AMP-activated protein kinase : Screening for novel membrane substrates and creatine kinase phosphorylation linked to specific subcellular compartment

Sacnicte Ramirez Rios

UNIVERSITÉ DE GRENOBLE

THÈSE

Pour obtenir le grade de

DOCTEUR DE L'UNIVERSITÉ DE GRENOBLE

Spécialité : **Biologie Cellulaire**

Arrêté ministériel : 7 août 2006

Présentée par

Sacnicte RAMIREZ RIOS

Thèse dirigée par **Uwe SCHLATTNER**

préparée au sein du **Laboratoire de Bioénergétique Fondamentale et Appliquée**
dans **l'École Doctorale Chimie et Sciences du Vivant**

La protéine kinase activée par AMP : Criblage de nouveaux substrats membranaires et phosphorylation de la créatine kinase liée à une compartimentation subcellulaire

Thèse soutenue publiquement le « **20 décembre 2010** », devant le jury composé de :

Pr. Theo WALLIMANN
Professeur à l'ETH Hönggerberg HPM, (Rapporteur)
Pr. Bé WIERINGA
Professeur, Department of Cell Biology, Nijmegen University (Rapporteur)
Dr. Marie-Lise LACOMBE
Professeur INSERM UMRS (Examinateur)
Pr. Uwe SCHLATTNER
Professeur au Laboratoire de Bioénergétique Fondamentale et Appliquée (Membre)

Table of Contents

AIM OF THE THESIS

Two key enzymes take center in the regulation of cellular energy metabolism. Creatine kinases (CK) serves as an acute energy buffer and transport system, while AMP-activated protein kinase (AMPK) senses and regulates cellular and whole body energy delivery and consumption in short and long term. Both kinases are presented in detail in Chapter 1.

The principal aim of this thesis was to extend our knowledge on the mechanisms of how AMPK can fulfill its pleioropic functions in regulating not only cellular energy homeostasis, but also many more ATP-dependent cellular functions like growth, shape and proliferation. To this end, it was envisaged to analyze the downstream signaling network of AMPK by identifying and characterizing novel direct substrates of AMPK. As a model system, the brain was chosen, because information on AMPK signaling in brain is still scarce.

In a first step, we established suitable purification procedures for different AMPK isoform combinations, potentially also applicable to any other protein. To obtain highly pure AMPK heterotrimeric complexes, we aimed at an automated, multidimensional protein purification protocol (Chapter 2). Such purified AMPK protein proofed to be an invaluable tool for studies of signaling pathways.

In continuation of previous efforts, applying an *in vitro* phosphoproteomic screen, brain-type creatine kinase (BCK) was identified as a putative substrate of AMPK. In this main project of the thesis, the aim was to confirm BCK as an AMPK substrate and to characterize this phosphorylation *in vitro* and *in vivo* (Chapter 3).

Finally, the large majority of known AMPK substrates are soluble cytosolic proteins. A secondary aim of the thesis was thus to extend the *in vitro* phosphoproteomic screen to proteins associated to unsoluble cellular structures, such as membranes (Chapter 4).

- CHAPTER 1 -

Regulation of cellular and whole body energy homeostasis

Introduction

1.1. Cellular energy metabolism

Energy metabolism in living organism is supported by the oxidation of carbohydrates (glucose) and lipids (fatty acids) provided by food intake (Stryer, 1988). Breakdown of glucose and fatty acids results in adenosine triphosphate (ATP) production, the universal energy currency in all organisms and cells. The initial step of energy metabolism consists in cell membrane transport of glucose and fatty acids across cell membrane followed by activation of two principal pathways of ATP production: glycolysis and oxidative phosphorylation (OxPhos). Glucose transport is regulated by a family of 13 carriers (GLUT), which differ in their kinetic characteristics and are stored in cytoplasmic vesicles and translocated to the plasma membrane in response to energy requiring conditions (Joost and Thorens, 2001). Similar events occur in fatty acid transport. FAT/CD36 carrier is stored in the cytoplasm upon appropriated signaling events (Ishiki and Klip, 2005). Glycolysis reactions take place in the cytoplasm of the cell. Once transported, glucose is phosphorylated by hexokinase and subsequent enzymatic steps convert glucose-6-phosphate into pyruvate, yielding 2 ATP and 2 NADH molecules. Under aerobic conditions, pyruvate is further metabolized in mitochondria, where it enters the tricarboxic acid cycle (TCA) after conversion into acetyl-CoA. Alternatively, under anaerobic conditions (e.g. during exercise) pyruvate is converted into lactate reducing NADH to NAD^+ again available to be reduced in glycolysis. The stepwise breakdown of the fatty acids chains also generates acetyl-CoA, which is further metabolized in mitochondria by the TCA cycle and OxPhos-mediated ATP synthesis.

1.2. Cellular Energy Homeostasis

The term homeostasis refers to the stability of the internal milieu in the face of external perturbations; these in principle may be caused by extracellular factors or by change in intracellular biological function (Hochachka, 2003). All living cells, to our knowledge, rely on the usage of 5'-Adenosine TriphosPhate (ATP) as the major fuel for cellular processes. The levels of intracellular ATP are maintained remarkably stable, even in times of high energy demand, e.g. during muscle contraction or nerve cell activation. Additionally, the ATP/ADP ratio, which significantly affects the free energy change of ATP hydrolysis, is maintained high allowing optimal efficiency of ATP-dependent reactions (Hochachka, 2000). Therefore, the cellular system demands for very tight regulation and efficient mechanism allowing for immediate responses to fluctuating energy requirements. Disorders in energy homeostasis are related to diseases such as diabetes, obesity or cancer.

1.3. Phosphotransfer systems

Living cells rely on a permanent availability of high levels of ATP as the major fuel of cellular processes. ATP consumption and production have to be balanced very tightly. Balance is especially important for cells with high and fluctuating energy metabolism, using vast amounts of energy in form of ATP in a short period of time, e.g. skeletal and cardiac muscle, brain, retina photoreceptor cells, spermatozoa and electrocytes (Wallimann and Hemmer, 1994; Wallimann et al., 1992). ATP production by oxidative phosphorylation or by glycolysis does not obligatory coincide temporally and spatially with cellular energy requirements. To avoid local lack of energy, metabolic enzymes and mitochondria are able to relocalize to sites of high energy consumption. It has been reported that glycolytic enzymes can bind to Na^+/K^+ ATPase to provide subcellular ATP (Glitsch and Tappe, 1993). Indeed, a relocalization of mitochondria along microtubules and actin filaments has been observed in neurons (Boldogh et al., 2007).

In addition to the ability to directly couple ATP production sites to ATP consumption sites, cells possess energy transfer and storage systems based on phosphotransfer from ATP (Figure 1-1) (Ratto et al., 1989; Watts, 1971). These include three families of kinases: adenylate kinases (AK), nucleoside diphosphate kinases (NDPK), and creatine kinases (CK). AK can restore ATP levels in the cell by making the "energy-rich" β-phophoryl in ADP accessible in the reaction: $2ADP \leftrightarrow ATP + AMP$ (Dzeja et al., 1998). It is also considered as the major source of AMP and thus delivers an AMP signal under energy stress. NDPKs catalyze the reversible exchange of the γ-phosphate between tri- and diphosphonucleosides: $N_1TP + N_2DP \leftrightarrow N_1DP + N_2TP$ (Lascu and Gonin, 2000). According to cellular concentrations of the different nucleotides suggest that the reaction *in vivo* mainly proceeds in the direction of using ATP, e.g. formed by oxidative phosphorylation, to generate the other triphosphonucleosides in particular GTP. CK is the major phosphotransfer system in cells that copes with high and fluctuating energy demands to maintain cellular energy homeostasis (Wallimann T, 2007). CK enzymes catalyze the reversible phosphate transfer from ATP to creatine (Cr) yielding the high-energy compound phosphocreatine (PCr) and ADP: $ATP + Cr \leftrightarrow ADP + PCr$.

All these phosphotransfer kinases exist as mitochondrial and cytosolic enzymes. Mitochondrial isoforms localized in the intermembrane space can use preferentially mitochondrially generated ATP for their phosphorylation reactions, thus building up a PCr pool (up to 20 mM), rephosphorylating AMP to ADP or GTP (NDPs) into GTP (NTPs). Cytosolic isoforms of CK and AK partially coupled to ATPases use for a local recovery of ATP the PCr pool via CK (immediate response under energy stress) or ADP via AK (under prolonged energy stress). Cytosolic NDPK coupled to GTPases can use local ATP provided by CK or AK reactions (Figure 1-1).

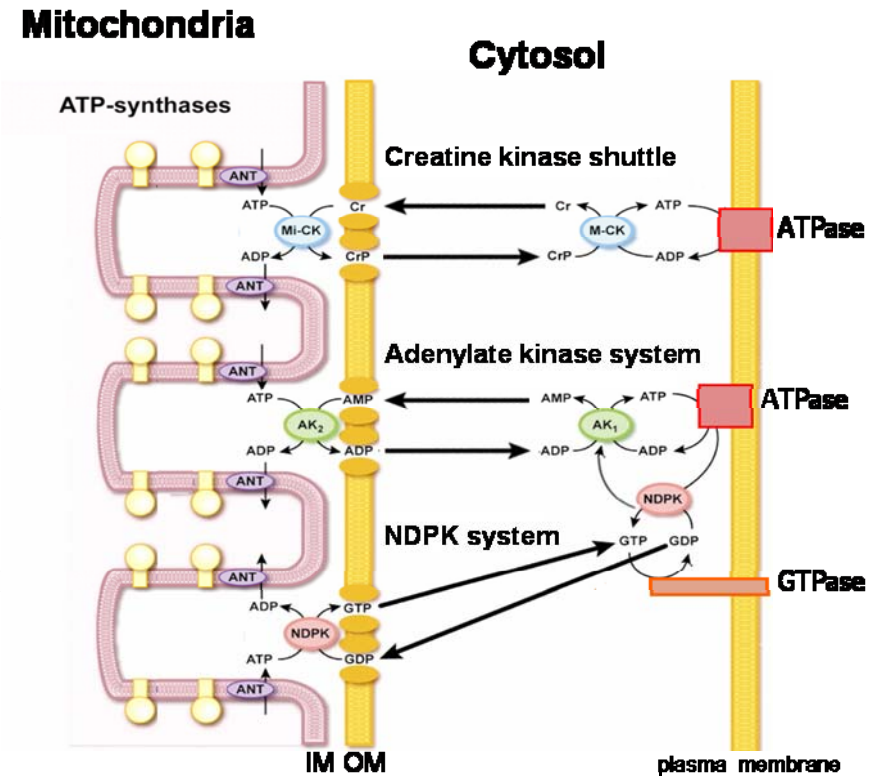

Figure 1-1. High-energy phosphoryl transfer networks. Integrated communication between cellular sites of ATP-generation (e.g. mitochondria) and ATP-utilization (e.g. plasma membrane). Creatine kinase (CK), adenylate kinase (AK), and the nucleoside dephosphate kinase (NDPK) systems are functionally coupled to oxidative phosphorylation in mitochondria via mitochondrial isoforms where they transfer the energy rich ~P from ATP to nucleotides or PCr. CK, AK and NDPK isoforms in the cytosol transfer the ~P through reversible reaction to ATP towards ~P consuming sites (e.g ATPases and GTPases). (Adapted from (Dzeja and Terzic, 2003)).

1.4. Creatine kinase

In vertebrates, five different CK isoenzymes are expressed in a tissue-specific manner and are localized to different intracellular compartments. For ATP homeostasis and maintenance of high ATP/ADP ratios, CK can efficiently regenerate ATP at the expense of phosphocreatine ($MgADP^-$ + PCr^{2-} +H^+ ↔ $MgATP^{2-}$ + Cr) and *vice versa* (Wallimann et al., 1998; Wallimann et al., 1992). In sarcomeric muscle, dimeric cytosolic muscle-type CK (MCK) and octameric sarcomeric mitochondrial CK (sMtCK) are always co-expressed, whereas in brain and other non-muscle tissues and cells, dimeric cytosolic brain-type CK (BCK) is co-expressed with octameric ubiquitous mitochondrial CK (uMtCK). In adult heart, where both cytosolic MCK and BCK are expressed, also the MB-CK heterodimer is found (Wallimann et al., 1992). MtCKs are located in the mitochondrial intermembrane space (Kottke et al., 1991), along the entire inner membrane and also at peripheral contact sites (Kottke et al., 1988; Schlattner et al., 1998), where inner and outer membranes are in close proximity (Biermans et al., 1989; Brdiczka and Wallimann, 1994). There, MtCKs can directly transphosphorylate intra-mitochondrial ATP into PCr (Jacobus, 1985; Saks et al., 1985), which is then exported into the cytosol. The presence of mitochondrial and cytosolic CK suggests that compartmentalized CK isoenzymes are necessary to fulfill specific functions as discussed above.

1.4.1. Temporal and spatial buffering functions of creatine kinases

The 'cytosolic' and 'mitochondrial' CKs reversibly convert Cr to the high-energy compound phosphocreatine (PCr). This conversion mainly occurs in close proximity to ATP-generating processes, such as glycolysis in the cytosol or oxidative phosphorylation in mitochondria, thereby building up a large pool of rapidly diffusing and available PCr. This pool can act as temporal and spatial buffer preventing a rapid decreased in global ATP concentration upon cell activation or sudden stress conditions. Cytosolic CKs are often associated with ATP-utilizing processes (e.g. ATPase) and ensure high local ATP/ADP ratios through the regeneration of ATP at the expense of PCr (Figure 1-2) (Wallimann et al., 1992). An *in vivo* model system with spermatozoa confirmed that a CK-mediated ATP relay from mitochondria (near the sperm head) to the flagellum, where the main ATP sink is located to maintain tail movement (Tombes and Shapiro, 1989). The CK system also requires an adequate Cr supply which is maintained by a specific creatine transporter (CRT) (Speer et al., 2004). Evidence for the crucial function of this Na^+/Cl^--dependent creatine transporter emerged from studies of CRT deficient patients, suffering severe retardation of speech and mental development, accompanied by the absence of Cr in the brain.

The highest expression of CK is evident in tissues or cells with a high energy demand. In skeletal muscle, PCr concentration may reach 20-35 mM or more, and the ATP regeneration capacity of CK is very high. Knockout mice lacking cytosolic MCK show no alterations in absolute muscle force, but lack the ability to perform burst activity (van Deursen et al., 1993). Remarkable, this muscle phenotype becomes more severe if both MCK and sMtCK genes are deleted simustaneously. PCr and ATP levels are normal in resting MCK-deficient muscles, but rates of high energy phosphate exchange between PCr and ATP are at least 20% reduced. CK-deficient muscles displayed adaptations to compensate the CK energy transfer by increasing the intermyofibrillar mitochondrial volume and glycolytic potential. By these metabolic and structural adaptations, the diffusion distance for ATP from mitochondria to myofibrils is shortened because PCr shuttling is no longer possible. These compensatory adaptations in CK double-knockout mice seem to be even more prominent in the cardiac muscle, to safeguard the performance of this organ that is essential for life (Bonz et al., 2002). In brain, the CK system was studied using a mouse models deficient in BCK. Knockout mice presented a significantly reduced flux capacity for high-energy phosphoryl transfer between PCr and ATP, but elementary functions were not perturbed. Interestingly, mice lacking BCK exhibited a decreased spatial learning acquisition and habituation in a Morris water maze test (Jost et al., 2002). Electron microscopy analysis of knockout mice brain revealed an increased intra- and infrapyramidal mossy fiber field size (IIP-MF) in comparison with wild type animal. The IIP-MF area, has been reported to correlate with alterations in behavioral traits and spatial learning taks (Ramirez-Amaya et al., 2001; Schwegler and Crusio, 1995). More details on the importance of CK for brain function were obtained with mice lacking both BCK and uMtCK. These mice exhibit a reduced body weight and are severely hampered in spatial learning, and display lower nest building activity and altered acoustic

startle reflex responses (Streijger et al., 2005). In addition CK double knockout mice present problems with the maintenance of temperature homeostasis and incidentally succumb due to a sudden and severe drop in body temperature (Streijger et al., 2009). In addition, morphological analysis of CK double knockout brains showed a reduction in brain weight and hippocampal size. All these physiological problems caused by the absence of brain-specific CK isoform fully support the importance of CK for normal brain function.

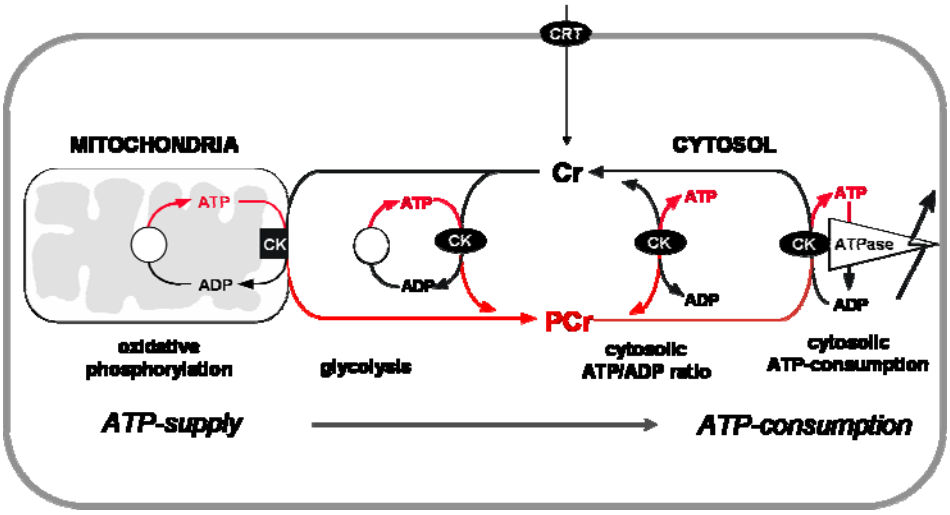

Figure 1-2. The CK/PCr system. Creatine (Cr) is transported into the cell by a specific creatine transporter (CRT). Imported Cr is reversibly converted into the high-energy compound phosphocreatine (PCr) by the action of creatine kinase (CKs) which are coupled to ATP processes such as oxidative phosphorylation (OxPhos) in mitochondria or glycolysis in the cytosol. PCr serves as energy store and transport compound allowing immediate ATP regeneration by cytosolic CKs globally or locally, when associated with ATP-consuming processes (ATPases). Adapted from (Schlattner et al., 2006).

1.4.2. Creatine metabolism and brain energetics

In mammals, creatine (Cr) is principally taken-up from diet but also synthesized endogenously by a two-step mechanism (Braissant et al., 2001; Braissant et al., 2005). Mainly in the kidney, guanidinoacetate (GAA) is formed from arginine and glycine by L-arginine:glycine amidinotransferase (AGAT). Via the blood stream, GAA enters the liver where it is subsequently methylated by S-adenosyl-L-methionine:N-guanidinoacetate methyltransferase (GAMT) converting GAA into Cr (Wyss and Kaddurah-Daouk, 2000). Cr, which leaves the liver and is then transported through the blood stream is finally taken up via a specific creatine transporter (CRT) by target tissues, such muscle or brain, where Cr is phosphorylated by CK to high-energy PCr (Figure 1-3A,B). Intracellular Cr and PCr are non-enzymatically converted to creatinine, with a constant daily turnover of 1.5% of body creatine. Creatinine is excreted through the urine and the daily urinary creatine excretion is directly proportional to total body creatine. The central nervous system (CNS) is the main organ affected in Cr deficiency syndromes.

Two main categories of disorders in Cr metabolism are distinguished according to the metabolic pathway of Cr: disorder of Cr synthesis including AGAT and GAMT deficiencies, and disorders of cellular Cr transport CRT deficiency(Salomons et al., 2001; Schulze et al., 1997; Stockler et al., 1994). Patients suffering of these deficiencies present neurological symptoms in infancy, including mental retardation and delays in speech acquisition. GAMT, and often CRT deficiencies, also can cause epilepsy. GAMT and AGAT deficiencies are treatable by oral creatine supplementation, while patients with CRT deficiency do not respond to this type of treatment. In the brain, Cr is taken up by cells that express the CRT. However, certain cells like astrocytes lacking the CRT are able to synthesize creatine endogenously by co-expressing AGAT and GAMT, especially in the developing brain (Braissant et al., 2001) (Figure 1-3C). Recently, it was demonstrated that AGAT, GAMT and CRT are expressed independently of each other in CNS, at the level of transcription and translation (Braissant et al., 2010). Interestingly, in many brain structures, cells that are fully equipped for Cr synthesis (co expressing AGAT + GAMT) represent less than 20%, and a higher proportion of cells expresses AGAT without GAMT, or GAMT without AGAT. This suggested that for Cr synthesis to occur, GAA must be transported from AGAT- to GAMT-expressing cells. In addition, Braissant et al, presented evidence that brain cells can take up GAA probably through CRT, and convert it to Cr. This evidence proposes that all brain cells seem to have the capacity for endogenous Cr biosynthesis, but whether it is functional depends on in the expression of AGAT, GAMT and CRT. It was proposed that Cr synthesized by astrocytes can be taken up by neurons indicating a novel neuron-glial relationship involving Cr traffic (Figure 1-3D). Furthermore, Cr is exocytotically released from central neurons and acts as partial agonist on central GABA post-synaptic receptors (Koga et al., 2005), suggesting a neuron-modulator function of Cr in the brain (Almeida et al., 2006). Interestingly, positive effects of Cr supplementation on the skeletomuscular health status of elderly patients as well as for those with muscle, neuromuscular, and heart diseases have been reported (Chetlin et al., 2004; Tarnopolsky et al., 2001; Woo et al., 2005). In addition, rat and mouse cerebral ischemia models treated with oral Cr administration resulted in neuroprotection and remarkable reduction in ischemic brain infarction. This is due to the fact that newly introduced Cr is phosphorylated inside of the cell by CK, leading to an increase PCr/ATP ratio, and thus a higher energy charge in the cell (Adcock et al., 2002; Zhu et al., 2004). Moreover, traumatic brain injury (TBI) animal models have shown that Cr supplementation protects against TBI neuropathology through mechanisms involving maintenance of mitochondrial bioenergetics and preservation of ATP levels (Sullivan et al., 2000). Notably, Cr is assumed to have additional non-energy-related functions, for example Cr supplementation was demonstrated to have antioxidant properties via a mechanism involving a direct scavenging of reactive oxygen species (Sestili et al., 2006) and a protective effect of Cr against oxidant and UV stress has been detected in keratinocytes (Lenz et al., 2005). Different questions concerning Cr metabolism, like regulation of trans-cellular transport, uptake of Cr into the brain and intracellular trafficking and exocytotic release of Cr after neuronal stimulation have still to be clarified in detail.

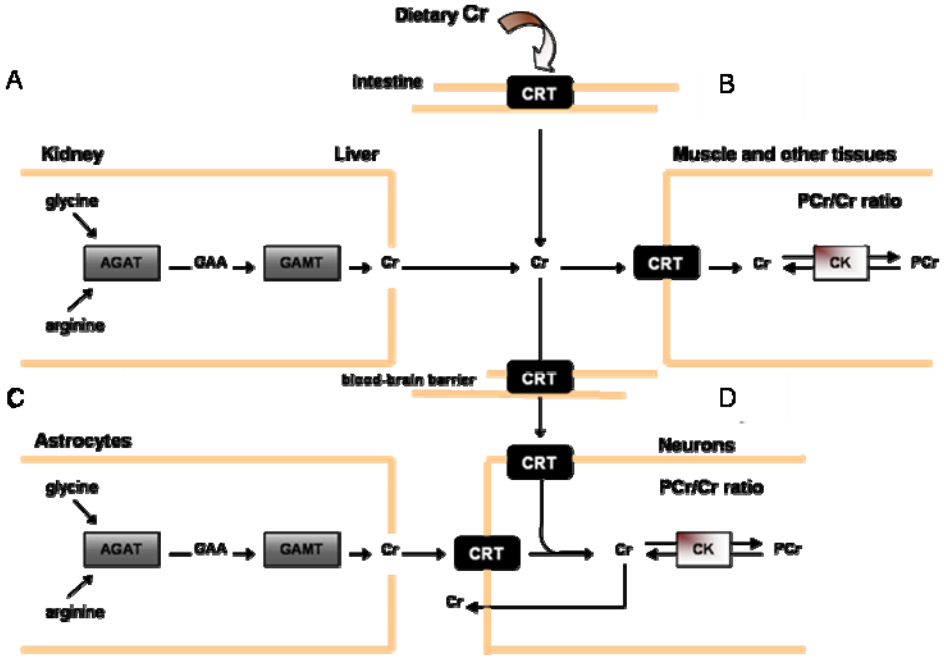

Figure 1-3. **Scheme of whole-body creatine metabolism with emphasis on the brain.** A certain fraction of Cr is endogenously synthesized in liver by a two-step involving AGAT and GAMT. AGAT, which produces guanidino acetate (GAA) as intermediate, is expressed preferentially in the kidney. GAMT is found mostly in liver, the main organ of the final step of endogenous Cr synthesis (A). Cr leaves the liver and is transported through the bloodstream and is actively taken up via a specific creatine transporter (CRT) by cells with high energy requirements, such as muscle cells where Cr is phosphorylated by CK to PCr (B). To get into the brain, Cr needs to pass the blood-brain barrier by the CRT. From there, Cr is taken up by those brain cells that express the CRT, represented mainly by neurons but not by astrocytes, which lack the CRT (C,D). On the other hand, dietary Cr, present in fresh fish and meat, is taken up by an intestinal CRT and transported into the bloodstream, where it mixes with endogenously synthesized Cr. A possible traffic of Cr between astrocytes and neurons and exocytotic release of Cr from neurons is proposed. Adapted from (Wallimann T, 2007).

1.4.3. Subcellular localization of CK isoforms

In cells with high energy demands, cytosolic CKs are generally co-expressed with MtCKs in a tissue specific manner. Mitochondrial CK isoenzymes are synthesized in the cytosol but then imported into mitochondria. There they are localized in both, peripheral intermembrane space (IMS) and the cristae space of mitochondria, interacting functionally with two transmembrane proteins, adenine nucleotide translocase (ANT) of the inner membrane and porin voltage-dependent anion channel (VDAC) of the outer membrane (Schlattner et al., 1998; Wyss et al., 1992) in the so-called contact sites, where inner and outer membranes are in even closer apposition. A functional coupling between MtCKs and oxidative phosphorylation has been demonstrated (Guzun et al., 2009; Saks et al., 1976). In this system, ATP produced by oxidative phosphorylation and provided by ANT, is converted into PCr by MtCKs and channeled into the cytosol via VDAC. These interactions are essential for the specific functions of the MtCKs in the CK/PCr circuit.

In the cytosol, BCK or MCK maintain ATP regeneration form PCr at cellular sites of energy demand. In muscle, CK localization and function has been well described (Figure 1-4). A small fraction between 5-10% of cytosolic MCK is specifically bound to the myofibrillar M-band (Hornemann et al., 2000; Turner et al., 1973) where CK is tightly functionally coupled to the myofibrillar, actin-activated myosin Mg^{2+}-ATPase. This localization is specific for MCK isoform (Wallimann et al., 1983b). The amount of MCK bound to the M-band is sufficient to regenerate the ATP hydrolysed by the actomyosin ATPase during muscle contraction (Wallimann et al., 1984). Besides its enzymatic function as an ATP regenerator, several authors have proposed an important function of MCK for the structural integrity of the myosin filament lattice (Wallimann et al., 1983a). Although cytosolic CKs are mainly localized in the cytoplasm, it is evident that in certain processes CK is membrane-associated. MCK has been found to be specifically associated with the sarcoplasmic reticulum (SR). Here, a functional coupling of citosolic CK to the ATP-dependent Ca^{2+} has been identified (Levitsky et al., 1978; Rossi et al., 1990). The CK system supports the ATP-driven Ca^{2+} uptake into SR vesicles to maintain Ca^{2+} homeostasis but also to regulate the local ATP/ADP ratios in the proximity of the Ca^{2+} pump (Rossi et al., 1990) allowing for adequate muscle function. The Ca^{2+} uptake in SR was affected in muscle lacking MCK or both MCK and sMtCK, resulting in affected muscle performance (van Deursen et al., 1993). Interestingly, the association of CK with SR was resistant to high-salt and low salt/EDTA treatment, suggesting that the specific association of CK with the SR can be due to a strong anchorage of CK fractions either directly with the SR membrane and/or an association with SR proteins, likely by a post-translational modification of CK (Rossi et al., 1990). Recently, MCK was found to interact with the Na^{+}/Ca^{2+} exchanger (NCX1). Under energy stress conditions, MCK is recruited to the plasma membrane and colocalizes with NCX1 leading to a recovery of NCX1 activity that is lost under energy-compromised conditions (Yang et al., 2010).

The brain is another excitable tissue with high ATP demands. Here, BCK is especially abundant and displays a mainly cytosolic distribution (Sistermans et al., 1995) (Figure 1-5). However, a certain fraction of total BCK is associated with the plasma membrane, where the enzyme is functionally coupled to the Na^{+}/K^{+}-ATPase ion pump (Guerrero et al., 1997). BCK has also been found to interact to membrane-associated proteins like the thrombin receptor-1 (PAR-1). In astrocytes, BCK is required by PAR-1 to induce and mediate cytoskeletal remodeling via the RhoA pathway in response to thrombin (Mahajan et al., 2000). It was suggested that interaction of BCK and PAR-1 is important to provide an ATP generating system during cytoskeletal reorganization precisely at the membrane site of receptor signaling. The neuron-specific K^{+}-Cl^{-} cotransporter, KCC2 has been reported as an interaction partner of BCK (Inoue et al., 2004). KKC2 is involved in the developmental regulation of $[Cl^{-}]$ in neurons. To elucidate the functional significance of this interaction, BCK activity was inhibited using dominant-negative BCK expression or utilizing a pharmacological inhibitor in mouse cortical neurons. In both systems, the absence of BCK activity led to a decrease in the ability of KKC2 to maintain adequate concentration of $[Cl^{-}]$ (Inoue et al., 2006). Bürklen et al. demonstrated a specific interaction of BCK with the *cis*-Golgi matrix protein (GM130). GM130 is a cytoplasmic protein that is

tightly bound to Golgi membranes and participles in the disassembly of the Golgi complex (Lowe et al., 2000). *In vivo*, BCK co-localizes with the GM130 only during early prophase of mitosis characterized by a condensation in the perinuclear area. In this phase, energy is needed to initiate Golgi apparatus fragmentation and various phosphorylation processes (including GM130 phosphorylation). It's likely that interaction between GM130 and BCK facilitates GM130 phosphorylation by ATP-requiring protein kinase. It was suggested that BCK can be linked to signaling cascades regulating the integrity of the Golgi apparatus and thus may be involved in the control of cell cycle (Burklen et al., 2007). Recently, Kuiper et al, demostrated that, in macrophages, BCK co-accumulates transiently with F-actin at the nascent phagosome were it seems to play a role in active and ATP-dependent actin polymerization and particle adhesion (Kuiper et al., 2008). BCK also co-localizes with F-actin in peripheral membranes ruffles in actively spreading astrocytes (Kuiper et al., 2009). The authors confirmed that cell motility is coupled to on-site availability of ATP generated by BCK, and that the absence of BCK activity affects the migration capacity of astrocytes and other cells types (Kuiper et al., 2009).

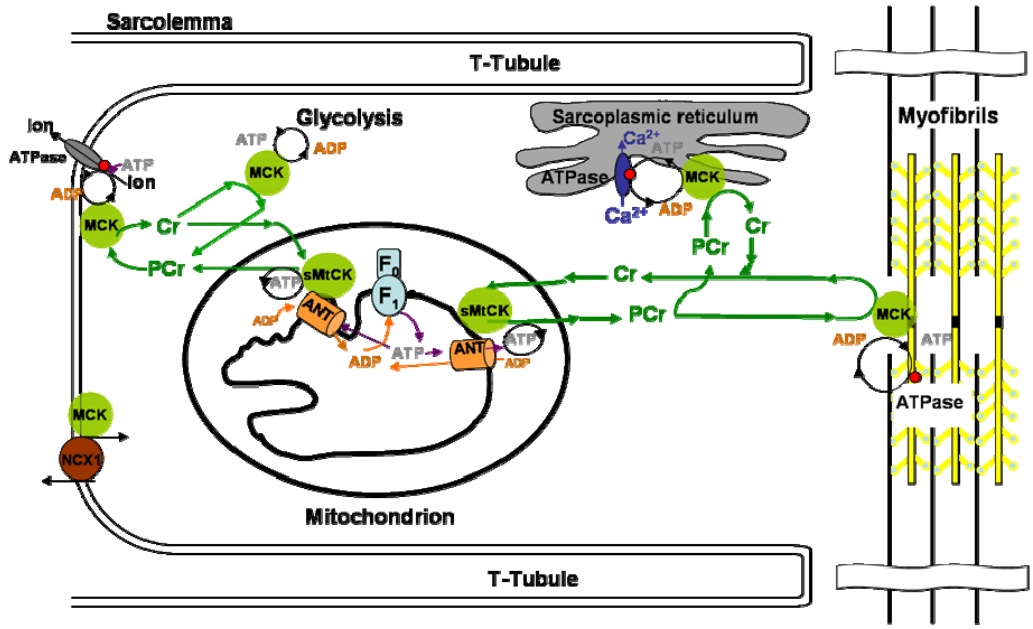

Figure 1-4. Subcellular compartmentation of sarcomeric mitochondrial CK (sMtCK) and cytosolic MCK. ATP produced by mitochondria is converted into PCr by sMtCK and channeled into the cytosol. Similarly, in more glycolytic tissues, cytosolic MCK coupled to glycolytic enzymes can add to this PCr pool. At the receiving end of the CK/PCr shuttle, cytosolic CK coupled to ATP-consuming processes such as the myofibrillar calcium-activated MgATPase, the SR Ca^{2+}-pump ATPase (SERCA), or the Na^{+}/Ca^{2+} exchanger (NCX1) can regenerate local ATP levels. Adapted from (Saks et al., 2001).

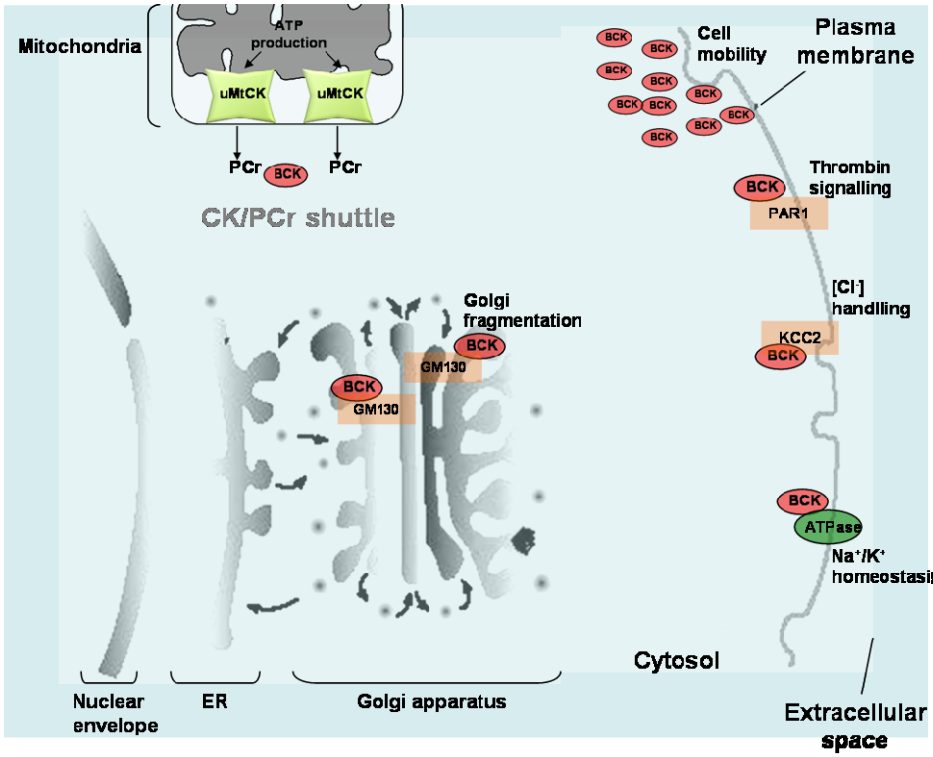

Figure 1-5. Subcellular compartmentation of cytosolic BCK. In brain, BCK transport energy through the CK/PCr shuttle to energy demanding compartments. ATP produced by mitochondria is converted into PCr by uMtCK and channeled into the cytosol. Energy consuming processes are among other cytoskeletal reorganization, cell mobility, golgi fragmentation.

1.4.4. BCK structure

Cytosolic BCK dimers display an elongated "banana-like" shape with a molecular mass of 2 X 43 kDa and overall dimensions of ~ 92 X 42 X 65 Å (Figure 1-6A). The fold of the monomer BCK is very similar to that of the mitochondrial isoform and also to cytosolic muscle MCK. BCK consists of a small N-terminal domain comprising residues 2-100 and a larger C-terminal domain (residues 125-381) connected by a long linker region (101-124) (Figure 1-6B). The large domain contains an eight-stranded antiparallel β-sheet flanked by seven α-helices. The N-terminal domain of BCK differs between monomers. The N-terminus of monomer A is localized at the surface of the dimer, while the first eight residues of monomer B protrude into the contact region between the two monomers (Figure 1-6A). The finding of two remarkable different N-terminal conformations in a homodimeric protein seems to be noteworthy and differs from the structure of the MCK or sMtCK, where the two monomers of the dimer are identical. Whether this is a unique feature to BCK or a general property of cytosolic creatine kinases cannot be answered at the moment, since in the structure of rabbit MCK residues 2-7 were not defined by electron (Rao et al., 1998). Additional structural differences between the monomers are found in residues at the surface and for flexible loop regions of the enzyme. Otherwise, structural differences between the monomers are rare, especially in the highly conserved "common core" of all guanidine kinases.

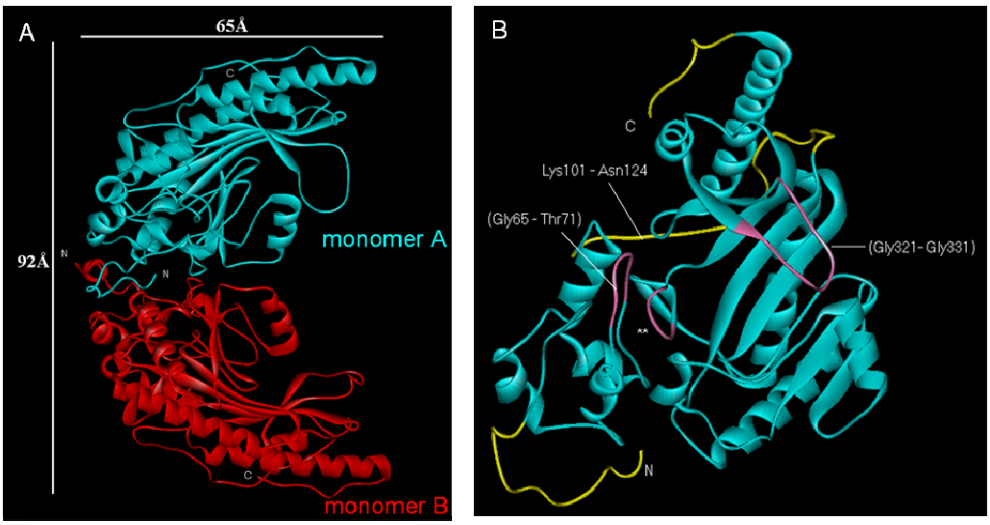

Figure 1-6. Molecular structure of the biologically active dimer and the monomer of chicken BCK in a ribbon representation. A) Monomer A and B are shown in cyan and red, respectively. Note the different topology of the N-termini located between the monomers. B) Monomer structure of BCK, The conserved "common core" of all CK isoenzymes is shown in cyan, isoenzyme-specific sequences of the N- and C- terminal are coded in yellow, together with the long linker region (101-124). Two flexible loops conserved in all CKs and known to be important for catalysis are depicted in light red with the respective residue numbers in brackets. The loop 280-285 contains the highly reactive "essential" Cys283 represent by **.

Creatine kinase contains several conserved arginines in the active site (Arg96, 130, 132, 135, 236, 292 and 320). By comparison with the structures of chicken sMtCK with bound Na-ATP (Fritz-Wolf et al., 1996), arginines 130, 132, 236, 292 and 320 of BCK are expected to interact with the phosphate groups of the adenine nucleotide. Site-directed mutagenesis was applied to elucidate function of CKs. In human BCK replacement of the reactive cysteine, Cys283 by either serine or tyrosine led to a total loss of activity. The reduced activity was not due to problems with dimerization as each of the mutants was able to produce a heterodimer. Based on these results, the authors concluded that Cys283 is essential for catalysis. The presence of a single cis-proline at position 212, as already postulated for sMtCK is also present in BCK. This cis-proline is localized between β-strand 3 (216-220) and a loop (residues 204-211), which covers part of the active site cleft. Mutation of this proline leads to a reduction of enzyme activity and a pH shift in the pH optimum of the CK reaction by 1.3 pH units toward acidic pH (Forstner et al., 1998). Two flexible loops are conserved in all CKs, in BCK these loops are residues Gly65-Thr71 and Gly321-Gly331, which seem to be important for catalysis. Mutation of His61 in sMtCK (corresponding to His66 in BCK) severely hampers enzyme activity (Forstner et al., 1997) confirmed the proximity of this loop to the active site in the enzyme. Interestingly, guanidino kinases differ significantly in the length of this loop depending on the size of their substrates. BCK isoform share 77-82% amino acid sequences identity with the cytosolic MCK (Muhlebach et al., 1994), suggesting a similarity of their three-dimensional structures. Thus, no significant divergence in the overall fold is seen. Interestingly, the N-terminal region, where cytosolic CK isoenzymes diverge most significantly in their amino acid sequences, seem to be important for specific interactions between CK and certain structures (Stolz and Wallimann, 1998).

1.4.5. MtCK structure

In contrast to dimeric cytosolic CK, MtCK not only form dimers, but also associates into octamers. The octameric species is the predominant oligomeric form *in vitro* as well as *in vivo*. The highly ordered, large cuboidal octamer has overall dimensions of about 105 x 105 x 86 Å (Figure 1-7A). It assembles from four elongated "banana-shaped" dimers that are arranged around its fourfold axis. Along this axis, a central channel of about 20 Å diameter extends through the entire octamer (Figure 1-7B). The N-termini of all monomers protrude into this channel. The top and bottom faces that are perpendicular to the fourfold octamer axis each expose the C-termini of four monomers (Figure 1-7A). The monomer consists of a small N-terminal domain (residues 1-100) and a larger C-terminal domain (residues 113-end) connected by a long linker region without secondary structure (residues 101-112). The small N-terminal domain is exclusively α-helical. It contains 5 conserved α-helices and one α1(3_{10})-helix (chicken sMtCK) or an additional α-helix (human uMtCK). The core of the C-terminal large domain is formed by an eight-stranded antiparallel β-sheet, which is flanked by seven α-helices. All α–helices except α8 are on the convex side of the β–sheet, while the enzyme's active site is on the concave side. The β–sheet and the α8-helix form the common core of CK isoenzymes that is characterized by a conserved amino acid sequence and contains the enzyme's active site. Some aspects of the MtCK structures indicate a high degree of flexibility; two loops in the region of residues 61-65 and 316-326 are disordered in both sarcomeric and ubiquitous MtCK structures, but close down on the active site during catalysis, suggesting that CK undergoes flexible between the small and large domain during catalysis. The ability to form highly symmetrical cuboidal octamers is a unique feature of all MtCKs (Ellington et al., 1998; Schlattner et al., 2000). The octamer is held together by several interactions of two rather small regions, comprising some residues in the small domain and a predominant hydrophobic patch in the large domain around Trp264. Site directed mutagenesis demonstrated that N-terminal domain of MtCK is important for octamer stability (Kaldis et al., 1994). Deletion of the N-terminal heptapeptide and simultaneous mutation of the dimer/dimer interface Trp264 significantly reduces octamer formation of sMtCK. Membrane binding is another important characteristic of MtCKs. It was proposed that the linker region between N- and C-domain is one of the possible membrane binding motifs specific for the mitochondrial CK isoforms (Schlattner et al., 1998). Indeed, this linker region is located at the surface of the octamer with the side chains pointing toward the fourfold top or bottom faces of MtCK. The second putative membrane-binding region of MtCKs resides at the very C-terminal end of the molecule. There, MtCKs expose three to four basic residues (depending on the isoform), which could interact with the negative charged head groups of phospholipids in the mitochondrial membranes, in particular cardiolipin (Schlattner et al., 2009; Stachowiak et al., 1996; Vacheron et al., 1997). More interestingly, it was found that MtCK proteins are involved in the transfer of lipids from one mitochondria membrane to another (Epand et al., 2007a) as well as with MtCK-induced clustering of cardiolipin (Epand et al., 2007b).

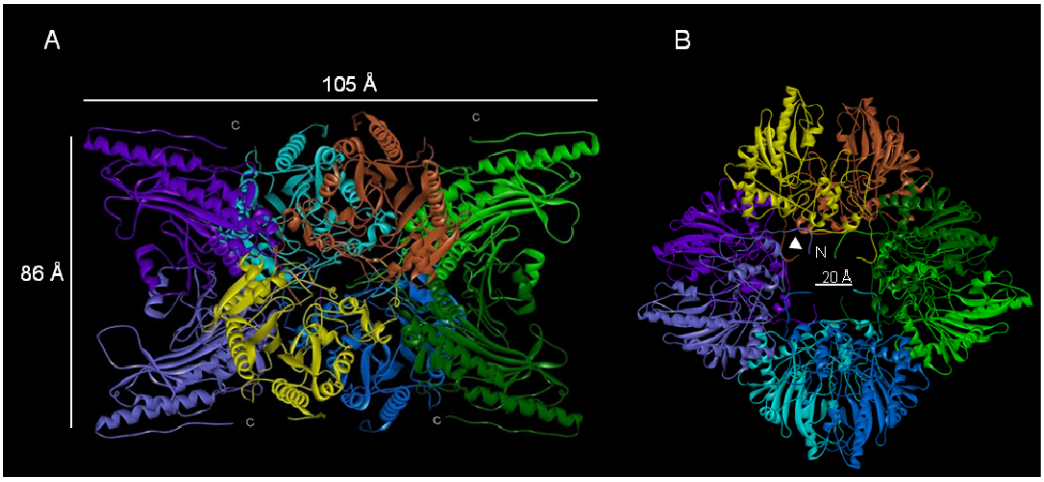

Figure 1-7. Molecular structure of uMtCK. The octameric structure of human uMtCK (solved at 2.7 Å (Eder et al., 2000)). a) The side view (right) shows a two-fold symmetry; the arrows indicate one of the eight C-terminal stretches that are involved in binding to anionic phospholipids. b) The top or bottom view (left) reveals a 4-fold rotational symmetry of the dimers arranged around a 20 Å large central channel. The arrows indicate one of the eight N-termini.

1.4.6. Creatine kinase regulation

Since intracellular ATP/ADP ratios regulate a variety of cellular processes and since CK system is involved in regulation of local ATP/ADP ratios, it was proposed that CK may also be subject of regulation e.g. by post-translational modification. Indeed, BCK was found phosphorylated in brain microtubule fractions (Mahadevan et al., 1984). Protein kinase C (PKC) was shown to phosphorylate BCK in chiken brain (Quest et al., 1990) and in mouse skin cells, resulting in an increased affinity of BCK for PCr (Chida et al., 1990a; Chida et al., 1990b). In addition, covalent modification of CKs by autophosphorylation has been reported (Hemmer et al., 1995). This autophosphorylation exerts a modulatory effect on ATP substrate binding, rather than on the catalytic mechanism (Stolz et al., 2002). It was proposed that CK autophosphorylation may possibly modulate the reversibility of the CK reaction. Creatine kinase was also suggested as a target for AMPK (Ponticos et al., 1998). It was shown that AMPK phosphorylates and thereby inactivates MCK. However, inhibition of CK activity by AMPK phosphorylation could not be confirmed by others (Ingwall, 2002). Nevertheless, association with subcellular structures or enzymatic activity of CK isoenzymes may be subject to regulation by secondary modifications. For example, it is conceivable that phosphorylation could act as a mechanism of reversible membrane targeting of CK isoenzymes. Furthermore, it is likely that CKs are connected to signal transduction pathways at a different level, that is, by locally providing ATP for protein kinases.

1.5. AMP-activated protein kinase: A key-regulator of energy metabolism

The phosphocreatine/creatine kinase (PCr/CK) shuttle constitutes a first mechanism to prevent sudden drops of ATP, but once the PCr pool exhausted, the ATP concentration also declines accompanied by a rise in ADP and AMP. Through the action of AK, which converts two ADP molecules in one ATP and one AMP molecule, the drop in ATP levels is slowed down, while AMP rises more rapidly than ADP. As indicated by its name, 5'-adenosine monophosphate-activated protein kinase (AMPK) is sensitive to intracellular AMP levels and is in the front line to sense energy decrease translated by a rise in AMP levels (Neumann D, 2007) (Figure 1-8).

1.5.1. AMPK as a multifunctional metabolic sensor

AMPK is a metabolic and stress sensor that has been functionally conserved throughout eukaryotic evolution. Functions described for AMPK include the coordination of anabolic and catabolic processes in various tissues, including cardiac and skeletal muscle, adipose tissue, pancreas and liver (Kahn et al., 2005). In these tissues, AMPK responds to diverse external (e.g. hormones) and internal (e.g. AMP) stimuli that signal an impaired energy state in diverse physiological and pathological situations. Activated AMPK inhibits ATP-consuming (anabolic) processes and stimulates ATP-generating (catabolic) processes. Earlier studies focused on the role of AMPK as metabolic sensor at the cellular level, but it is becoming evident that AMPK also plays more complex roles as a metabolic sensor for the entire organism (Carling, 2004).

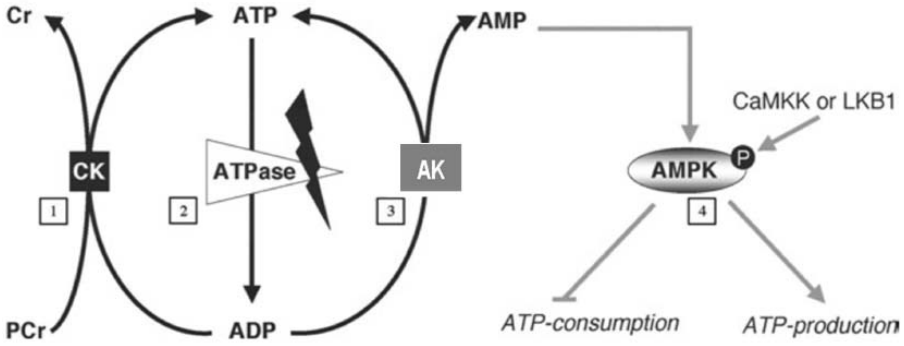

Figure 1-8. High-energy phosphoryl transfer networks and regulation of cellular energy status. ATP comsuption by ATPases (2) and the energy is converted, among other purposes, for muscle contraction, ion-pumps and protein synthesis. The cellular ATP/ADP ratio is kept high by the action of two energy-related kinases, creatine kinase (CK, (1) and adenylate kinase (AK)(3). The ADP generated upon hydrolysis by ATPases is recharged into ATP by the action of CK (1) which draws its energy from a large phosphocreatine (PCr) pool, and by AK (3) that uses two ADP molecules to regenerate one ATP and to generate one AMP molecule. AMP serves as an indicator for cellular energy stress and stimulates AMPK (4). Phosphorylation by either of the two upstream kinases, i.e. LKB1 or CaMKK, at Thr172 in the α subunit causes its activation, with AMP inhibiting dephosphorylation. Activated and fully AMP-stimulated AMPK then up-regulates catabolic pathways for ATP production and suppresses anabolic pathways that would consume ATP. Adapted from (Neumann D, 2007).

AMPK not only senses cellular energy status, but also functions at the tissue and organism levels to promote context-specific responses to physiological signals of metabolic status. In fact, AMPK modulates many aspects of cellular metabolism. It was first known to be activated by ATP depletion (increase AMP/ATP ratio) provoked by stimuli as exercise, starvation, or hypoxia. However, AMPK is also activated by certain drugs, hormones and cellular stressors that do not alter AMP/ATP ratio. Via these signals, the AMPK signaling pathway senses both physiological and pathophysiological stimuli (Kahn et al., 2005). It has recently proposed that AMPK is also involved in whole-body energy homeostasis, stimulating energy expenditure by promoting fatty acid and glucose oxidation in the periphery, while at the same time inhibiting energy in-take via effects on appetite in the hypothalamus (Kahn et al., 2005). In addition, AMPK now seems to control non-metabolic processes such as cell growth, autophagy and cytoskeleton reorganization.

1.5.2 Heterotrimeric Structure and expression

AMPK is a heterotrimeric Ser/Thr protein kinase, consisting of a catalytic α subunit and two regulatory β and γ subunits. AMPK subunit isoforms are encoded by distinct genes with two α subunits (Stapleton et al., 1996), two β subunits (Chen et al., 1999; Thornton et al., 1997) and three γ subunits (Cheung et al., 2000). Additionally, the gene encoding for the γ2 and γ3 subunits allow for alternative splicing, further increasing the subunit variety and generating a theoretical combination of at least 20 different heterotrimeric isoforms. However, it is unclear if all combinations occur *in vivo*. All three subunits present a characteristic domain structure. The catalytic α subunit comprises an N-terminal kinase domain followed by an autoinhibitory sequence (AIS) and a subunit interacting domain that binds β subunit. The β subunit contains two characterized elements, a glycogen binding domain (GBD) mediating AMPK association with glycogen (Hudson et al., 2003; Polekhina et al., 2003) and a C-terminal containing the binding sequence responsible for α and γ binding (α γ-SBS) (Iseli et al., 2005), in addition, the β-subunit presents a consensus sequence for myristoylation at the N-terminal. The γ subunit reveals four tandem repeat sequences called CBS motifs, and the β–binding region located N-terminal to the first CBS domain (Viana et al., 2007). The CBS motifs are functionally organized in two pairs, called Bateman domains, known to bind ATP or AMP in an exclusive manner (Adams et al., 2004) (Figure 1-9)..

AMPK subunits show differential tissue-specific expression and activation. In rat, AMPK α1 is evenly expressed in heart, liver, kidney, brain, spleen, lung and skeletal muscle, whereas AMPK α2 is highly abundant in skeletal muscle and to lesser extent in heart, liver, brain and kidney and detectable in lung (Stapleton et al., 1996). The β1 subunit shows a similar widespread expression profile as α1, whereas β2 is highly expressed in skeletal muscle and heart and to lesser extent in brain, placenta, liver and pancreas (Thornton et al., 1997). The γ1 and γ2 isoforms are ubiquitously expressed whereas γ3 expression seems to be limited to skeletal muscle. The expression profile of the different subunits let to the conclusion that AMPK α1β1γ1 is probably the predominant complex in most cell types.

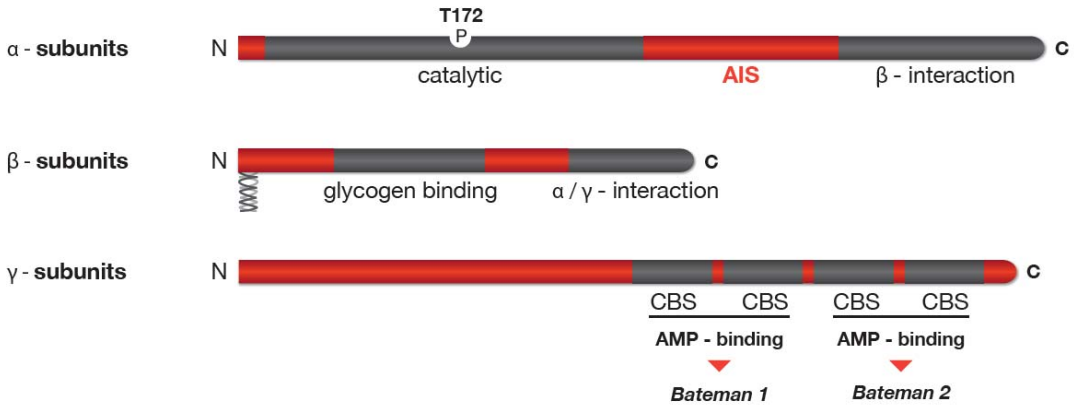

Figure 1-9. Domain structure of mammalian AMPK. Schematic representation of the domain structure of the three AMPK subunits. Isoforms exist for each subunit, with α1/α2 and β1/β2 being very homologous pairs, while the γ-subunit isoforms (γ1-3) and their splice variants (γ2/γ3 long and short) differ at their N-terminus. The α-subunit contains the Thr172 residue that must be phosphorylated (P) by upstram kinases for activity and an autoinhibitory sequence domain (AIS) that inhibits the activity of the kinase domain. The C-terminal domain is required for binding the β- subunit. The β-subunits contains central glycogen-binding domains and C-terminal domain that is required for binding the α- and γ subunits. In addition, β-subunits present a consensus sequence for myrostoylation at the N-terminus. The three γ-subunit isoforms have variable N-terminal domains and four conserved cystathionine beta-synthase motifs (CBS1–4). The CBS motifs act in pairs to form two Bateman domains that bind ATP or AMP in an exclusive manner.

1.6. AMPK regulation

1.6.1. Molecular regulation

Regulation by phosphorylation

AMPK is activated in response to an increase in the ratio of AMP to ATP within the cell and therefore acts as an efficient sensor for cellular energy state. However, the most critical step for activation of AMPK is phosphorylation of threonine 172 in the kinase domain of the α subunit (Hawley et al., 1996). Additional phosphorylation sites on the α and β subunits have been reported with possible effects on AMPK activity (Mitchelhill et al., 1997; Woods et al., 2003). Two major upstream kinases have been described to phosphorylate AMPK in vivo, namely LKB1 (Hawley et al., 2003) and Ca^{2+}/calmodulin-dependent kinase kinase, especially the β isoform (CaMKKβ) (Hawley et al., 2005; Hurley et al., 2005). LKB1 is a serine/threonine kinase with a tumor suppressor function. The active form of LKB1 is a heterotrimeric complex with the pseudokinase STRAD and the scaffolding protein MO25, both of which exist as two different isoforms, α and β. The association with STRAD and MO25 proteins is essential for the kinase activity of LKB1 (Boudeau et al., 2004). Mice lacking LKB1 develop hepatocellular carcinomas that are associated with loss of LKB1 expression (Nakau et al., 2002). Thus, the involvement of LKB1 in the regulation of energy metabolism by activation of AMPK suggests a possible connection between AMPK and cancer (Luo et al., 2005; Motoshima et al., 2006).

CaMKKβ and, to a lesser extent, CaMKKα are the second well-established upstream kinases capable of phosphorylation and activation of AMPK in a Ca^{2+} dependent manner. CaMKKs are activated by the complex Ca^{2+}-calmudulin (CaM) which is formed in response to elevated Ca^{2+} levels. The tissue distribution of CaMKKs, with high levels in brain, suggests that may play an important role in the nervous system. However, it has been reported that CaMKK mediates both thrombin and bradykinin-dependent AMPK activation and stimulation of fatty acid oxidation in endothelial cell (Stahmann et al., 2006). Similary, CaMKK also mediates receptor T cell activation (Tamas et al., 2006). In both cases this appeared to involve the Ca^{2+}-CaMKK-AMPK pathway in response to the increase energy turnover which usually accompanies Ca^{2+} release in certain cell types. The transforming growth factor (TGF)-β-activated kinase-1 (TAK1) was recently identified as a third possible upstream kinase of AMPK. Although strong evidence for a direct phosphorylation and activation of AMPK by TAK1 in vitro and in cell culture exist (Momcilovic et al., 2006) an alternative indirect regulation mechanism via LKB1 was proposed (Xie et al., 2006), thus the role of TAK1 in the AMPK system therefore remains uncertain. In addition, AMPK is also a direct target of Akt and PKA, which appear to phosphorylated the same sites on the catalytic subunit, i.e., α1 Ser485 (or α2Ser491) resulting in a negative regulation of AMPK (Horman et al., 2006; Hurley et al., 2006; Kovacic et al., 2003). Interestingly, phosphorylation of this site, also may be catalyzed by AMPK itself in an autophosphorylation reaction, appears to reduce the accessibility of Thr172 to upstream kinase.

AMPK activity also demands an effective negative control mechanism, which is the dephosphorylation of Thr172 by the protein phosphatase 2Cα (PP2Cα) (Davies et al., 1995). Regulation of this dephosphorylation has emerged as one mechanism by which dephosphorylation is controlled by AMP binding to γ subunit, making AMPK a better substrate for phosphorylation by upstream kinases and repressing dephosphorylation by PP2Cα (Sanders et al., 2007; Suter et al., 2006). In addition, the observed conformational change upon AMP binding also allosterically stimulates AMPK activity (Riek et al., 2008; Suter et al., 2006).

Allosteric regulation

As its name implies, AMPK is stimulated by elevated levels of AMP. This nucleotide acts a a sort of second messenger, since its concentration dramatically increases secondary to a fall in ATP concentration due to the adenylate kinase (AK) reaction. This important metabolic enzyme catalyses the reaction that converts 2 molecules of ADP to ATP + AMP (see section 3). AMP binds to the regulatory γ-subunit of AMPK, which contains two tandem Bateman domains, each of which binds one molecule of AMP or ATP (in a mutually exclusive manner). In the γ2 isoform, which is expressed at particularly high levels in cardiac muscle, several dominant-acting mutations are associated with heart diseases involving, cardiac hypertrophy, contractile dysfunction and arrhythmias. These mutations have been found to impair both the binding of AMP to the Bateman domains and the activation of the heterotrimeric complex by AMP (Burwinkel et al., 2005; Scott et al., 2004), proving that the Bateman domains represent the regulatory nucleotide-binding sites of the complex.

1.6.2. Cellular regulation

AMPK is activated by any stress that depletes cellular ATP, such as heat shock and metabolic poisons in hepatocytes (Corton et al., 1995; Shaw et al., 2005), exercise in skeletal muscle (Sakamoto et al., 2005; Winder and Hardie, 1996), ischemia (Marsin et al., 2000; Sakamoto et al., 2006), oxidative stress, hypoxia, or nutrient deprivation (Kahn et al., 2005; Salt et al., 1998). All these can be regarded as pathological stresses that interfere with ATP production. In addition, a physiological stress that activates AMPK by increasing ATP consumption is exercise during muscular contraction (Vavvas et al., 1997; Winder and Hardie, 1996).

The primary role of the AMPK orthologue in yeast is in response to glucose starvation. In cultured cells from mammals and Drosophila, AMPK is also activated by glucose deprivation; so this seems to have been an ancient role for the system. In mammals, AMPK acts as a fuel sensor in the hypothalamus and responds to a variety of metabolic and nutrients factors. Under fasting conditions hypothalamic AMPK activity is increased promoting food intake, in contrast, hyperglycemia and refeeding inhibit AMPK activity in the hypothalamus (Minokoshi et al., 2004). Hypothalamic AMPK activity is regulated by anorexigenic and orexigenic hormones such as leptin or ghrelin. Leptin inhibits hypothalamic AMPK activity repressing food intake, whereas is activated by ghrelin, a gut hormone that stimulates food intake (Nakazato et al., 2001). However, leptin's effects on metabolism are not limited to the hypothalamus as almost all tissues examined express leptin receptors. Leptin acts directly in isolated skeletal muscle to increase fatty acid oxidation and glucose uptake in an AMPK-dependent manner, and this process appears to involve an increase in the AMP/ATP ratio (Minokoshi et al., 2002). Future studies are required to delineate the upstream pathways mediating the effects of leptin on AMPK signaling and to understand how leptin mediates opposite effects on AMPK, activating in muscles but suppressing in hypothalamus. Adiponectin is another adipokine such as leptin, which actives AMPK and stimulates fatty acid oxidation and glucose uptake in skeletal muscle (Tomas et al., 2002; Yamauchi et al., 2002) and adipose tissue (Wu et al., 2003). The metabolic effects of adiponectin also involve the suppression of hepatic glucose output, an effect which is dependent on the activation of AMPK. Recently, it was found that adiponectin increase appetite via activation of AMPK in the hypothalamus (Kubota et al., 2007). Importantly, activation of hypothalamic AMPK by adiponectin reduces leptin sensitivity, suggesting that through their central action leptin and adiponectin have opposite roles but when acting in concert these two adipokines work to maintain fat level/energy stores through modulation of hypothalamic AMPK signaling (Steinberg and Kemp, 2007).

1.6.3. Pharmacological activation

Chemical compounds used to study AMPK activation *in vivo* include indirect or direct inhibitors of ATP synthesis like hydrogen peroxide, 2-deoxyglucose, oligomycin or dinitrophenol, and AMP mimics like 5-aminoimidazole-4-carboxyamide riboside (AICAR). AICAR is metabolized by the cell

and converted to inosine monophosphate (ZMP) which mimics the effects of AMP and activates AMPK by direct allosteric activation (Fryer et al., 2002).

Efforts to develop pharmacological activators of AMPK to treat the metabolic syndrome (see section 8.1) have gained momentum after metformin, the most widely prescribed anti-diabetic drug since decades, shown to activate AMPK (Musi et al., 2002). Metformin actives AMPK by inhibition of complex I of the respiratory chain (El-Mir et al., 2000), leading to an increase in intracellular AMP (Hawley et al., 2010). Possibly, many synthetic and natural compounds that positively affect the metabolic syndrome act on mitochondria and inhibition of respiration, e.g. galegine, troglitazone, phenobarbital, resveratrol, and berberine (Hawley et al., 2010). Recently, a novel AMPK synthetic activator A-769662 has been developped by Abbott laboratories. A-769662 is a cell-permeable activator which directly binds close to the GBD of the β-subunit thus activating AMPK in a specific manner (Goransson et al., 2007).

Another way to activate AMPK in the cell is an increase in Ca^{2+}-levels, e.g. via the the Ca^{2+} ionophore A23187, which activated AMPK via the CamKK upstream kinases (Goransson et al., 2007; Hawley et al., 2010). Figure 1-10 summarize the principal AMPK activation and regulation processes.

1.7. AMPK downstream signaling

Upon activation by upstream kinases, AMPK inhibits energy-consuming pathways such as glycogenesis, gluconeogenesis, fatty acid and cholesterol synthesis by direct phosphorylation of the enzymes controlling these pathways. At the same time, AMPK stimulates catabolic pathways to recruit substrates for ATP generation, and thus to sustain cellular energy balance. These effects on metabolic key enzymes are achieved through direct activatory or inhibitory phosphorylation or through changes in their gene expression levels by affecting transcription factors.

1.7.1. AMPK regulation of carbohydrate metabolism

The uptake of glucose across the plasma membrane is dependent on the glucose gradient as well as the expression of transmembrane proteins known as GLUTs (glucose transporter). In many tissues including skeletal muscle, GLUT4 is translocated to the plasma membrane for the uptake of glucose in response to stimuli such muscle contraction. AMPK facilitates translocation of GLUT4 to the plasma membrane through phosphorylation of Rab GTPases TBC1D1 and TBC1D4 (AS160) (Kane et al., 2002; Zeigerer et al., 2004). At the transcriptional level, AMPK regulates GLUT4 expression by phosphorylation of both peroxisome proliferator-activated receptor gamma co-activator-1 alpha (PGC-1α) and histone deacetylase (HDAC) 5, which both promote myocyte enhancer factor (MEF) dependent transcription, resulting in enhanced GLUT4 promoter activity (Jager et al., 2007; McGee et al., 2008).

AMPK then also increases the rate of glycolysis through phosphorylation of 6-phosphofructosekinase-2 (PFK2) at Ser-466 (Marsin et al., 2000), leading to higher ATP production. Via PGC-1α, AMPK also promotes the expression of mitochondrial oxidative proteins and thus oxidative ATP production (Winder et al., 2000; Wu et al., 1999).

Glucose levels are also affected by glycogen metabolism. The absolute level of glycogen is a function of both its production (glycogenesis) and its breakdown (glycogenolysis), which are mediated by the enzymes glycogen synthase (GS) and glycogen phosphorylase (GP), respectively. AMPK inhibits glycogenesis by direct phosphorylation of glycogen synthase at an inhibitory site of the enzyme (Young et al., 1996). Recently, it was demonstrated that AMPK also phosphorylates the glycogen targeting subunit R5/PTG of the type 1 protein phosphatase (PP1) (Vernia et al., 2009). R5/PTG phosphorylation inhibits the dephosphorylation of both, GS (supporting its inhibition) and GP (supporting its activation), thus decreasing glycogen synthesis.

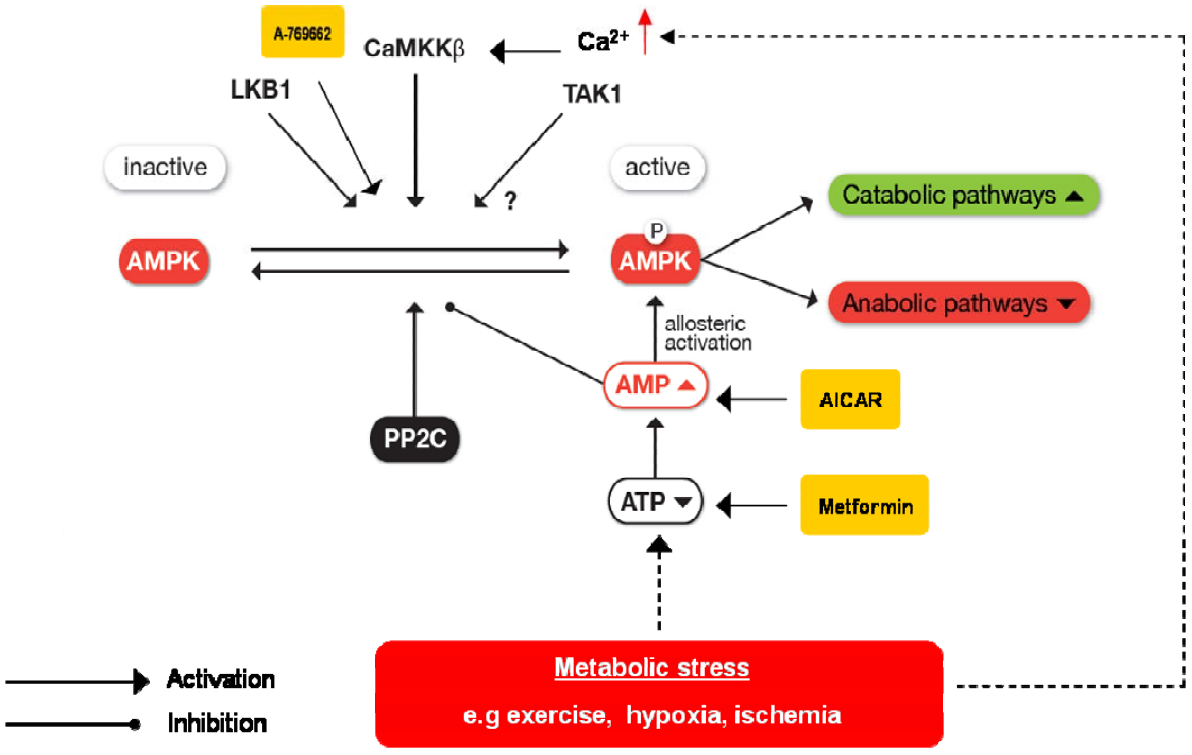

Figure 1-10. AMPK activation and regulation. AMPK is activated in response to metabolic stress, e.g exercise, ischemia, hypoxya. AMPK also response to stimuli by chemical compounds. Three upstream kinases, the tumor suppressor kinase LKB1, Ca^{2+}/Calmodulin-dependent kinase kinase (CaMKKβ) and transforming growth factor –activated kinase 1(TAK1), are known to phosphorylate AMPK at the main site Thr-172 *in vitro*. At least CaMKKβ and LKB1 reportedly regulate AMPK *in vivo*. Once phosphorylated, AMPK activity is further increased allosterically by AMP binding, which simultaneously prevents dephosphorylation and inactivation by PP2C. Active AMPK helps to restore cellular energy balance during times of energy stress through activation of catabolism and inhibition of anabolism pathways.

Another mechanism to maintain the glucose homeostasis is the gluconeogenesis. AMPK negatively regulates the transcription of the gluconeogenic enzymes L-type pyruvate kinase (L-PK) (Leclerc et al., 1998), phosphoenol-pyruvate carboxylase (PEPCK) (Lochhead et al., 2000) and

glucose-6—phosphatase (G-6-Pase) (Woods et al., 2000) in response to elevated glucose. L-PK and another genes involved in glucose and lipid metabolism, is regulated by the transcription factor 4α (HNF-4α) (Miquerol et al., 1994). AMPK phosphorylates HNF-4α, reducing the ability of the transcription factor to form the homodimers required for stability and DNA binding (Hong et al., 2003). CREB-regulated transcription fractor (CRTC2) has emerged as a critical regulator of gluconeogenesis (Koo et al., 2005). Under fasting conditions, glucagon triggers the transcription of gluconeogenic genes via the cAMP-responsive factor CREB (CRE binding protein) and subsequent recruitment of the co-activator CRTC2. This recruitment leads to the expression of PGC-1α, which in turn drives the transcription of PEPCK and G-6-Pase. CRTC2 phosphorylation by AMPK prevents the translocation of CRTC2 the nucleus, thereby reducing CREB-dependent mRNA expression of PEPCK and G-6-Pase (Koo et al., 2005). Figure 1-11 summarizes the function of AMPK in the regulation of glucose uptake, glycolysis and glycogen metabolism.

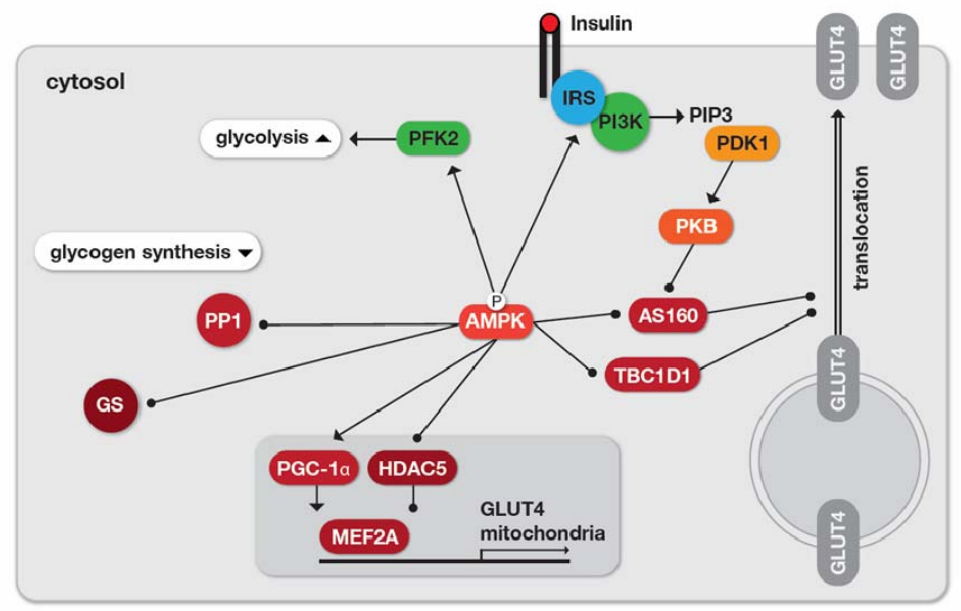

Figure 1-11. Regulation of glucose uptake, glycolysis and glycogen synthesis by AMPK. For increasing the cellular glucose uptake, AMPK phosphorylates the Rab GTPase activating proteins TBC1D4 (AS160) and TBC1D1, which reduces their association with vesicles thus enhancing GLUT4 translocation. Similarity, insulin-dependent glucose uptake is facilitated by Akt/PKB-mediated AS160 phosphorylation that, however, requires the upstream signaling cascade via IRS-1 and phosphoinositide 3-kinase (PI3K) capable of generating phosphotidylinositol 3-phosphate (PIP3), which subsequently activates 3- phosphoinositide dependent protein kinase-1 (PDK1). IRS-1 is also a direct substrate of AMPK. On the transcriptional level, expression of GLUT4 and mitochondrial proteins, is increased by phosphorylation of the transcriptional coactivator PGC1α and the histone deacetylase HDAC5, the latter is sequestered out of the nucleus in response to the phosphorylation. The rate of glycolysis is increased through activation of PFK2, whereas glycogen synthesis is inhibited by direct inhibition of glycogen synthase (GS) or by preventing glycogen association of protein phosphatase 1 (PP1). Adapted from (Steinberg and Kemp, 2009).

1.7.2. AMPK regulation of lipid metabolism

During fasting, post-absorptive conditioned lipids are the predominant substrate for the maintenance of whole body energy metabolism (Kiens, 2006). The first step in the regulation of fatty acid (FA) metabolism involves their movement across the plasma membrane. FAs enter the cell either via passive diffusion across the plasma membrane via flip-flop mechanism or via fatty acid translocase (FAT/CD36) and fatty acid binding protein (FABP) (Luiken et al., 2004). Acetyl-CoA carboxylase (ACC) is the major enzyme in the regulation of fatty acid oxidation and synthesis. ACC catalyzes the carboxylation of acetyl CoA to malonyl CoA, a metabolic intermediate during fatty acids synthesis. ACC exists in two isoforms (Abu-Elheiga et al., 1995), ACC1 and ACC2 which differ in their subcellular localization and tissue distribution (Abu-Elheiga et al., 2000). Malonyl CoA synthesized in the cytosol by ACC1 is incorporated into fatty acids synthesis by fatty acid synthase although malonyl CoA synthesized in mitochondria acts allosterically to inhibit carnitine palmitoyltransferase 1 (CPT1), which controls transport of activated fatty acids into mitochondria for oxidation. Regulation of ACC is achieved by reversible phosphorylation by AMPK, being the Ser79 (ACC1) or Ser221 (ACC2) the major sites responsible for the inhibition of ACC activity and therefore suppressing fatty acid synthesis and increasing mitochondrial β–oxidation (Munday, 2002) (Figure 1-12).

Hormone-sensitive lipase (HSL) is important for the degradation of triacylglycerol (TG) in adipose and muscle tissue. HSL is known to be activated by PKA phosphorylation at serines 563, 659, and 660 (Anthonsen et al., 1998) but activation of AMPK in adipocytes and skeletal muscle suggested that AMPK inhibits this activation through phosphorylation at Ser-565 (Watt et al., 2006). AMPK also appears to negatively regulate HSL activity during muscle contraction. In both resting and contraction muscle, TG hydrolysis is suppressed in response to AMPK activation by HMGR (3-hydroxy-3methylglutaryl-CoA reductase) which is the rate-limiting enzyme for isoprenoid and cholesterol synthesis and a substrate for AMPK. The catalytic activity of HMGR is inhibited by phosphorylation on Ser-872 by AMPK thus inhibiting cholesterol synthesis.

1.7.3. AMPK regulation of protein metabolism, cell proliferation and other pathways

Protein synthesis accounts for around 20% of energy turnover in growing cells, inhibition of this pathway is therefore an important mechanism by which to maintain cellular ATP under metabolic stress. AMPK inhibits protein synthesis at multiple levels; peptide elongation, peptide translation and ribosome biogenesis (Figure 1-13). It phosphoryles and actives eukaryote elongation factor 2 kinase (eEF2K) on Ser-398, which in turn phosphorylates eEF2 and inhibits protein synthesis (Browne et al., 2004). It also inhibits the mammalian target of rapacycin complex (mTORC) pathway. This pathway is regulated through phosphorylation of tuberous sclerosis 2 (TSC2) (Inoki et al., 2003), a GTPase-activating protein controlling the ability of the small GTPase Rheb to activate mTOR. Additionally, mTORC activation is also inhibited by AMPK-mediated phosphorylation of mTOR binding partner Raptor causing inactivation of the mTOR complex (Gwinn et al., 2008) and by direct phosphorylation of mTOR (Cheng et al., 2004)(Figure 1-13). Another mechanism by which AMPK activation affects

the expression of proteins is through effects on mRNA stability. AMPK activation reduces the cytoplasmic level of the RNA-binding protein HuR, which stabilizes specific mRNAs in the cytoplasm by binding to their 3'-untranslated regions (Wang et al., 2002). Target mRNAs for HuR include proteins that regulated the cell cycle, such as cyclin A and cyclin B1. Additional studies also implicate AMPK in the regulation of transcriptional factor and coactivators, which might regulate cell growth and proliferation, especially in cancer. AMPK phosphorylates and increase the accumulation of the tumor suppressor p53 and of the cyclin-dependent kinase inhibitors p27kip1, both contributing to cell cycle arrest (Imamura et al., 2001; Jones et al., 2005; Rattan et al., 2005). AMPK has also been shown *in vitro* to phosphorylate the transcriptional coactivator p300, reducing its affinity for nuclear receptors (Yang et al., 2001). The physiological significance of p300 phosphorylation by AMPK is still unknown; however, this event has the ability to influence transcription levels of a large set of genes, which may be critical for regulating cell growth and survival and may therefore be important under a number of conditions including cancer cell proliferation.

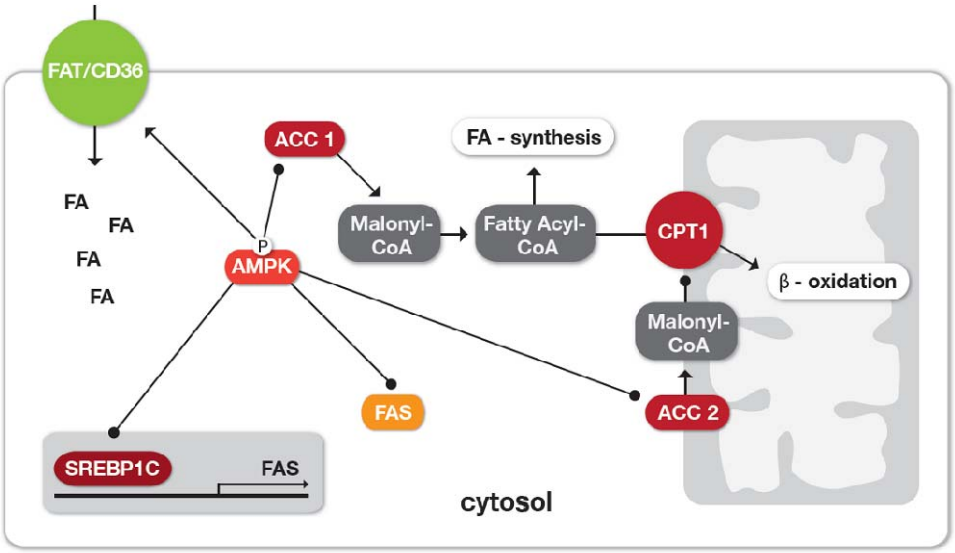

Figure 1-12. Role of AMPK in lipid metabolism. AMPK promotes the fatty acid uptake by inducing FAT/CD36 translocation to the plasma membrane. Through inactivation of ACC-1 and ACC-2 the concentration of malonyl-CoA is reduced, thereby promoting mitochondrial β-oxidation and simultaneously inhibiting fatty acid synthesis. The synthesis of fatty acids is further reduced by inhibition of FAS and downregulation of lipogenic gene transcription via phosphorylation of SREBP1C. However, the AMPK-dependent regulation of FAT/CD36, FAS and SREBP1C may be indirect. The exact mechanisms of control remain elusive. Adapted from (Steinberg and Kemp, 2009).

In addition to protein metabolism and cell cycle progression, AMPK is also implicated in the maintaining of cell membrane potential and intracellular ion homeostasis. Recently, different ion transporters seem to be regulated by AMPK. These include, cystic fibrosis transmembrane conductance regulator Cl^- channel (CFTR) (King et al., 2009), ATP-sensitive potassium (K_{ATP}) channel (Chang et al., 2009), and epithelial Na+ channel (eNaC) (Carattino et al., 2005) which are inhibited by AMPK whereas Na^+-K^+-$2Cl^-$ cotransporter (NKCC2) seems to be activated. Recently,

AMPK activity has also been reported to stimulate the sarcoplasmic/endoplasmic reticulum calcium ATPase by preventing its oxydation (Dong et al., 2010).

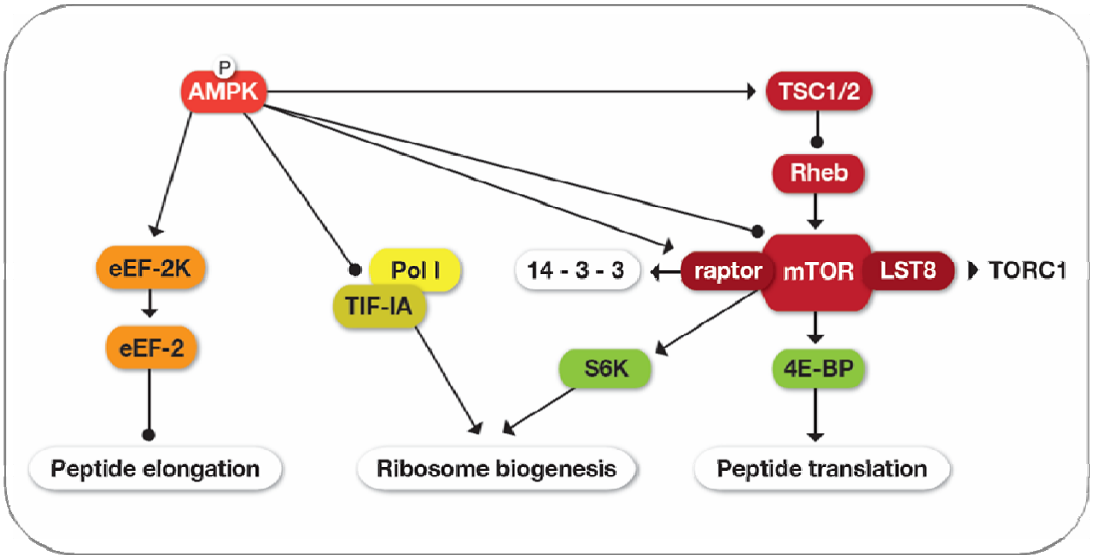

Figure 1-13. Role of AMPK in protein metabolism. AMPK inhibits mTOR signaling by different mechanism. AMPK inhibits TORC1 complex by phosphorylating the tumor suppressor complex TSC1/TSC2, which negatively regulates TORC1 by inactivating the GTPase Rheb. TORC1 activity is also impaired through phosphorylation of Raptor, which leads to 14-3-3 binding and physical separation of the TORC1 complex. Also, direct inhibitory phosphorylation of mTOR by AMPK has been described. Inhibition of TORC activity reduces protein synthesis by inhibition of protein translation and reduced ribosomal biogenesis. In addition, AMPK impairs the transcription of ribosomal RNA through phsophorylation of the transcription factor TIF-IA. Finally, peptide elongation is prevented by activation of eEF-2 kinase which in turn inactivates eEF-2. Adapted from (Steinberg and Kemp, 2009).

1.8. AMPK Role of AMPK in human physiopathology

1.8.1. AMPK and the metabolic syndrome

Obesity is associated with a number of health problems that are often summarized as the metabolic syndrome. These include insulin resistance, type 2 diabetes, cardiovascular disease and fatty liver disease. Currently more than 170 million patients suffer of type 2 diabetes, and this figure is expected to double by 2030 in line with the increasing obesity (Farag and Gaballa, 2010). Type 2 diabetes is characterized by insulin resistance and high blood glucose due to impaired cellular glucose uptake. As outlined above, AMPK is a major kinase regulating both lipid and glucose metabolism, the principal processes impaired in diabetes and obesity (Viollet et al., 2007). In rodents, many (but not all) disorders that are associated with insulin resistance are accompanied by decreases in AMPK activity and several abnormalities in the mentioned metabolic pathways. Studies with AICAR reveled that AMPK activation increased glucose uptake and fatty oxidation in obese diabetic rodents, suggesting a therapeutic potential of AMPK activators to treat type 2 diabetes (Winder and Hardie, 1999). Interest in AMPK as a therapeutic target for the treatment of metabolic syndrome increased after AMPK was shown to be activated by metformin (Musi et al., 2002) and to be responsible to the beneficial effects of metformin at least in liver (Shaw et al., 2005). Metformin is an orally applied bioguanidine that reduces plasma glucose and lipids and improves insulin sensitivity in patients with

type 2 diabetes. Metformin-activation of AMPK is dependent on cellular uptake by the organic cation transporter (OCT1). This leads to a preferential accumulation of metformin in liver, mild inhibition of mitochondrial complex 1 and increased AMP/ATP ratios that activate AMPK. To circumvent such an indirect mechanism, several pharmaceutical companies currently try to develop direct activators of AMPK

1.8.2. AMPK and cancer

AMPK is likely to be involved in cancer signaling as well, mainly due to the tumor suppressor properties of its upstream kinase LKB1 and the downstream link to mTOR signaling, controlling and cell proliferation (Hardie, 2005). LKB1, found to be mutated in patients with inheritable Peutz-Jeghers syndrome and in sporadic lung tumors. The mechanism by which LKB1 suppresses tumorigenesis is unclear but in part at least, appears to be mediated by inhibition of mTOR. Recently studies demonstrate that activation of AMPK inhibits protein synthesis by phosphorylating several important regulators (Inoki et al., 2003) (see section 7.3). Thus, at least some effects important for the tumor suppressor function of LKB1 are mediated by activated AMPK. Recently, studies have revealed a reduced incidence of cancer in diabetic patients on metformin therapy (Libby et al., 2009). Authors have proposed that metformin activates AMPK by inhibiting mitochondrial respiration and increasing 5′-AMP, which enhances activation of AMPK by LKB1 (Hardie, 2007), thus the anticancer properties of metformin are likely to be mediated by AMPK's ability to preserve cellular energy levels by phosphorylating proteins such as p27KIP and TSC2 that lead to inhibition of cell growth and proliferation signaling networks (Carling, 2007; Inoki et al., 2003). In addition, activation of AMPK by AICAR treatment of the breast cancer cell line MDA-MB-231 blocks proliferation and colony formation in culture as well as reducing tumor growth in nude mice (Swinnen et al., 2005). Metformin has also been shown to act as a growth inhibitor of MCF7 breast cancer cells, an effect dependent on the presence of AMPK. The growth inhibition was associated with decreased mTOR activation (Zakikhani et al., 2006). The growth suppressor effects were specific, as shown by the fact that HeLa cells, which are deficient in LKB1, were unaffected by the metformin treatment.

1.8.3. AMPK mutation in human pathology

Mutations in the AMPK γ2 subunit, expressed at particularly high levels in the heart, impairs AMP binding and thus AMP-dependent AMPK activation (Burwinkel et al., 2005; Scott et al., 2004). However, AMPK carrying these mutations shows low levels of endogenous, constitutive activity. These mutations are associated with heart disease of varying degree of severity, involving cardiac hypertrophy, contractile dysfunction and arrhythmias. The major cause of AMPK related heart disease is the accumulation of glycogen in cardiac myocytes due to the increased basal AMPK activity that impairs heart muscle development and intercellular signal transduction (Burwinkel et al., 2005).

1.9. References

Abu-Elheiga, L., W.R. Brinkley, L. Zhong, S.S. Chirala, G. Woldegiorgis, and S.J. Wakil. 2000. The subcellular localization of acetyl-CoA carboxylase 2. *Proc Natl Acad Sci U S A*. 97:1444-9.

Abu-Elheiga, L., A. Jayakumar, A. Baldini, S.S. Chirala, and S.J. Wakil. 1995. Human acetyl-CoA carboxylase: characterization, molecular cloning, and evidence for two isoforms. *Proc Natl Acad Sci U S A*. 92:4011-5.

Adams, J., Z.P. Chen, B.J. Van Denderen, C.J. Morton, M.W. Parker, L.A. Witters, D. Stapleton, and B.E. Kemp. 2004. Intrasteric control of AMPK via the gamma1 subunit AMP allosteric regulatory site. *Protein Sci*. 13:155-65.

Adcock, K.H., J. Nedelcu, T. Loenneker, E. Martin, T. Wallimann, and B.P. Wagner. 2002. Neuroprotection of creatine supplementation in neonatal rats with transient cerebral hypoxia-ischemia. *Dev Neurosci*. 24:382-8.

Almeida, L.S., G.S. Salomons, F. Hogenboom, C. Jakobs, and A.N. Schoffelmeer. 2006. Exocytotic release of creatine in rat brain. *Synapse*. 60:118-23.

Anthonsen, M.W., L. Ronnstrand, C. Wernstedt, E. Degerman, and C. Holm. 1998. Identification of novel phosphorylation sites in hormone-sensitive lipase that are phosphorylated in response to isoproterenol and govern activation properties in vitro. *J Biol Chem*. 273:215-21.

Biermans, W., I. Bernaert, M. De Bie, B. Nijs, and W. Jacob. 1989. Ultrastructural localisation of creatine kinase activity in the contact sites between inner and outer mitochondrial membranes of rat myocardium. *Biochim Biophys Acta*. 974:74-80.

Boldogh, I.R., L.A. Pon, M.P. Sheetz, and K.J. De Vos. 2007. Cell-free assays for mitochondria-cytoskeleton interactions. *Methods Cell Biol*. 80:683-706.

Bonz, A.W., S. Kniesch, U. Hofmann, S. Kullmer, L. Bauer, H. Wagner, G. Ertl, and M. Spindler. 2002. Functional properties and [Ca(2+)](i) metabolism of creatine kinase--KO mice myocardium. *Biochem Biophys Res Commun*. 298:163-8.

Boudeau, J., J.W. Scott, N. Resta, M. Deak, A. Kieloch, D. Komander, D.G. Hardie, A.R. Prescott, D.M. van Aalten, and D.R. Alessi. 2004. Analysis of the LKB1-STRAD-MO25 complex. *J Cell Sci*. 117:6365-75.

Braissant, O., E. Beard, C. Torrent, and H. Henry. 2010. Dissociation of AGAT, GAMT and SLC6A8 in CNS: relevance to creatine deficiency syndromes. *Neurobiol Dis*. 37:423-33.

Braissant, O., H. Henry, M. Loup, B. Eilers, and C. Bachmann. 2001. Endogenous synthesis and transport of creatine in the rat brain: an in situ hybridization study. *Brain Res Mol Brain Res*. 86:193-201.

Braissant, O., H. Henry, A.M. Villard, O. Speer, T. Wallimann, and C. Bachmann. 2005. Creatine synthesis and transport during rat embryogenesis: spatiotemporal expression of AGAT, GAMT and CT1. *BMC Dev Biol*. 5:9.

Brdiczka, D., and T. Wallimann. 1994. The importance of the outer mitochondrial compartment in regulation of energy metabolism. *Mol Cell Biochem*. 133-134:69-83.

Browne, G.J., S.G. Finn, and C.G. Proud. 2004. Stimulation of the AMP-activated protein kinase leads to activation of eukaryotic elongation factor 2 kinase and to its phosphorylation at a novel site, serine 398. *J Biol Chem*. 279:12220-31.

Burklen, T.S., A. Hirschy, and T. Wallimann. 2007. Brain-type creatine kinase BB-CK interacts with the Golgi Matrix Protein GM130 in early prophase. *Mol Cell Biochem*. 297:53-64.

Burwinkel, B., J.W. Scott, C. Buhrer, F.K. van Landeghem, G.F. Cox, C.J. Wilson, D. Grahame Hardie, and M.W. Kilimann. 2005. Fatal congenital heart glycogenosis caused by a recurrent activating R531Q

mutation in the gamma 2-subunit of AMP-activated protein kinase (PRKAG2), not by phosphorylase kinase deficiency. *Am J Hum Genet*. 76:1034-49.

Carattino, M.D., R.S. Edinger, H.J. Grieser, R. Wise, D. Neumann, U. Schlattner, J.P. Johnson, T.R. Kleyman, and K.R. Hallows. 2005. Epithelial sodium channel inhibition by AMP-activated protein kinase in oocytes and polarized renal epithelial cells. *J Biol Chem*. 280:17608-16.

Carling, D. 2004. The AMP-activated protein kinase cascade--a unifying system for energy control. *Trends Biochem Sci*. 29:18-24.

Carling, D. 2007. The role of the AMP-activated protein kinase in the regulation of energy homeostasis. *Novartis Found Symp*. 286:72-81; discussion 81-5, 162-3, 196-203.

Chang, T.J., W.P. Chen, C. Yang, P.H. Lu, Y.C. Liang, M.J. Su, S.C. Lee, and L.M. Chuang. 2009. Serine-385 phosphorylation of inwardly rectifying K+ channel subunit (Kir6.2) by AMP-dependent protein kinase plays a key role in rosiglitazone-induced closure of the K(ATP) channel and insulin secretion in rats. *Diabetologia*. 52:1112-21.

Chen, Z., J. Heierhorst, R.J. Mann, K.I. Mitchelhill, B.J. Michell, L.A. Witters, G.S. Lynch, B.E. Kemp, and D. Stapleton. 1999. Expression of the AMP-activated protein kinase beta1 and beta2 subunits in skeletal muscle. *FEBS Lett*. 460:343-8.

Cheng, S.W., L.G. Fryer, D. Carling, and P.R. Shepherd. 2004. Thr2446 is a novel mammalian target of rapamycin (mTOR) phosphorylation site regulated by nutrient status. *J Biol Chem*. 279:15719-22.

Chetlin, R.D., L. Gutmann, M.A. Tarnopolsky, I.H. Ullrich, and R.A. Yeater. 2004. Resistance training exercise and creatine in patients with Charcot-Marie-Tooth disease. *Muscle Nerve*. 30:69-76.

Cheung, P.C., I.P. Salt, S.P. Davies, D.G. Hardie, and D. Carling. 2000. Characterization of AMP-activated protein kinase gamma-subunit isoforms and their role in AMP binding. *Biochem J*. 346 Pt 3:659-69.

Chida, K., K. Kasahara, M. Tsunenaga, Y. Kohno, S. Yamada, S. Ohmi, and T. Kuroki. 1990a. Purification and identification of creatine phosphokinase B as a substrate of protein kinase C in mouse skin in vivo. *Biochem Biophys Res Commun*. 173:351-7.

Chida, K., M. Tsunenaga, K. Kasahara, Y. Kohno, and T. Kuroki. 1990b. Regulation of creatine phosphokinase B activity by protein kinase C. *Biochem Biophys Res Commun*. 173:346-50.

Corton, J.M., J.G. Gillespie, S.A. Hawley, and D.G. Hardie. 1995. 5-aminoimidazole-4-carboxamide ribonucleoside. A specific method for activating AMP-activated protein kinase in intact cells? *Eur J Biochem*. 229:558-65.

Davies, S.P., N.R. Helps, P.T. Cohen, and D.G. Hardie. 1995. 5'-AMP inhibits dephosphorylation, as well as promoting phosphorylation, of the AMP-activated protein kinase. Studies using bacterially expressed human protein phosphatase-2C alpha and native bovine protein phosphatase-2AC. *FEBS Lett*. 377:421-5.

Dong, Y., M. Zhang, B. Liang, Z. Xie, Z. Zhao, S. Asfa, H.C. Choi, and M.H. Zou. 2010. Reduction of AMP-activated protein kinase alpha2 increases endoplasmic reticulum stress and atherosclerosis in vivo. *Circulation*. 121:792-803.

Dzeja, P.P., and A. Terzic. 2003. Phosphotransfer networks and cellular energetics. *J Exp Biol*. 206:2039-47.

Dzeja, P.P., R.J. Zeleznikar, and N.D. Goldberg. 1998. Adenylate kinase: kinetic behavior in intact cells indicates it is integral to multiple cellular processes. *Mol Cell Biochem*. 184:169-82.

Eder, M., K. Fritz-Wolf, W. Kabsch, T. Wallimann, and U. Schlattner. 2000. Crystal structure of human ubiquitous mitochondrial creatine kinase. *Proteins*. 39:216-25.

El-Mir, M.Y., V. Nogueira, E. Fontaine, N. Averet, M. Rigoulet, and X. Leverve. 2000. Dimethylbiguanide inhibits cell respiration via an indirect effect targeted on the respiratory chain complex I. *J Biol Chem*. 275:223-8.

Ellington, W.R., K. Roux, and A.O. Pineda, Jr. 1998. Origin of octameric creatine kinases. *FEBS Lett*. 425:75-8.

Epand, R.F., U. Schlattner, T. Wallimann, M.L. Lacombe, and R.M. Epand. 2007a. Novel lipid transfer property of two mitochondrial proteins that bridge the inner and outer membranes. *Biophys J*. 92:126-37.

Epand, R.F., M. Tokarska-Schlattner, U. Schlattner, T. Wallimann, and R.M. Epand. 2007b. Cardiolipin clusters and membrane domain formation induced by mitochondrial proteins. *J Mol Biol*. 365:968-80.

Farag, Y.M., and M.R. Gaballa. 2010. Diabesity: an overview of a rising epidemic. *Nephrol Dial Transplant*.

Forstner, M., M. Kriechbaum, P. Laggner, and T. Wallimann. 1998. Structural changes of creatine kinase upon substrate binding. *Biophys J*. 75:1016-23.

Forstner, M., A. Muller, M. Stolz, and T. Wallimann. 1997. The active site histidines of creatine kinase. A critical role of His 61 situated on a flexible loop. *Protein Sci*. 6:331-9.

Fritz-Wolf, K., T. Schnyder, T. Wallimann, and W. Kabsch. 1996. Structure of mitochondrial creatine kinase. *Nature*. 381:341-5.

Fryer, L.G., A. Parbu-Patel, and D. Carling. 2002. Protein kinase inhibitors block the stimulation of the AMP-activated protein kinase by 5-amino-4-imidazolecarboxamide riboside. *FEBS Lett*. 531:189-92.

Glitsch, H.G., and A. Tappe. 1993. The Na+/K+ pump of cardiac Purkinje cells is preferentially fuelled by glycolytic ATP production. *Pflugers Arch*. 422:380-5.

Goransson, O., A. McBride, S.A. Hawley, F.A. Ross, N. Shpiro, M. Foretz, B. Viollet, D.G. Hardie, and K. Sakamoto. 2007. Mechanism of action of A-769662, a valuable tool for activation of AMP-activated protein kinase. *J Biol Chem*. 282:32549-60.

Guerrero, M.L., J. Beron, B. Spindler, P. Groscurth, T. Wallimann, and F. Verrey. 1997. Metabolic support of Na+ pump in apically permeabilized A6 kidney cell epithelia: role of creatine kinase. *Am J Physiol*. 272:C697-706.

Guzun, R., N. Timohhina, K. Tepp, C. Monge, T. Kaambre, P. Sikk, A.V. Kuznetsov, C. Pison, and V. Saks. 2009. Regulation of respiration controlled by mitochondrial creatine kinase in permeabilized cardiac cells in situ. Importance of system level properties. *Biochim Biophys Acta*. 1787:1089-105.

Gwinn, D.M., D.B. Shackelford, D.F. Egan, M.M. Mihaylova, A. Mery, D.S. Vasquez, B.E. Turk, and R.J. Shaw. 2008. AMPK phosphorylation of raptor mediates a metabolic checkpoint. *Mol Cell*. 30:214-26.

Hardie, D.G. 2005. New roles for the LKB1-->AMPK pathway. *Curr Opin Cell Biol*. 17:167-73.

Hardie, D.G. 2007. AMP-activated protein kinase as a drug target. *Annu Rev Pharmacol Toxicol*. 47:185-210.

Hawley, S.A., J. Boudeau, J.L. Reid, K.J. Mustard, L. Udd, T.P. Makela, D.R. Alessi, and D.G. Hardie. 2003. Complexes between the LKB1 tumor suppressor, STRAD alpha/beta and MO25 alpha/beta are upstream kinases in the AMP-activated protein kinase cascade. *J Biol*. 2:28.

Hawley, S.A., M. Davison, A. Woods, S.P. Davies, R.K. Beri, D. Carling, and D.G. Hardie. 1996. Characterization of the AMP-activated protein kinase kinase from rat liver and identification of threonine 172 as the major site at which it phosphorylates AMP-activated protein kinase. *J Biol Chem*. 271:27879-87.

Hawley, S.A., D.A. Pan, K.J. Mustard, L. Ross, J. Bain, A.M. Edelman, B.G. Frenguelli, and D.G. Hardie. 2005. Calmodulin-dependent protein kinase kinase-beta is an alternative upstream kinase for AMP-activated protein kinase. *Cell Metab*. 2:9-19.

Hawley, S.A., F.A. Ross, C. Chevtzoff, K.A. Green, A. Evans, S. Fogarty, M.C. Towler, L.J. Brown, O.A. Ogunbayo, A.M. Evans, and D.G. Hardie. 2010. Use of cells expressing gamma subunit variants to identify diverse mechanisms of AMPK activation. *Cell Metab*. 11:554-65.

Hemmer, W., E.M. Furter-Graves, G. Frank, T. Wallimann, and R. Furter. 1995. Autophosphorylation of creatine kinase: characterization and identification of a specifically phosphorylated peptide. *Biochim Biophys Acta*. 1251:81-90.

Hochachka, P.W. 2000. Oxygen, homeostasis, and metabolic regulation. *Adv Exp Med Biol*. 475:311-35.

Hochachka, P.W. 2003. Intracellular convection, homeostasis and metabolic regulation. *J Exp Biol*. 206:2001-9.

Hong, Y.H., U.S. Varanasi, W. Yang, and T. Leff. 2003. AMP-activated protein kinase regulates HNF4alpha transcriptional activity by inhibiting dimer formation and decreasing protein stability. *J Biol Chem*. 278:27495-501.

Horman, S., D. Vertommen, R. Heath, D. Neumann, V. Mouton, A. Woods, U. Schlattner, T. Wallimann, D. Carling, L. Hue, and M.H. Rider. 2006. Insulin antagonizes ischemia-induced Thr172 phosphorylation of AMP-activated protein kinase alpha-subunits in heart via hierarchical phosphorylation of Ser485/491. *J Biol Chem*. 281:5335-40.

Hornemann, T., M. Stolz, and T. Wallimann. 2000. Isoenzyme-specific interaction of muscle-type creatine kinase with the sarcomeric M-line is mediated by NH(2)-terminal lysine charge-clamps. *J Cell Biol*. 149:1225-34.

Hudson, E.R., D.A. Pan, J. James, J.M. Lucocq, S.A. Hawley, K.A. Green, O. Baba, T. Terashima, and D.G. Hardie. 2003. A novel domain in AMP-activated protein kinase causes glycogen storage bodies similar to those seen in hereditary cardiac arrhythmias. *Curr Biol*. 13:861-6.

Hurley, R.L., K.A. Anderson, J.M. Franzone, B.E. Kemp, A.R. Means, and L.A. Witters. 2005. The Ca2+/calmodulin-dependent protein kinase kinases are AMP-activated protein kinase kinases. *J Biol Chem*. 280:29060-6.

Hurley, R.L., L.K. Barre, S.D. Wood, K.A. Anderson, B.E. Kemp, A.R. Means, and L.A. Witters. 2006. Regulation of AMP-activated protein kinase by multisite phosphorylation in response to agents that elevate cellular cAMP. *J Biol Chem*. 281:36662-72.

Imamura, K., T. Ogura, A. Kishimoto, M. Kaminishi, and H. Esumi. 2001. Cell cycle regulation via p53 phosphorylation by a 5'-AMP activated protein kinase activator, 5-aminoimidazole- 4-carboxamide-1-beta-D-ribofuranoside, in a human hepatocellular carcinoma cell line. *Biochem Biophys Res Commun*. 287:562-7.

Ingwall, J.S. 2002. Is creatine kinase a target for AMP-activated protein kinase in the heart? *J Mol Cell Cardiol*. 34:1111-20.

Inoki, K., T. Zhu, and K.L. Guan. 2003. TSC2 mediates cellular energy response to control cell growth and survival. *Cell*. 115:577-90.

Inoue, K., S. Ueno, and A. Fukuda. 2004. Interaction of neuron-specific K+-Cl- cotransporter, KCC2, with brain-type creatine kinase. *FEBS Lett*. 564:131-5.

Inoue, K., J. Yamada, S. Ueno, and A. Fukuda. 2006. Brain-type creatine kinase activates neuron-specific K+-Cl- co-transporter KCC2. *J Neurochem*. 96:598-608.

Iseli, T.J., M. Walter, B.J. van Denderen, F. Katsis, L.A. Witters, B.E. Kemp, B.J. Michell, and D. Stapleton. 2005. AMP-activated protein kinase beta subunit tethers alpha and gamma subunits via its C-terminal sequence (186-270). *J Biol Chem*. 280:13395-400.

Ishiki, M., and A. Klip. 2005. Minireview: recent developments in the regulation of glucose transporter-4 traffic: new signals, locations, and partners. *Endocrinology*. 146:5071-8.

Jacobus, W.E. 1985. Theoretical support for the heart phosphocreatine energy transport shuttle based on the intracellular diffusion limited mobility of ADP. *Biochem Biophys Res Commun*. 133:1035-41.

Jager, S., C. Handschin, J. St-Pierre, and B.M. Spiegelman. 2007. AMP-activated protein kinase (AMPK) action in skeletal muscle via direct phosphorylation of PGC-1alpha. *Proc Natl Acad Sci U S A*. 104:12017-22.

Jones, R.G., D.R. Plas, S. Kubek, M. Buzzai, J. Mu, Y. Xu, M.J. Birnbaum, and C.B. Thompson. 2005. AMP-activated protein kinase induces a p53-dependent metabolic checkpoint. *Mol Cell*. 18:283-93.

Joost, H.G., and B. Thorens. 2001. The extended GLUT-family of sugar/polyol transport facilitators: nomenclature, sequence characteristics, and potential function of its novel members (review). *Mol Membr Biol*. 18:247-56.

Jost, C.R., C.E. Van Der Zee, H.J. In 't Zandt, F. Oerlemans, M. Verheij, F. Streijger, J. Fransen, A. Heerschap, A.R. Cools, and B. Wieringa. 2002. Creatine kinase B-driven energy transfer in the brain is important for habituation and spatial learning behaviour, mossy fibre field size and determination of seizure susceptibility. *Eur J Neurosci*. 15:1692-706.

Kahn, B.B., T. Alquier, D. Carling, and D.G. Hardie. 2005. AMP-activated protein kinase: ancient energy gauge provides clues to modern understanding of metabolism. *Cell Metab*. 1:15-25.

Kaldis, P., R. Furter, and T. Wallimann. 1994. The N-terminal heptapeptide of mitochondrial creatine kinase is important for octamerization. *Biochemistry*. 33:952-9.

Kane, S., H. Sano, S.C. Liu, J.M. Asara, W.S. Lane, C.C. Garner, and G.E. Lienhard. 2002. A method to identify serine kinase substrates. Akt phosphorylates a novel adipocyte protein with a Rab GTPase-activating protein (GAP) domain. *J Biol Chem*. 277:22115-8.

Kiens, B. 2006. Skeletal muscle lipid metabolism in exercise and insulin resistance. *Physiol Rev*. 86:205-43.

King, J.D., Jr., A.C. Fitch, J.K. Lee, J.E. McCane, D.O. Mak, J.K. Foskett, and K.R. Hallows. 2009. AMP-activated protein kinase phosphorylation of the R domain inhibits PKA stimulation of CFTR. *Am J Physiol Cell Physiol*. 297:C94-101.

Koga, Y., H. Takahashi, D. Oikawa, T. Tachibana, D.M. Denbow, and M. Furuse. 2005. Brain creatine functions to attenuate acute stress responses through GABAnergic system in chicks. *Neuroscience*. 132:65-71.

Koo, S.H., L. Flechner, L. Qi, X. Zhang, R.A. Screaton, S. Jeffries, S. Hedrick, W. Xu, F. Boussouar, P. Brindle, H. Takemori, and M. Montminy. 2005. The CREB coactivator TORC2 is a key regulator of fasting glucose metabolism. *Nature*. 437:1109-11.

Kottke, M., V. Adam, I. Riesinger, G. Bremm, W. Bosch, D. Brdiczka, G. Sandri, and E. Panfili. 1988. Mitochondrial boundary membrane contact sites in brain: points of hexokinase and creatine kinase location, and control of Ca2+ transport. *Biochim Biophys Acta*. 935:87-102.

Kottke, M., V. Adams, T. Wallimann, V.K. Nalam, and D. Brdiczka. 1991. Location and regulation of octameric mitochondrial creatine kinase in the contact sites. *Biochim Biophys Acta*. 1061:215-25.

Kovacic, S., C.L. Soltys, A.J. Barr, I. Shiojima, K. Walsh, and J.R. Dyck. 2003. Akt activity negatively regulates phosphorylation of AMP-activated protein kinase in the heart. *J Biol Chem*. 278:39422-7.

Kubota, N., W. Yano, T. Kubota, T. Yamauchi, S. Itoh, H. Kumagai, H. Kozono, I. Takamoto, S. Okamoto, T. Shiuchi, R. Suzuki, H. Satoh, A. Tsuchida, M. Moroi, K. Sugi, T. Noda, H. Ebinuma, Y. Ueta, T. Kondo, E. Araki, O. Ezaki, R. Nagai, K. Tobe, Y. Terauchi, K. Ueki, Y. Minokoshi, and T. Kadowaki. 2007. Adiponectin stimulates AMP-activated protein kinase in the hypothalamus and increases food intake. *Cell Metab*. 6:55-68.

Kuiper, J.W., H. Pluk, F. Oerlemans, F.N. van Leeuwen, F. de Lange, J. Fransen, and B. Wieringa. 2008. Creatine kinase-mediated ATP supply fuels actin-based events in phagocytosis. *PLoS Biol*. 6:e51.

Kuiper, J.W., R. van Horssen, F. Oerlemans, W. Peters, M.M. van Dommelen, M.M. te Lindert, T.L. ten Hagen, E. Janssen, J.A. Fransen, and B. Wieringa. 2009. Local ATP generation by brain-type creatine kinase (CK-B) facilitates cell motility. *PLoS One*. 4:e5030.

Lascu, I., and P. Gonin. 2000. The catalytic mechanism of nucleoside diphosphate kinases. *J Bioenerg Biomembr*. 32:237-46.

Leclerc, I., A. Kahn, and B. Doiron. 1998. The 5'-AMP-activated protein kinase inhibits the transcriptional stimulation by glucose in liver cells, acting through the glucose response complex. *FEBS Lett*. 431:180-4.

Lenz, H., M. Schmidt, V. Welge, U. Schlattner, T. Wallimann, H.P. Elsasser, K.P. Wittern, H. Wenck, F. Stab, and T. Blatt. 2005. The creatine kinase system in human skin: protective effects of creatine against oxidative and UV damage in vitro and in vivo. *J Invest Dermatol*. 124:443-52.

Levitsky, D.O., T.S. Levchenko, V.A. Saks, V.G. Sharov, and V.N. Smirnov. 1978. The role of creatine phosphokinase in supplying energy for the calcium pump system of heart sarcoplasmic reticulum. *Membr Biochem*. 2:81-96.

Libby, G., L.A. Donnelly, P.T. Donnan, D.R. Alessi, A.D. Morris, and J.M. Evans. 2009. New users of metformin are at low risk of incident cancer: a cohort study among people with type 2 diabetes. *Diabetes Care*. 32:1620-5.

Lochhead, P.A., I.P. Salt, K.S. Walker, D.G. Hardie, and C. Sutherland. 2000. 5-aminoimidazole-4-carboxamide riboside mimics the effects of insulin on the expression of the 2 key gluconeogenic genes PEPCK and glucose-6-phosphatase. *Diabetes*. 49:896-903.

Lowe, M., N.K. Gonatas, and G. Warren. 2000. The mitotic phosphorylation cycle of the cis-Golgi matrix protein GM130. *J Cell Biol*. 149:341-56.

Luiken, J.J., S.L. Coort, D.P. Koonen, D.J. van der Horst, A. Bonen, A. Zorzano, and J.F. Glatz. 2004. Regulation of cardiac long-chain fatty acid and glucose uptake by translocation of substrate transporters. *Pflugers Arch*. 448:1-15.

Luo, Z., A.K. Saha, X. Xiang, and N.B. Ruderman. 2005. AMPK, the metabolic syndrome and cancer. *Trends Pharmacol Sci*. 26:69-76.

Mahadevan, L.C., S.A. Whatley, T.K. Leung, and L. Lim. 1984. The brain isoform of a key ATP-regulating enzyme, creatine kinase, is a phosphoprotein. *Biochem J*. 222:139-44.

Mahajan, V.B., K.S. Pai, A. Lau, and D.D. Cunningham. 2000. Creatine kinase, an ATP-generating enzyme, is required for thrombin receptor signaling to the cytoskeleton. *Proc Natl Acad Sci U S A*. 97:12062-7.

Marsin, A.S., L. Bertrand, M.H. Rider, J. Deprez, C. Beauloye, M.F. Vincent, G. Van den Berghe, D. Carling, and L. Hue. 2000. Phosphorylation and activation of heart PFK-2 by AMPK has a role in the stimulation of glycolysis during ischaemia. *Curr Biol*. 10:1247-55.

McGee, S.L., B.J. van Denderen, K.F. Howlett, J. Mollica, J.D. Schertzer, B.E. Kemp, and M. Hargreaves. 2008. AMP-activated protein kinase regulates GLUT4 transcription by phosphorylating histone deacetylase 5. *Diabetes*. 57:860-7.

Minokoshi, Y., T. Alquier, N. Furukawa, Y.B. Kim, A. Lee, B. Xue, J. Mu, F. Foufelle, P. Ferre, M.J. Birnbaum, B.J. Stuck, and B.B. Kahn. 2004. AMP-kinase regulates food intake by responding to hormonal and nutrient signals in the hypothalamus. *Nature*. 428:569-74.

Minokoshi, Y., Y.B. Kim, O.D. Peroni, L.G. Fryer, C. Muller, D. Carling, and B.B. Kahn. 2002. Leptin stimulates fatty-acid oxidation by activating AMP-activated protein kinase. *Nature*. 415:339-43.

Miquerol, L., S. Lopez, N. Cartier, M. Tulliez, M. Raymondjean, and A. Kahn. 1994. Expression of the L-type pyruvate kinase gene and the hepatocyte nuclear factor 4 transcription factor in exocrine and endocrine pancreas. *J Biol Chem*. 269:8944-51.

Mitchelhill, K.I., B.J. Michell, C.M. House, D. Stapleton, J. Dyck, J. Gamble, C. Ullrich, L.A. Witters, and B.E. Kemp. 1997. Posttranslational modifications of the 5'-AMP-activated protein kinase beta1 subunit. *J Biol Chem*. 272:24475-9.

Momcilovic, M., S.P. Hong, and M. Carlson. 2006. Mammalian TAK1 activates Snf1 protein kinase in yeast and phosphorylates AMP-activated protein kinase in vitro. *J Biol Chem*. 281:25336-43.

Motoshima, H., B.J. Goldstein, M. Igata, and E. Araki. 2006. AMPK and cell proliferation--AMPK as a therapeutic target for atherosclerosis and cancer. *J Physiol*. 574:63-71.

Muhlebach, S.M., M. Gross, T. Wirz, T. Wallimann, J.C. Perriard, and M. Wyss. 1994. Sequence homology and structure predictions of the creatine kinase isoenzymes. *Mol Cell Biochem*. 133-134:245-62.

Munday, M.R. 2002. Regulation of mammalian acetyl-CoA carboxylase. *Biochem Soc Trans*. 30:1059-64.

Musi, N., M.F. Hirshman, J. Nygren, M. Svanfeldt, P. Bavenholm, O. Rooyackers, G. Zhou, J.M. Williamson, O. Ljunqvist, S. Efendic, D.E. Moller, A. Thorell, and L.J. Goodyear. 2002. Metformin increases AMP-activated protein kinase activity in skeletal muscle of subjects with type 2 diabetes. *Diabetes*. 51:2074-81.

Nakau, M., H. Miyoshi, M.F. Seldin, M. Imamura, M. Oshima, and M.M. Taketo. 2002. Hepatocellular carcinoma caused by loss of heterozygosity in Lkb1 gene knockout mice. *Cancer Res*. 62:4549-53.

Nakazato, M., N. Murakami, Y. Date, M. Kojima, H. Matsuo, K. Kangawa, and S. Matsukura. 2001. A role for ghrelin in the central regulation of feeding. *Nature*. 409:194-8.

Neumann D, W.T., Rider M H, Tokarska-Schlattner M, Hardie D G, Schlattner. 2007. Signaling by AMP-activated Protein kinase. *Molecular System Bioenergetics: Energy for life*:303-338.

Polekhina, G., A. Gupta, B.J. Michell, B. van Denderen, S. Murthy, S.C. Feil, I.G. Jennings, D.J. Campbell, L.A. Witters, M.W. Parker, B.E. Kemp, and D. Stapleton. 2003. AMPK beta subunit targets metabolic stress sensing to glycogen. *Curr Biol*. 13:867-71.

Ponticos, M., Q.L. Lu, J.E. Morgan, D.G. Hardie, T.A. Partridge, and D. Carling. 1998. Dual regulation of the AMP-activated protein kinase provides a novel mechanism for the control of creatine kinase in skeletal muscle. *Embo J*. 17:1688-99.

Quest, A.F., T. Soldati, W. Hemmer, J.C. Perriard, H.M. Eppenberger, and T. Wallimann. 1990. Phosphorylation of chicken brain-type creatine kinase affects a physiologically important kinetic parameter and gives rise to protein microheterogeneity in vivo. *FEBS Lett*. 269:457-64.

Ramirez-Amaya, V., I. Balderas, J. Sandoval, M.L. Escobar, and F. Bermudez-Rattoni. 2001. Spatial long-term memory is related to mossy fiber synaptogenesis. *J Neurosci*. 21:7340-8.

Rao, J.K., G. Bujacz, and A. Wlodawer. 1998. Crystal structure of rabbit muscle creatine kinase. *FEBS Lett*. 439:133-7.

Rattan, R., S. Giri, A.K. Singh, and I. Singh. 2005. 5-Aminoimidazole-4-carboxamide-1-beta-D-ribofuranoside inhibits cancer cell proliferation in vitro and in vivo via AMP-activated protein kinase. *J Biol Chem*. 280:39582-93.

Ratto, A., B.M. Shapiro, and R. Christen. 1989. Phosphagen kinase evolution. Expression in echinoderms. *Eur J Biochem*. 186:195-203.

Riek, U., R. Scholz, P. Konarev, A. Rufer, M. Suter, A. Nazabal, P. Ringler, M. Chami, S.A. Muller, D. Neumann, M. Forstner, M. Hennig, R. Zenobi, A. Engel, D. Svergun, U. Schlattner, and T. Wallimann. 2008. Structural properties of AMP-activated protein kinase: dimerization, molecular shape, and changes upon ligand binding. *J Biol Chem*. 283:18331-43.

Rossi, A.M., H.M. Eppenberger, P. Volpe, R. Cotrufo, and T. Wallimann. 1990. Muscle-type MM creatine kinase is specifically bound to sarcoplasmic reticulum and can support Ca2+ uptake and regulate local ATP/ADP ratios. *J Biol Chem*. 265:5258-66.

Sakamoto, K., A. McCarthy, D. Smith, K.A. Green, D. Grahame Hardie, A. Ashworth, and D.R. Alessi. 2005. Deficiency of LKB1 in skeletal muscle prevents AMPK activation and glucose uptake during contraction. *Embo J*. 24:1810-20.

Sakamoto, K., E. Zarrinpashneh, G.R. Budas, A.C. Pouleur, A. Dutta, A.R. Prescott, J.L. Vanoverschelde, A. Ashworth, A. Jovanovic, D.R. Alessi, and L. Bertrand. 2006. Deficiency of LKB1 in heart prevents

ischemia-mediated activation of AMPKalpha2 but not AMPKalpha1. *Am J Physiol Endocrinol Metab*. 290:E780-8.

Saks, V.A., T. Kaambre, P. Sikk, M. Eimre, E. Orlova, K. Paju, A. Piirsoo, F. Appaix, L. Kay, V. Regitz-Zagrosek, E. Fleck, and E. Seppet. 2001. Intracellular energetic units in red muscle cells. *Biochem J*. 356:643-57.

Saks, V.A., A.V. Kuznetsov, V.V. Kupriyanov, M.V. Miceli, and W.E. Jacobus. 1985. Creatine kinase of rat heart mitochondria. The demonstration of functional coupling to oxidative phosphorylation in an inner membrane-matrix preparation. *J Biol Chem*. 260:7757-64.

Saks, V.A., N.V. Lipina, G.B. Chernousova, V.G. Sharov, V.N. Smirnov, E.I. Chazov, and R. Grosse. 1976. [The functional coupling between MM isozyme of creatine phosphokinase (EC 2.7.3.2.) and MgATPase of myofibrils and (Na, K)ATPase of plasma membrane in heart cells]. *Biokhimiia*. 41:2099-109.

Salomons, G.S., S.J. van Dooren, N.M. Verhoeven, K.M. Cecil, W.S. Ball, T.J. Degrauw, and C. Jakobs. 2001. X-linked creatine-transporter gene (SLC6A8) defect: a new creatine-deficiency syndrome. *Am J Hum Genet*. 68:1497-500.

Salt, I.P., G. Johnson, S.J. Ashcroft, and D.G. Hardie. 1998. AMP-activated protein kinase is activated by low glucose in cell lines derived from pancreatic beta cells, and may regulate insulin release. *Biochem J*. 335 (Pt 3):533-9.

Sanders, M.J., P.O. Grondin, B.D. Hegarty, M.A. Snowden, and D. Carling. 2007. Investigating the mechanism for AMP activation of the AMP-activated protein kinase cascade. *Biochem J*. 403:139-48.

Schlattner, U., M. Eder, M. Dolder, Z.A. Khuchua, A.W. Strauss, and T. Wallimann. 2000. Divergent enzyme kinetics and structural properties of the two human mitochondrial creatine kinase isoenzymes. *Biol Chem*. 381:1063-70.

Schlattner, U., M. Forstner, M. Eder, O. Stachowiak, K. Fritz-Wolf, and T. Wallimann. 1998. Functional aspects of the X-ray structure of mitochondrial creatine kinase: a molecular physiology approach. *Mol Cell Biochem*. 184:125-40.

Schlattner, U., M. Tokarska-Schlattner, S. Ramirez, A. Bruckner, L. Kay, C. Polge, R.F. Epand, R.M. Lee, M.L. Lacombe, and R.M. Epand. 2009. Mitochondrial kinases and their molecular interaction with cardiolipin. *Biochim Biophys Acta*. 1788:2032-47.

Schlattner, U., M. Tokarska-Schlattner, and T. Wallimann. 2006. Mitochondrial creatine kinase in human health and disease. *Biochim Biophys Acta*. 1762:164-80.

Schulze, A., T. Hess, R. Wevers, E. Mayatepek, P. Bachert, B. Marescau, M.V. Knopp, P.P. De Deyn, H.J. Bremer, and D. Rating. 1997. Creatine deficiency syndrome caused by guanidinoacetate methyltransferase deficiency: diagnostic tools for a new inborn error of metabolism. *J Pediatr*. 131:626-31.

Schwegler, H., and W.E. Crusio. 1995. Correlations between radial-maze learning and structural variations of septum and hippocampus in rodents. *Behav Brain Res*. 67:29-41.

Scott, J.W., S.A. Hawley, K.A. Green, M. Anis, G. Stewart, G.A. Scullion, D.G. Norman, and D.G. Hardie. 2004. CBS domains form energy-sensing modules whose binding of adenosine ligands is disrupted by disease mutations. *J Clin Invest*. 113:274-84.

Sestili, P., C. Martinelli, G. Bravi, G. Piccoli, R. Curci, M. Battistelli, E. Falcieri, D. Agostini, A.M. Gioacchini, and V. Stocchi. 2006. Creatine supplementation affords cytoprotection in oxidatively injured cultured mammalian cells via direct antioxidant activity. *Free Radic Biol Med*. 40:837-49.

Shaw, R.J., K.A. Lamia, D. Vasquez, S.H. Koo, N. Bardeesy, R.A. Depinho, M. Montminy, and L.C. Cantley. 2005. The kinase LKB1 mediates glucose homeostasis in liver and therapeutic effects of metformin. *Science*. 310:1642-6.

Sistermans, E.A., Y.J. de Kok, W. Peters, L.A. Ginsel, P.H. Jap, and B. Wieringa. 1995. Tissue- and cell-specific distribution of creatine kinase B: a new and highly specific monoclonal antibody for use in immunohistochemistry. *Cell Tissue Res*. 280:435-46.

Speer, O., L.J. Neukomm, R.M. Murphy, E. Zanolla, U. Schlattner, H. Henry, R.J. Snow, and T. Wallimann. 2004. Creatine transporters: a reappraisal. *Mol Cell Biochem*. 256-257:407-24.

Stachowiak, O., M. Dolder, and T. Wallimann. 1996. Membrane-binding and lipid vesicle cross-linking kinetics of the mitochondrial creatine kinase octamer. *Biochemistry*. 35:15522-8.

Stahmann, N., A. Woods, D. Carling, and R. Heller. 2006. Thrombin activates AMP-activated protein kinase in endothelial cells via a pathway involving Ca2+/calmodulin-dependent protein kinase kinase beta. *Mol Cell Biol*. 26:5933-45.

Stapleton, D., K.I. Mitchelhill, G. Gao, J. Widmer, B.J. Michell, T. Teh, C.M. House, C.S. Fernandez, T. Cox, L.A. Witters, and B.E. Kemp. 1996. Mammalian AMP-activated protein kinase subfamily. *J Biol Chem*. 271:611-4.

Steinberg, G.R., and B.E. Kemp. 2007. Adiponectin: starving for attention. *Cell Metab*. 6:3-4.

Steinberg, G.R., and B.E. Kemp. 2009. AMPK in Health and Disease. *Physiol Rev*. 89:1025-78.

Stockler, S., U. Holzbach, F. Hanefeld, I. Marquardt, G. Helms, M. Requart, W. Hanicke, and J. Frahm. 1994. Creatine deficiency in the brain: a new, treatable inborn error of metabolism. *Pediatr Res*. 36:409-13.

Stolz, M., T. Hornemann, U. Schlattner, and T. Wallimann. 2002. Mutation of conserved active-site threonine residues in creatine kinase affects autophosphorylation and enzyme kinetics. *Biochem J*. 363:785-92.

Stolz, M., and T. Wallimann. 1998. Myofibrillar interaction of cytosolic creatine kinase (CK) isoenzymes: allocation of N-terminal binding epitope in MM-CK and BB-CK. *J Cell Sci*. 111 (Pt 9):1207-16.

Streijger, F., F. Oerlemans, B.A. Ellenbroek, C.R. Jost, B. Wieringa, and C.E. Van der Zee. 2005. Structural and behavioural consequences of double deficiency for creatine kinases BCK and UbCKmit. *Behav Brain Res*. 157:219-34.

Streijger, F., H. Pluk, F. Oerlemans, G. Beckers, A.C. Bianco, M.O. Ribeiro, B. Wieringa, and C.E. Van der Zee. 2009. Mice lacking brain-type creatine kinase activity show defective thermoregulation. *Physiol Behav*. 97:76-86.

Stryer, L. 1988. Biochemistry. New York, W.H. Freeman and Company:350-356, 374-424.

Sullivan, P.G., J.D. Geiger, M.P. Mattson, and S.W. Scheff. 2000. Dietary supplement creatine protects against traumatic brain injury. *Ann Neurol*. 48:723-9.

Suter, M., U. Riek, R. Tuerk, U. Schlattner, T. Wallimann, and D. Neumann. 2006. Dissecting the role of 5'-AMP for allosteric stimulation, activation, and deactivation of AMP-activated protein kinase. *J Biol Chem*. 281:32207-16.

Swinnen, J.V., A. Beckers, K. Brusselmans, S. Organe, J. Segers, L. Timmermans, F. Vanderhoydonc, L. Deboel, R. Derua, E. Waelkens, E. De Schrijver, T. Van de Sande, A. Noel, F. Foufelle, and G. Verhoeven. 2005. Mimicry of a cellular low energy status blocks tumor cell anabolism and suppresses the malignant phenotype. *Cancer Res*. 65:2441-8.

Tamas, P., S.A. Hawley, R.G. Clarke, K.J. Mustard, K. Green, D.G. Hardie, and D.A. Cantrell. 2006. Regulation of the energy sensor AMP-activated protein kinase by antigen receptor and Ca2+ in T lymphocytes. *J Exp Med*. 203:1665-70.

Tarnopolsky, M.A., A. Parshad, B. Walzel, U. Schlattner, and T. Wallimann. 2001. Creatine transporter and mitochondrial creatine kinase protein content in myopathies. *Muscle Nerve*. 24:682-8.

Thornton, C., M.A. Snowden, and D. Carling. 1997. Identification of a novel AMPK beta subunit that is highly expressed in skeletal muscle. *Biochem Soc Trans*. 25:S667.

Tomas, E., T.S. Tsao, A.K. Saha, H.E. Murrey, C. Zhang Cc, S.I. Itani, H.F. Lodish, and N.B. Ruderman. 2002. Enhanced muscle fat oxidation and glucose transport by ACRP30 globular domain: acetyl-CoA carboxylase inhibition and AMP-activated protein kinase activation. *Proc Natl Acad Sci U S A*. 99:16309-13.

Tombes, R.M., and B.M. Shapiro. 1989. Energy transport and cell polarity: relationship of phosphagen kinase activity to sperm function. *J Exp Zool*. 251:82-90.

Turner, D.C., T. Wallimann, and H.M. Eppenberger. 1973. A protein that binds specifically to the M-line of skeletal muscle is identified as the muscle form of creatine kinase. *Proc Natl Acad Sci U S A*. 70:702-5.

Vacheron, M.J., E. Clottes, C. Chautard, and C. Vial. 1997. Mitochondrial creatine kinase interaction with phospholipid vesicles. *Arch Biochem Biophys*. 344:316-24.

van Deursen, J., A. Heerschap, F. Oerlemans, W. Ruitenbeek, P. Jap, H. ter Laak, and B. Wieringa. 1993. Skeletal muscles of mice deficient in muscle creatine kinase lack burst activity. *Cell*. 74:621-31.

Vavvas, D., A. Apazidis, A.K. Saha, J. Gamble, A. Patel, B.E. Kemp, L.A. Witters, and N.B. Ruderman. 1997. Contraction-induced changes in acetyl-CoA carboxylase and 5'-AMP-activated kinase in skeletal muscle. *J Biol Chem*. 272:13255-61.

Vernia, S., M.C. Solaz-Fuster, J.V. Gimeno-Alcaniz, T. Rubio, L. Garcia-Haro, M. Foretz, S.R. de Cordoba, and P. Sanz. 2009. AMP-activated protein kinase phosphorylates R5/PTG, the glycogen targeting subunit of the R5/PTG-protein phosphatase 1 holoenzyme, and accelerates its down-regulation by the laforin-malin complex. *J Biol Chem*. 284:8247-55.

Viana, R., M.C. Towler, D.A. Pan, D. Carling, B. Viollet, D.G. Hardie, and P. Sanz. 2007. A conserved sequence immediately N-terminal to the Bateman domains in AMP-activated protein kinase gamma subunits is required for the interaction with the beta subunits. *J Biol Chem*. 282:16117-25.

Viollet, B., R. Mounier, J. Leclerc, A. Yazigi, M. Foretz, and F. Andreelli. 2007. Targeting AMP-activated protein kinase as a novel therapeutic approach for the treatment of metabolic disorders. *Diabetes Metab*. 33:395-402.

Wallimann, T., T.C. Doetschman, and H.M. Eppenberger. 1983a. Novel staining pattern of skeletal muscle M-lines upon incubation with antibodies against MM-creatine kinase. *J Cell Biol*. 96:1772-9.

Wallimann, T., M. Dolder, U. Schlattner, M. Eder, T. Hornemann, T. Kraft, and M. Stolz. 1998. Creatine kinase: an enzyme with a central role in cellular energy metabolism. *Magma*. 6:116-9.

Wallimann, T., and W. Hemmer. 1994. Creatine kinase in non-muscle tissues and cells. *Mol Cell Biochem*. 133-134:193-220.

Wallimann, T., H. Moser, and H.M. Eppenberger. 1983b. Isoenzyme-specific localization of M-line bound creatine kinase in myogenic cells. *J Muscle Res Cell Motil*. 4:429-41.

Wallimann, T., T. Schlosser, and H.M. Eppenberger. 1984. Function of M-line-bound creatine kinase as intramyofibrillar ATP regenerator at the receiving end of the phosphorylcreatine shuttle in muscle. *J Biol Chem*. 259:5238-46.

Wallimann T, T.-S.M., Neumann D, Epand RM, Epand RF, Andres RH, Widmer HR, Hornemann T, Saks V, Agarkova I, Schlattner U 2007. The phospho-creatine circuit: Molecular and cellular physiology of creatine kinases, sensitivity to free radicals and enhancement by creatine supplementation. . *In: Saks VA (ed) Molecular Systems Bioenergetics: Energy for Life. Wiley-VCH, Weinheim, pp 195-264*.

Wallimann, T., M. Wyss, D. Brdiczka, K. Nicolay, and H.M. Eppenberger. 1992. Intracellular compartmentation, structure and function of creatine kinase isoenzymes in tissues with high and fluctuating energy demands: the 'phosphocreatine circuit' for cellular energy homeostasis. *Biochem J*. 281 (Pt 1):21-40.

Wang, W., J. Fan, X. Yang, S. Furer-Galban, I. Lopez de Silanes, C. von Kobbe, J. Guo, S.N. Georas, F. Foufelle, D.G. Hardie, D. Carling, and M. Gorospe. 2002. AMP-activated kinase regulates cytoplasmic HuR. *Mol Cell Biol*. 22:3425-36.

Watt, M.J., A.G. Holmes, S.K. Pinnamaneni, A.P. Garnham, G.R. Steinberg, B.E. Kemp, and M.A. Febbraio. 2006. Regulation of HSL serine phosphorylation in skeletal muscle and adipose tissue. *Am J Physiol Endocrinol Metab*. 290:E500-8.

Watts, D.C. 1971. Evolution of phosphagen kinases, . *Biochemical Evolution and the Origin of life (Schoffeniels, E. Ed.)*:150-173.

Winder, W.W., and D.G. Hardie. 1996. Inactivation of acetyl-CoA carboxylase and activation of AMP-activated protein kinase in muscle during exercise. *Am J Physiol*. 270:E299-304.

Winder, W.W., and D.G. Hardie. 1999. AMP-activated protein kinase, a metabolic master switch: possible roles in type 2 diabetes. *Am J Physiol*. 277:E1-10.

Winder, W.W., B.F. Holmes, D.S. Rubink, E.B. Jensen, M. Chen, and J.O. Holloszy. 2000. Activation of AMP-activated protein kinase increases mitochondrial enzymes in skeletal muscle. *J Appl Physiol*. 88:2219-26.

Woo, Y.J., T.J. Grand, S. Zentko, J.E. Cohen, V. Hsu, P. Atluri, M.F. Berry, M.D. Taylor, M.A. Moise, O. Fisher, and S. Kolakowski. 2005. Creatine phosphate administration preserves myocardial function in a model of off-pump coronary revascularization. *J Cardiovasc Surg (Torino)*. 46:297-305.

Woods, A., D. Azzout-Marniche, M. Foretz, S.C. Stein, P. Lemarchand, P. Ferre, F. Foufelle, and D. Carling. 2000. Characterization of the role of AMP-activated protein kinase in the regulation of glucose-activated gene expression using constitutively active and dominant negative forms of the kinase. *Mol Cell Biol*. 20:6704-11.

Woods, A., D. Vertommen, D. Neumann, R. Turk, J. Bayliss, U. Schlattner, T. Wallimann, D. Carling, and M.H. Rider. 2003. Identification of phosphorylation sites in AMP-activated protein kinase (AMPK) for upstream AMPK kinases and study of their roles by site-directed mutagenesis. *J Biol Chem*. 278:28434-42.

Wu, X., H. Motoshima, K. Mahadev, T.J. Stalker, R. Scalia, and B.J. Goldstein. 2003. Involvement of AMP-activated protein kinase in glucose uptake stimulated by the globular domain of adiponectin in primary rat adipocytes. *Diabetes*. 52:1355-63.

Wu, Z., P. Puigserver, U. Andersson, C. Zhang, G. Adelmant, V. Mootha, A. Troy, S. Cinti, B. Lowell, R.C. Scarpulla, and B.M. Spiegelman. 1999. Mechanisms controlling mitochondrial biogenesis and respiration through the thermogenic coactivator PGC-1. *Cell*. 98:115-24.

Wyss, M., and R. Kaddurah-Daouk. 2000. Creatine and creatinine metabolism. *Physiol Rev*. 80:1107-213.

Wyss, M., J. Smeitink, R.A. Wevers, and T. Wallimann. 1992. Mitochondrial creatine kinase: a key enzyme of aerobic energy metabolism. *Biochim Biophys Acta*. 1102:119-66.

Xie, M., D. Zhang, J.R. Dyck, Y. Li, H. Zhang, M. Morishima, D.L. Mann, G.E. Taffet, A. Baldini, D.S. Khoury, and M.D. Schneider. 2006. A pivotal role for endogenous TGF-beta-activated kinase-1 in the LKB1/AMP-activated protein kinase energy-sensor pathway. *Proc Natl Acad Sci U S A*. 103:17378-83.

Yamauchi, T., J. Kamon, Y. Minokoshi, Y. Ito, H. Waki, S. Uchida, S. Yamashita, M. Noda, S. Kita, K. Ueki, K. Eto, Y. Akanuma, P. Froguel, F. Foufelle, P. Ferre, D. Carling, S. Kimura, R. Nagai, B.B. Kahn, and T. Kadowaki. 2002. Adiponectin stimulates glucose utilization and fatty-acid oxidation by activating AMP-activated protein kinase. *Nat Med*. 8:1288-95.

Yang, W., Y.H. Hong, X.Q. Shen, C. Frankowski, H.S. Camp, and T. Leff. 2001. Regulation of transcription by AMP-activated protein kinase: phosphorylation of p300 blocks its interaction with nuclear receptors. *J Biol Chem*. 276:38341-4.

Yang, Y.C., M.J. Fann, W.H. Chang, L.H. Tai, J.H. Jiang, and L.S. Kao. 2010. Regulation of sodium-calcium exchanger activity by creatine kinase under energy-compromised conditions. *J Biol Chem*. 285:28275-85.

Young, M.E., G.K. Radda, and B. Leighton. 1996. Activation of glycogen phosphorylase and glycogenolysis in rat skeletal muscle by AICAR--an activator of AMP-activated protein kinase. *FEBS Lett*. 382:43-7.

Zakikhani, M., R. Dowling, I.G. Fantus, N. Sonenberg, and M. Pollak. 2006. Metformin is an AMP kinase-dependent growth inhibitor for breast cancer cells. *Cancer Res*. 66:10269-73.

Zeigerer, A., M.K. McBrayer, and T.E. McGraw. 2004. Insulin stimulation of GLUT4 exocytosis, but not its inhibition of endocytosis, is dependent on RabGAP AS160. *Mol Biol Cell*. 15:4406-15.

Zhu, S., M. Li, B.E. Figueroa, A. Liu, I.G. Stavrovskaya, P. Pasinelli, M.F. Beal, R.H. Brown, Jr., B.S. Kristal, R.J. Ferrante, and R.M. Friedlander. 2004. Prophylactic creatine administration mediates neuroprotection in cerebral ischemia in mice. *J Neurosci*. 24:5909-12.

- CHAPTER 2 -

A versatile multidimensional protein purification system with full Internet remote control based on a standard HPLC system

Uwe Riek[1,2], Sacnicte Ramirez[1], Theo Wallimann[2], and Uwe Schlattner[1]

[1]Inserm U884, University Joseph Fourier, Laboratory of Fundamental and Applied Bioenergetics, Grenoble, France, and [2]Institute of Cell Biology, Zurich, Switzerland

BioTechniques 46: ix-xii (BioTechniques for Preclinical Development May 2009) doi 10.2144/000113130

Abstract: The standard Äkta Explorer high-performance liquid chromatography (HPLC) system has limitations for the automation of multidimensional protein purification. Here, we describe simple modifications that allow for automated multidimensional purification protocols to extend the possibilities of the Äkta three-dimensional purification kit in terms of column number, flexibility of volumes stocked for re-injection of samples, and available choice of buffers. These modifications do not preclude the use of standard one-dimensional purification protocols. Additionally, we demonstrate a technology for encrypted full remote control of the machine over the Internet by cost-effective use of standard asymmetric digital subscriber line (ADSL) that enables direct remote interaction with the machine without preventing local control. A 4-column purification scheme, including equilibration and cleaning in place (CIP) procedures, was implemented on such a system. It significantly increased reproducibility and shortened processing time by 85%, as compared with manual operation, thus allowing for automated protein purification overnight.

Keywords: multidimensional protein chromatography; automated protein purification; remote control. Supplementary material for this article is available at www.BioTechniques.com/article/113130

- CHAPTER 2 -

Un système multidimensionnel pour la purification des protéines avec contrôle complet via Internet sur un système standard d'HPLC

Uwe Riek[1,2], Sacnicte Ramirez[1], Theo Wallimann[2] and Uwe Schlattner[1]

[1] Inserm, U884, University Joseph Fourier, Laboratory of Fundamental and Applied Bioenergetics, Grenoble, France, [2] Institute of Cell Biology, ETH Zurich, Switzerland

BioTechniques 46: ix-xii (BioTechniques for Preclinical Development May 2009) doi 10.2144/000113130

Résumé: L'Äkta Explorer HPLC système a ses limites pour l'automatisation de la purification multidimensionnelle des protéines. Ici, nous décrivons des modifications simples qui permettent la automatisation de la purification multidimensionnelle avec l'extension du kit standard de la purification en trois dimensions de l'Äkta en termes de nombre de colonnes, la flexibilité de volumes stockés pour réinjection des échantillons, et le choix disponible de tampons. Ces modifications ne font pas l'obstacle à l'utilisation des protocoles standard pour la purification unidimensionnelle. En outre, nous démontrons une technologie de contrôle complète chiffrée à distance de la machine sur l'Internet par l'utilisation rentable des asymétrique standard en ligne d'abonné numérique (ADSL) qui permet l'interaction directe avec la machine à distance sans pour autant empêcher le contrôle local. Un schéma de purification de 4-colonnes, y compris l'équilibration et le nettoyage en place (CIP), a été mis en œuvre sur un tel système. Il a considérablement augmenté la reproductibilité et raccourci le temps de traitement de 85%, par rapport à le fonctionnement manuel, permettant ainsi une purification des protéines automatique pendant la nuit.

Mots-clés: chromatographie multidimensionnelle des protéines, purification de protéines automatisé; control à distance. Information supplémentaire pour cet article est disponible sur www.BioTechniques.com/article/113130

2.1. Introduction

Protein purification protocols, once established, have to be highly reproducible to guarantee the success of subsequent applications such as protein crystallography (1,2). Reproducibility is a decisive issue if a protein is difficult to crystallize, but this is true also for other structural or kinetic studies such as inhibitor screening. The critical factor is not only the degree of purity itself (3), but also the capability to maintain constant quality over extended time periods and with different operators.

To achieve the highest purity, many protein purification protocols involve sequential separation over several chromatographic columns that work according to different separation principles, optimized for a given protein. Such multidimensional protocols start with complex mixtures (mostly crude extracts or homogenates) to end up with a fraction containing the highly enriched protein of interest (4). Although the addition of an affinity tag for heterologously expressed proteins facilitates the purification procedure, several different columns may still be necessary, even when using automated high-throughput systems (2,5–8). Such multidimensional protocols are generally based on biocompatible integrated high-performance liquid chromatography (HPLC) systems, such as the Äkta Explorer (GE Healthcare, Zurich, Switzerland). However, if each column is run separately and operated manually, it is a very time-consuming procedure with the risk of significant batch-to-batch variability due to the human factor. There are commercial solutions to automated multidimensional chromatography, but these have limitations as well. For example, the 3D Kit for Äkta systems only allows for three-dimensional (3-D) purifications, and sample volumes recovered for re-injection between columns are limited. Furthermore, the standard setup only allows connecting up to 11 buffers or solutions, which is insufficient for equilibration, run, and cleaning in place (CIP) of more than three columns.

These system limitations would necessitate manual interventions, which inevitably would lead to time loss while waiting for an operator, and batch-to-batch variability affecting the quality of the final protein preparation. To circumvent these problems, we have modified the system layout to take advantage of a certain flexibility of this system. We report here a fully automated Äkta setup for 4- and higher-dimensional protein purifications with remote control via the Internet. Based on this setup, an exemplary purification protocol is presented that is completed in only 19 h as compared with ~1 week with manual operation, and yields protein of consistently high quality.

2.2. Experimental procedures

2.2.1. System hardware

All products are from GE Healthcare unless mentioned otherwise. An Äkta 100 Explorer Air with a preparative, green tubing kit, including a P960 sample pump, a 10-mm UV/VIS flow cell, and a fraction collector Frac 950 was placed in a chromatography refrigerator (Unichromat 2025; Uniequip,

Munich, Germany). The standard setup was modified in 10 places as follows, described in order from buffer preparation to fraction collection (for a detailed connectivity diagram, see Supplementary Figure 1):

1. An additional 8-port valve (Cat. no. IV-908, new UniNet address 8) was installed in front of input B2.0 This allowed for connecting 7 additional buffers (i.e., the solutions to run CIP procedures for all columns sequentially by a method queue) to pump B.

2. A large polycarbonate canister (20-L Nalgene Clearboy; Nalgene/Thermo Fisher Scientific, Rochester, NY, USA) for distilled water was connected via a degasser (Cat. no. VE 7510, Viscotec, Stuttgart, Germany) to inputs B1 and A1.8. The latter allows for flushing of the flow path between V6 and pump A, thus separating incompatible solvents used for CIP (e.g., pure ethanol and 8 M urea). In this setup, the inputs A1.1, A2, B1 and B2 can still be used for the standard "buffer preparation" mode of the Äkta in case of manual runs. In addition, the water canister was connected to the sample valve (V5, position 8) for flushing pump P960.

3. The 5-mL Mixer (Cat. no. M-925) was equipped with a new, self-made magnetic stirrer, containing two strong (N38 magnetization) NdFeB magnets (Cat. no. K-08-C; Supermagnete, Uster, Switzerland) in a glass fiber-armed polytetrafluoroethylene (PTFE) rotor. The latter was cut out of a PTFE block on a lathe with a mortise, and the NdFeB magnets were fixed inside by Araldite epoxy resin (Migros, Thusis, Switzerland) and radially aligned by an external magnetic field until hardening of the resin. This allowed strong and more efficient mixing as necessary for highly viscous buffers (>5 mPa·s) containing, for example, glycerol and/or sucrose for protein stabilization.

4. An additional injection valve (Cat. no. INV-907, new UniNet address 9) was placed between the existing injection (V1) and flow direction valves (V7). This allowed connecting V9 for "direct load" via the sample pump P960, while maintaining V1 for using a Super Loop (Cat.no. 19-7850-01; or any other loop) with the system pumps (see point 8 below).

5. The outlet valve (V4) at position 8 was connected to the sample valve (V5) at position 7. This enabled the system pumps to flush the flow path between V5 and the second injection valve (V9), including the P960, with buffer.

6. A homemade three-way connector (made from 3 standard fingertight fittings and glued together with Araldite epoxy resin) was inserted into the latter tubing and linked to a flow restrictor (4 bar) to work as an overpressure valve. This was necessary to protect the UV/VIS flow cell from exceeding backpressure in case that outlet valve (V4, position 8) would direct flow toward sample valve (V5) without the latter being correctly switched to position 7.

7. A purge valve was mounted between sample valve (V5) and the air sensor (ASP960) in front of the sample pump (P960). This allowed manual filling and cleaning of sample tubing before starting the chromatographic run, an essential procedure for using the air sensor as a detector of completed sample application to stop injection by pump P960.

8. The outlet valve (V4) at position 7 was connected to the first injection valve (V1) at position 3 (normally the fill port for manual operation) to collect an elution peak fraction directly into a Super Loop. This allows more precise re-injection via the system pump, as compared with direct load via pump P960 with its tolerance of ±2 mL. The tubing connector can be easily replaced by a needle-fill port for manual injection and operation of the machine.

9. Outlet valve (V4) positions 3 to 6 were passed into glass vessels to collect large fractions that can be re-injected via the tubing connected to the sample valve (V5) and pump P960.

10. Additional air sensors have been added between valve V8 and input B2 and in front of the upper column valve V2. They prevent the system from sucking air into pump B or pumping air into the column matrices, respectively, by using the watch function of the Unicorn software.

2.2.2. System software

UNICORN 5.01 software was run on a standard Windows XP (SP1) PC connected to a private, physically separated network (labnet) administered by a Debian Linux server. Encrypted remote access to the Äkta and the labnet was provided by running OpenVPN 2.0 (http://openvpn.net) on the server, providing LZO-compressed IP tunneling. An unencrypted real Virtual Network Computing (VNC) server was run on the control PC and VNC clients on the remote computers, allowing for platform-independent access to the HPLC as if sitting in front of the machine (see Supplementary Material for details).

2.2.3. 4-D Chromatography implementation

Using the modified Äkta HPLC setup placed into a refrigerator, a four-dimensional (4-D) purification of His_6-tagged heterotrimeric $\alpha_2\beta_2\gamma_1$ AMP activated protein kinase [AMPK (9–11)] was implemented (see Figure 2-1 for the flow paths, Figure 2-2 for protein elution profiles, and Figure 1A in Reference 12 for an SDS-PAGE of the final preparation). Protein was heterologously expressed in bacteria as described (12–14). Seventy grams of wet-weight bacterial pellet was lysed in 200 mL lysis buffer (30% glycerol, 0.5 M sucrose, 2 mM $MgCl_2$, and 50 mM HEPES, pH 8.0, at 7°C) by sonication. The lysate was centrifuged at 23,00× *g* for 1 h (Avanti J-20; Beckman Coulter, Roissy, France), the clear supernatant applied to sample vessel 1 and injected by “direct load” (pump P960) onto column 1 [NTA metal affinity chromatography (XK 26/40 column with 140 mL Protino Ni-IDA; Macherey

Nagel, Oensingen, Switzerland), Figures 2-1A and 2-2A] until air was detected by the air sensor ASP960 in front of the pump. The column was washed with lysis buffer and eluted with 250 mM imidazol into sample vessel 2 (V4, position 4).

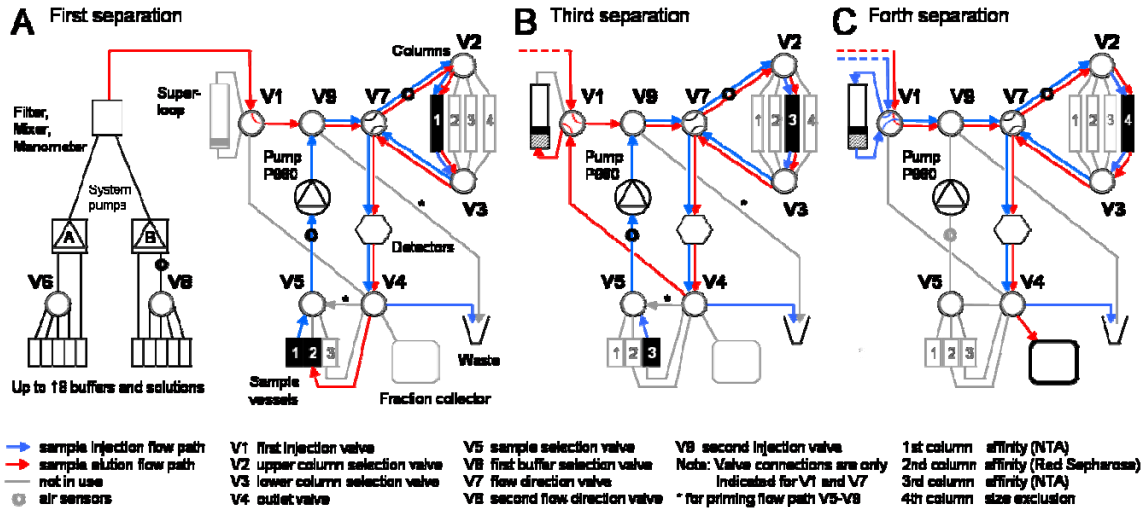

Figure 2-1. Flow path of a 4-dimensional Äkta setup used to purify AMPK complex. Main tubing connect-ions are given, showing the complete flow path for sample injection (blue arrows) and sample elution (red arrows) of (A) the first chromatography (NTA metal affinity, XK 26/40 column with 140 mL Protino Ni-IDA) and the analogous second chromatography (affinity, XK26/20 column with 45 mL Reactive Red 120 Sepharose), (B) the third chromatography (NTA metal affinity, 2 mL Ni-HP column), and (C) the forth chromatography (size exclusion chromatography, Superdex 200 16/60 column). The flow path for equilibration and CIP is not shown, except for priming the V5-V9 tubing (*), but the necessary tubing is included. Further details are given in Materials and Methods, and a more detailed connectivity diagram is given in Supplementary Figure 1.

Prior to elution, pump P960 and the tubing to the second injection valve (V9) were primed with 20 mL buffer (250 mM imidazol) using the system pumps via V9 (position 1), V7 (position 2), V4 (position 8) and V5 (position 7; for flow path, see Supplementary Figure 1). The elution fraction in vessel 2 was then loaded as above onto column 2 [Red Sepharose affinity chromatography (XK26/20 column with 45 mL Reactive Red 120 Sepharose; Sigma-Aldrich, Buchs, Switzerland), Figure 2B], and the column washed with lysis buffer and eluted by an additional 600 mM NaCl into vessel 3. The pump P960 was primed again as before and the elution fraction loaded onto column 3 [NTA metal affinity chromatography (2 mL Ni-HP column; GE Healthcare), Figures 1B and 2C] for concentration and buffer exchange. After a wash with lysis buffer, the column was eluted by 250 mM imidazol, 2 mM tris(2-carboxyethyl)phosphine (TCEP) and 200 mM NaCl. The AMPK elution peak was monitored by automated peak recognition and directed to the fraction collector, except for those 5 mL containing the highest protein concentrations. The latter fraction was directed into the Super Loop (V4, position 7), where it remained in the presence of TCEP to ensure a fully reduced AMPK. Column 4 [size exclusion chromatography (Superdex 200 16/60 column; GE Healthcare), Figures 1C and 2D] was equilibrated with 200 mM NaCl, 2 mM $MgCl_2$, 2 mM TCEP and 50 mM HEPES pH 8.0 at 7°C.

Finally, the sample was injected onto column 4, and the AMPK peak was eluted into the fraction collector. The entire purification procedure was carried out at 7°C except for the Superdex column, which was run at 25°C; further experimental details may be found in Reference 12. This protocol, which needed only 18.5 h for full completion, was followed by an automated CIP regeneration procedure. It consisted of serial injections of the following solutions, all separated by an injection of distilled water: 8 M urea and 0.05% SDS (for NTA and Red Sepharose columns), 0.4 M EDTA (pH 7.4) and 0.9 M $NiSO_4$ (additionally for NTA columns), and 0.1 M NaOH (for the Superdex 200 size exclusion column). Following this procedure, no carry-over to subsequent purifications was observed. The purity of the preparation and the lack of carryover was confirmed by Coomassie Blue–stained SDS-PAGE gels of peak fractions, showing the three AMPK subunits as distinct protein bands at the expected molecular weight (see Figure 1A in Reference 12). Quality and reproducibility of this protein preparation were essential for an extended biophysical characterization of the AMPK complex (12). The protocol has been also successfully applied to other AMPK subunit isoform combinations ($\alpha_1\beta_1\gamma_1$, $\alpha_2\beta_1\gamma_1$, and $\alpha_1\beta_2\gamma_1$) (12), as well as isoforms of creatine kinase (unpublished data).

2.3. Results and discussion

A 4-D purification protocol on an Äkta Explorer system has been successfully set up for automated and remote-controlled operation in a minimum time span, including equilibration and regeneration of all columns (Figures 1 and 2). The standard setup had to be modified and extended to meet the following requirements: (*i*) The availability of at least four consecutive purification steps with recovered and re-injected volumes of unknown size, ranging from milliliters up to several liters, possibly without limitation; (*ii*) the possibility to inject, in the same protocol, fractions of unknown, large size (e.g., bacterial lysate) and fractions of known, precise volume in the milliliter range (e.g., for size exclusion chromatography); (*iii*) overcoming the limitation of connecting only eleven buffers to the system, which is an insufficient number for equilibration, chromatography, and CIP procedures of more than three columns; (*iv*) a technical environment that allows continuous operation of the instrument (24 h/day, 7 days/week) at any temperature between 4°C and 20°C, even when using solutions with high viscosity; and (*v*) implementation of a feasible way for controlling the machine from offsite during purification procedures that last several days.

The commercially available 3D Kit for the Äkta did not offer a solution to these problems. It can only handle three dimensions, the column volumes have to be compatible with each other, and only smaller volumes can be stored in between the runs. However, we found that the problems could be solved by the addition of two valves, a flow restrictor, some additional tubing connections and a Linux PC (Supplementary Figure 1). One additional valve serves as a second buffer/solution selection valve, which not only allows accessing several large vessels (2–20 L) for solvents that are frequently used in automated mode, but also continues to work with the standard built-in “buffer preparation” mode. The other additional valve is used as a second injection valve, which enables the parallel use of “direct

load" and Super Loop for sample application in the same protocol, and also an easy set-up for quick one-dimensional runs with manual injection.

CIP procedures to regenerate all columns and to flush the tubing and the Super Loop have been implemented in an analogous, automated way to prevent carry over or contamination in subsequent purifications (see Figure 1A in Reference 12). Stock solutions for CIP (8 M urea, 0.05% SDS, 0.5 M EDTA, 1 M $NiSO_4$, 0.5 M NaOH) and all buffers are supplied by large vessels permanently connected to the system, using the increased number of connectable solutions due to the additional valve V8.

Some additional instruments had to be modified to ensure proper functioning of the entire setup for continuous operation. All instruments were placed inside a refrigerator and checked for their proper functioning down to 4°C. A degasser failed to keep its vacuum at 4°C, so its vacuum pump and valve had to be installed outside the refrigerator. The refrigerator itself has to be operated in a way to avoid local temperature fluctuations that could lead to baseline instability of the UV/VIS signal (likely by the thermal expansion of the fiber optic). Therefore, the built-in air circulation fan of the refrigerator had to be set to permanent function instead of switching on only together with the compressor of the cooling system. Finally, the mixing cell of the Äkta system may fail when using buffers with high viscosity, also resulting in baseline oscillations of the detectors. Already at 20°C, a mixture of 46% glycerol in water exceeds the viscosity limits of the mixer (M-925) (15). An efficient countermeasure was the replacement of the weak magnetic stirrer by a stronger, homemade one, resulting in efficient mixing of solutions up to 60% glycerol at 4°C.

For a convenient control of the purification progress, remote control via OpenVPN using standard internet connectivity was added. We tested various implementations for the remote access to the machine. However, the one described here was by far the most convenient and in particular, it works reliably and with a bandwidth as slow as 128 Kb/s downstream and 68 Kb/s upstream. The OpenVPN and VNC clients exist for various platforms and the encrypted tunnel can collapse at any time without bringing the Unicorn software on the control PC into a fatal situation. With connections over 10 Mb/s, implementations with the Unicorn-internal remote access capability are also feasible, either by a network drive or by socket over a special port. However, an additional installation of Unicorn on the remote system is necessary, and the flexibility is limited, since the remote system has to connect to the Unicorn server and then blocks local input, making simultaneous remote and local handling practically impossible. With slower connections (e.g., 500 Kb/s downstream and 300 Kb/s upstream with ADSL), remote work with the Unicorn networking installation was very slow or impossible due to internal timeouts, even when using LZO compression. In addition, standard Unicorn-Unicorn connections are not encrypted, so a VPN tunnel has to be built up anyway. Thus, sending the entire graphical output of the control-PC by VNC over a LZO-compressed tunnel proved more practical and much faster than the Unicorn-Unicorn connection.

The automated purification system presented here was used to implement a purification scheme for the heterotrimeric 5′-AMP–activated protein kinase (AMPK) (12) and creatine kinase (unpublished data). AMPK protein was expressed in *E. coli* grown in large bioreactor batch cultures (14). To further decrease batch-to-batch variability, frozen aliquots of bacterial pellet obtained from a single expression were used as starting material. The purification protocol included 4 different columns (12), some of them producing large elution peaks (Figure 2). Manual operation of this purification procedure would take ~1 week (5 working days) and necessitate frequent intervention by an operator, while an automated run took <19 h, with only the initial set-up requiring manual operation. Such a reduction in processing time (by about 85%) has several advantages. First, for example, if one decides to purify a protein from cell lysates in the morning, highly pure protein is available the next day in the afternoon. Furthermore, if the protein is rather unstable in any of the chosen separation conditions, its activity and yield will both be improved during the shorter automated runs, as was the case with the preparation of AMPK.

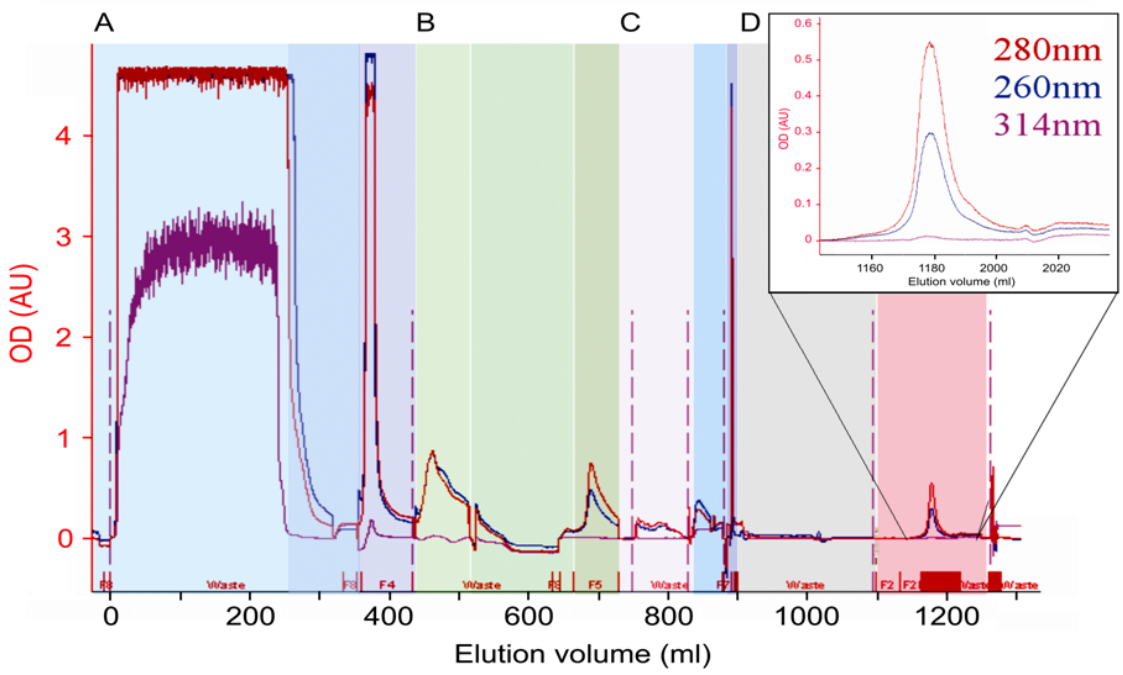

Figure 2-2. Protein elution profile of a 4-dimensional chromatography run. Purification of α2β2γ1 AMPK on an Äkta setup as shown in Figure 1 (for details, see "System hardware" section.) (A) First chromatography (NTA metal affinity matrix). Light blue, sample loading; dark blue, column washing and flushing the system with elution buffer; violet, elution of the first column into sample vessel 2 (V4, position 4). (B) Second chromatography (Red Sepharose affinity matrix). Light green, loading of the elution of the first column; dark green, column washing; olive, elution into sample vessel 2 (V4, position 5). (C) Third chromatography (NTA metal affinity matrix), necessary for concentration and buffer exchange. Pink, loading of the elution of the second column; blue, column washing; dark blue, concentrated peak eluted into the Super Loop (V4, position 7) connected to the first injection valve. (D) Forth chromatography (size exclusion chromatography). Grey, equilibration of the column while sample is in the Super Loop; red, size exclusion chromatography. The insert shows a magnification of the final elution peak of purified protein. Elution was monitored at 280 nm (protein), 260 nm (nucleotides), and 314 nm.

The automated multidimensional protein purification setup improves the reliability of multidimensional protein purifications as compared with manual handling. It also proved to be an efficient tool for method development. Based on established purification steps, columns and separation conditions of a new step can be designed by storing pre-purified sample in the machine and then using it to perform scouting runs by method queuing. This avoids problems due to variability in pre-purified starting material. The automation is not only convenient, it also allows for a much more time-efficient utilization of the expensive equipment. In our hands, the modified Äkta Explorer setup was in use for more than 95% of time (in a 24 h/day, 7 day/week scheme) over three months without major problems. The full remote accessibility via ADSL saves additional time: for example, a cleaning procedure can be quickly evaluated and repeated if necessary from home in the morning before arriving in the laboratory. Remote control, even from several hundred kilometers away, enables supervision of ongoing work and online briefing collaborators at the local PC in the laboratory.

Given the multiple advantages of the automated HPLC system, the investment in the necessary hardware is modest and the additional software freely available. Most importantly, the advantages and benefits of the modifications are significantly increased productivity and reproducible results in protein purification.

2.4. Acknowledgments

This work was supported by EU FP6 contract LSHM-CT-2004-005272 (EXGENESIS); the French Agence Nationale de Recherche (“Chaire d’excellence” given to the U.S.); and grants from ETH Zurich (graduate training fellowship for U.R.), the National Council on Science and Technology of Mexico (to S.R.), the Swiss National Science Foundation (Nr. 3100AO-102075 to T.W. and U.S., Nr. 3100+0-11437/1 to T.W. and D. N.), and Swiss Re. We thank Dietbert Neumann for AMPK plasmids and all members of the Wallimann and Schlattner groups for help and discussion.

2.5. Supplementary Material and Methods

A versatile multidimensional protein purification system with full Internet remote control based on a standard HPLC system

2.6. System Software

The UNICORN 5.01 (strategy ECAF400B) software was run in the stand-alone installation on a standard Windows XP (SP1) PC connected to a private, physically separated network (labnet). This was network address translation (NAT)–routed and administered by a Debian Linux (stable) server using MAC address-bound dynamic host configuration protocol (DHCP) and a DNS server for Linux (PDNSD). The Linux server also provided mirrored RAID1 (redundant array of inexpensive disks) and offsite backup storage space by a Samba network drive (www.samba.org). An encrypted remote access to the Äkta and the labnet was provided by running OpenVPN 2.0 (http://openvpn.net) on the server. Using the built-in LZO compression and IP tunneling, the appropriate IP range was routed from remote through the tunnels into the labnet. Then, an unencrypted real virtual network computing (VNC) server was run on the control PC and VNC clients on the remote computers, allowing for platform-independent access to the high-performance liquid chromatography (HPLC) as if sitting in front of the machine. For increased performance over 300 Kb/s ADSL, graphical effects of limited usefulness (Fade Effect, shadows, contents during dragging, screen saver, desktop picture etc.) from Windows XP were turned off as well as its “automated update” function to maintain the system’s productivity into the future.

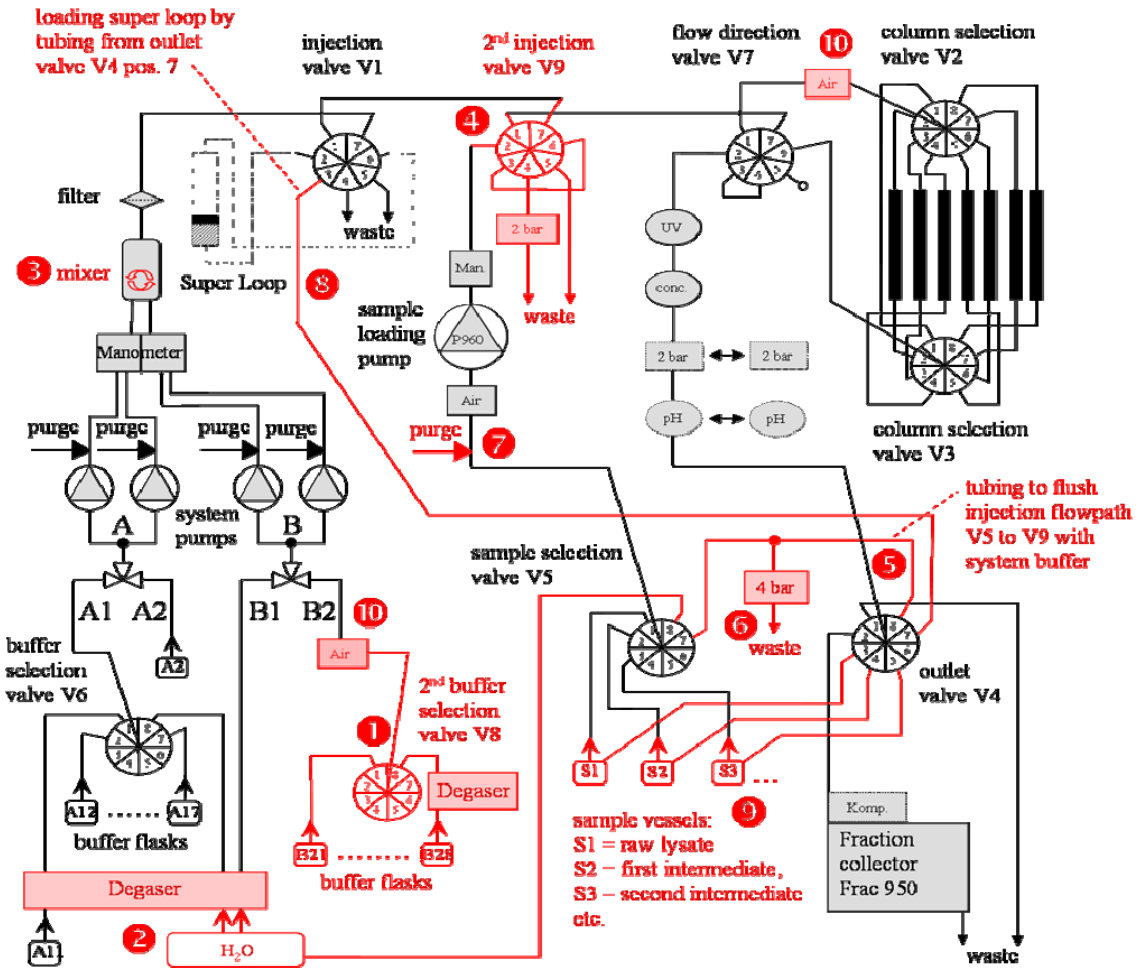

Supplementary Figure 2-1. Connectivity scheme of a modified Äkta 100 Explorer Air HPLC system. All custom added or modified parts are shown in red and are numbered according to the description in the main text. Double arrows indicate detectors that can be optionally removed from the flow path. The Super Loop can be optionally replaced by a standard tubing loop (dotted line), depending on the required volume. Note the two additional valves (V8: IV-908, second buffer selection valve, and V9: INV-907, second injection valve) as well as the additional tubing between outlet valve (V4) and other system components (valve V5, sample vessels, and valve V1). The two injection valves allow sample application either in the "direct load" mode with pump P960 (via V9) or with a loop and the system pump (via V1, port 3 connected to outlet valve V4) in the same multidimensional protocol. For normal manual injections at V1, the tubing at port 3 has to be replaced by the fill port. Man., manometer; Air, air sensor; 2 bar, 4 bar, flow restrictors; UV, flow cell for UV-900 monitor; conc., flow cell for conductivity; pH, flow cell for pH electrode.

2.7. References

1. **Chapman, T.** 2005. Protein purification: pure but not simple. Nature *434*:795-798.

2. **Stromberg, P., J. Rotticci-Mulder, R. Bjornestedt, and S.R. Schmidt.** 2005. Preparative parallel protein purification (P4). J. Chromatogr. B Analyt. Technol. Biomed. Life Sci. *818*:11-18.

3. **Caylor, C.L., I. Dobrianov, S.G. Lemay, C. Kimmer, S. Kriminski, K.D. Finkelstein, W. Zipfel, W.W. Webb, et al.** 1999. Macromolecular impurities and disorder in protein crystals. Proteins *36*:270-281.

4. **Berkowitz, S.A.** 1989. Protein purification by multidimensional liquid chromatography. Adv. Chromatogr. *29*:175-219.

5. **Scheich, C., V. Sievert, and K. Bussow.** 2003. An automated method for high-throughput protein purification applied to a comparison of His-tag and GST-tag affinity chromatography. BMC Biotechnol. *3*:12.

6. **Opiteck, G.J., S.M. Ramirez, J.W. Jorgenson, and M.A. Moseley 3rd.** 1998. Comprehensive two-dimensional high-performance liquid chromatography for the isolation of overexpressed proteins and proteome mapping. Anal. Biochem. *258*:349-361.

7. **Sigrell, J.A., P. Eklund, M. Galin, L. Hedkvist, P. Liljedahl, C.M. Johansson, T. Pless, and K. Torstenson.** 2003. Automated multi-dimensional purification of tagged proteins. J. Struct. Funct. Genomics *4*:109-114.

8. **Steen, J., M. Uhlen, S. Hober, and J. Ottosson.** 2006. High-throughput protein purification using an automated set-up for high-yield affinity chromatography. Protein Expr. Purif. *46*:173-178.

9. **Hardie, D.G.** 2007. AMP-activated protein kinase as a drug target. Annu. Rev. Pharmacol. Toxicol. *47*:185-210.

10. **Hardie, D.G. and D. Carling.** 1997. The AMP-activated protein kinase--fuel gauge of the mammalian cell? Eur. J. Biochem. *246*:259-273.

11. **Hardie, D.G., S.A. Hawley, and J.W. Scott.** 2006. AMP-activated protein kinase--development of the energy sensor concept. J. Physiol. *574*:7-15.

12. **Riek, U., R. Scholz, P. Konarev, A. Rufer, M. Suter, A. Nazabal, P. Ringler, M. Chami, et al.** 2008. Structural properties of AMP-activated protein kinase. Dimerization, molecular shape, and changes upon ligand binding. J. Biol. Chem. *283*:18331-18343.

13. **Suter, M., U. Riek, R. Tuerk, U. Schlattner, T. Wallimann, and D. Neumann.** 2006. Dissecting the role of 5′-AMP for allosteric stimulation, activation and deactivation of AMP-activated protein kinase. J. Biol. Chem. *281*:32207-32216.

14. **Riek, U., R. Türk, T. Wallimann, U. Schlattner, and D. Neumann.** 2008. A home-built low cost bioreactor for large-scale bacterial expression of proteins in *E. coli.* Biotechniques *45*:187-189.

15. **Lide, D.R., ed.** 2006. CRC Handbook of Chemistry and Physics, 87th ed., CRC Press, Boca Raton, FL.

- CHAPTER 3 -

AMP-activated protein kinase phosphorylates brain-type creatine kinase *in vivo* to regulate subcellular localization, not enzyme activity

Sacnicte Ramirez-Rios[1], Frédéric Lamarche[1], Anna Brückner[1], Roland Tuerk[2], Cécile Cottet[1], Yolanda Auchli[3], Luc Barret[1], René Brunisholz[3], Dietbert Neumann[2], Malgorzata Tokarska-Schlattner[1], and Uwe Schlattner[1*]

[1] Inserm, U884, Grenoble, France; Laboratory of Fundamental and Applied Bioenergetics, University Joseph Fourier, Grenoble, France, [2] Institute of Cell Biology, ETH Zurich, Switzerland, [3] Functional Genomics Center Zurich, ETH Zurich/University of Zurich, Switzerland.

Submitted to EMBO J

Abstract: AMP-activated protein kinase (AMPK) and cytosolic brain-type creatine kinase (BCK) cooperate to maintain cellular energy homeostasis in many non-muscle tissues. While activated AMPK stimulates ATP-generating pathways and inhibits ATP consuming pathways, CK can directly regenerate ATP from a cellular phosphocreatine pool. Here we report on AMPK-dependent phosphorylation of BCK identified in a non-biased *in vitro* screen for AMPK substrates in the brain. Based on our results with phosphorylation assays, mass spectrometry, protein sequencing, site-directed mutagenesis, yeast-two-hybrid analysis, and a phosphosite-specific antibody, we show phosphorylation of several vertebrate BCK species that involves transient interaction of active AMPK with non-phosphorylated BCK and occurs at serine 6 with about one phosphorylation per BCK dimer. AMPK-mediated BCK phosphorylation did not affect enzymatic activity of BCK, but led to specific perinuclear localization of P-Ser6-BCK corresponding to endoplasmic reticulum. We propose that cellular energy stress, often linked to cytosolic Ca^{2+}-overload, is sensed via the CamKK-AMPK signaling pathway to a recruitment of BCK to the ER for efficient refueling of the ER Ca^{2+}-pump that finally lowers cytosolic [Ca^{2+}].

- CHAPTER 3 -

La protéine kinase active par l'AMP (AMPK) phosphoryle la créatine kinase cytosolique du cerveau *in vivo* pour réguler sa localisation subcellulaire et pas son activité enzymatique

Sacnicte Ramirez-Rios[1], Frédéric Lamarche[1], Anna Brückner[1], Roland Tuerk[2], Cécile Cottet[1], Yolanda Auchli[3], Luc Barret[1], René Brunisholz[3], Dietbert Neumann[2], Malgorzata Tokarska-Schlattner[1], and Uwe Schlattner[1*]

[1] Inserm, U884, Grenoble, France; Laboratory of Fundamental and Applied Bioenergetics, University Joseph Fourier, Grenoble, France, [2] Institute of Cell Biology, ETH Zurich, Switzerland, [3] Functional Genomics Center Zurich, ETH Zurich/University of Zurich, Switzerland.

Soumis à EMBO J

Résume: La protéine kinase active par l'AMP (AMPK) et la créatine kinase cytosolique du cerveau (BCK) coopère pour maintenir l'homéostasie énergétique cellulaire dans divers tissus non musculaires. Cependant que l'AMPK stimule les voies génératrices de l'ATP et inhibe les voies de consommation de l'ATP, CK réagit directement pour régénérer de l'ATP à partir du pool de phosphocréatine cellulaire. Dans ce travail, nous rapportons la phosphorylation de la BCK par l'AMPK, laquelle a été identifiée dans un criblage *in vitro* pour des nouvelles cibles de l'AMPK dans le cerveau. Cette phosphorylation a été mise en évidence à l'aide d'un test de phosphorylation, spectrométrie de masse, séquençage de protéine, mutagenèse dirigée, le système de double hybride en levure et d'un anticorps généré spécifique. On a montré que cette phosphorylation se produit en diverses espèces et implique une interaction sélective entre l'AMPK active et la BCK non phosphorylée. La phosphorylation se produit sur la serine 6 avec une stoechiométrique de 1 par dimère de la BCK. La phosphorylation médiée par l'AMPK n'affecte pas l'activité enzymatique de la BCK mais localise la kinase dans le réticulum endoplasmique (RE) *in vivo*. Nous proposons que le stress énergétique cellulaire, souvent liée à une surcharge de calcium [Ca^{2+}] cytosolique est capté par la voie de signalisation CamKK-AMPK induisent le recrutement de la BCK au RE pour l'apporte d'énergie à la pompe du calcium qui finalement abaisse la concentration du calcium cytosolique [Ca^{2+}].

3.1. Introduction

A key element in sensing energy stress at the cellular and whole-body level is AMP-activated protein kinase (AMPK). This evolutionary conserved, heterotrimeric serine/threonine kinase integrates various inputs sensing energy and nutritional state to finally trigger a large variety of cellular responses to relieve energy stress (Hardie et al., 2006). AMPK is activated allosterically by high AMP/ATP ratios via its γ-subunit and covalently by phosphorylation of its α-subunit at Thr172 via different upstream kinases that relay signals from calcium, various hormones, and others. Activated AMPK directly acts on enzymes to regulate metabolic pathways or other signaling cascades, or to activate transcription factors for long term adaptations of energy metabolism. More recently, roles of AMPK beyond cellular energy homeostasis have been reported, e.g. in controlling cell cycle and shape. Due to its links to metabolic and proliferation signaling, AMPK became also a prime pharmacological target for treating type II diabetes, the metabolic syndrome or cancer.

Isoforms of creatine kinase (CK) are essential parts of an intricate cellular energy buffer and transport system. CK catalyzes the reversible transfer of high-energy phosphates between ATP and creatine to yield ADP and the high energy intermediate phosphocreatine (PCr). In cells with elevated, variable and/or local energy demands, in particular in muscle and brain, the CK system maintains stable ATP/ADP ratios and thus maintains energy homeostasis (Wallimann et al., 1998). CK isoforms accumulate PCr within the cell to high concentrations (up to 15 mM in brain) and use this otherwise inert PCr to regenerate global and local ATP pools under conditions of increased workload (energy buffer function). They also exploit the rapid diffusibility of PCr to connect cellular sites of ATP generation (e.g. mitochondria) with sites of high ATP consumption (e.g. myofibrils or ion pumps; energy shuttle function). To fulfill these specific cellular functions, CK isoforms do not behave as strictly soluble enzymes, but also associate with defined cellular structures. For efficient PCr generation, mitochondrial CK isoenzymes (MtCK) co-localizes with adenylate translocase in proteolipid complexes (Schlattner et al., 2009) to access matrix ATP. Cytosolic muscle-type CK (MCK) interacts, among others, with proteins in the myofibrillar M-line (myomesin, M-protein) using a charge-clamp mechanism to sustain massive, local regeneration of ATP from PCr (Hornemann et al., 2003; Hornemann et al., 2000). These interactions have been characterized in detail at the molecular level based on different X-ray structures solved by us and others (Fritz-Wolf et al., 1996; Rao et al., 1998). These structures revealed cytosolic CKs as banana-shaped dimers, and MtCKs as highly symmetric, cuboidal octamers (Eder et al., 2000; Eder et al., 1999).

As compared to MCK and MtCK isoforms, few is known about the functions and subcellular localizations of the cytosolic brain-type CK isoform (BCK) found in different non-muscle tissues, including most cell types in the brain. However, there is evidence from BCK knockout mice and subcellular localization studies that energy buffer and transport functions of the CK system are required to support high energy turnover and correct functioning of brain cells. BCK knockout mice lacking also brain MtCK (uMtCK), showed a marked cognitive phenotype with deficiencies in learning and memory (Streijger et al., 2005), spatial orientation (Jost et al., 2002), and in functioning

of hair bundle cells in the auditory system (Shin et al., 2007). In astrocytes, BCK is found in peripheral regions and pseudopodia and seems to associate with the cytoskeleton and to contribute to cell shape and motility (Kuiper et al., 2009). In macrophages, also expressing BCK, the kinase is associated with F-actin at the nascent phagosome (Kuiper et al., 2008), possibly involved in ATP-dependent actin polymerization and particle adhesion. However, only very few direct interaction partners were identified so far. In brain, BCK enhances the activity of neuron-specific K^+-Cl^- co-transporter (KCC2) (Inoue et al., 2004), indicating an ATP/ADP handling role of BCK without revealing the precise regulatory mechanism. In other tissues, BCK interacts with heat-shock protein 84/metallothionein-3 (Lahti et al., 2005), cis-Golgi matrix protein (GM130, (Burklen et al., 2007)), the SOCS box-containing protein Abs-9 (Debrincat et al., 2007) and protein G-coupled thrombin receptor PAR-1 (Mahajan et al 2000). In the latter case, it was shown that BCK provides high-energy phosphates for thrombin receptor signaling during cytoskeletal reorganization. Thus, in the brain, it remains largely unknown how BCK functionally couples to ATP-dependent processes, in particular under conditions of energy stress. Phosphorylation of BCK has been reported in some earlier studies, but without that stoichiometries or functions could be clearly shown (Chida et al., 1990a; Chida et al., 1990b; Mahadevan et al., 1984; Quest et al., 1990).

AMPK and CK thus fulfill similar cellular functions and cooperate for the maintenance of energy homeostasis. While the CK system can react very rapidly at the metabolic level, AMPK is more involved in medium and long term adaptations. A cross-talk between both systems has been postulated in an earlier paper on MCK phosphorylation by AMPK (Ponticos et al 1998). However, the reported inhibition of MCK enzyme activity and, *vice versa*, AMPK-regulation by PCr/Cr ratios (Ponticos et al 1998) could not be confirmed by follow-up studies (Ingwall, 2002; Suter et al., 2006; Taylor et al., 2006). Here we report on a specific phosphorylation of the BCK isoform at Ser6 by different AMPK isoforms that involves only transient interaction with AMPK. This phosphorylation does not affect enzymatic catalysis, but leads to a pool of phospho-BCK localized to the endoplasmatic reticulum (ER). There, it probably contributes to an effective cellular energy transfer towards the ER, in particular for refueling the ER Ca^{2+}-pump. This is the first evidence that AMPK-mediated phosphorylation is not activating or inactivating an enzyme, but promoting a specific subcellular localization. These data also suggest that CK phosphorylation in general may be rather linked to subcellular localization than to regulation of enzyme activity.

3.2. Results

3.2.1. BCK is phosphorylated by AMPK *in vitro*

An *in vitro* screen to identify new soluble AMPK targets has been developed and successfully applied to proteins from rat brain (Tuerk et al., 2007). This “Mudseek” approach combines multi-dimensional protein prepurification from brain extracts, followed by phosphorylation assays, 2D-PAGE and mass spectrometry. In continuation of these efforts, further putative AMPK targets have been identified, one of them being the rat BCK isoform (unpublished data). To confirm whether BCK

is a true *in vitro* substrate for AMPK, we repeated *in vitro* phosphorylation assays with a panel of pure BCKs including rabbit, Strep-tagged human and chicken BCK, using constitutive active αT172Dβ1γ1 AMPK (111TD) and a 24-fold excess of BCK. All three BCK species incorporated radioactive label only in the presence of AMPK, along with the autophosphorylation of α and β subunits confirming AMPK activity (Figure 3-1). Difference in gel migration between human and the other BCK species correspond to the presence of Strep-tagged in the N-terminal of human BCK protein.

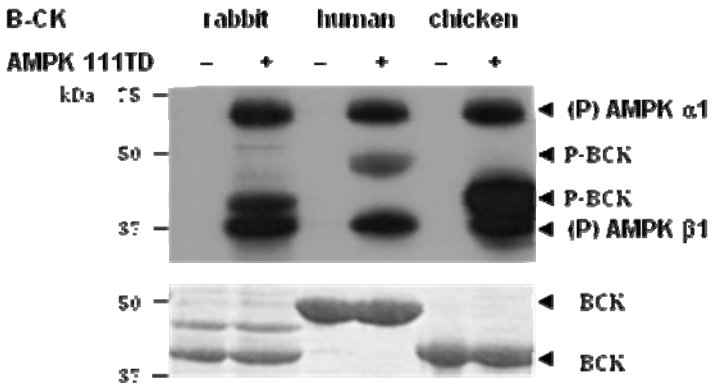

Figure 3-1. ***In vitro*** **phosphorylation of BCK from different species by constitutively active AMPK**. Pure BCK proteins (240 pmol) were incubated with [γ -^{32}P]ATP in presence (+) or absence (-) of constitutive active α1T172Dβ1γ1 AMPK (111TD, 10 pmol). Proteins used: tissue-purified rabbit BCK, recombinant human BCK with N-terminal Strep tag, recombinant chicken BCK. Reaction mixtures were analyzed by SDS-PAGE and autoradiography. Coomassie Blue staining (lower panel) is shown as loading control. P-BCK, phosphorylated BCK; (P) AMPKα1 and (P) AMPKβ1, autophosphorylated α1- and β1-subunits of AMPK.

3.3. BCK displays two putative AMPK phosphosites

To identify the phosphorylation sites in the BCK amino acid sequence, we first subjected untagged huBCK to *in vitro* phosphorylation by AMPK 111TD, followed by tryptic digest and HPLC separation. Three radioactive fractions (2, 10 and 35) eluting from an HPLC column (Suppl. Figure 3-1) were subjected to MALDI-MS/MS. Fractions 10 and 35, but not fraction 2, contained phosphopeptides as identified by the loss of a phosphoric acid moiety (-98 Da; Table 3-1, Suppl. Figures 3-2 and 3-3). There was some ambiguity concerning the phosphorylated residue in the phosphopeptide of fraction 10 which contains two serine residues. Therefore, all peptides were in addition sequenced by Edman degradation (Figure 3-2). Two phosphorylation sites, serine 6 in fraction 10 and threonine 35 in fraction 35 were thus determinated by MALDI-MS/MS and unequivocally confirmed by Edman sequencing. Both of these sites are located in the N-terminal small domain of the enzyme. Alignment of the amino acid sequences of different BCKs species revealed conservation of the N-terminal phosphorylation sites (Ser or Thr at positions 6 and 35) across different vertebrate species (Table 3-2).

TABLE 3-1. Putative [^{32}P]-phosphopeptides identified by MALDI-MS/MS in tryptic digests of AMPK-phosphorylated human BCK.

Fraction (HPLC)	*MH+*	*Score*	*Sequence*
10	1194.53	*407*	PFSN**S**HNALK 5: Phospho (ST)
10	1096.553 (-98Da)	*777*	PFSN**S**HNALK 5: Dehydroalanine
10	1194.53	*347*	PF**S**NSHNALK 3: Phospho (ST)
10	1096.553 (-98Da)	*330*	PF**S**NSHNALK 3: Dehydroalanine
35	1383.692	*91*	VL**T**PELYAELR 3: Phospho (ST)
35	1285.715 (-98Da)	*89*	VL**T**PELYAELR 3: Dehydroaminobutyric acid

Human brain BCK phosphorylated by constitutive active AMPK111. Fraction numbers correspond to RC-HPLC runs of tryptic peptides; no phosphopeptide was found in fraction 2 (see Suppl Figure 3-1). -98 Da denotes the loss of phosphoric acid.

3.3.1. Mutation of BCK at Ser6 prevents phosphorylation by activated AMPK α1 and α2

To investigate the importance of Ser6 and Thr35 phosphorylation for *in vitro* BCK phosphorylation, both residues were individually or together mutated into the phospho-mimetic aspartic acid by site-directed mutagenesis, yielding single mutants S6D and T35D or double mutant S6D/T35D (DM). Enzymes were expressed in a bacterial system and purified by two-step column chromatography, including affinity chromatography with Blue Sepharose and cation exchange chromatography with Resource Q resin. The resulting BCK preparations of high purity (see Suppl. Figure 3-4) were subjected to *in vitro* phosphorylation using α2β2γ1 wild type AMPK (221WT) previously activated by the AMPK upstream kinase CamKKβ and a 60-fold excess of substrate. Incorporation of ^{32}P was revealed by phosphoimager. As shown in Figure 3-3A, S6D and S6D/T35D (DM) mutants did not incorporate radioactive label, whereas the T35D mutant still became strongly phosphorylated (Figure 3-3A). This phosphorylation was dependent on the presence of AMPK, and not on the AMPK kinase CamKKβ (Suppl. Figure 3-5).

We then aimed to compare BCK phosphorylation efficiency by AMPK α1 and α2 isoforms. Like above, BCK wild type and S6D mutant were incubated *in vitro* with [γ-^{32}P]ATP in presence or absence of α2β2γ1 wild-type AMPK (221WT) and α1β1γ1 wild-type AMPK (111WT) isoforms previously activated by CamKKβ (Figure 3-3B). To correct for slightly different specific activities of the AMPK preparations, similar experiments with both AMPK complexes were performed with the well established AMPK substrate acetyl-CoA carboxylase (ACC), purified as a GST-tagged fusion protein (not shown).

TABLE 3-2. Sequence alignment of BCK isoform species.

```
sec. struct.      hhhhhhhh  hhhh          hhhhh  hhhhh

                1         10         20         30         40
human    BCK MPFSNSHNALKLRFPAEDEFPDLSAHNNHMAKVLTPELYA
mouse    BCK MPFSNSHNTQKLRFPAEDEFPDLSSHNNHMAKVLTPELYA
rat      BCK MPFSNSHNTQKLRFPAEDEFPDLSSHNNHMAKVLTPELYA
rabbit   BCK MPFSNTHNTLKLRFPAEDEFPDLSAHNNHMAKVLTPEMDA
chicken  BCK MPFSNSHNLLKMKYSVDDEYPDLSVHNNHMAKVLTLDLYK
```

Sequences are given for cytosolic BCKs from human (**P12277**, KCRB_HUMAN), mouse (**Q04447,** KCRB_MOUSE), rat (**P07335**, KCRB_RAT), rabbit (**P00567,** KCRB_RABIT) and chicken (**P05122**, KCRB_CHICK). Sequences of the proteins (with starting methionines and targeting peptides) are given. The conserved secondary structure is indicated on top (h, α-helix), AMPK-phosphorylated residues are indicated in bold letters.

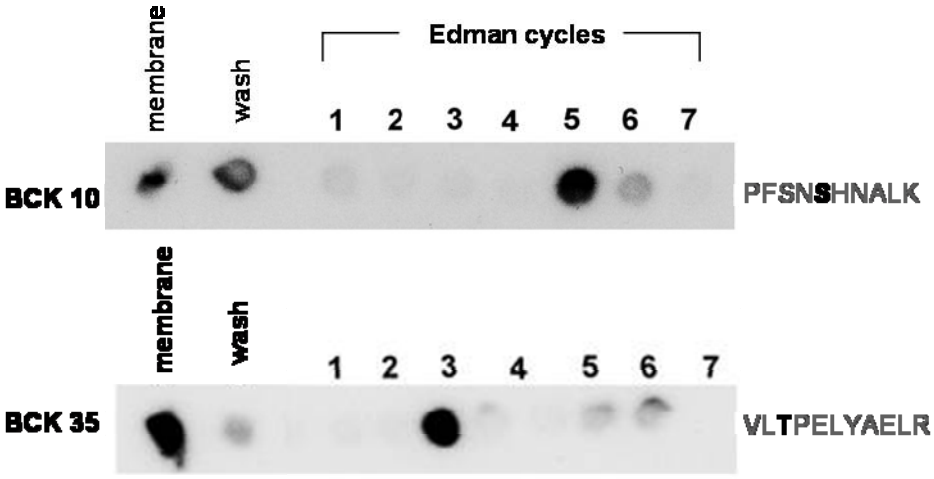

Figure 3-2. Identification of BCK phospho-sites by solid phase Edman sequencing. Pure recombinant human BCK was phosphorylated by constitutively active recombinant αT172Dβ1γ1 AMPK (111TD) using [γ -^{32}P]ATP. Two tryptic BCK-peptides that incorporated ^{32}P (see Suppl Figure 3-1) were isolated by reversed-phase chromatography, identified by MS/MS (see Table 3-1) and subjected to solid phase Edman sequencing for seven cycles. The autoradiograph shows the position of the radiolabeled amino acid in the peptide. Membrane, residual peptide after last Edman cycle; wash, unbound peptide.

Both AMPK complexes phosphorylated huBCK wild-type and only residual phosphorylation was observed for S6D mutant. When ^{32}P-incorporation was quantified, the phosphorylation ratio for activated 221WT/ activated 111WT was 2,5 for BCK and only 1,5 for ACC. These results confirm that Ser6 is the major phosphorylation site in the BCK sequence. In addition, BCK is phosphorylated by both AMPK 111 and 221 isoforms being AMPK 221 more efficient.

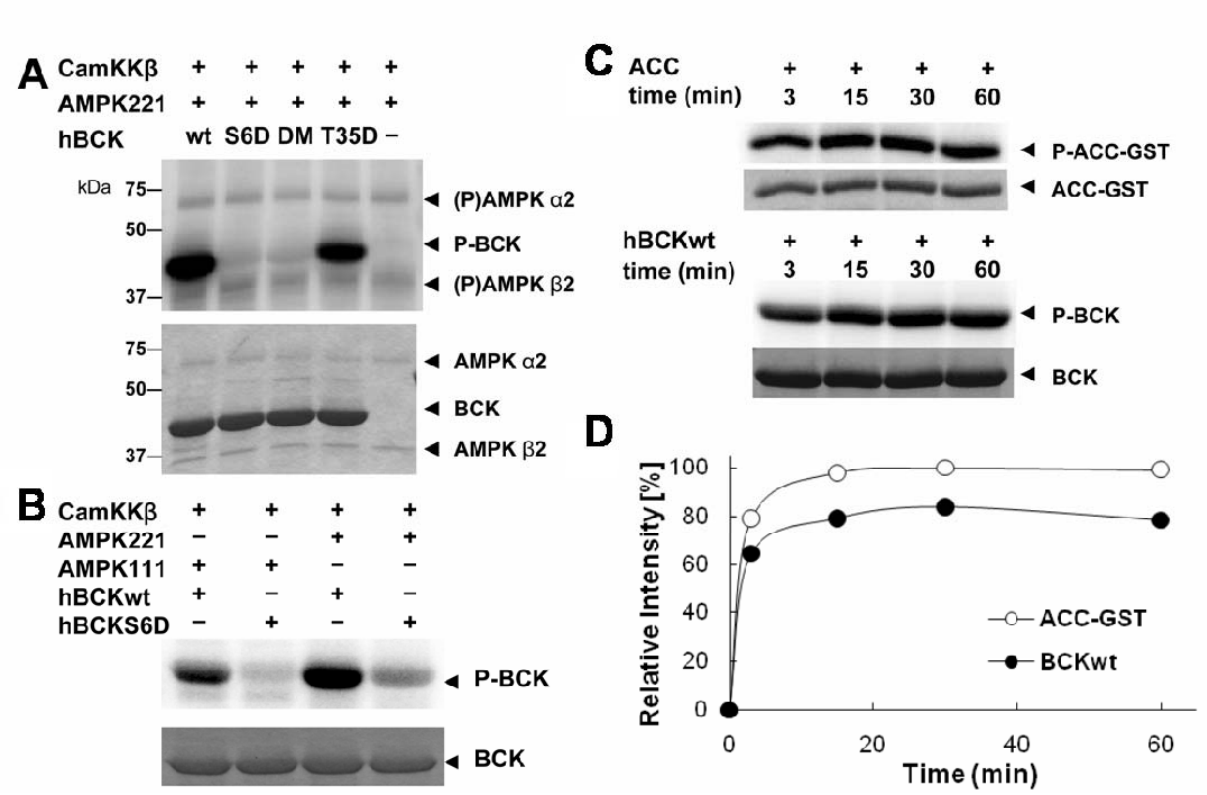

Figure 3-3. Mutation of BCK at Ser 6 prevents phosphorylation by activated AMPK. BCK is phosphorylated by activated AMPK in a similar manner that ACC substrate. *(A) BCK Ser6 is essential for phosphorylation by AMPK.* Highly purified, non-tagged wild-type BCK and mutants (200 pmol) were subjected to *in vitro* phosphorylation assays with [γ-^{32}P]ATP, using AMPK α2β2γ1 wild-type (221WT, 3.5 pmol) activated by CamKKβ (1 pmol). *(B) BCK is phosphorylated by different AMPK isoforms.* Wild type BCK and S6D mutant (200 pmol) were subjected to *in vitro* phosphorylation assay using AMPK α1β1γ1 wild-type (111WT, 3.5 pmol) or α2β2γ1 wild-type (221WT, 3.5 pmol), both activated by CamKKβ (1 pmol). *(C,D) BCK and acetyl-CoA carboxylase (ACC) are phosphorylated at similar rates and stoichiometries.* (C) GST-ACC (80 pmol) and wild type BCK (200pmol) were subjected to an *in vitro* phosphorylation assay for 3, 15, 30 and 60 min in the presence of AMPK 221WT (3.5 pmol) previously activated by CamKKβ (1 pmol). (D) Quantification of incorporated radiolabel data showing in (C) into ACC (○) and wild type BCK (●) normalized to protein amount (monomeric ACC and dimeric BCK) and relative to ACC phoshorylation (set to 100%). All reaction mixtures were analyzed by SDS-PAGE, Coomassie Blue-staining and quantified by Typhoon phosphoimager. Note: Mutants containing the S6D mutation are no longer phosphorylated by AMPK; AMPK α and β subunits are autophosphorylated, see (P) AMPKα2 and (P) AMPKβ2 labels.

3.3.2. Ser6 is phosphorylated rapidly and with high stoichiometry

We then analyzed the phosphorylation time course of huBCK wild-type by AMPK. huBCK and ACC proteins were incubated *in vitro* with [γ-^{32}P]ATP in the presence or absence of recombinant AMPK 221WT previously activated by the upstream kinase CamKKβ. For both proteins we observed a strong phosphorylation signal already after 3 min of incubation, which then reached a maximum after 15-30 min (Figure 3-3D). Incorporation of phospholabel into both proteins was quantified by phosphoimager analysis and expressed relative to protein amount and GST-ACC as reference (Figure 3-3C). This clearly revealed a time course of BCK phosphorylation similar to ACC (Figure 3-3D). Since ACC has one AMPK phosphosite that can be completely phosphorylated by AMPK (Davies et al., 1990), stoichiometry of BCK phosphorylation can be estimated to be close to one per BCK dimer, i.e. one monomer per BCK dimer carries a phospho-Ser6.

3.3.3. Active AMPK interacts transiently with BCK wild-type via its α subunit N-terminal domain

We further tested whether BCK phosphorylation requires strong interaction with the protein kinase by applying a cytosolic yeast two-hybrid (CytoY2H) assay. Cyto-Y2H is a cytosolic, split-protein-based assay where bait/prey interaction leads to reconstitution of ubiquitin, subsequent release of transcription factor by ubiquitin-specific proteases, and transcription of reporter genes that allow growth on nutrient-deficient medium. Such transcriptional read-out is very sensitive and can detect also weak or transient interactions. BCK monomer-monomer interaction leading to dimerization served as positive control, while *Simian virus* Large T antigen was used as negative control. This cyto-Y2H assay clearly revealed interaction of BCK wild-type with constitutive active AMPK α2T172D (α2TD), but not with inactive wild-type α1 or α2 subunits (Figure 3-4), while the S6D mutation prevented any formation of BCK/AMPK complexes. The β subunits did not interact with BCK neither. Using co-immunoprecipitation, interaction between BCK wild-type and AMPK α2TD was not detectable. These results suggest that activation of AMPK is needed to allow for a direct but transient interaction of the AMPK α subunit with non-phosphorylated BCK.

3.3.4. BCK wild-type and phospho-mimetic mutant S6D do not differ in enzymatic activity

Protein phosphorylation is known to be a post-translational regulatory mechanism that can modify conformation or activity of enzymes. We therefore compared wild-type BCK with the phospho-mimetic mutants by using gel filtration chromatography with a calibrated Superose 12 column. Stokes radii of all proteins corresponded to 86 kDa of BCK dimers, confirming that quaternary structure of BCK is conserved in the phospho-mimetic mutants (Figure 3-5). However, a slight shift to larger Stokes radii was observed in the mutant proteins, in particular those containing the S6D mutation.

We further analyzed whether phosphorylation by AMPK has an effect on the two-substrate reaction of BCK. The precise kinetic parameters of recombinant wild-type and phosphorylation-mimicking S6D mutant were determined in both, forward and reverse reaction. As shown in detail in Table 3-3, phosphorylation did not modify enzyme kinetic parameters. Neither total specific activity in both directions of the reaction, nor the affinity values of all four substrates, including K_m (binding as first substrate) and K_d (binding as second substrate), were significantly altered (Table 3-3, Suppl. Figure 3-6). We could neither detect an effect of AMPK activation on endogenous BCK enzyme activity in astrocytes (Suppl. Figure 3-7).

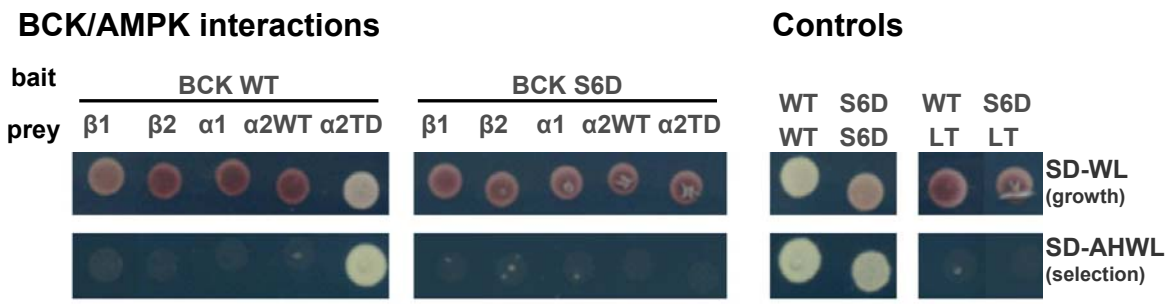

Figure 3-4. BCK wild-type, but not S6D mutant, interacts with AMPK αT172D, but not wild-type, in yeast-two-hybrid assay. Interaction of AMPK with wild-type (WT) or S6D mutant BCK with different AMPK subunits or αT172D (TD) mutant was analyzed with a cytosolic split-ubiquitin yeast two-hybrid assay. BCKs were expressed as plasma membrane-anchored fusion proteins (bait), while AMPK subunits were expressed as soluble fusion proteins (prey). Interactions activating reporter gene transcription allow growth on nutrient-deficient medium (for more details see Experimental Procedures). Spots represent yeast grown for 72 h at 30°C. Dimerization of BCK WT and S6D mutant served as positive controls, assays with BCK WT or S6D mutant and Large T antigen *(Simian virus)* served as negative control. SD-AHWL, supplement-deficient in adenine, histidine, tryptophan and leucine.

3.3.5. Specificity of phospho-BCK detection using a purified polyclonal anti P-Ser6-BCK antibody

For further studies on enzyme activity-independent functions of phosphorylated BCK, an antibody specific for phosphorylated Ser6 in human BCK was obtained by immunization of rabbits with the P-peptide PFSN(P~S)HNALKL, corresponding to the very N-terminal part of BCK (amino acids 1-12) and affinity purification from the serum using the antigenic peptide. In immunoblot analysis with recombinant protein huBCK, the anti P-Ser6-BCK antibody did not show cross-reactivity with non-phosphorylated enzyme (Figure 3-6A) or other proteins in cellular extracts (not shown). The detection limit was however at about 400 ng recombinant BCK and thus at the limit of what can be expected in cellular extracts (Figure 3-6A).

Table 3-3. Enzyme kinetic constants of BCK wild-type and S6D mutant.

Kinetic parameter		*huBCK proteins*	
		WT	***S6D***
Forward reaction			
Specific activity	[U/mg protein]	29.0 ± 2.94	29.5 ± 2.78
K_d (MgATP)	[mM]	1.15 ± 0.05	1.11 ± 0.08
K_m (MgATP)	[mM]	0.88 ± 0.02	0.86 ± 0.05
K_d (Cr)	[mM]	6.94 ± 0.26	7.05 ± 0.11
K_m (Cr)	[mM]	5.80 ± 0.16	6.07 ± 0.10
Reverse reaction			
Specific activity	[U/mg protein]	128 ± 3.51	127 ± 5.19
K_d (MgADP)	[mM]	0.19 ± 0.01	0.21 ± 0.02
K_m (MgADP)	[mM]	0.26 ± 0.01	0.29 ± 0.32
K_d (PCr)	[mM]	1.99 ± 0.12	2.02 ± 0.17
K_m (PCr)	[mM]	3.10 ± 0.17	3.00 ± 0.05

Constants for the CK wild-tpye (WT) and mutant (S6D) forward and reverse reactions at pH 8 and 7, respectively, were calculated from initial rate data by global fitting using Sigma Plot software (see Experimental Procedures).

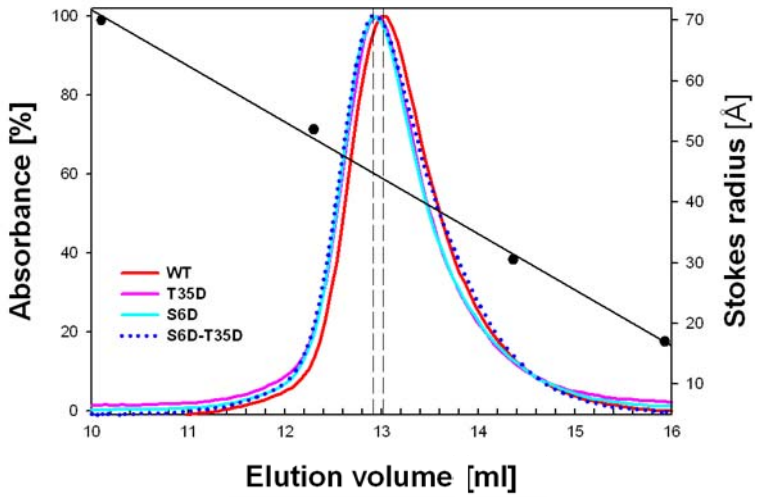

Figure 3-5. BCK phospho-mimetic mutant proteins display slightly increased Stokes radius. Size exclusion chromatography of BCK wt and mutants, using elution of 0.3 mg injected protein on a calibrated Superose 12 column at 1 ml/min. Elution volumes were (with Stokes radii): BCK wild-type (red); 13.02 ml, 43.9 Å, BCK S6D (cyan); 12.92 ml, 44.7 Å, DM (blue); 12.90, 44.88 Å and T35D (magenta); 12.94 ml; 44.5 Å.

3.3.6. BCK is phosphorylated at Ser6 in astrocytes treated with A769662 or AICA-riboside

To characterize BCK phosphorylation by AMPK *in vivo*, we established cell culture of primary mouse astrocytes. Astrocytes are cells with high and fluctuating energy demand that express high levels of BCK (Kuiper et al., 2009). We first examined the effect of pharmacological activators of AMPK. More recently, the Abbott compound A-769662 has been used as a cell-permeable activator of AMPK that acts very specifically through direct binding to the β1 subunit (Goransson et al., 2007). Treatment of astrocytes with 50 μM A-769662 for only 30 min led to rapid activation of AMPK, as judged by an increase in AMPK Thr172 phosphorylation (Figure 3-6B). This increase was already detectable after 15 min and persisted for at least 4 h (data not show). Using the anti-P-Ser6-BCK antibody, we detected concomitant appearance of phospho-BCK, which was absent in untreated controls (Figure 3-6B), thus demonstrating AMPK-dependent BCK phosphorylation *in vivo*.

As another pharmacological activator of AMPK, we used AICA-riboside (AICAR). Mouse primary astrocytes were treated with 1mM AICAR for 30 min. This led to phosphorylation of AMPK at Thr172 and of its direct substrate, acetyl-CoA carboxylase (ACC) at Ser79 (Figure 3-7A). About 500 μg of soluble proteins were then analyzed by 2D-electrohoresis and immunoblotting with p-Ser6-BCK antibody. While controls again did not show P-Ser6-BCK signals (not shown), three P-Ser6-BCK spots with different isolectric points were revealed after AICAR treatment, indicating the presence P-Ser6 in different phospho-BCK species (Figure 3-7B). The presence of several spots can be due to autophosphorylation of cytosolic BCK (Hemmer et al., 1995; Quest et al., 1990; Rosenberg et al., 1981; Stolz et al., 2002). In addition, 2D-electrophoresis showed also specificity of P-Ser6-BCK antibody. The major spot corresponding to an unphosphorylated BCK isoform was not detected by the antibody (Figure 3-7B).

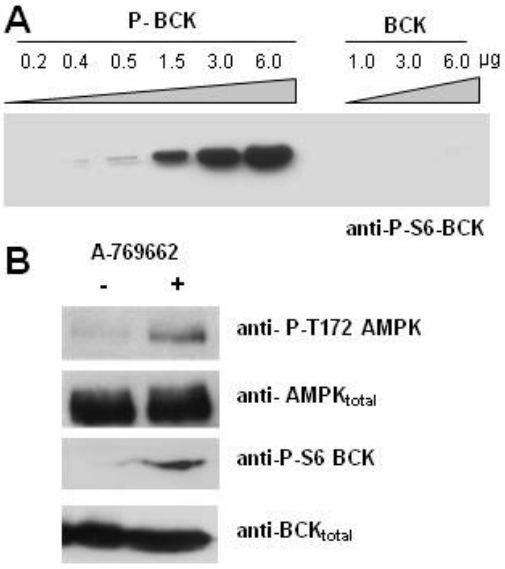

Figure 3-6. Detection of P-Ser6-BCK phosphorylated *in vitro* and in A769662-treated astrocytes by using specific antibody. *(A) Specificity and affinity of P-Ser6-specific antibody.* A specific antibody against an N-terminal BCK peptide phosphorylated at Ser6 was obtained by rabbit immunization and affinity purification. The antibody was tested at a dilution of 1:1000 in immunoblots of 0,2 – 6,0 µg recombinant human BCK, either phosphorylated *in vitro* with constitutive active AMPK 221TD or non-phosphorylated controls. Note: Even at 6 µg, the antibody does not cross-react with non-phosphorylated BCK. *(B) BCK is phosphorylated at Ser6 in mouse astrocytes treated with A769662.* Primary mouse cortical astrocytes cultured for 14 days were incubated in DMED medium containing vehicle (DMSO) or 50µM A769662 for 30 min at 37°C. Total cell lysates (60 µg protein) were analyzed by PAGE-immunoblotting using antibodies specific for P-αThr172-AMPK, P-Ser6-BCK, or total αAMPK and BCK.

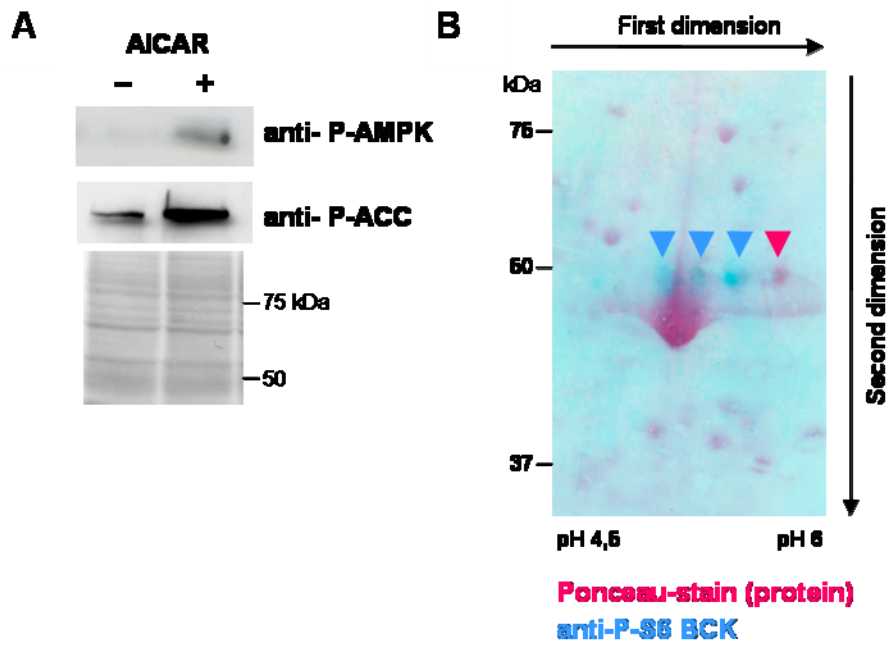

Figure 3-7. Detection of P-Ser6-BCK spots in astrocytes treated with AICAR. Primary mouse cortical astrocytes cultured for 14 days were incubated in DMED medium containing vehicle (dH_20) or 1 mM AICAR for 30 min at 37 °C. *(A) AMPK activation by AICAR.* Phosphorylation of acetyl-CoA carboxylase (ACC) and AMPK in total cell lysates (60 µg) was analyzed by PAGE immunoblotting using phospho-specific antibodies against P-αThr172-AMPK and P-Ser79-ACC. *(B) Overlay of protein stain and P-Ser6-BCK detection in 2D-PAGE.* Total soluble protein (500 µg) was subjected to 2D-PAGE followed by blotting, Ponceau-staining (red spots) and immunodetection with antibodies against P-Ser6 BCK (blue spots).

3.3.7. Ser6-phosphorylated BCK localizes to perinuclear regions in astrocytes and fibroblasts

As AMPK-mediated phosphorylation did not affect enzymatic activity of BCK, we investigated whether subcellular localization may be altered. First, confocal microscopy was applied to the model system described above. In mouse primary astrocytes, activation of AMPK by two different pharmacological activators, AICAR and A769662, induced perinuclear localization of phospho-BCK (Figure 3-8C-D). While untreated astrocytes presented low levels of phospho-BCK (Figure 3-8B), AMPK activation led to a strong perinuclear signal (Figure 3-8C-D). Since total astrocyte BCK gave a diffuse cytosolic staining with some enrichment near the plasma membrane before and after AMPK activation (Suppl. Figure 3-8), the P-Ser6-BCK probably corresponds to a minor fraction of the cytosolic BCK pool.

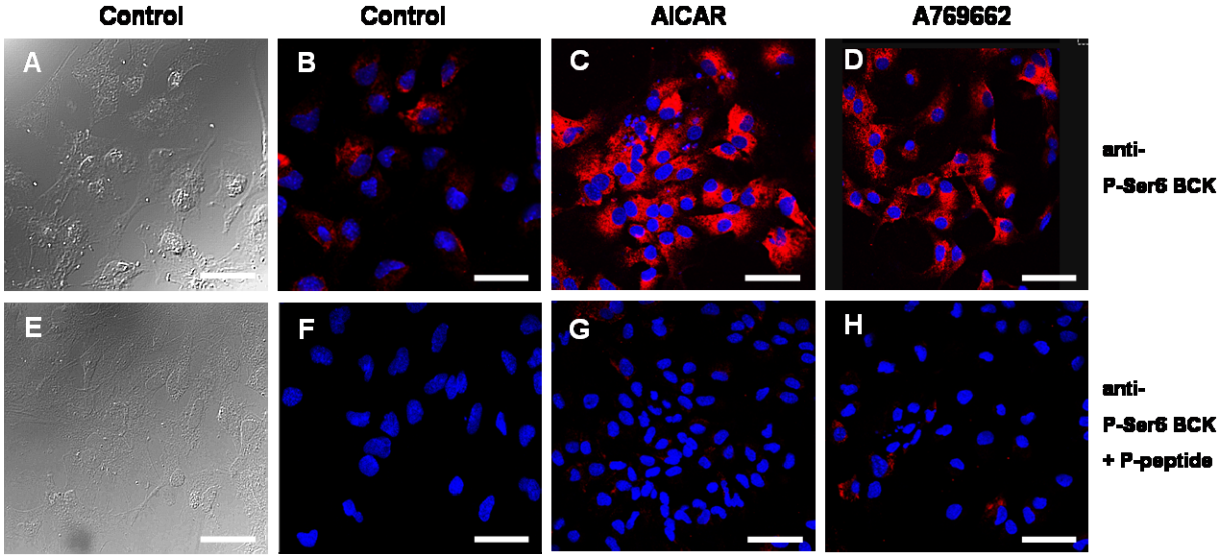

Figure 3-8. Astrocyte BCK phosphorylated at Ser6 upon AMPK activation localizes to perinuclear regions. Cultures of primary mouse cortical astrocytes in (A) phase contrast microscopy or (B-D) confocal microscopy after staining for P-Ser6-BCK (red fluorescence) and nuclei (Hoechst 33342 dye, blue fluorescence). Astrocytes cultured for 14 days were incubated in DMEM medium containing (B) vehicle (dH_20 or DMSO), (C) 1 mM AICAR, or (D) 50µM A769662 for 30 min at 37 °C. Antibody specificity was confirmed applying a competition assay with the P-peptide using for the generation of the anti-P-Ser6 antibody. Astrocytes incubated in DMEM medium containing (F) vehicle (dH_20 or DMSO), (G) 1 mM AICAR, or (H) 50µM A769662 for 30 min at 37 °C were stained for P-Ser6-BCK (red fluorescence) and nuclei (Hoechst 33342 dye, blue fluorescence) in the presence of the mix P-Ser6 BCK/P-peptide. Cells were permeabilized and immunostained with anti-P-Ser6 BCK antibody and DyLight 649 conjugated goat-anti rabbit secondary antibody. Note: P-Ser6-BCK increases with AMPK activation in a perinuclear region. Bars correspond to 47 µm.

In an effort to ascertain the specificity of the anti-P-S6 antibody in such *in vivo* applications, two different control experiments were performed. First, we applied a competition assay with the P-peptide that had been used for generation of the anti-P-Ser6 antibody. This led to an almost complete disappearance of the phospho-BCK signal (Figure 3-8G). Second, we used immortalized mouse embryonic fibroblasts (MEFs) derived from CK-B/AK1 double knock-out animals (MEF-BAK-/-) (Kuiper et al., 2009). Wild-type and BAK-/- MEFs cultured for 3 days until confluence were treated

with A769662, leading to activation of AMPK as detected by αT172 phosphorylation (Figure 3-9). When immunostained with anti-P-S6 antibody under the same conditions as for astrocytes, wild-type MEFs showed a perinuclear staining very similar to what had been observed in astrocytes (Fig. 3-9A-C). However, BAK-/- MEFs analyzed under identical conditions did not show this perinuclear staining (Figure 3-9D-F). These experiments provided clear evidence for the fluorescent staining corresponding to Ser6-phosphorylated BCK.

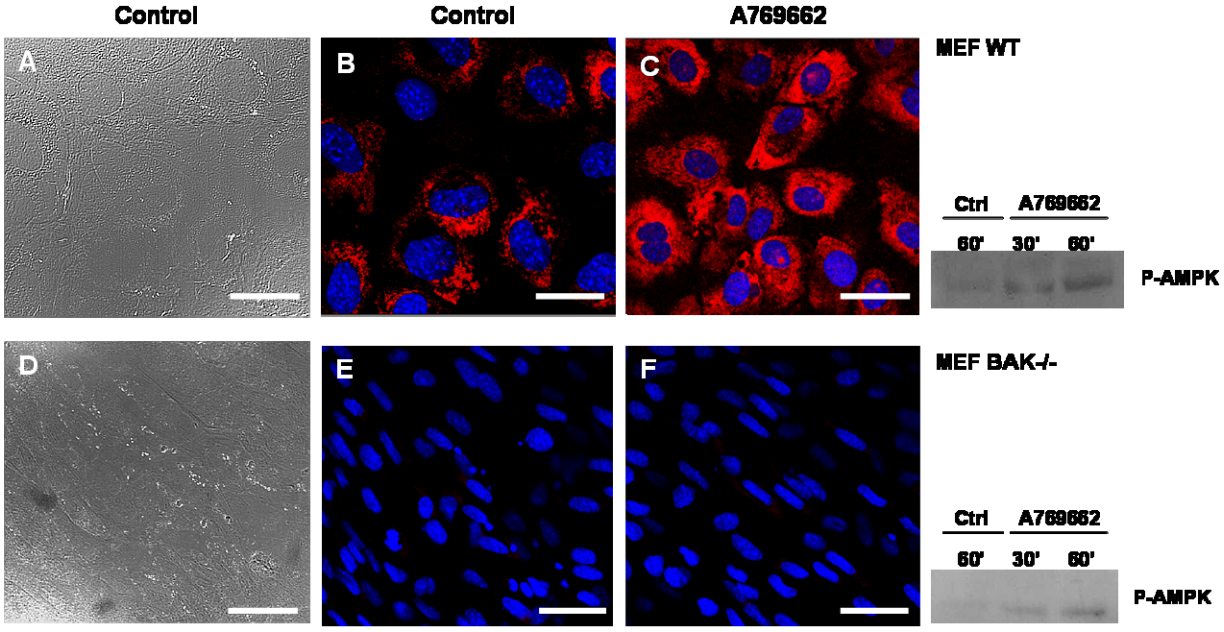

Figure 3-9. Phospho-Ser6-BCK is detected upon AMPK activation in wild-type, but not BAK-/- MEFs. Cultures of immortalized mouse embryonic fibroblasts (MEFs) from control (A-C) and BAK-/- knockout mice (D-F) were stained for P-Ser6-BCK (red fluorescence) and nuclei (Hoechst 33342 dye, blue fluorescence) and analyzed by confocal microscopy. MEFs cultured for 3 days were incubated in DMEM medium containing (B,E) vehicle (DMSO) or (C,F) 50µM A769662 for 30 min at 37 °C. Cells were labeled with Hoechst 33342 dye and permeabilized and immunostained with anti-P-Ser6 BCK antibody and DyLight 649 conjugated goat-anti rabbit secondary antibody. Activation of AMPK in MEF wild type or BAK-/- was confirmed by immunoblot. Fibroblasts were treated with 50µM A769662 for 30 and 60 min at 37 °C. Total cell lysates (40 µg) were analyzed by immunoblotting using the antibody specific for P-αThr172-AMPK. Note: Knockout MEFs lack P-Ser6-BCK. However, P-Ser6-BCK is also very low in wt MEFs and only increased by AMPK activation. Bars correspond to 35 µm (A-C) or 47 µm (D-F).

3.3.8. Phospho-BCK is targeted to the endoplasmic reticulum.

The defined localization of BCK in perinuclear regions raised the question whether the Ser-6 phosphorylated BCK species is bound to a specific subcellular structure. Cell fractionation followed by immunoblotting with anti-S6-BCK antibody remained inconclusive, probably because the low affinity of the antibody in detecting denatured phospho-BCK (see Figure 3-6A). Therefore, cellular co-localization of BCK with different marker proteins *in vivo* was studied by confocal microscopy in primary mouse cortical astrocytes treated with A769662. Different marker proteins for organelles like mitochondria or Golgi apparatus showed only minimal or at least incomplete cellular co-localization

(Suppl. Figures 3-9 and 3- 10). Only protein disulfide-isomerase (PDI), a marker for the endoplasmic reticulum, showed full colocalization with phospho-BCK in all stainings (Figure 3-10).

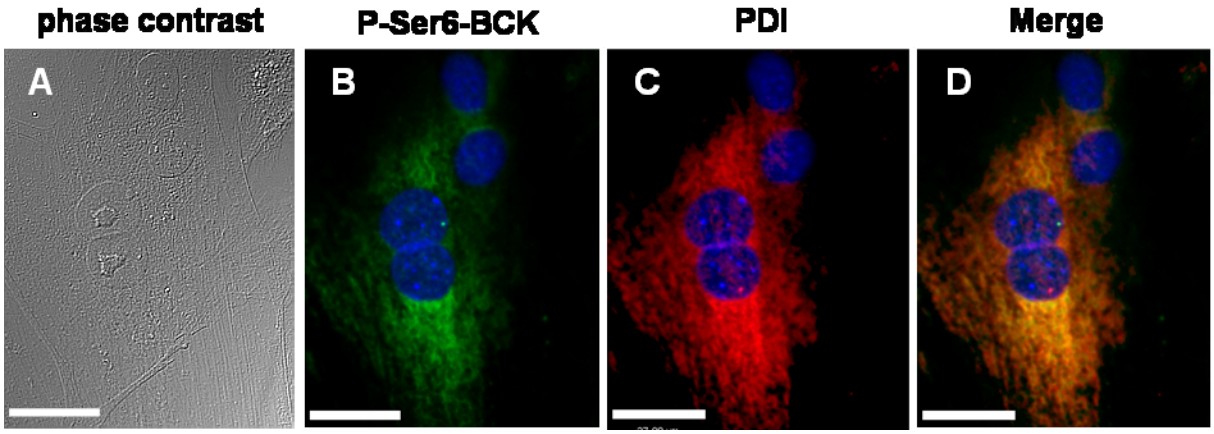

Figure 3-10. Astrocyte BCK phosphorylated at Ser6 fully co-localizes with endoplasmic reticulum. Cultures of primary mouse cortical astrocytes in (A) phase contrast microscopy or confocal microscopy after staining for (B) P-Ser6-BCK (green fluorescence), (C) protein disulfide isomerase (PDI, marker for endoplasmic reticulum, red fluorescence), and (D) merge image of (B) and (C). Nuclei were stained with Hoechst 33342 dye (blue fluorescence). Astrocytes cultured for 14 days were incubated in DMED medium containing 50 µM A769662 for 30 min, permeabilized and immunostained. Primary antibodies were rabbit-anti-P-Ser6 BCK, mouse-anti-PDI and DyLight 488 conjugated goat-anti rabbit and DyLight 649 conjugated donkey-anti mouse secondary antibodies. Note: P-Ser6-BCK stain fully overlaps with PDI stain. Bars correspond to 27 µm.

3.4. Discussion

The brain-type isoform of creatine kinase has been identified in this study unambiguously as an *in vitro* and *in vivo* substrate of AMPK. Following its detection in a non-biased *in vitro* screen for novel AMPK substrates in the brain, the involved phospho-site was unambiguously identified and verified by site-directed mutagenesis, and finally this secondary modification was shown not to regulate enzyme activity, but to localize BCK *in vivo* to sites at the endoplasmic reticulum (ER) under situations of AMPK activation as occurring in cellular energy stress.

Phosphorylation events have been repeatedly associated with CK isoforms since the description of BCK as a phosphoprotein in 1984 (Mahadevan et al., 1984), without however providing clear evidence for *in vivo* phosphorylation by specific protein kinases or for the induced putative functional changes. Cytosolic creatine kinases can undergo autophosphorylation at multiple residues close to the active site, albeit at low stoichiometries (Hemmer et al., 1995; Quest et al., 1990; Rosenberg et al., 1981; Stolz et al., 2002). This may modulate substrate binding, without having major effects. For this reason, it cannot be ruled out that the minor changes in enzyme activity reported for phosphorylated MCK in hibernating animals (Abnous and Storey, 2007), frog muscle (Dieni and Storey, 2009) or diabetic heart (Lin et al., 2009) are due to autophosphorylation events. However, recent proteomics studies revealed some CK phosphorylation sites possibly targeted by protein kinases: Ser128 in MCK as potential PKC site (Lin et al., 2009), Ser319, Ser343 and Thr361 in sMtCK (Boja et al., 2009) and

Tyr115 in uMtCK (Lewandrowski et al., 2008). A role of PKC isoforms in a specific phosphorylation of cytosolic BCK (Chida et al., 1990a; Chida et al., 1990b; Chida et al., 1988) or MCK (Lin et al., 2009; Reiss et al., 1996; Yang et al., 2010) remain still elusive, since these studies have not combined unambiguous phosphoprotein identification with mutational studies and functional assays. Finally, AMPK was reported to phosphorylate MCK, without that the residue had been identified, and both enzymes were co-localized in myofibrils (Ponticos et al., 1998). Functionally, it was postulated that MCK phosphorylation by activated AMPK inhibits MCK, while, *vice versa,* a high PCr/Cr ratio maintained by non-phosphorylated, active MCK would inhibit AMPK. However, these regulations were not confirmed by follow-up studies (Ingwall, 2002; Suter et al., 2006; Taylor et al., 2006).

In this study, we present extensive *in vitro* and *in vivo* evidence showing that the BCK isoform is specifically phosphorylated by AMPK. BCK was identified in an *in vitro* screen as already applied to identify novel soluble AMPK targets in brain (Tuerk et al., 2007) and erythrocytes (Thali et al., 2010) and which already yielded other, confirmed AMPK substrates (Hallows et al., 2010). The AMPK-BCK signaling axis was thoroughly confirmed by (i) identification of the involved phosphosite by MALDI-MS/MS and Edman sequencing of phospho-peptides, together with mutagenesis of identified sites into phospho-mimicking aspartate, (ii) detailed analysis of enzyme catalytic parameters, (iii) validation of a specific phospho-BCK antibody *in vitro* and *in vivo*, using peptide competition and BCK-deficient fibroblasts, and (iv) *in vivo* study of BCK phosphorylation using two mechanistically different AMPK activators, AICAR and A769662.

In vitro assays confirmed that BCK phosphorylation mediated by AMPK 221 and somewhat less by AMPK 111 occurs in humans and also in other vertebrate species, including rabbit and chicken. It targets mainly Ser6 and is comparable to acetyl-CoA carboxylase in its kinetics and stoichiometry. This residue is highly conserved in the majority of BCK species (Table 3-2). Importantly, AMPK-dependent Ser6 phosphorylation also occurs *in vivo* (see below). The presence of different P-Ser6-BCK spots in 2D-PAGE of AICAR-treated astrocytes suggests that phosphorylation by AMPK adds to (auto) phosphorylation at different other sites that occur *in vivo* and have been yet reported (Hemmer et al., 1995; Quest et al., 1990; Rosenberg et al., 1981; Stolz et al., 2002). The Ser6 residue and its N-flanking region are conserved across vertebrates, while the C-flanking region is identical except the +3 and +4 residues. The Ser6 site does not fit entirely with the general consensus motif for AMPK derived from some long known substrates (Φ(X,β)XXS/TXXXΦ, where Φ is a hydrophobic residue, β a basic residue and the order within parentheses is not critical; (Scott et al., 2002)), but conforms reasonably well to residues identified in a peptide library profiling for an optimal AMPK phosphorylation motif (Gwinn et al., 2008). AMPK substrate recognition requires active AMPK αTD and non-phosphorylated BCK. It is abolished with AMPK α wild-type or the phospho-mimicking S6D BCK mutant, suggesting that only AMPK activation allows for its interaction with BCK. Since the interaction can only be detected by Y2H assay, it is of rather low affinity, rapid “kiss-and-run” character. As for the stoichiometry of almost one phosphorylation per BCK dimer, this corresponds

very well to the molecular structure of BCK that we solved 10 years ago (Eder et al., 1999). BCK always occurs in homodimeric form, but folds into a structural heterodimer (Figure 3-11A). Only one monomer has its N-terminus exposed at the convex side of the banana-shaped dimer, while the N-terminus of the second monomer folds back into the monomer/monomer interface (Figure 3-11B,C). Thus, effectively only one Ser6 per BCK dimer would be accessible for AMPK phosphorylation.

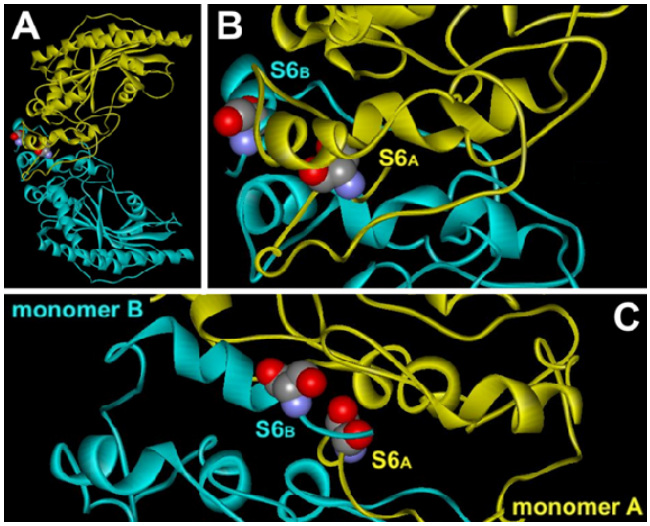

Figure 3-11. Location of the Ser6 phosphosite within the BCK dimeric structure. The high resolution chicken BCK structure (Eder et al., 1999) is shown in backbone representation with schematic secondary structure elements. (A) Banana-shaped BCK dimer with monomer A in yellow and monomer B in cyan, (B) Close-up of the N-termini at the monomer/monomer interface. Ser6 is represented in CPK representation. Note the divergent N-termini in the two monomers, with monomer B folding inwards thus shielding Ser6 from the surface. (C) Close-up of (B), rotated by 90° to view the convex side of the dimer. Note: exposure of the hydroxyl function of Ser6 in monomer B. (Figure prepared with WebLab ViewerPro 4.0).

All studies addressing the function of CK phosphorylation so far tested mainly for specific activities and affinity values for the substrates, reporting changes at or below 50%, as e.g. for the purported inhibition of MCK by PKC (Lin et al., 2009) or AMPK (Ponticos et al., 1998). Studies using ^{31}P NMR spectroscopy of intact rat heart revealed that an increase rather than a decrease in MCK activity occurs at increased workload that is associated with higher AMP levels and AMPK reaction velocity, suggesting that AMPK itself does not inhibit CK activity at least in the heart. In this study, we did neither observe any significant change in the catalytic parameters with the phospho-mimetic BCK S6D mutant. It may also be questioned whether the reported activity changes would be sufficient to effectively regulate a high turnover enzyme like CK *in vivo*, as heterozygous CK knockout animals with strongly reduced CK levels have no obvious phenotype (van Deursen et al., 1994).

Effects of BCK phosphorylation on subcellular localization have not been addressed so far. Only interaction of MCK with the plasma membrane sodium-calcium exchanger has been reported to depend on a putative Ser123 phosphorylation of MCK (Yang et al., 2010); MCK was thus able to reactivate the exchanger under energy-compromised conditions, seemingly without requiring changes

in enzymatic activity. In the study presented here, we analyzed subcellular localization of phosphorylated BCK in mouse primary astrocytes or fibroblasts treated with two different AMPK activators, AICAR or A-769662, and using confocal microscopy with a highly specific anti-P-Ser6-BCK antibody. Taken together, the results show that (i) basic levels of phospho-BCK are low in astrocytes and fibroblasts, (ii) BCK is phosphorylated *in vivo* by activated AMPK in both cell types, (iii) detection of phospho-BCK by anti-P-Ser6 antibody is specific as seen with transgenic MEFs lacking BCK, (iv) localization of phospho-BCK after treatment with A-769662 or AICAR is exclusively perinuclear, (v) only a small part of total BCK enters in this phosphorylated perinuclear pool, and (vi) this localization perfectly superimposes with markers of the endoplasmic reticulum. Such a phosphorylation-induced targeting may involve the small conformational change indicated by the shift in Stokes radius of S6D mutant protein compared to wild-type. In fact, the phospho-residue is well located at the convex side of the BCK dimer to engage into interactions without disturbing the active sites located at the concave side of the dimer (Figure 3-11A). The Ser6-site is also close to the domain which in homologous MCK mediates binding to myomesin and M-protein in the myofibrillar M-band (Hornemann et al., 2003; Hornemann et al., 2000).

Our data indicate that AMPK activated during cellular energy stress phosphorylates BCK to direct it to sites at the endoplasmic reticulum. Although BCK is mainly distributed homeogenously in the cytoplasm, it is well known that it also partially associates with different cellular structures. In astrocytes, BCK is found in peripheral regions and pseudopodia and seems to associate with the cytoskeleton and to contribute to cell shape and motility (Kuiper et al., 2009). At the plasma membrane, BCK binds to and activates membrane-associated thrombin receptor PAR-1 (Mahajan et al., 2000) and potassium-chloride-channel, KCC2 (Inoue et al., 2004), and at the Golgi it interacts transiently with GM130 (Burklen et al., 2007). At all these specific sites, BCK can locally regenerate ATP and provide it to ATP-dependent processes in close vicinity, building-up so called microcompartments. In particular at membrane surfaces, where ATP diffusion may become limiting much earlier during energy stress, such BCK microcompartments can overcome diffusional limitations. We thus propose that phosphorylation of BCK in cells as astrocytes or fibroblasts is a molecular mechanism to recruit BCK into ER microenvironments where it is functionally coupled to ATP-requiring reactions.

The ER is known for its high ATP requirements related to different functions such as protein translation, protein folding and assembly, posttranslational protein modifications, or calcium sequestration (Chen et al., 2010). ER function is highly sensitive to stress that perturbs cellular energy levels, redox state or Ca^{2+}. Although localization at the ER membrane has not yet been described for BCK, association of the homologous MCK isoform with ER and its functional importance in particular for the activity of sarcomeric/endoplasmic reticulum Ca^{2+} ATPase (SERCA) are well established (Levitsky et al., 1978; Rossi et al., 1990). The phenotype of MCK knockout mice clearly points to dysregulated calcium homeostasis due to lower SERCA activity (de Groof et al., 2002; Steeghs et al., 1997). ATP consumption by SERCAs may explain up to 20% of whole body total daily

energy expenditure (Norris et al., 2010) and SERCA function strongly depends on a high local ATP/ADP ratio. Under energy-compromised conditions mostly linked to cytosolic Ca^{2+}-overload, AMPK might thus support SERCA activity by providing an energy buffering microenvironment. Indeed, also the calcium ionophore A-23187 activated AMPK in astrocytes via CaMKK, the main AMPK upstream kinase in brain, and resulted in the same ER-associated phospho-BCK signal (data not shown). Thus, high cytosolic [Ca^{2+}] would be directly sensed by the CamKK-AMPK cascade to phosphorylate BCK and improve SERCA activity. In direct support of such a mechanism, Dong et al. have shown recently that SERCA activity was altered in AMPK α2-/- endothelial cells and could be restored by transfection of constitutive active AMPK (Dong et al., 2010). Increasing intracellular [Ca^{2+}] and a decrease of SERCA activity due to the absence of AMPK finally induced ER stress, suggesting that AMPK can act as a physiological suppressor of ER stress, possibly via BCK. Most recently, an analogous situation has been described for intracellular Ca^{2+} handling at the plasma membrane. MCK was found to translocate from the cytosol to the plasma membrane, where it co-localized and interacted with the Na^{+}/Ca^{2+} exchanger (NCX1; (Yang et al., 2010)) for removing Ca^{2+} from the cytosol (Bonz et al., 2002).

ATP is necessary for different ATP-dependent processes at the ER surface, but also must be imported inside the lumen space to maintain multiple functions. Lack of ATP in this compartment may induce ER stress (Schroder, 2008). Recently, ER-ANT1, an ATP/ADP transporter was localized in the ER membrane in *Arabidopsis* (Leroch et al., 2008). ER-ANT1 knockout showed an impaired ER metabolism due to ATP deficiency within the ER lumen. Although in mammals the corresponding ATP carrier has not yet been identified, ATP transport across ER membranes has been shown to occur (reviewed in Hirschberg et al., 1998). We therefore hypothesized that phosphorylation-mediated BCK confinement to ER may be also important to assure ATP supply into the ER lumen in a hypothetical microcompartment associating phospho-BCK with a putative ER ATP-transporter.

Taken together, we have characterized in this study a post-translational regulation of BCK by AMPK that may be important under energy stress. Ser6 is the major BCK site phosphorylated by AMPK, and this does not affect enzymatic activity of BCK but instead influences BCK localization with the ER membrane. Further investigations are required to determine the precise regulation mechanisms that connects AMPK activation to BCK mediated ATP supply and ER function.

3.5. Experimental Procedures

3.5.1. Materials

AICA-Riboside (AICAR) was from Biotrend Chemicals (Zurich, Switzerland). A769662 was gently provided by Grahame Hardie (Division of Molecular Physiology, College of Life Sciences and University of Dundee, UK), wild type and BAK-/- (BCK/AK1 double knockout) mouse embryonic fibroblasts (MEFs) were gently provided by Bé Wieringa (Nijmegen Center for Molecular Life Sciences, NCMLS, University of Nijmegen, The Netherlands). If not stated otherwise, antibodies were from Cell Signaling (Cell Signaling Technology, Danvers, MA, USA). The antibody against the N-terminal phosphorylated Ser6-residue of BCK was obtained by immunization of rabbits with the synthetic peptide MPFSN(P~S)HNALKL (Eurogenetec, Angers, France). Anti-peptide antibody was purified against the peptide used for immunization and used at 1/100 or 1/1000 dilution.

3.5.2. Creatine kinase proteins, mutants and their purification

Rabbit BCK purified from brain tissue was obtained from Sigma (St Louis, USA). Chicken BCK (b subtype, B_b-CK, GeneID: 396248) subcloned into pET-3b (Novagen, Madison, USA; Stolz & Wallimann 1998), human BCK (GeneID: 1152) subcloned into streptavidin-fusion vector and human BCK non-tagged subcloned into pET42(+) vector (Novagen) were expressed in bacteria and purified as described earlier (Eder et al., 1999) with minor modifications. In particular, the entire procedure was adapted to an automated HPLC system (ÄKTA Explorer 100, GE Healthcare) run at 10°C. Briefly, cells were lysed by sonication in 50 mM Tris-HCl, pH 8.0, 15% sucrose, 125 U benzonase (Merck, Whitehouse station, NJ, USA), unsoluble material was removed by centrifugation (25000 g, 40 min, 4°C), the supernatant was adjusted to pH 5.8 and loaded onto a Blue Sepharose column (GE Healthcare, Buckinghamshire, UK) equilibrated with 50 mM NaPi buffer (pH 5.8). After washing BCK was eluted with NaPi-buffer (pH 8.0) containing 10 mM MgADP. Samples were desalted with a HiPrep 26/10 desalting column against 25 mM Tris-HCl (pH 8.0) and further purified on a Resource Q column. BCK proteins eluted at ~ 240 mM NaCl and were essentially pure as judged by SDS-PAGE (Suppl. Figure 3-4).

Site-directed mutagenesis of Ser6 in human BCK was performed by PCR with Phusion DNA polymerase (Finnzymes) using mutagenic primers given in Suppl. Table 3-1. PCR products were purified using a Nucleo Spin Extract II (Macherey Nagel), self-ligated using T4 DNA ligase (New England Biolabs). All constructs were verified by DNA sequencing.

Wild type AMPK α1β1γ1 (111WT) and α2β2γ1 (221WT) isoform combinations, as well as the corresponding constitiutively active forms mutated at αT172, α1T172Dβ1γ1 (111TD) or α2T172Dβ2γ1 (221TD) were expressed in bacteria from polycistronic vectors and purified by multi-dimensional HPLC as described earlier (Neumann et al., 2003; Riek et al., 2009). CamKKβ GST fusion from pGEX-PreS-CamKKβ (gently provided by H. Tokumitsu, Kagawa Medical University, Japan) and GST-ACC fusion construct (gently provided by G. Hardie, Univ. of Dundee, UK) were expressed and purified with standard protocols as described (Tokumitsu et al. 2001., Scott et al. 2002).

3.5.3. Phosphorylation of BCK by AMPK *in vitro*

For phosphorylation of different BCK species 240 pmol protein were incubated for 3 min at 37°C in the presence or absence of 10 pmol AMPK 111TD in kinase buffer (200 mM [γ-^{32}P]ATP with a specific activity of 400 mCi/mmol ATP, 50 mM AMP, 5 mM $MgCl_2$, 1 mM DTT, and 10 mM HEPES, pH 7.4). Alternatively, AMPK 111WT or AMPK 221WT was activated by 20 min incubation at 30°C with 1 pmol CamKKβ in kinase buffer without radiolabel. BCK WT or mutants (200 pmol) were incubated for 3 min at 37 °C in the presence or absence of 3.5 pmol pre- activated 111WT or 221WT in kinase buffer (200 mM [γ-^{32}P]ATP with a specific activity of 400 mCi/mmol ATP, 50 mM AMP, 5 mM $MgCl_2$, 1 mM DTT, and 10 mM HEPES, pH 7.4). Kinase reactions were stopped by addition of SDS sample buffer. Aliquots containing 9 µg of protein were subjected to 10% SDS-PAGE and autoradiography or analysis on a Typhoon scanner (GE Healthcare).

3.5.4. Mass spectrometry and Edman sequencing

Purified untagged human BCK was phosphorylated *in vitro* by constitutively active AMPK 111TD as described above. Gels were dried, gel bands corresponding to BCK were excised and rehydrated in water, and protein was digested in-gel with trypsin as described (Benvenuti et al., 2002). A volume of 1-5 µl of concentrated tryptic peptides were applied to a microbore reversed-phase column (ZORBAX SB C_{18}, Agilent Technologies, Santa Clara, CA, USA) connected to an Agilent 1100 capillary LC system that was equipped with a microcollection/spotting system (for PAC, Prespotted AnchorChip) to separate the peptides derived from digestion. The flow rate for peptide elution was 7 µl/min, and peptide separation was monitored at 220 and 280 nm. After the run, the PAC was allowed to dry at room temperature and exposed to autoradiography film. The presence of radiolabeled phosphopeptides were analyzed by MALDI-MS and MALDI tamdem MS (MS^2) using an upgraded Bruker Daltonics Ultraflex TOF/TOF II MALDI mass spectrometer as described (Tuerk et al., 2007). Selected radioactive peptides were subjected to sequencing by Edman degradation as described (Tuerk et al., 2009).

3.5.5. Determination of catalytic properties of CK

Enzymatic activity of purified BCK WT and mutants were determined using a coupled enzyme assay as described (Schlattner et al., 2000). Briefly, ATP production (reverse reaction) was coupled by hexokinase (400 U/ml) and glucose-6-phosphate dehydrogenase (150 U/ml) to NADPH production, using 2 mM ADP, 5 mM $MgCl_2$, 20 mM PCr, 40 mM D-glucose and 1 mM NADP in 0.1 M triethanolamine buffer pH 7. PCr production (forward reaction) was coupled by pyruvate kinase (160 U/ml) and lactate dehydrogenase (800 U/ml) to NADH oxidation, using 4 mM ATP, 4.5 mM Mg-acetate, 20 mM Cr, 3 mM PEP and 0.45 mM NADH in 0.1 M triethanolamine buffer pH 8. Changes in the redox state of pyridine nucleotides were followed at 340 nm in a Specord 210 spectrophotometer (Analytikjena, Jena, Germany) thermostated at 25°C. For the determination of dissociation rate constants (Kd, Km) a matrix of initial velocity data was recorded by varying 5 different concentrations

of each substrate at 5 different, fixed concentrations of the second substrate. Fixed concentrations were 0.5, 1, 2, 4 and 20 mM PCr; 0.02, 0.1, 0.2, 0.4 and 2.0 mM ADP; 0.5, 1, 2, 5 and 10 mM Cr; 0.1, 0.2, 0.8, 2 and 4 mM ATP, always keeping the ratio Mg^{2+}/nucleotide constant. The data were analyzed by global fitting with a random equilibrium model (Sigma Plot Enzyme Kinetics Module).

3.5.6. Cellulose polyacetate electrophoresis (CPAE).

Astrocytes cultured for 14 days were incubated in presence or absence of 50 μM A769662 for 30 min at 37 °C. Astrocytes lysates were prepared as described (Kuiper et al., 2009). CK isoenzymes from astrocytes were separated by native cellulose polyacetate electrophoresis (CPAE) for 1 h at 150 V at room temperature (Tokarska-Schlattner et al., 2005). Electrophoresis was performed on Cellogel strips (No. OlA42, Biotec-Fischer, Reiskirchen, Germany) in an electrophoresis tank purchased from the same company, with a running buffer containing 11.7 mM barbiturate, 52.4 mM diethylbarbiturate, 1.4 mM β-mercaptoethanol, pH 8.6. Subsequently, the CK bands were visualized by a color reaction coupled to the CK enzyme activity (Tokarska-Schlattner et al., 2005).

3.5.7. Yeast two-hybrid assay

Potential interaction of BCK WT and S6D mutant with AMPK WT subunits α1, α2 and the constitutive active α2 T172D, as well as β1 and β2 subunit domains (aa 1-54), was analyzed by a cytosolic yeast-two-hybrid (Y2H) technique based on reconstitution of split-ubiquitin (cytoY2H, Dualsystems Biotech, Schlieren, Switzerland) with the novelty that the bait is anchored at the plasma membrane and not the ER (Brückner et al, 2009).Cloning procedures using Sfi1 sites, transformation of yeast cell line NMY51 and yeast spotting were performed as described earlier (Mockli et al., 2007). Yeast cells were spotted on selective medium lacking tryptophan and leucine (SD-WL) for growth verification in order to verify the presence of bait and prey plasmid and on medium lacking tryptophan, leucine, adenine and histidine (SD-AHWL) for protein interaction analysis. The spotted plates were incubated 72 h at 30°C. The dimerization of BCK served as positive and the interaction of BCK with Large T antigen *(Simian virus)* as negative control.

3.5.8. Gel filtration chromatography

Pure BCK WT and mutant proteins were separated by HPLC using a Superose 12 gel filtration column (Pharmacia) in GF buffer (25 mM Tris-HCl, 150 mM NaCl and 2 mM β-mercaptoethanol, pH 8.0) at 1.0 ml/min and 10°C. The column was calibrated for Stokes' radii with the following marker proteins myoglobin (17 Å, 17.81 kDa), ovalbumin (30.5 Å, 45.7 kDa), gamma globulin (52 Å, 158 kDa), and thyroglobulin (70 Å, 669 kDa).

3.5.9. Cell culture and treatments

Primary cortical astrocytes were prepared aseptically from cerebral hemispheres of 3-4-day-old mice pups, according to previously described methods (Booher and Sensenbrenner, 1972), with some modifications. Pups were sacrificed by decapitation under sterile conditions. Cerebral hemispheres were dissected free of meninges and gently dispersed in a DMEM/F12 high glucose supplemented with 10% inactivated fetal calf serum and 1% penicillin, streptomycin and amphotericin B. In typical cultures, more than 95% of the cells were identified as astrocytes by immunostaining for glial fibrillary acidic protein (GFAP). Mouse embryonic fibroblasts (MEFs) wild type or BAK-/- were cultured as described (Kuiper et al., 2009). When cultures were close to confluence, they were treated with 50 μM A769662 or 1 mM AICAR (dissolved in DMSO or water respectively) for 30 min at 37°C.

3.5.10. Immunoblotting

Cortical astrocyte lysates were prepared as described (Kuiper et al., 2009). Cell extracts were prepared in lysis buffer containing protease inhibitor cocktail (Roche Diagnostics, Mannheim, Germany) and phosphatase inhibitor cocktail (GE, Healthcare). Samples were resolved by 10% SDS-PAGE or 2D-PAGE and transferred to Hybond ECL nitrocellulose membrane (Amersham Biosciences, Buckinghamshire, UK). Membranes were washed 3x in Tris-buffered saline with 0.1% Tween-20 (TBST), incubated in TBST with 5% nonfat dry milk (TBST-M) for 1h at room temperature (RT), washed again 3x in TBST, and incubated with the following primary antibodies diluted in TBST-M for 1h at RT or overnight at 4°C: rabbit polyclonal antibodies against P-αThr172-AMPK (1:1000, Cell Signaling), P−Ser79 acetyl-CoA carboxylase (1:1000, Cell Signaling), P−Ser6 BCK (1:1000), total AMP-activated protein kinase alpha (1:1000, Cell Signaling) and total BCK (1:2000; generated and characterized previously by Schlattner et al., 2002). Washed 3x in TBST, membranes were incubated in a TBST-M dilution of secondary antibodies coupled to horseradish peroxidase for 1h at RT (1:5000, Cell Signaling). After 3x washing in TBST, immunoreactive bands were visualized using enhanced chemiluminescence (ECL plus, Amersham Biosciences, Buckinghamshire, UK) and film or quantified by a ImageQuant LAS4000 (GE Healthcare).

3.5.11. 2D-PAGE

Cortical astrocytes were suspended in 1 ml sample buffer (7 M urea, 2 M thiourea, 4% CHAPS, 40 mM DTT, 1.0% v/v IPG buffer, 0.5% v/v Triton X-100, protease inhibitor cocktail (Roche Diagnostics, Mannheim, Germany) and phosphatase inhibitor cocktail (GE, Healthcare), sonicated on ice and left for 1 h at 4°C to allow full solubilization. The suspension was centrifuged at 14 000g for 60 min at 4°C, desalted with a 2-D clean-up kit (GE Healthcare, Buckinghamshire, UK). The protein content was determined by the 2D-Quant kit (GE Healthcare). Approximately 0.5 mg extracted or pure proteins were separated in a first dimension on an EttanIPGphor 3 using immobilized pH 3-10 nonlinear gradient gel strips (24 cm, GE Healthcare). For isoelectric focusing voltage was gradually

increased from 0 V to 10 000 V during 12 h and then kept constant for 4 h to achieve about 64 500 Vh in total. Strips were then equilibrated in 75 mM Tris-HCl pH 8.8, 6 M Urea, 29.3% glycerol, 2% SDS, and 0.002% bromophenol blue, in presence of first 1% DTT (w/v) and then 2.5% iodoacetamide (w/v). For protein separation in the second dimension, strips were applied to large 10% SDS-PAGE gels. After protein fixation with 50% ethanol and 10% acetic acid for 1 h, gels were stained with colloidal Coomassie Blue (Roth, Germany) for 12 h. Excess of the dye was washed out with distilled water.

3.5.12. Immunofluorescence

Astrocytes were grown onto Lab-Tek chamber slides (Thermo Scientific Nunc, Rochester, NY, USA), treated with AMPK activators as described above, rinsed twice with pre-warmed phosphate-buffered saline (PBS), and fixed with 3% paraformaldehyde in PBS. Following three washing steps in PBS, cells were permeabilized with 0.2% Triton X-100 in PBS. After extensive washing with PBS, cells were blocked for 1h in PBS containing 3% bovine serum albumin (BSA) and 0.1% Tween 20, incubated 1h at RT or overnight at 4°C with primary antibodies diluted in blocking buffer, washed three times with blocking buffer and incubated with secondary antibodies in blocking buffer for 45min at RT. Applied primary antibodies were rabbit anti-P-Ser6 BCK (1:100, Eurogenetec), mouse anti-PDI (1:100, ER marker, Abcam, Cambridge, UK) and chicken-anti-BCK (1:200, generated and characterized previously by Schlattner et al., 2002). Applied secondary antibodies were DyLight 649 (red fluorescence) conjugated goat-anti rabbit (1:250, Jackson ImmunoResearch, Baltimore, USA) or DyLight 488 (green fluorescence) conjugated goat-anti rabbit (1:250, Jackson ImmunoResearch), DyLight 649 (red fluorescence) conjugated donkey anti-mouse (1:250, Jackson ImmunoResearch) and DyLight 649 (red fluorescence) conjugated donkey-anti chicken (1:250, Jackson ImmunoResearch). Different cellular structures (plasma membrane, Golgi) were stained with 50 µg/µl of WGA (wheat germ agglutinin) directly coupled to Alexa Fluor 350 (Invitrogen, USA). Nuclei were stained with 1 µM Hoechst dye (Interchim, Montlucon, France) and mitochondria with 250 nM Mitotracker Red CMXRos (Invitrogen). Images were collected with a Leica TCS SP2 Acoustico Optical Beam Splitter (AOBS) inverted laser scanning confocal microscope equipped with a coherent 351-364 UV laser using a x63 water immersion objective (HCX PL APO 63.0 x 1.20 water corrected). Laser excitation was 351/364 nm for Hoechst (nuclei) and WGA, 488 nm for DyLight 488, 633 nm for DyLight 649 and 579 for Mitotracker Red CMXRos. Confocal pinhole (Airy units) was 1. In double staining of phospho BCK and PDI, confocal sections of both fluorescent signals were taken simultaneously, the 3D reconstruction images were recorded, and merged images of the two signals were obtained using confocal microscope software. Each experiment was performed on a randomly chosen field containing several cells.

3.6. Supplementary Tables

SUPPL. TABLE 3-1. **Mutagenic primers used for mutation of human BCK phosphosites.**

Mutation	Sense/antisense	Primer code	Sequence
S6D	Sense	S6Dfw	CTTCTCCAACGACCACAACGCACTG
	Antisense	S6DRv	CAGTGCGTTGTGGTCGTTGGAGAAG
T35D	Sense	T35Dfw	GCCAAGGTGCTGGACCCCGAGCTGTAC
	Antisense	T35DRv	GTACAGCTCGGGGTCCAGCACCTTGGC
S6DT35D	Sense	S6Dfw	CTTCTCCAACGACCACAACGCACTG
	Antisense	T35DRv	GTACAGCTCGGGGTCCAGCACCTTGGC

Mutagenic mismatches with the template are underlined.

3.7. Supplementary Figures

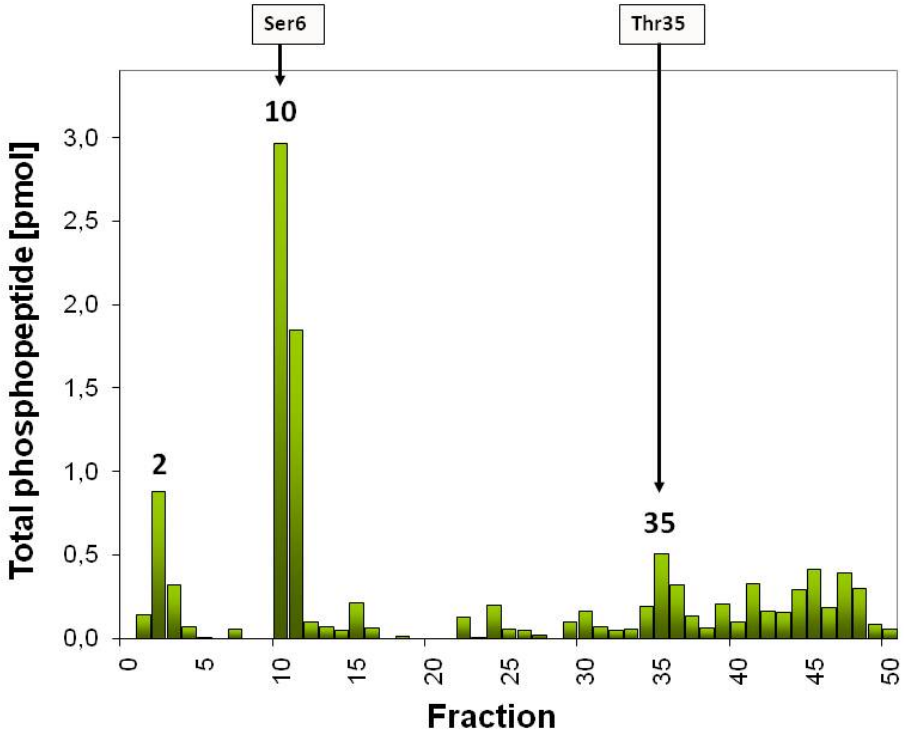

SUPPL. FIGURE 3-1. RC-HPLC profile of tryptic BCK [^{32}P]-phosphopeptides. Pure recombinant huBCK was phosphorylated by constitutive active recombinant α1β1γ1 (111) AMPK (αT172D mutant). Fractions 10 and 35 have been analyzed by MS/MS (Table 1) and Edman sequencing (Figure 3-2). No Phosphopeptide was found in fraction 2.

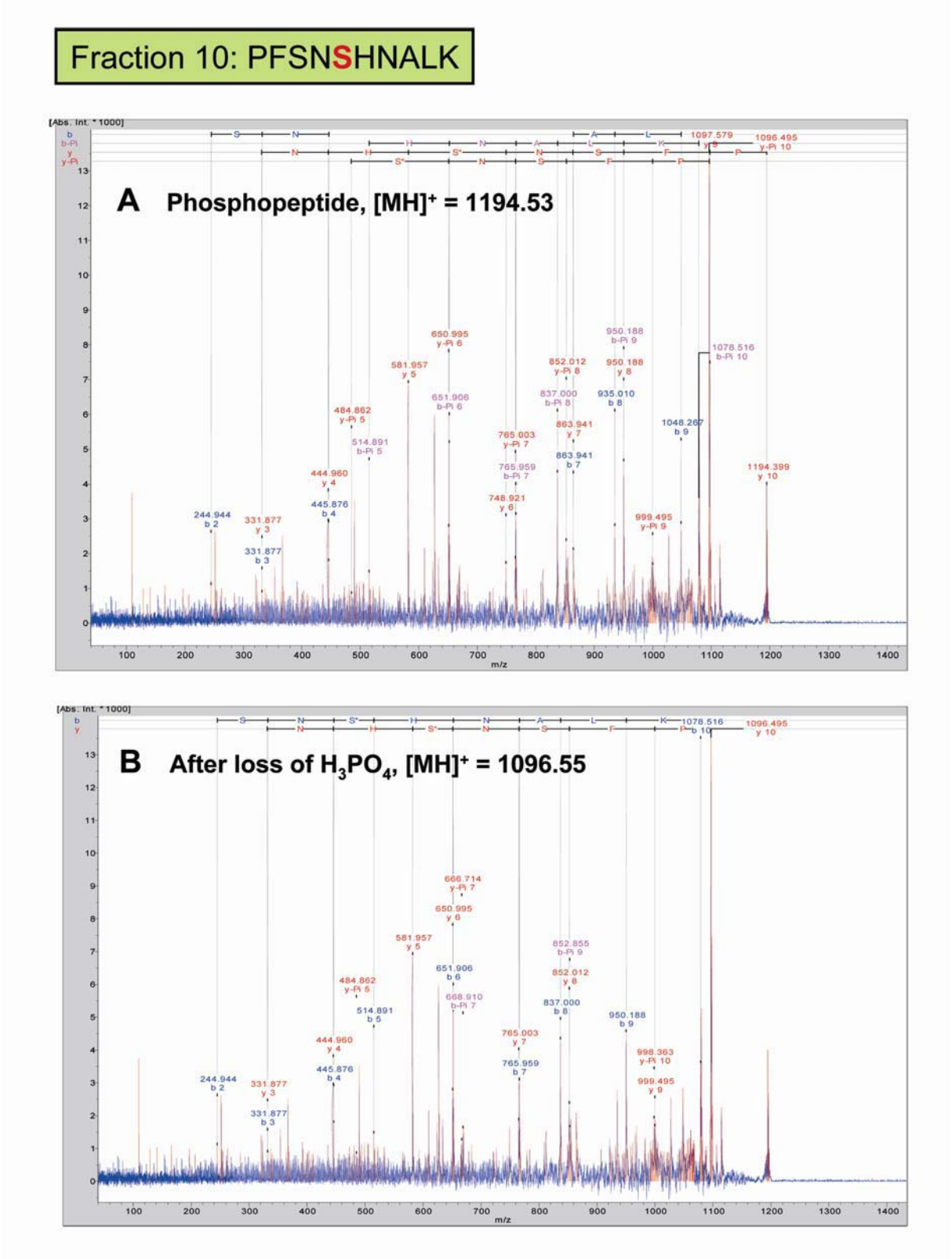

SUPPL. FIGURE 3-2. MS/MS spectrum of fraction 10. Identified peptide PFSNSHNALK as phosphopeptide ($[MH]^+$ = 1194.53, top) or after loss of H_3PO_4 ($[MH]^+$ = 1096.55, bottom).

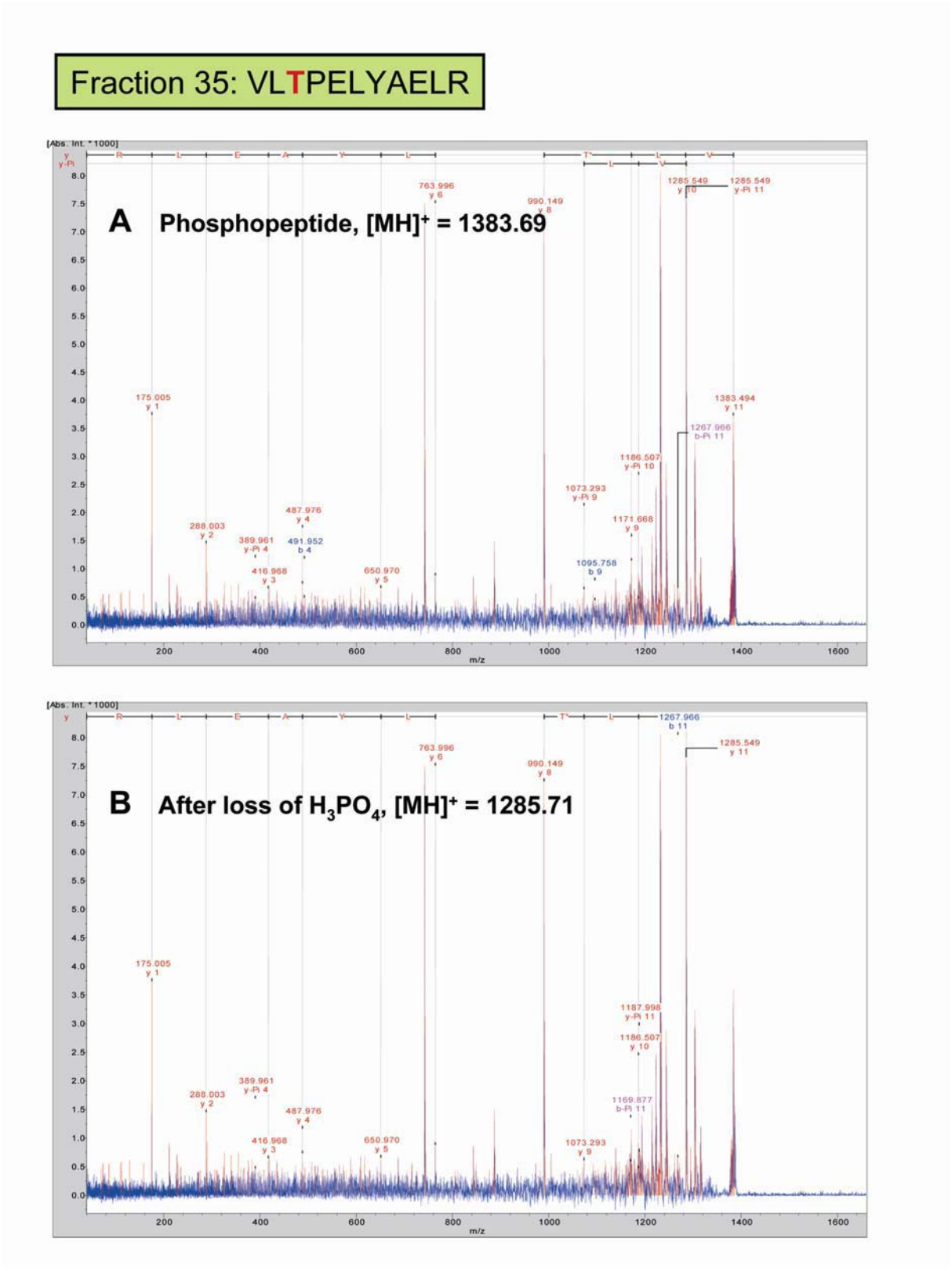

SUPPL. FIGURE 3-3. MS/MS spectrum of fraction 35. Identified peptide VLTPELYAELR as phosphopeptide ($[MH]^+$ = 1383.69, top) or after loss of H_3PO_4, ($[MH]^+$ = 1285.71, bottom).

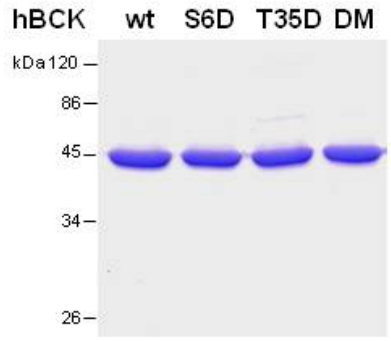

SUPPL FIGURE 3-4. Wild-type and mutant BCK proteins purified by a multidimensional protocol. Coomassie Blue-stained 12 % SDS-PAGE, showing the purity of untagged human BCK wild-type and mutant proteins purified by two steps column chromatography including affinity chromatography with Blue Sepharose and cation exchange chromatography with Resource Q resin. 5 µg protein per lane. Wt; wild type BCK, S6D; Ser6 mutant, T35D; Thr35 mutant, DM; Ser6-Thr35 mutant.

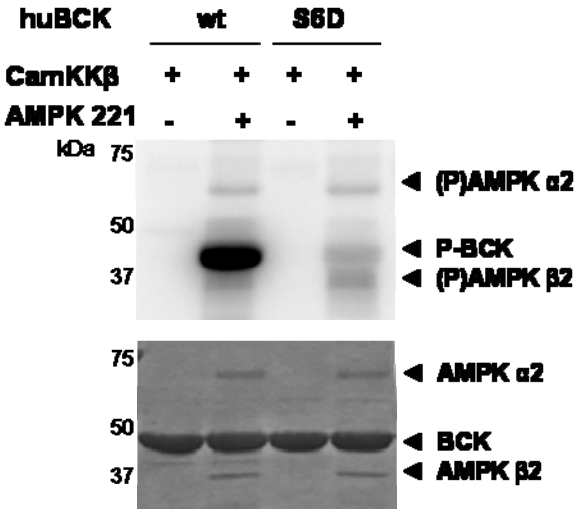

SUPPL. FIGURE 3-5. Phosphorylation of BCK wild-type depends on AMPK, not the upstream kinase CamKKβ. Non-tagged wild type BCK and S6D mutant (200 pmol) were subjected to *in vitro* phosphorylation assays with [γ-^{32}P]ATP, in presence or absence of AMPK $\alpha2\beta2\gamma1$ wild-type (221WT, 3.5 pmol) previously activated by CamKKβ (1 pmol). Reaction mixtures were analyzed by SDS-PAGE, Coomassie Blue-staining and Typhoon phosphoimager. Note: S6D is no longer phosphorylated by AMPK; AMPK α and β subunits are autophosphorylated, see (P)AMPKα2 and (P)AMPKβ2.

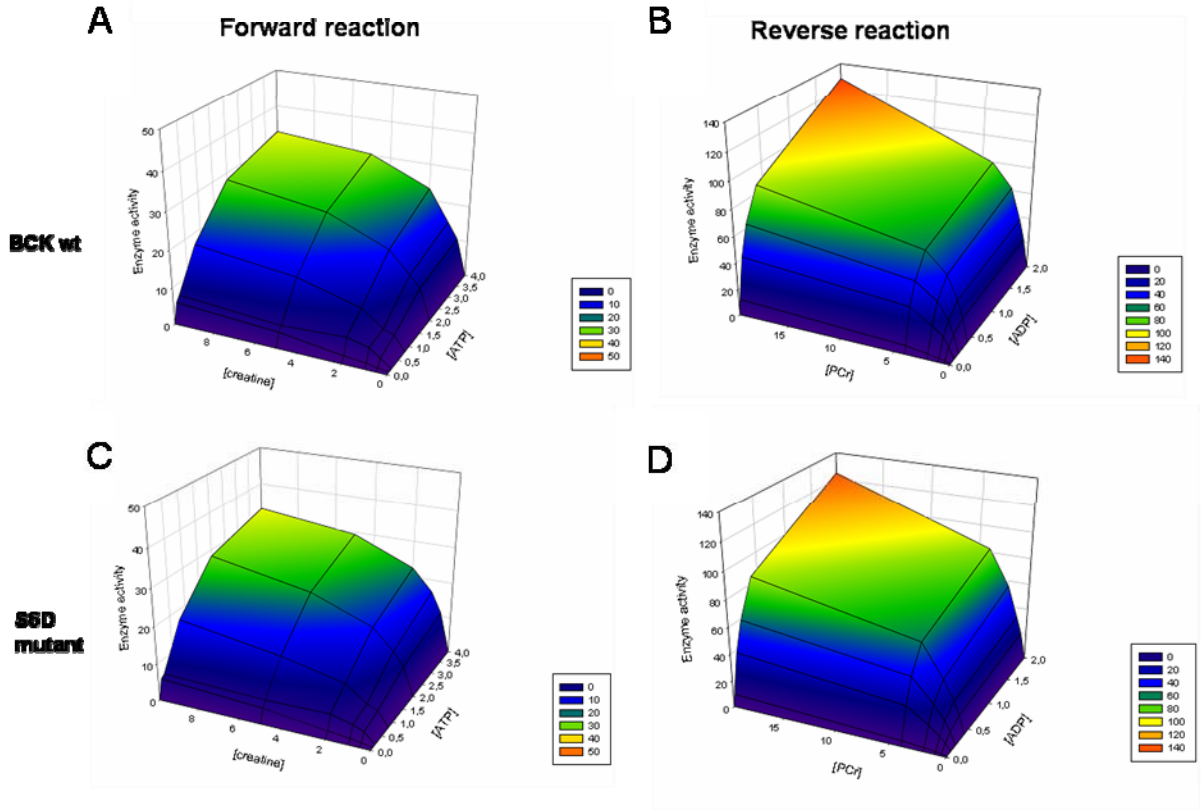

SUPPL. FIGURE 3-6. BCK wild-type and phospho-mimetic mutant S6D do not differ in enzymatic activity. Analysis of enzymatic activity of human wild-type BCK (A,B) or S6D mutant (C,D) in the (A,C) forward reaction with MgATP and creatine (Cr), or (B, D) reverse reaction with MgADP and phosphocreatine (PCr).

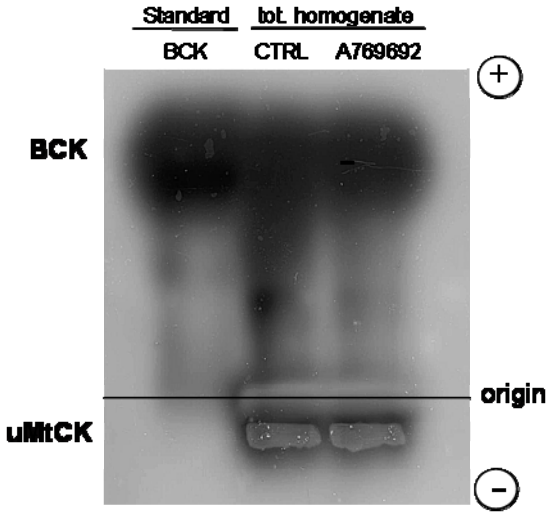

SUPPL. FIGURE 3-7. Effect of A769662 on the BCK activity in astrocytes. Astrocytes cultured for 14 days were incubated in DMEM medium containing vehicle dH20 (CTRL) or 50µM A769662 for 30 min at 37 °C. CK isoenzymes were separated by native cellulose polyacetate electrophoresis (CPAE) and detected by their enzymatic activity. Equal amounts of total protein (40µg) were loaded on each lane for control and treated astrocytes. Purified recombinant BCK was used as standard. Note: BCK activity is not affected by treatment with A769662 as shown by CPAE separation of homogenates with optimized coloration of BCK isoenzymes activities.

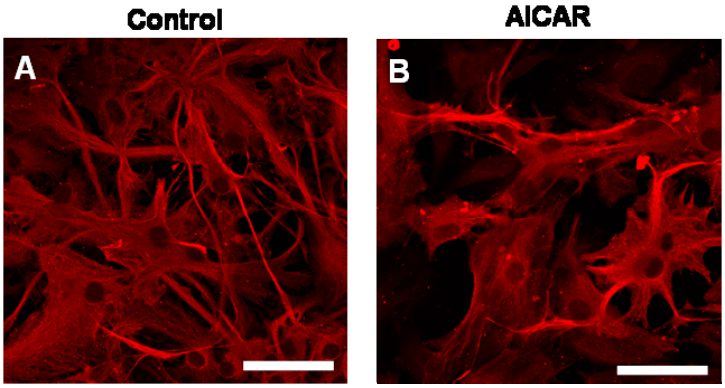

SUPPL. FIGURE 3-8. BCK in astrocytes before and after AMPK activation. Astrocytes cultured for 14 days were incubated in DMEM medium containing (A) vehicle (dH_20), (B) 1 mM AICAR for 30 min at 37 °C. Cells were permeabilized and immunostained with anti-chicken-BCK first antibody and DyLight 649 conjugated goat-anti chicken secondary antibody. Bars correspond to 32 µm.

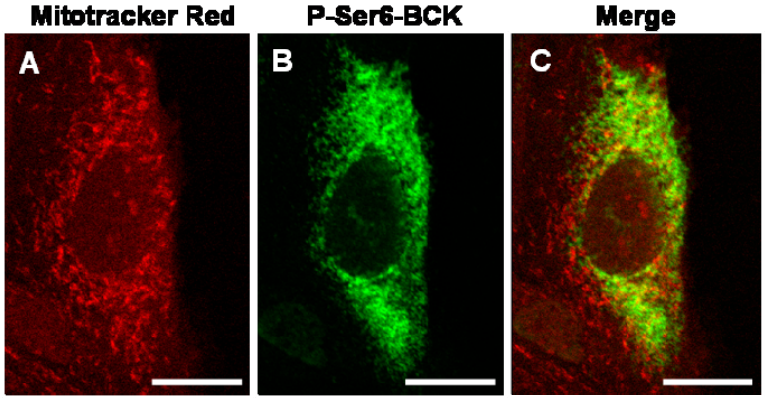

SUPPL. FIGURE 3-9. Astrocyte BCK phosphorylated at Ser6 does not fully co-localize with mitochondria. Cultures of primary mouse cortical astrocytes stained (A) with Mitotracker Red or (B) for P-Ser6-BCK (green fluorescence); (C) merge image. Astrocytes cultured for 14 days were incubated in DMEM medium containing 50µM A769662 for 30 min at 37 °C. After treatment cells were incubated with 250 nM of Mitotracker Red CMXRos for 30min at 37°C and then fixed, permeabilized and immunostained with anti-P-Ser6 BCK antibody and DyLight 488 conjugated goat-anti rabbit secondary antibody. Bars correspond to 22 µm.

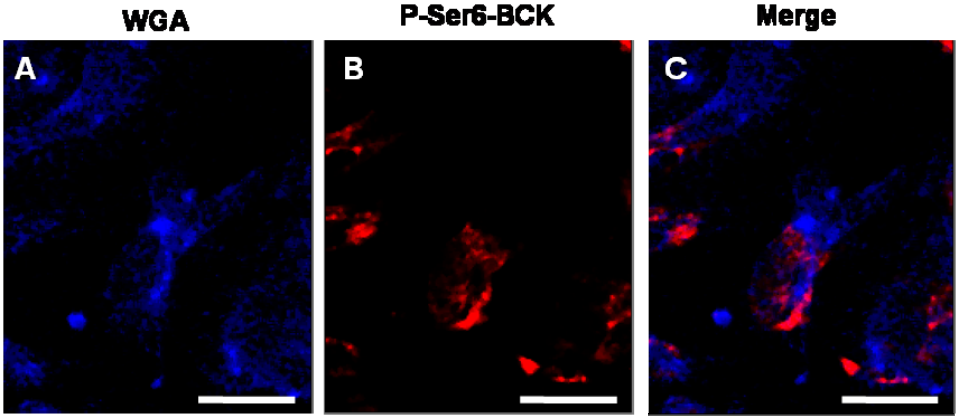

SUPPL. FIGURE 3-10. Astrocyte BCK phosphorylated at Ser6 does not fully co-localize with Golgi apparatus. Cultures of primary mouse cortical astrocytes (A) stained for WGA (wheat germ agglutinin) Golgi marker (blue fluorescence) and (B) P-Ser6-BCK (red fluorescence); (C) merge image. Astrocytes cultured for 14 days were incubated in DMEM medium containing 50µM A769662 for 30 min at 37 °C. After treatment cells were incubated with 50 µg/µl of WGA (wheat germ agglutinin) for 10min at 37°C and then fixed, permeabilized and immunostained with anti-P-Ser6 BCK antibody and DyLight 649 conjugated goat-anti rabbit seconday antibody. Bars correspond 26 µm.

3.8. Footnotes

* This work was supported by EU FP6 contract LSHM-CT-2004-005272 (EXGENESIS), the French Agence Nationale de Recherche ("chaire d'excellence" given to U.S.), and a personal grant no. 183832 of CONACYT (Mexico) to S.R. We thank G. Hardie (University of Dundee, UK), B. Wieringa (Nijmegen University, The Netherlands) and H. Tokumitsu (Kagawa Medical University, Japan) for generously providing reagents. The abbreviations used are: ACC, acetyl-CoA carboxylase; AMPK, AMP activated protein kinase; CaMKK, Ca^{2+}/calmodulin-dependent protein kinase kinase; SD-AHWL, SD-WL, supplement deficient medium lacking Ade-His-Trp-Leu or Trp-Le; Y2H, yeast two-hybrid; AICAR, AICA-riboside; AK1, adenylate kinase 1.

3.9. References

Abnous, K., and K.B. Storey. 2007. Regulation of skeletal muscle creatine kinase from a hibernating mammal. *Arch Biochem Biophys*. 467:10-9.

Benvenuti, S., R. Cramer, J. Bruce, M.D. Waterfield, and P.S. Jat. 2002. Identification of novel candidates for replicative senescence by functional proteomics. *Oncogene*. 21:4403-13.

Boja, E.S., D. Phillips, S.A. French, R.A. Harris, and R.S. Balaban. 2009. Quantitative mitochondrial phosphoproteomics using iTRAQ on an LTQ-Orbitrap with high energy collision dissociation. *J Proteome Res*. 8:4665-75.

Bonz, A.W., S. Kniesch, U. Hofmann, S. Kullmer, L. Bauer, H. Wagner, G. Ertl, and M. Spindler. 2002. Functional properties and [Ca(2+)](i) metabolism of creatine kinase--KO mice myocardium. *Biochem Biophys Res Commun*. 298:163-8.

Booher, J., and M. Sensenbrenner. 1972. Growth and cultivation of dissociated neurons and glial cells from embryonic chick, rat and human brain in flask cultures. *Neurobiology*. 2:97-105.

Bruckner, A., C. Polge, N. Lentze, D. Auerbach, and U. Schlattner. 2009. Yeast two-hybrid, a powerful tool for systems biology. *Int J Mol Sci*. 10:2763-88.

Burklen, T.S., A. Hirschy, and T. Wallimann. 2007. Brain-type creatine kinase BB-CK interacts with the Golgi Matrix Protein GM130 in early prophase. *Mol Cell Biochem*. 297:53-64.

Chen, X., A. Karnovsky, M.D. Sans, P.C. Andrews, and J.A. Williams. 2010. Molecular characterization of the endoplasmic reticulum: Insights from proteomic studies. *Proteomics*.

Chida, K., K. Kasahara, M. Tsunenaga, Y. Kohno, S. Yamada, S. Ohmi, and T. Kuroki. 1990a. Purification and identification of creatine phosphokinase B as a substrate of protein kinase C in mouse skin in vivo. *Biochem Biophys Res Commun*. 173:351-7.

Chida, K., M. Tsunenaga, K. Kasahara, Y. Kohno, and T. Kuroki. 1990b. Regulation of creatine phosphokinase B activity by protein kinase C. *Biochem Biophys Res Commun*. 173:346-50.

Chida, K., S. Yamada, N. Kato, and T. Kuroki. 1988. Phosphorylations of Mr 34,000 and 40,000 proteins by protein kinase C in mouse epidermis in vivo. *Cancer Res*. 48:4018-23.

Davies, S.P., A.T. Sim, and D.G. Hardie. 1990. Location and function of three sites phosphorylated on rat acetyl-CoA carboxylase by the AMP-activated protein kinase. *Eur J Biochem*. 187:183-90.

de Groof, A.J., J.A. Fransen, R.J. Errington, P.H. Willems, B. Wieringa, and W.J. Koopman. 2002. The creatine kinase system is essential for optimal refill of the sarcoplasmic reticulum Ca2+ store in skeletal muscle. *J Biol Chem*. 277:5275-84.

Debrincat, M.A., J.G. Zhang, T.A. Willson, J. Silke, L.M. Connolly, R.J. Simpson, W.S. Alexander, N.A. Nicola, B.T. Kile, and D.J. Hilton. 2007. Ankyrin repeat and suppressors of cytokine signaling box protein asb-9 targets creatine kinase B for degradation. *J Biol Chem*. 282:4728-37.

Dieni, C.A., and K.B. Storey. 2009. Creatine Kinase Regulation by Reversible Phosphorylation in Frog Muscle. *Comp Biochem Physiol B Biochem Mol Biol*.

Dong, Y., M. Zhang, B. Liang, Z. Xie, Z. Zhao, S. Asfa, H.C. Choi, and M.H. Zou. 2010. Reduction of AMP-activated protein kinase alpha2 increases endoplasmic reticulum stress and atherosclerosis in vivo. *Circulation*. 121:792-803.

Eder, M., K. Fritz-Wolf, W. Kabsch, T. Wallimann, and U. Schlattner. 2000. Crystal structure of human ubiquitous mitochondrial creatine kinase. *Proteins*. 39:216-25.

Eder, M., U. Schlattner, A. Becker, T. Wallimann, W. Kabsch, and K. Fritz-Wolf. 1999. Crystal structure of brain-type creatine kinase at 1.41 A resolution. *Protein Sci*. 8:2258-69.

Fritz-Wolf, K., T. Schnyder, T. Wallimann, and W. Kabsch. 1996. Structure of mitochondrial creatine kinase. *Nature*. 381:341-5.

Goransson, O., A. McBride, S.A. Hawley, F.A. Ross, N. Shpiro, M. Foretz, B. Viollet, D.G. Hardie, and K. Sakamoto. 2007. Mechanism of action of A-769662, a valuable tool for activation of AMP-activated protein kinase. *J Biol Chem*. 282:32549-60.

Gwinn, D.M., D.B. Shackelford, D.F. Egan, M.M. Mihaylova, A. Mery, D.S. Vasquez, B.E. Turk, and R.J. Shaw. 2008. AMPK phosphorylation of raptor mediates a metabolic checkpoint. *Mol Cell*. 30:214-26.

Hallows, K.R., P.F. Mount, N.M. Pastor-Soler, and D.A. Power. 2010. Role of the energy sensor AMP-activated protein kinase in renal physiology and disease. *Am J Physiol Renal Physiol*.

Hardie, D.G., S.A. Hawley, and J.W. Scott. 2006. AMP-activated protein kinase--development of the energy sensor concept. *J Physiol*. 574:7-15.

Hemmer, W., E.M. Furter-Graves, G. Frank, T. Wallimann, and R. Furter. 1995. Autophosphorylation of creatine kinase: characterization and identification of a specifically phosphorylated peptide. *Biochim Biophys Acta*. 1251:81-90.

Hirschberg, C.B., P.W. Robbins, and C. Abeijon. 1998. Transporters of nucleotide sugars, ATP, and nucleotide sulfate in the endoplasmic reticulum and Golgi apparatus. *Annu Rev Biochem*. 67:49-69.

Hornemann, T., S. Kempa, M. Himmel, K. Hayess, D.O. Furst, and T. Wallimann. 2003. Muscle-type creatine kinase interacts with central domains of the M-band proteins myomesin and M-protein. *J Mol Biol*. 332:877-87.

Hornemann, T., M. Stolz, and T. Wallimann. 2000. Isoenzyme-specific interaction of muscle-type creatine kinase with the sarcomeric M-line is mediated by NH(2)-terminal lysine charge-clamps. *J Cell Biol*. 149:1225-34.

Ingwall, J.S. 2002. Is creatine kinase a target for AMP-activated protein kinase in the heart? *J Mol Cell Cardiol*. 34:1111-20.

Inoue, K., S. Ueno, and A. Fukuda. 2004. Interaction of neuron-specific K+-Cl- cotransporter, KCC2, with brain-type creatine kinase. *FEBS Lett*. 564:131-5.

Jost, C.R., C.E. Van Der Zee, H.J. In 't Zandt, F. Oerlemans, M. Verheij, F. Streijger, J. Fransen, A. Heerschap, A.R. Cools, and B. Wieringa. 2002. Creatine kinase B-driven energy transfer in the brain is important for habituation and spatial learning behaviour, mossy fibre field size and determination of seizure susceptibility. *Eur J Neurosci*. 15:1692-706.

Kuiper, J.W., H. Pluk, F. Oerlemans, F.N. van Leeuwen, F. de Lange, J. Fransen, and B. Wieringa. 2008. Creatine kinase-mediated ATP supply fuels actin-based events in phagocytosis. *PLoS Biol*. 6:e51.

Kuiper, J.W., R. van Horssen, F. Oerlemans, W. Peters, M.M. van Dommelen, M.M. te Lindert, T.L. ten Hagen, E. Janssen, J.A. Fransen, and B. Wieringa. 2009. Local ATP generation by brain-type creatine kinase (CK-B) facilitates cell motility. *PLoS One*. 4:e5030.

Lahti, D.W., J.D. Hoekman, A.M. Tokheim, B.L. Martin, and I.M. Armitage. 2005. Identification of mouse brain proteins associated with isoform 3 of metallothionein. *Protein Sci*. 14:1151-7.

Leroch, M., H.E. Neuhaus, S. Kirchberger, S. Zimmermann, M. Melzer, J. Gerhold, and J. Tjaden. 2008. Identification of a novel adenine nucleotide transporter in the endoplasmic reticulum of Arabidopsis. *Plant Cell*. 20:438-51.

Levitsky, D.O., T.S. Levchenko, V.A. Saks, V.G. Sharov, and V.N. Smirnov. 1978. The role of creatine phosphokinase in supplying energy for the calcium pump system of heart sarcoplasmic reticulum. *Membr Biochem*. 2:81-96.

Lewandrowski, U., A. Sickmann, L. Cesaro, A.M. Brunati, A. Toninello, and M. Salvi. 2008. Identification of new tyrosine phosphorylated proteins in rat brain mitochondria. *FEBS Lett*. 582:1104-10.

Lin, G., Y. Liu, and K.M. MacLeod. 2009. Regulation of muscle creatine kinase by phosphorylation in normal and diabetic hearts. *Cell Mol Life Sci*. 66:135-44.

Mahadevan, L.C., S.A. Whatley, T.K. Leung, and L. Lim. 1984. The brain isoform of a key ATP-regulating enzyme, creatine kinase, is a phosphoprotein. *Biochem J*. 222:139-44.

Mahajan, V.B., K.S. Pai, A. Lau, and D.D. Cunningham. 2000. Creatine kinase, an ATP-generating enzyme, is required for thrombin receptor signaling to the cytoskeleton. *Proc Natl Acad Sci U S A*. 97:12062-7.

Mockli, N., A. Deplazes, P.O. Hassa, Z. Zhang, M. Peter, M.O. Hottiger, I. Stagljar, and D. Auerbach. 2007. Yeast split-ubiquitin-based cytosolic screening system to detect interactions between transcriptionally active proteins. *Biotechniques*. 42:725-30.

Neumann, D., A. Woods, D. Carling, T. Wallimann, and U. Schlattner. 2003. Mammalian AMP-activated protein kinase: functional, heterotrimeric complexes by co-expression of subunits in Escherichia coli. *Protein Expr Purif*. 30:230-7.

Norris, S.M., E. Bombardier, I.C. Smith, C. Vigna, and A.R. Tupling. 2010. ATP consumption by sarcoplasmic reticulum Ca2+ pumps accounts for 50% of resting metabolic rate in mouse fast and slow twitch skeletal muscle. *Am J Physiol Cell Physiol*. 298:C521-9.

Ponticos, M., Q.L. Lu, J.E. Morgan, D.G. Hardie, T.A. Partridge, and D. Carling. 1998. Dual regulation of the AMP-activated protein kinase provides a novel mechanism for the control of creatine kinase in skeletal muscle. *Embo J*. 17:1688-99.

Quest, A.F., T. Soldati, W. Hemmer, J.C. Perriard, H.M. Eppenberger, and T. Wallimann. 1990. Phosphorylation of chicken brain-type creatine kinase affects a physiologically important kinetic parameter and gives rise to protein microheterogeneity in vivo. *FEBS Lett*. 269:457-64.

Rao, J.K., G. Bujacz, and A. Wlodawer. 1998. Crystal structure of rabbit muscle creatine kinase. *FEBS Lett*. 439:133-7.

Reiss, N., J. Hermon, A. Oplatka, and Z. Naor. 1996. Interaction of purified protein kinase C with key proteins of energy metabolism and cellular motility. *Biochem Mol Biol Int*. 38:711-9.

Riek, U., S. Ramirez, T. Wallimann, and U. Schlattner. 2009. A versatile multidimensional protein purification system with full internet remote control based on a standard HPLC system. *Biotechniques*. 46:ix-xii.

Rosenberg, U.B., H.M. Eppenberger, and J.C. Perriard. 1981. Occurrence of heterogenous forms of the subunits of creatine kinase in various muscle and nonmuscle tissues and their behaviour during myogenesis. *Eur J Biochem*. 116:87-92.

Rossi, A.M., H.M. Eppenberger, P. Volpe, R. Cotrufo, and T. Wallimann. 1990. Muscle-type MM creatine kinase is specifically bound to sarcoplasmic reticulum and can support Ca2+ uptake and regulate local ATP/ADP ratios. *J Biol Chem*. 265:5258-66.

Schlattner, U., M. Eder, M. Dolder, Z.A. Khuchua, A.W. Strauss, and T. Wallimann. 2000. Divergent enzyme kinetics and structural properties of the two human mitochondrial creatine kinase isoenzymes. *Biol Chem*. 381:1063-70.

Schlattner, U., N. Mockli, O. Speer, S. Werner, and T. Wallimann. 2002. Creatine kinase and creatine transporter in normal, wounded, and diseased skin. *J Invest Dermatol*. 118:416-23.

Schlattner, U., M. Tokarska-Schlattner, S. Ramirez, A. Bruckner, L. Kay, C. Polge, R.F. Epand, R.M. Lee, M.L. Lacombe, and R.M. Epand. 2009. Mitochondrial kinases and their molecular interaction with cardiolipin. *Biochim Biophys Acta*. 1788:2032-47.

Schroder, M. 2008. Endoplasmic reticulum stress responses. *Cell Mol Life Sci*. 65:862-94.

Scott, J.W., D.G. Norman, S.A. Hawley, L. Kontogiannis, and D.G. Hardie. 2002. Protein kinase substrate recognition studied using the recombinant catalytic domain of AMP-activated protein kinase and a model substrate. *J Mol Biol*. 317:309-23.

Shin, J.B., F. Streijger, A. Beynon, T. Peters, L. Gadzala, D. McMillen, C. Bystrom, C.E. Van der Zee, T. Wallimann, and P.G. Gillespie. 2007. Hair bundles are specialized for ATP delivery via creatine kinase. *Neuron*. 53:371-86.

Steeghs, K., A. Benders, F. Oerlemans, A. de Haan, A. Heerschap, W. Ruitenbeek, C. Jost, J. van Deursen, B. Perryman, D. Pette, M. Bruckwilder, J. Koudijs, P. Jap, J. Veerkamp, and B. Wieringa. 1997. Altered Ca2+ responses in muscles with combined mitochondrial and cytosolic creatine kinase deficiencies. *Cell*. 89:93-103.

Stolz, M., T. Hornemann, U. Schlattner, and T. Wallimann. 2002. Mutation of conserved active-site threonine residues in creatine kinase affects autophosphorylation and enzyme kinetics. *Biochem J*. 363:785-92.

Streijger, F., F. Oerlemans, B.A. Ellenbroek, C.R. Jost, B. Wieringa, and C.E. Van der Zee. 2005. Structural and behavioural consequences of double deficiency for creatine kinases BCK and UbCKmit. *Behav Brain Res*. 157:219-34.

Suter, M., U. Riek, R. Tuerk, U. Schlattner, T. Wallimann, and D. Neumann. 2006. Dissecting the role of 5'-AMP for allosteric stimulation, activation, and deactivation of AMP-activated protein kinase. *J Biol Chem*. 281:32207-16.

Taylor, E.B., W.J. Ellingson, J.D. Lamb, D.G. Chesser, C.L. Compton, and W.W. Winder. 2006. Evidence against regulation of AMP-activated protein kinase and LKB1/STRAD/MO25 activity by creatine phosphate. *Am J Physiol Endocrinol Metab*. 290:E661-9.

Thali, R.F., R.D. Tuerk, R. Scholz, Y. Yoho-Auchli, R.A. Brunisholz, and D. Neumann. 2010. Novel candidate substrates of AMP-activated protein kinase identified in red blood cell lysates. *Biochem Biophys Res Commun*. 398:296-301.

Tokarska-Schlattner, M., M. Zaugg, R. da Silva, E. Lucchinetti, M.C. Schaub, T. Wallimann, and U. Schlattner. 2005. Acute toxicity of doxorubicin on isolated perfused heart: response of kinases regulating energy supply. *Am J Physiol Heart Circ Physiol*. 289:H37-47.

Tuerk, R.D., Y. Auchli, R.F. Thali, R. Scholz, T. Wallimann, R.A. Brunisholz, and D. Neumann. 2009. Tracking and quantification of 32P-labeled phosphopeptides in liquid chromatography matrix-assisted laser desorption/ionization mass spectrometry. *Anal Biochem*. 390:141-8.

Tuerk, R.D., R.F. Thali, Y. Auchli, H. Rechsteiner, R.A. Brunisholz, U. Schlattner, T. Wallimann, and D. Neumann. 2007. New candidate targets of AMP-activated protein kinase in murine brain revealed by a novel multidimensional substrate-screen for protein kinases. *J Proteome Res*. 6:3266-77.

van Deursen, J., W. Ruitenbeek, A. Heerschap, P. Jap, H. ter Laak, and B. Wieringa. 1994. Creatine kinase (CK) in skeletal muscle energy metabolism: a study of mouse mutants with graded reduction in muscle CK expression. *Proc Natl Acad Sci U S A*. 91:9091-5.

Wallimann, T., M. Dolder, U. Schlattner, M. Eder, T. Hornemann, T. Kraft, and M. Stolz. 1998. Creatine kinase: an enzyme with a central role in cellular energy metabolism. *Magma*. 6:116-9.

Yang, Y.C., M.J. Fann, W.H. Chang, L.H. Tai, J.H. Jiang, and L.S. Kao. 2010. Regulation of sodium-calcium exchanger activity by creatine kinase under energy-compromised conditions. *J Biol Chem*. 285:28275-85.

- CHAPTER 4 -

In search of novel AMPK substrates:

Extending non-biased *in vitro* screening to mitochondrial and membrane proteins

Sacnicte Ramirez-Rios[1], Malgorzata Tokarska-Schlattner[1], Laurence Kay[1], Yolanda Auchli[2], René Brunisholz[2] and Uwe Schlattner[1*]

[1] Inserm, U884, Grenoble, France; Laboratory of Fundamental and Applied Bioenergetics, University Joseph Fourier, Grenoble, France, [2] Functional Genomics Center Zurich, ETH Zurich/University of Zurich, Switzerland.

Abstract. AMP-activated protein kinase (AMPK) is a sensor of the cellular energy state and a key player in the regulation of energy metabolism at cellular and whole body level. Although a number of AMPK substrate proteins have been described, downstream signaling of AMPK is far from being fully understood. Most of the known AMPK targets are soluble proteins localized in cytoplasm and nucleus. Few is known on AMPK substrates associated with unsoluble cellular structures such as membranes in general or mitochondria in particular. Here we combine two-dimensional prefractionation (subfractionation of mitochondria) with standard SDS-PAGE separation, or simple isolation of heavy cellular fractions with two-dimensional blue native PAGE (2D-BN-PAGE) for separation of unsoluble proteins, identify putative AMPK substrate candidates by MALDI-MS/MS, and confirm two of them as *in vitro* AMPK substrates: glutamate dehydrogenase and protein disulfide isomerase. Our approach provides proof-of-principle for such a screening being a useful tool to identify candidate substrates. Putative targets as well as the strengths and pitfalls of the screening approach are discussed.

- CHAPTER 4 -

Criblage des nouvelles cibles de l'AMPK: Extension des outils pour le criblage *in vitro* de protéines mitochondriales et membranaires

Sacnicte Ramirez-Rios[1], Malgorzata Tokarska-Schlattner[1], Laurence Kay[1], Yolanda Auchli[2], René Brunisholz[2] and Uwe Schlattner[1*]

[1] Inserm, U884, Grenoble, France; Laboratory of Fundamental and Applied Bioenergetics, University Joseph Fourier, Grenoble, France, [2] Functional Genomics Center Zurich, ETH Zurich/University of Zurich, Switzerland.

Résume: La protéine kinase active par l'AMP (AMPK), est un senseur de l'état énergétique cellulaire que régule au niveau cellulaire et du corps en entier la livraison et la consommation d'énergie. Bien qu'un certain nombre des substrats de l'AMPK ont été décrits, la signalisation en aval de l'AMPK est loin d'être pleinement compris. La plupart des cibles connues de l'AMPK sont des protéines solubles localisées dans le cytoplasme et le noyau. Peu est connu sur les substrats de l'AMPK associés aux structures insolubles cellulaires comme les membranes en général ou les mitochondries en particulier. Ici, nous combinons le préfractionnement en deux dimensions (sous fractionnement des mitochondries) avec séparation par SDS-PAGE, ou l'isolement simple de fractions cellulaires lourdes avec séparation en deux dimensions par gel type bleu natif-PAGE (2D-BN-PAGE) pour la séparation de protéines insolubles, et l'identification des substrats candidats de l'AMPK par MALDI-MS/MS. Deux nouveaux substrats de l'AMPK ont été confirmé *in vitro* : la glutamate déshydrogénase et la protéine disulfure isomérase. Notre approche fournit des outils pour le criblage de cibles membranaires de l'AMPK ainsi qu'une liste de cibles potentielles.

4.1. Introduction

AMP-activated protein kinase (AMPK) is a heterotrimeric serine/threonine kinase consisting of a catalytic α subunit and two regulatory β and γ subunits. This kinase is activated in response to an increase in the AMP/ATP ratio within the cell and therefore acts as an efficient sensor for cellular energy state (Carling, 2004; Hardie, 2007). However, the most critical step for activation of AMPK is phosphorylation of threonine 172 in the kinase domain of the α subunit (Hawley et al., 1996; Suter et al., 2006). Once activated AMPK inhibits ATP-consuming (anabolic) processes such as protein synthesis, gluconeogenesis, or FA synthesis and stimulates ATP-generating (catabolic) processes like glucose uptake, glycolysis, or FA oxidation to restore cellular ATP levels (Hardie et al., 2006). In addition, AMPK is also involved in whole-body energy homeostasis, stimulating energy expenditure by promoting FA and glucose oxidation in the periphery, while at the same time inhibiting energy intake via effects on appetite in the hypothalamus (Kahn et al., 2005).

AMPK is a generally soluble enzyme localized in cytoplasm and nucleus, where it phosphorylates specific targets, including key metabolic enzymes or transcription factors (Kodiha et al., 2007; Steinberg and Kemp, 2009) respectively. Little is known about an association of AMPK with unsoluble cellular structures such as membranes or cytoskeleton and putative AMPK targets therein. In view of the importance of membranes in energy transformation and transduction, metabolite and ion transport or signal processing, which are all energy-dependent, membrane-associated proteins would be plausible targets of AMPK. However, only few membrane proteins have been identified as AMPK substrates so far (Chang et al., 2009; Fraser et al., 2007; Kuramoto et al., 2007; Wyatt et al., 2007). As for mitochondrial function, it is known to be affected by AMPK via two main pathways: regulation of FA oxidation and mitochondrial biogenesis. For the former regulation, partial location of acetyl-CoA carboxylase 2 (ACC2) at the mitochondrial surface is important (Ha et al., 1996). ACC carboxylates acetyl-CoA into malonyl-CoA which inhibits mitochondrial carnitine palmitoyltransferase 1 (CPT1) and thus turns down mitochondrial FA import. When AMPK is activated, it phosphorylates and thus inhibits ACC, which reduces malonyl-CoA levels and relieves inhibition of CPT1. By this mechanism, AMPK increases mitochondrial FA β-oxidation (Hopkins et al., 2003). At the same time, since ACC isoforms catalyze a rate-limiting step in FA synthesis, their inhibition by AMPK-mediated phosphorylation reduces FA synthesis. Mitochondrial biogenesis on the other hand is stimulated by AMPK via its substrate peroxisome proliferator-activated receptor-γ coactivator-1α (PGC-1α) (Bergeron et al., 2001; Jager et al., 2007; Winder et al., 2000). Furthermore, it should be mentioned that further components of the AMPK signaling pathway including upstream kinase LKB1 (Hawley et al., 2003) and the well-established downstream target mTOR were also found associated with mitochondria (Abu-Elheiga et al., 2000; Ha et al., 1996; Schieke et al., 2006).

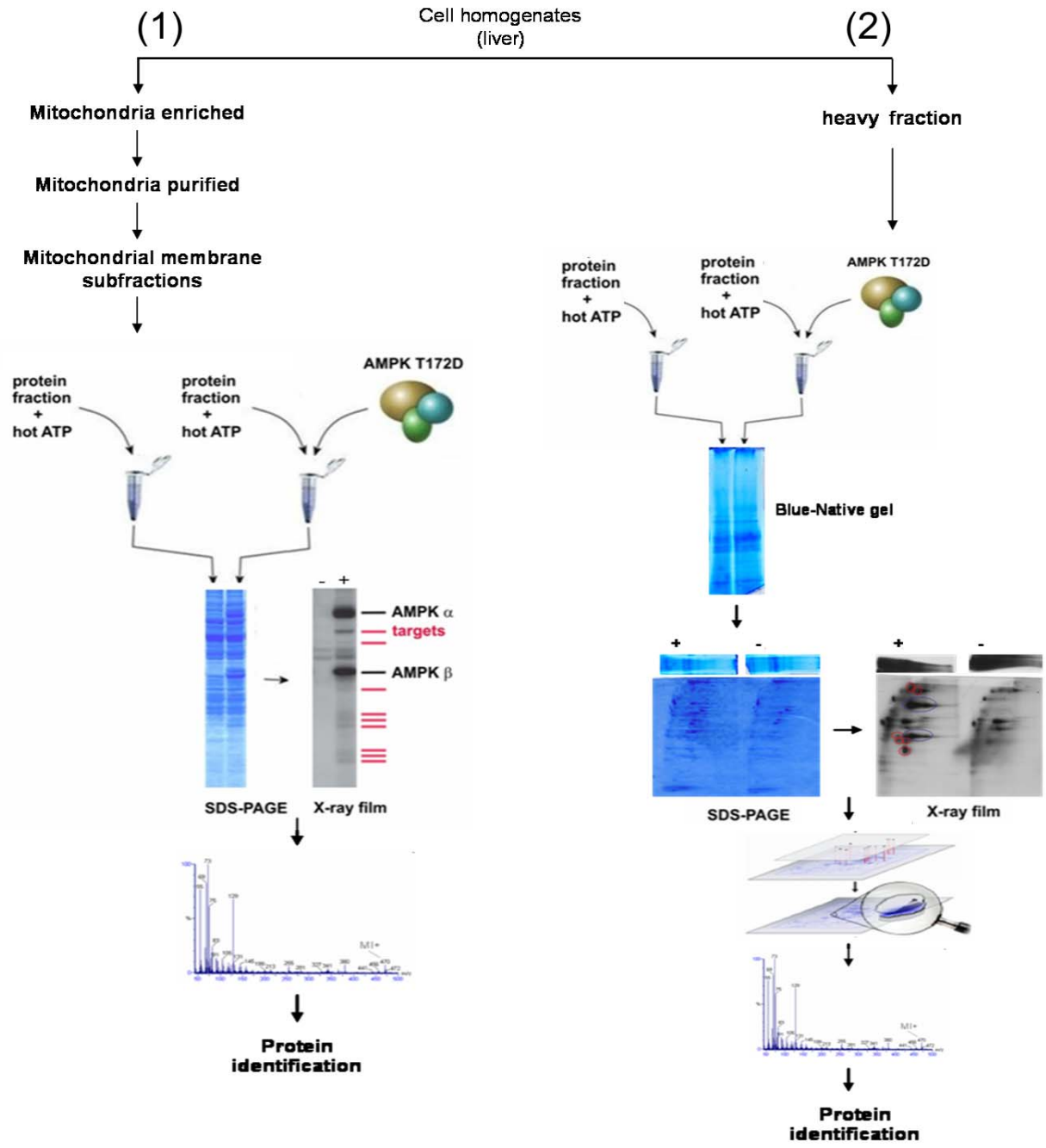

Figure 4-1. Screening of AMPK targets in membrane fractions. *(1) Prefractionation and 1D-SDS-PAGE.* Mitochondria are isolated and purified by differential centrifugation and density gradients, respectively, and then subfractionated to obtain inner and outer membrane. Mitochondria and mitochondrial subfractions are incubated with [γ^{32}P]-ATP in presence (+) or absence (-) of constitutive active AMPK α1T172Dβ1γ1 (AMPK 111TD). Proteins are separated by large SDS-PAGE. (2) *2D-native BN-PAGE.* Heavy cellular fractions containing unsoluble structures and associated proteins (including plasma, nuclear and ER membranes) are incubated with [γ^{32}P]-ATP in presence (+) or absence (-) of constitutive active AMPK 111TD. Proteins are resolved by two-dimensional blue native PAGE (BN-PAGE). In both strategies, gels are stained with colloidal Coomassie and autoradiographed. AMPK-specific signals identified by autoradiography are assigned to the protein bands/spots on Coomassie-stained gels, excised, trypsin-digested and subjected to MALDI-MS/MS mass spectrometry.

Further mitochondrial and membrane proteins were proposed as AMPK targets by an unbiased *in vitro* screen of brain extracts (Tuerk et al., 2007). The role of phosphorylation at the surface or within

mitochondria, including the involved kinases, phosphatases and their targets, has been underestimated for a long time. It is only now emerging as an important regulator of mitochondrial function.

In this study, we provide proof-of-concept that *in vitro* screening procedures for AMPK substrates can be adapted to search for proteins associated with unsoluble cellular fractions, such as mitochondrial membranes and proteins in the heavy cellular fraction. Our experimental approach is based on a multidimensional screen for protein kinase substrates (MudSeek) established by Tuerk and co-workers (Thali et al., 2010; Tuerk et al., 2007). This method, which was initially developed to screen for cytosolic, soluble AMPK targets, had to be adapted to include potentially unsoluble proteins. We applied either two-dimensional prefractionation (subfractionation of mitochondria) together with standard SDS-PAGE, or crude cell fractionation together with two-dimensional blue native PAGE (2D-BN-PAGE) combined with MALDI-MS/MS to identify putative AMPK targets (Figure 4-1).

4.2. Results

4.2.1. Screening for mitochondrial substrates of AMPK using two-dimensinal prefractionation combined with SDS-PAGE

Our first approach to screen for putative AMPK substrates was focused on mitochondrial proteins (Figure 4-2). Rat liver mitochondria were isolated by a combination of differential and Percoll gradient centrifugation (Figure 4-2A). To reduce complexity of the samples, mitochondria have been further sub-fractionated. A swelling-shrinking procedure combined with centifugation on a sucrose gradient were applied to separate the inner and outer membrane fractions (Figure 4-2B). Enrichment and final purity of mitochondria and sub-mitochondrial fractions were controlled by immunoblotting for markers of the inner membrane (adenine nucleotide translocator, ANT) and outer membrane (voltage-dependent anion channel, VDAC) (Figure 4-2C)**.** Residual cross-contamination of the membrane fractions is due to the interaction of ANT and VDAC in the so-called contact sites (Nicolay et al., 1990; Reichert and Neupert, 2002).

Three fractions, i.e. total mitochondria, inner and outer membrane were used to screen for putative downstream targets of AMPK. They were incubated with [γ-^{32}P]-ATP in the presence or absence of constitutively active AMPK α1T172Dβ1γ1 (AMPK 111TD). The reaction mixtures were separated by SDS-PAGE and phosphorylated proteins were visualized by autoradiography. PAGE autoradiographs representative for at least six independent experiments are shown in Figure 4-3. Activity of AMPK is already indicated by the autophosphorylation of AMPK α- and β-subunits. Additional signals appearing exclusively in presence of active AMPK were considered to be AMPK specific. It is to note, that incorporation of ^{32}P in the absence of AMPK was almost absent in mitochondrial fractions, indicating a low level of endogenous protein kinases and autophosphorylation events.

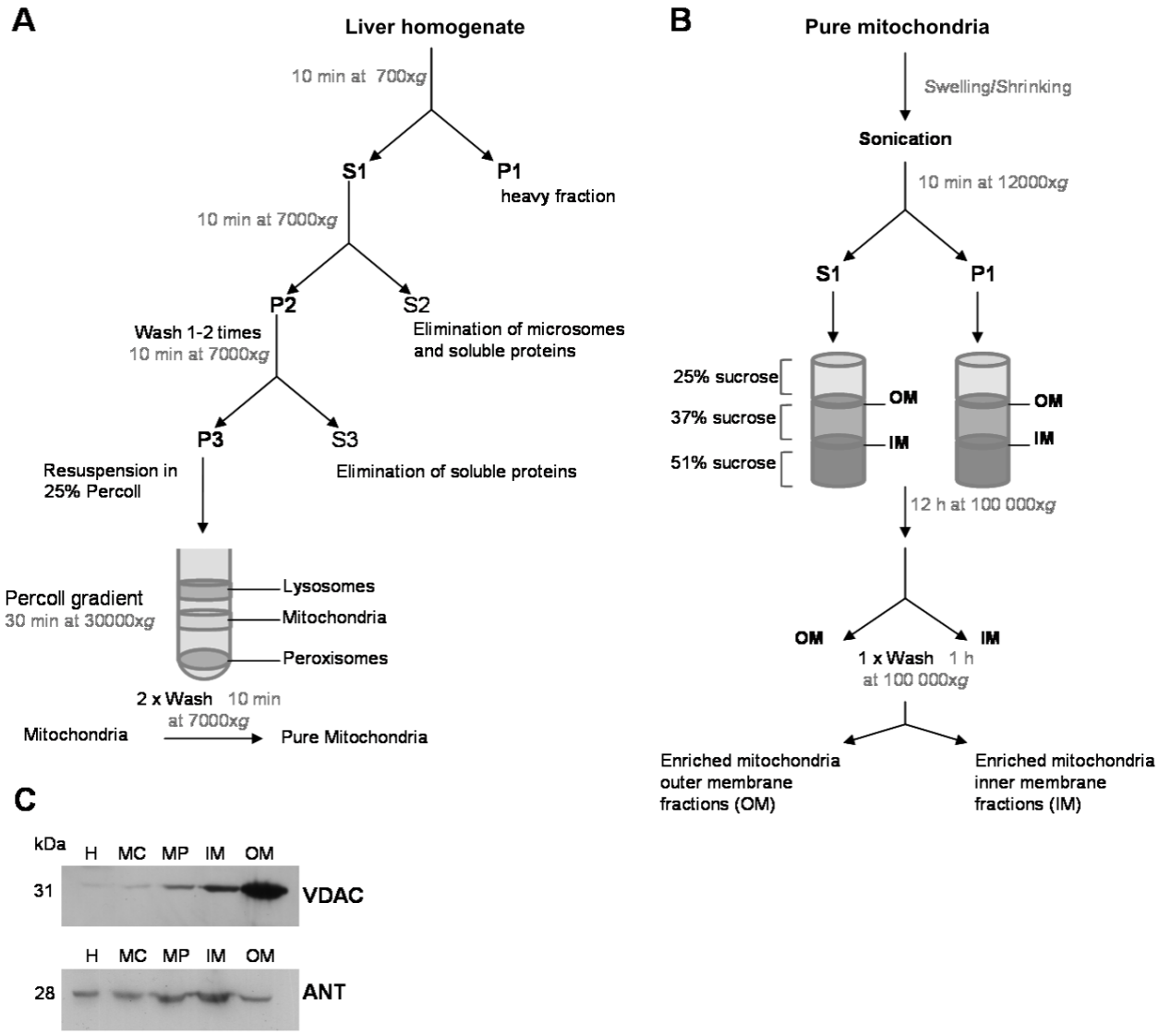

Figure 4-2. **Purification and subfractionation of rat liver mitochondria.** (A) Schematic representation of differential centrifugation steps and Percoll purification of liver mitochondria. (B) Schematic representation of inner and outer membrane enrichment by swelling-shrinking procedure and sucrose gradient. (C) Enrichment of inner and outer membrane controlled by immunoblotting using antibodies against markers of the inner membrane (adenine nucleotide translocator, ANT) and the mitochondrial outer membrane (voltage dependent anion channel, VDAC). H, liver homogenate; MC, crude mitochondria; MP, Percoll mitochondria; MIM, inner membrane fraction; MOM, outer membrane fraction.

Potential substrates were found in all fractions and over the entire range of molecular weight, with most and strongest specific ^{32}P-signals in the total mitochondria fraction (Figure 4-3). In total, 51 bands from at least 6 phosphorylation assays (see supplemental data) were excised, subjected to tryptic in-gel digestion, and analyzed by MALDI-MS/MS mass spectrometry. Fourteen proteins listed in Table 4-1 could be identified with a significant probability-based MOWSE. These are principally localized in the mitochondria matrix and the inner membrane, only two correspond to the outer membrane fraction (Figure 4-4). Four proteins were extra-mitochondrial and co-purified with intact mitochondria (two cytoplasmic proteins and two endoplasmic reticulum proteins). The physiogical functions of these proteins cover various mitochondrial processes such as ATP synthesis, oxidative

phosphorylation, gluconeogenesis, detoxification, FA oxidation, alcohol metabolism and metabolite transport.

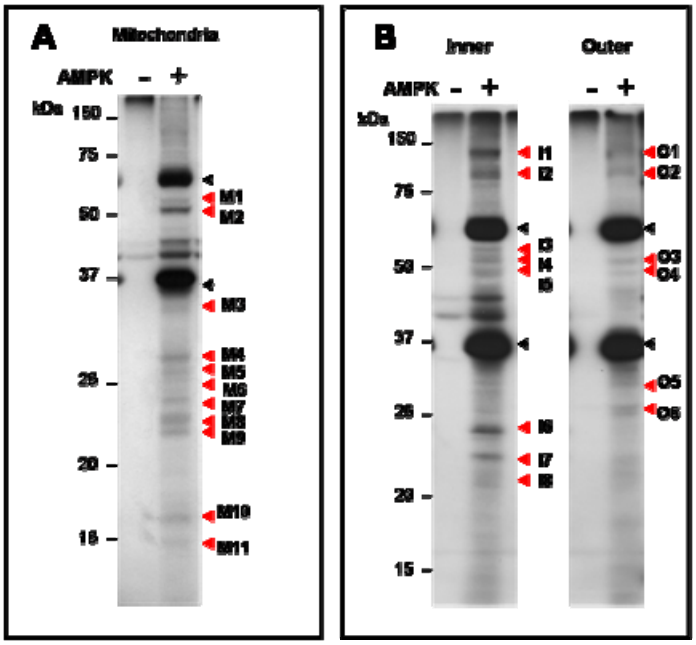

Figure 4-3. Autoradiogram of representative *in vitro* phosphorylation assays with mitochondrial fractions. (A) Total mitochondria. (B) Mitochondrial membrane fractions : inner, inner membrane; outer, outer membrane. Fractions were incubated with [γ-^{32}P]-ATP in presence (+) or absence (-) of exogenous constitutively active AMPK 111TD. After separation of the reaction mixtures by one-dimensional, large format SDS-PAGE gels (200 mm width x 220 mm length), these were dried and incorporation of ^{32}P was detected by autoradiography. Black arrows indicate autophosphorylation of the AMPK α- and β-subunits, whereas the red arrows point to other specifically radiolabeled proteins (i.e. labeled only in presence of AMPK 111TD). Some additional bands were detected in parallel phosphorylation assays (see supplemental data). Proteins identified by MALDI-MS/MS are listed in Table 4-1.

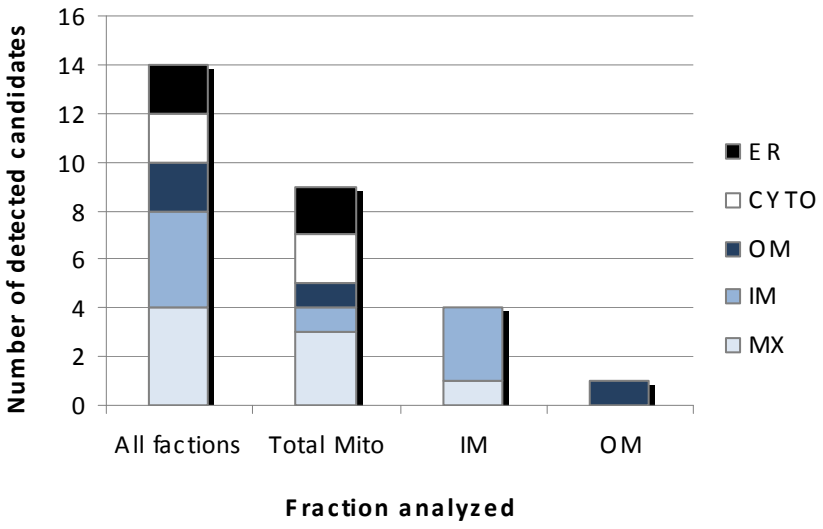

Figure 4-4. Subcellular localization of proteins identified in mitochondrial and submitochondrial fractions. Proteins identified by mass spectrometry were distributed in different compartments of mitochondria. ER, endoplasmic reticulum; CYTO, cytoplasm; OM, outer membrane fractions; IM, inner membrane; MX, matrix.

Table 4-1. **Proteins identified in mitochondrial and submitochondrial fractions by mass spectrometry.**

Protein name	*Swiss Prot ID*	*Function*	*Location*	*Score* [a]	*Band* [b]	*MW(kDa)*	*Reported phosphorylated* [c]
ADP/ATP translocase 2	Q09073	Exchange of ADP and ATP	Inner	150	M4	33	YES [2]
Aldehyde dehydrogenase	P11884	Alcohol metabolism	Matrix	176	M1	56	YES [1]
ATP synthase subunit alpha	P15999	ETC Complex V	Inner	541	I3	60	YES [1]
ATP synthase subunit beta	P10719	ETC Complex V	Inner	124	I11	56	YES [1]
Cytochrome b5	P00173	Electron transport	ER	175	M11	15	NO
Electron transfer flavoprotein, β subunit	Q68FU3	Fatty acid oxidation	Matrix	251	M16	28	YES [1]
Glutamate dehydrogenase 1	P10860	Glutamate metabolism	Matrix	415	M23	60	YES [1]
Glutathione S-transferase alpha-3	P04904	Detoxyfication metabolism	Cytoplasmic	111	M33	25	NO
Glutathione S-transferase Mu1	P04905	Detoxyfication metabolism	Cytoplasmic	117	M5	25	NO
Microsomal glutathione S-transferase 1	P08011	Detoxyfication metabolism	Outer	102	M10	17	NO
NADH dehydrogenase [ubiquinone]Fe-S	Q9DCT2	ETC Complex I	Inner	154	I4	52	YES [1]
Protein disulfide-isomerase A3	P11598	Protein folding	ER	150	M13	57	NO
Pyruvate carboxylase	P52873	Gluconeogenesis	Matrix	183	I14	129	NO
Voltage-dependent anion channel 3	Q6GSZ1	Outer membrane permeability	Outer	366	O5	31	YES [2]

[a] Probability-based MOWSE score. Protein scores above 79 are significant ($p<0.05$)
[b] Specification of analyzed bands. M, mitochondria; I, Inner membrane; O, Outer membrane
[c] Protein previously identified phosphorylated
ETC; electron traonsport chain; ER, endoplasmic reticulum
[1] Reported by Aponte et al. 2009
[2] Reported by Zhao et al. 2010

4.2.2. Screening for membrane substrates of AMPK using 2D-BN-PAGE

In a complementary approach, we were interested to analyze potentially unsoluble proteins by applying blue native 2D-PAGE. Here, proteins and protein complexes including membrane proteins are resolved in a first dimension in their native state by a PAGE lacking reducing agents and denaturing detergents. Addition of Coomassie blue G250 that binds to proteins provides a negative surface charge and allows protein separation mainly due to size differences (see also Experimental Procedures). To set-up this technique, we used the heavy fraction obtained after a first centrifugation of cellular extracts, which contains unsoluble material including membranes and associated proteins. This fraction was subjected to phosphorylation assays with [γ-^{32}P]-ATP and AMPK 111TD as above. As expected, MALDI-MS/MS analysis of ^{32}P-signals occurred to be unsuccessful when separating the reaction mixtures only on large SDS-PAGE as before (Figure 4-5A). However, separation with 2D-BN-PAGE largely improved this situation (Figure 4-5B). Six AMPK-specific spots could be detected and, after tryptic digestion and mass spectrometry, one protein in each spot could be identified with a significant probability-based MOWSE score (Table 4-2). Most were of mitochondrial origin, possibly sticking to mitochondrial fragments present in this heavy fraction. A number of other spots incorporated ^{32}P already in absence of AMPK 111TD due to endogenous protein kinase activities and autophosphorylation events, including autophosphorylation of AMPK α- and β-subunits (black arrows in Figure 4-5B).

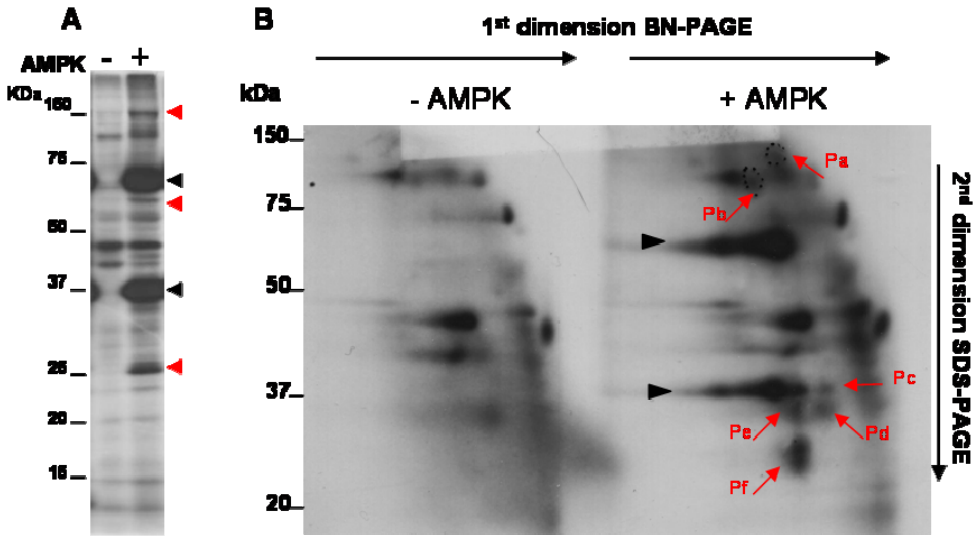

Figure 4-5. Autoradiograms of representative *in vitro* phosphorylation assays with heavy cellular fractions. Fractions incubated with [γ-^{32}P]-ATP in presence (+) or absence (-) of exogenous constitutively active AMPK 111TD were separated by (A) large 1D- SDS-PAGE or (B) 2D-BN-PAGE (5-16.5% linear gradient separating gel and a 4% stacking gel, followed by a large 12% SDS-PAGE). Gels were stained with colloidal Coomassie, dried and autoradiographed. Black arrows, autophosphorylation of AMPK α- and β-subunits; red arrows, proteins specifically radiolabeled in presence of active AMPK 111TD. Six specifically labeled spots were excised, trypsin-digested and subjected to MALDI-MS/MS mass spectrometry. Identified proteins are listed in Table 4-2.

Table 4-2. Proteins identified in heavy fraction by mass spectrometry.

Protein name	*Swiss Prot ID*	*Function*	*Location*	*Score[a]*	*Spot[b]*	*MW(kDa)*	*Reported phosphorylated[c]*
Carbamoyl-phosphate synthase 1	P07756	Urea cycle	Matrix	284	Pa	164	YES [1]
Glycogen phosphorylase	P09811	Glycogen metabolism	Cytoplasmic	282	Pb	97	NO
Enoyl-CoA hydratase	P14604	Fatty acid oxidation	Matrix	109	Pf	31	NO
Malate dehydrogenase 2	P04636	Tricarboxylic acid cycle	Matrix	178	Pd	35	YES [1]
Thiosulfate sulfurtransferase	P24329	Iron-sulfur cluster assembly	Matrix	191	Pe	33	YES [1]

[a] Probability-based MOWSE score. Protein scores above 79 are significant ($p<0.05$)
[b] Specification of analyzed bands. M, mitochondria; I, Inner membrane; O, Outer membrane
[c] Protein previously identified phosphorylated
[1] Reported by Aponte et al. 2009
[2] Reported by Zhao et al. 2010

4.2.3. *In vitro* verification of identified putative substrates of AMPK

The screening for putative AMPK substrates in mitochondrial and heavy cellular fractions revealed a total of 19 candidate proteins (Suppl. Table 4-1). We first analyzed the presence of the consensus AMPK substrate recognition motif in these proteins (Gwinn et al., 2008; Hardie, 2008; Scott et al., 2002). Seven out of the 19 candidates showed at least one such recognition motif (Table 4-3). However, the consensus sequence is only an indication. Identified sites may not be phosphorylated or sites slightly differing from this motif may still be phosphorylated (Chen et al., 1999).

Table 4-3. Putative membrane AMPK substrates identified in the phosphoscreening presenting the AMPK recognition motif.

Protein name	*Location*	*AMPK recognition motif*
ADP/ATP translocase 2	Inner	VKVETTEDLV
ATP synthase subunit alpha	Inner	IKAVDSLVPI
ATP synthase subunit beta	Inner	LKDATSKVAL
Glycogen phosphorylase	Cytosolic	IKLVTSVAEV
Malate dehydrogenase 2	Matrix	LSHIETRANV
Pyruvate carboxylase	Matrix	MRVVHSYEEL
Protein disulfide-isomerase A3	ER	FSHELSDFGL

*The core substrate recognition motif for AMPK is Φ(X, β)XXS/TXXXΦ where Φ is a hydrophobic residue (M, V, L, I, or F) and β is a basic residue (R, K or H), and the parentheses indicate that the order of residues at the P-4 and P-3 positions is not critical.

A subset of four identified proteins was finally chosen to verify *in vitro* phosphorylation: proteins with a hypothetical consensus sequence like glycogen phosphorylase (GP), malate dehydrogenase 2 (MDH), and protein disulfide-isomerase (PDI), and in addition glutamate dehydrogenase (GDH). Pure proteins together with acetyl-CoA carboxylase (ACC), an AMPK substrate as a positive control, were incubated *in vitro* with [γ-^{32}]-ATP in presence or absence of constitutively active AMPK 111TD and analyzed as before (Figure 4-6). Under these rather stringent phosphorylation conditions, AMPK-dependent phosphorylation was clearly detectable for GDH and PDI, but not for MDH and GP.

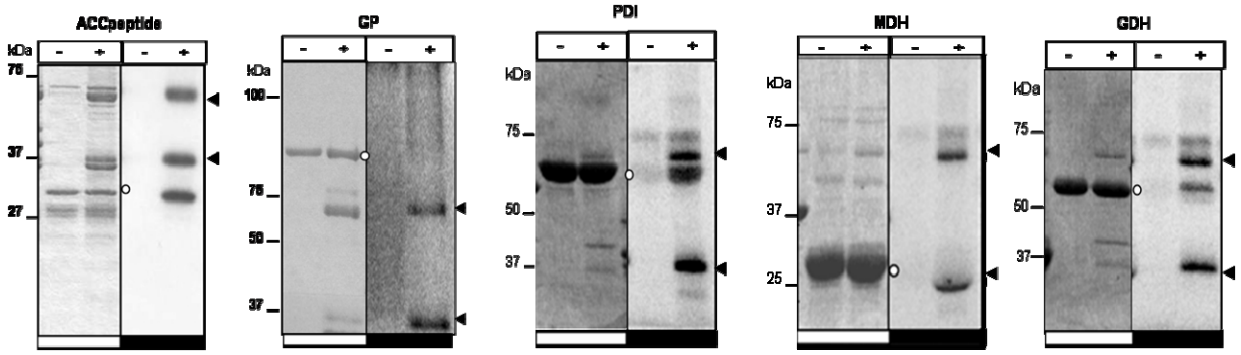

Figure 4-6. *In vitro* phosphorylation of AMPK substrate candidates. Coomassie Blue-stained gel (left, open bars below) and the autoradiograph (right, filled bars below) are shown. Purified candidate targets (200 pmol) were incubated with [γ-^{32}P]-ATP in the presence (+) or absence (-) of AMPK 111TD. Reaction mixtures were analyzed by SDS-PAGE and gels were Coomassie Blue-stained, dried and autoradiographed. Autophosphorylation of AMPK α- and β-subunits is indicated by black arrows, candidate targets are indicated by open circles (○). GST-ACC peptide containing the AMPK motif was used as a positive control of the phosphorylation assay. Characteristics of separating gel were adapted to the molecular weight of the targets.

4.2.4. AMPK may associate with mitochondria

Since there is no specific study on the association of AMPK with mitochondria, we did some initial analysis using purified liver mitochondrial fractions as above. These membranes contained traces of immunodetectable AMPK (Figure 4-7A). When exogenous, recombinant AMPK was added, it persisted to co-sediment with mitochondria even after four washing steps (Figure 4-7B). These data show that AMPK associates with membranes present in the fraction of purified liver mitochondria.

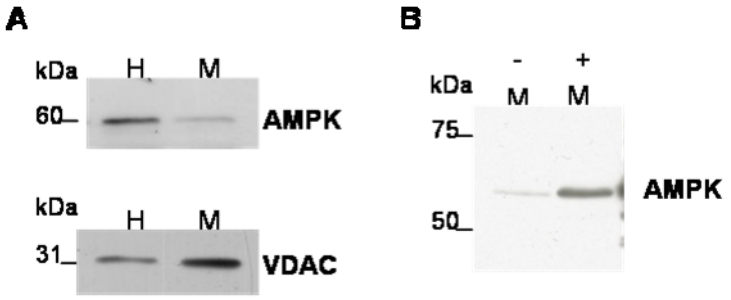

Figure 4-7. **Association of AMPK with mitochondria**. (A) Immunoblot detection of AMPK in crude mitochondria. Mitochondrial enrichment was confirmed by immunoblotting against VDAC. (B) Isolated liver mitochondria were incubated without (-) or with exogenous recombinant (+) AMPK 111WT for 1h at 37°C. After 4 washing steps mitochondria were subjected to anti-AMPK immunoblotting. H, liver homogenate and M, crude mitochondrial fraction.

4.3. Discussion

In this study, we have attempted to screen novel substrates of AMPK associated to unsoluble cellular structures like membranes, in particular mitochondrial membranes. Two strategies based on *in vitro* phosphorylation with pure, active AMPK were set-up, including membrane subfractionation and native 2D gel electrophoresis. We provide proof-of-principle for the reduction of complexity of this protein population and for successful identification of putative AMPK substrates by mass spectrometry.

Cellular surfaces, in particular membranes, are sites of intense metabolism, comprising energy conversion and transduction, metabolite and ion transport, maintenance of ion gradients, cell signaling, cell motility and many others. Since all these processes are highly ATP-dependent, it is likely that some of them are targeted by AMPK, although only very few of them have been identified so far. These include the transmembrane proteins Ca^{2+}-activated potassium channel subunit alpha-1 (Evans et al., 2009; Wyatt et al., 2007), cystic fibrosis transmembrane conductance regulator (CFTR; (King et al., 2009)) GABA type B receptor subunit 1 (Kuramoto et al., 2007) and Kidney-specific Na^{+}-K^{+}-$2Cl^{-}$ cotransporter (NKCC2; (Fraser et al., 2007)).

Different approaches have been developed in the past to identify substrates of a specific protein kinase. A straightforward *in vitro* approach is labeling of proteins from cellular extracts with a kinase of interest in the presence of [γ^{32}P]-ATP and identification of ^{32}P-labeled proteins by mass spectrometry. This approach has been successfully applied in the past to soluble proteins (Cohen and Knebel, 2006; Thali et al., 2010; Tuerk et al., 2007). However, it requires a number of conditions to successfully identify kinase candidates: (i) high purity and activity of the added protein kinase together with short incubation time to avoid unspecific protein phosphorylation, (ii) reduced complexity of the protein mixture by prefractionation, preferentially multi-dimensional, to enrich for low-abundance proteins, and (iii) high resolution separation of labeled proteins, preferentially multi-dimensional, to ascertain unequivocal identification of ^{32}P-labeled phosphorylated proteins by mass spectrometry.

This type of *in vitro* protein kinase substrate screen is extended by our study to unsoluble cellular structures and the proteins associated with them. Disposing of highly purified AMPK and a well established *in vitro* phosphorylation protocol, the principal problem has been an appropriate separation of proteins. For a protein fraction including very hydrophobic proteins, simple multidimensional column chromatography to reduce complexity and classical 2D-PAGE for the separation of ^{32}P-labeled proteins as used in the earlier studies is not or only partially applicable. We established here two different strategies to circumvent this problem.

In a first one, we optimized subcellular fractionation of membranes at the example of mitochondrial membranes and obtained purified mitochondria and highly enriched inner and outer mitochondrial membranes. The limited number of proteins present in such purified inner and outer membrane fractions then allowed proceeding with classical, large 1D-SDS-PAGE, compatible with membrane proteins, and successful protein identification by MALDI-MS/MS. In a second strategy, we used the crude heavy fraction obtained by low speed pelleting of liver homogenates, and which contains unsoluble cellular material, mainly membranes, cytoskeletal elements and proteins associating to them. In this case, combination of blue native PAGE combined with classical SDS-PAGE (2D-BN-PAGE) was essential to reach sufficient resolution power for MALDI-MS/MS protein identification. Resolution power was also important to identify AMPK-specific ^{32}P-labeling. While background phosphorylation already present in absence of AMPK due to endogenous protein kinases or autophosphorylation was almost absent in mitochondrial fractions, it was high in crude heavy fractions, possibly masking some AMPK specific signals.

As expected, mainly mitochondrial proteins were identified in mitochondrial fractions. In addition, two cytosolic glutathione-S-transferases were found, which are known to associate with or translocated to mitochondria (Robin et al., 2003). Finally, protein disulfide isomerase (PDI) located in the ER was identified, probably since ER is often connected to and co-purifies with mitochondria (de Brito and Scorrano, 2010). This result corroborates that prefractionation/purification of membrane systems is a useful strategy to obtain organelle-specific targets. The crude heavy cellular fraction revealed mostly soluble proteins that apparently co-sedimented with unsoluble structures. The lack of transmembrane proteins in this screen may be due to their low abundance or inaccessible phosphorylation sites in the labeling assay, since detergent was avoided. Astonishingly, also in the crude heavy cellular fraction mostly mitochondrial proteins were identified, possibly because destroyed mitochondria were largely present in this fraction.

A number of mitochondrial proteins was also detected in an earlier *in vitro* screen for AMPK substrates in brain (Tuerk et al., 2007) and other mitochondrial phosphoprotein screens (Aponte et al., 2009; Reinders et al., 2007; Zhao et al., 2010). For AMPK, which has been reported as strictly cytosolic/nuclear enzyme so far, signaling should be limited to the mitochondrial surface. However, AMPK could phosphorylate the nascent preproteins before their import into the organelle. Indeed, regulation of mitochondrial import by phosphorylation has been shown for several proteins (Dasari et al., 2006; Lee et al., 2006; Robin et al., 2002). Alternatively, it is conceivable that AMPK could

activate another, mitochondria-associated downstream kinase present in the examined fractions. At least, we have found some evidence for a local AMPK pool at the mitochondrial surface, since in addition to traces of AMPK co-purifying with liver mitochondria, recombinant AMPK can be re-bound to these mitochondria

Out of 19 proteins identified by both screening strategies, seven contained the stringent AMPK substrate consensus sequence, and four were tested by using pure protein for confirmatory *in vitro* phosphorylation assays. Two proteins were found phosphorylated *in vitro* by AMPK: glutamate dehydrogenase (GDH) and protein disulfide isomerase A3 (PDI). The other two probably represent false-positives due to multiple reasons: (i) problems in the assignment of ^{32}P-bands/spots to corresponding bands/spots on Coomassie stained gels, (ii) phosphorylation of a minor protein in a band/spot different from the identified major protein, or (iii) phosphorylation mediated by AMPK-activation of another protein kinase in a particular fraction.

The matrix enzyme glutamate dehydrogenase (GDH) is an important branch-point enzyme between carbon and nitrogen metabolism by catalyzing the reversible conversion of glutamate into α-ketoglutarate (Hudson and Daniel, 1993). GDH is reversibly regulated by cellular energy state; it is inactivated by high matrix ATP and GTP levels and by reversible cystein-specific ADP-ribosylation via sirtuins, and activated by high matrix ADP and GDP levels (Smith et al., 2001). Activation in response to caloric restriction and low blood glucose leads to increased amino acids breakdown into α-ketoglutarate, catalyzed by trough GDH, which enters the Krebs cycle to ultimately produce GTP and ATP. GDH has also tissue-specific functions like in pancreatic β-cells, where it is involved in energy state-dependent regulation of insulin secretion (Li et al., 2006). Compared to these short term regulations, AMPK could provide long term adaptation of GDH levels or activity in the mitochondrial matrix.

Protein disulfide isomerase (PDI), a member of the thioredoxin superfamily, assists in protein folding by catalyzing the formation, isomerization and reduction of disulfide bonds that stabilize protein structure (Hatahet and Ruddock, 2009). PDIs also serve as molecular chaperons to prevent protein aggregation, since accumulation of misfolded proteins can cause ER stress. They are mainly present in the ER, but more recently some PDI isoforms have been reported at different subcellular sites (e.g. cell surface and extracellular space, cytosol, and nucleus) (Bennett et al., 2000; Turano et al., 2002). AMPK may target PDI in these non-ER locations, where PDIs are present in smaller amounts and their role is less clear, but may include cellular adhesion and protein import (Bennett et al., 2000).

Taken together, we have made a first attempt to screen for novel substrates of AMPK associated with unsoluble cellular structures like membranes. Several proteins could be identified by mass spectrometry and two of them have been verified so far to be *in vitro* AMPK substrates. Our data provide proof-of-principle for the described screening protocols. However, these protocols could be further improved by extended prefractionation procedures that allow detection of less abundant proteins and further reduce protein complexity for unambiguous identification of phosphoprotein.

Such approaches may include specific depletion of abundant proteins (like VDAC in the outer mitochondrial membrane) or separation techniques such as free flow electrophoresis. Also native 2D-BN-PAGE may be scaled-up to improve resolution power.

4.4. Experimental procedures

4.4.1. Materials

Essentially FA free BSA and Triton X-100 were purchased from GE (GE Healthcare, USA). Percoll was obtained from Pharmacia (Uppsala, Sweden). Coomassie blue G250 dye from Thermo Scientific (Rockford, USA). [γ-^{32}P]ATP was purchased from GE Healthcare (Buckinghamshire, UK). Recombinant constitutively active AMPK $\alpha1\beta1\gamma1$ isoform containing an aspartic acid instead of a threonine at position 172 was expressed in *E. coli* and purified by the method described in chapter 2.

4.4.2. Isolation of heavy cellular fraction and mitochondria from liver

Mitochondria were isolated from male Wistar rat liver as described previously by (Tokarska-Schlattner et al., 2007). Briefly, the entire procedure was realized at 4°C. Liver tissue was homogenized with a Teflon/glass potter in 30 ml Mannitol-Hepes-Sucrose buffer (220 mM mannitol, 70 mM sucrose, 10 mM HEPES, pH 7.4), containing 0.1% bovine serum albumin, 0.2 mM EDTA. The homogenate was centrifuged for 10 min at 700 *g*. The resulting pellet, the "heavy" cellular fraction containing unsoluble material and many membranes, was resuspended in 250 mM sucrose, 10 mM HEPES, pH 7.4 buffer and solubilized with 0.5% Triton X-100, incubated for 30 min and centrifuged at 20000 *g* at 4°C for 30 min to recover the supernatant. These solubilized membranes proteins were used for the phosphorylation assay (see below).

The supernatant was centrifuged again for 10 min at 7000 g. The resulting pellet containing mainly mitochondria was resuspended in 250 mM sucrose, 10 mM HEPES, pH 7.4, 100 µM EGTA, 25% Percoll and centrifuged for 30 min at 100 000 g. These highly purified mitochondria were washed twice with 250 mM sucrose, 10 mM HEPES, pH 7.4, 100µM EGTA by centrifugation at 7000 x g for 10 min. Washed mitochondria were then recovered and resuspended in the washing buffer.

4.4.3. Isolation of inner and outer membrane

Mitochondrial subfractions (inner membrane and outer membrane) were prepared by a swelling-shrinking procedure as previously described (Hovius et al., 1990). The inner and outer membranes as well as a soluble fraction were separated by ultracentrifugation in a sucrose gradient. Briefly, Percoll-pure mitochondria (about 50 mg protein) were resuspended in 6 ml of 10 mM KH_2PO_4 buffer, pH 7.4, at 4°C. After 15 min of agitation to allow swelling, 6 ml of 10 mM KH_2PO_4 containing 30% (w/v) sucrose, 30% (v/v) glycerol, 10 mM $MgCl_2$, and 4 mM ATP were added. After 60 min of incubation at 4°C to allow shrinking, the mitochondrial suspension was sonicated using a Branson device at position 3A (3 cycles of 15 s separated by 60 s intervals to avoid heating). A first crude inner membrane fraction was pelleted at 12,000 *g* for 10 min. The pellet was resuspended in 3 ml of 10 mM KH_2PO_4,

pH 7.4 buffer. Pellet and supernatant were layered separate onto a discontinuous sucrose gradient consisting out of 51%, 37% and 25% (w/v) sucrose and centrifuged in a swinging bucket rotor at 100,000 *g* for at least 12 h at 4°C. The clear top of the gradient contained the soluble protein fraction, the 25-37% interphase contained the light outer membrane subfraction, and the 37-51% interphase contained the pure inner membrane subfraction. The membrane fractions were collected carefully from the gradient and washed twice with 10 mM KH_2PO_4, pH 7.4 buffer.

4.4.4. Immunoblotting detection of membrane markers

Mitochondria, submitochondrial fractions, and crude membrane fractions were analyzed by immunoblotting detection of marker proteins with primary antibodies (dilution in brackets): VDAC (outer mitochondrial membrane) using goat anti-species VDAC 1 (1:300, Santa Cruz), ANT (inner mitochondrial membrane) using rabbit anti-species ANT-2 (1:300, Santa Cruz), calreticulin (ER membrane) using rabbit anti-species calreticulin (1:2000, BD Biosciences), Na^+K^+ATPase (cytoplasmic membrane) using rabbit anti-species Na^+K^+ATPase (1:1:10000, Millipore). The secondary antibodies used were anti-goat IgG (1:2000, Cell signaling) and anti-rabbit IgG (1:2000, Cell Signaling). The blots were revealed using the Amersham Biosciences ECL Plus Western blotting detection system from GE Healthcare.

4.4.5. Screening for membrane AMPK substrates

In vitro phosphorylation assays

Radioactive phosphorylation assays were performed similar as in (Tuerk et al., 2007). Fractions (80 µg protein) were incubated with or without recombinant constitutively active AMPK 111TD (60 pmol, 8 µg) at 37°C for 4 min in kinase buffer (200 µM [γ-^{32}P]ATP, 50 µM AMP, 5 mM $MgCl_2$, 1 mM DTT and 10 mM HEPES, pH 7.4) at a final volume of 40 µl. The kinase reactions were then stopped after 4 min by addition of 10 µl of SDS sample buffer for 1D-PAGE and with 10 µl of loading buffer (750 mM ε-aminocaproic acid, 5% (w/v) Coomassie G 250 and 10% (v/v) glycerol) for native PAGE.

1D electrophoresis (SDS-PAGE)

The phosphorylation mixture (40 µl) complemented with 10 µl of SDS sample buffer (105 mM Tris-HCl, pH 6.8, 4% (w/v) SDS, 15% (v/v) glycerol, 1.2 M 2-mercaptoethanol, and 0.02% (w/v) bromophenol blue) was heated to 95°C for 5 min and separated by SDS-PAGE using large 12% gels (200 x 220 mm). Proteins were fixed in 40% ethanol (v/v) and 10% acetic acid (v/v) for 2 h and stained with colloidal Coomassie (Carl Roth GmbH, Germany) overnight. Gels were then covered with plastic film, dried on a Whatman paper as a support, and exposed to ECL-film (GE Healthcare, USA) for 2 days to detect radioactively labeled protein bands.

Blue Native 2D-PAGE

Blue native polyacrylamide gel electrophoresis (BN-PAGE) is an alternative strategy to separating membrane proteins with high resolution separation from tissue homogenates, cell and cell

fractions. Membrane proteins are separated well after solubilization with adequate neutral detergents such as triton X-100, β-dodecyl-n-maltoside and digitonin. The separation principle of membrane proteins relies on binding of the dye Coomassie blue G250 to proteins which provides negative charges to the surface of the protein. During migration to the anode, proteins are separated according to molecular mass and/or size and high resolution is obtained by the decreasing pore size of a polyacrylamide gradient gel. This method was established in order to have a better resolution and separation of complex mixture of membrane proteins and thus of potential membrane targets of AMPK. The first dimension (BN-PAGE) was realized as described in (Schagger and von Jagow, 1991) and (Wittig et al., 2006) with minor modifications. After the phosphorylation assay, the mixtures were separated by BN-PAGE with a 5-16.5% linear gradient separating gel and a 4% stacking gel. Electrophoresis was carried out in the presence of 0.02% (w/v) of Coomassie blue G250 as a component in the cathode buffer. Protein separation was carried out at 100 V for 3,5 h at 4°C. The molecular mass of the resolved complexes was determinated by the HMW (high molecular weight) native protein marker (Thyroglobulin, apoferritin and BSA protein mix). After electrophoresis, strips of the first dimension gels were cut and protein were denaturated in presence of 2 % (w/w) SDS, 1% (v/v) β-mercaptoethanol and 1X anti-protease mix (GE Healthcare) for 1 h. After protein denaturation, stripes were applied to the second dimension (large 12% SDS-PAGE gel). After SDS-PAGE, proteins were stained with colloidal Coomassie overnight. Gels were dried and exposed to film for autoradiography as above.

4.4.6. Trypsin digestion and mass spectrometry

After development, the autoradiography films were realigned to the dried one-dimensional or two-dimensional gels. Radioactively labeled bands and spots on autoradiogrammes were located on Coomassie stained gels and marked for later excision. To avoid contamination by keratin and dust particles, all procedures including in-gel digestion, were performed in a laminar flow sterile bench. Excised gel pieces, containing bands and spots of interest, were subjected to in-gel digestion with trypsin (Promega, Wallisellen, Switzerland). Extracted peptides were lyophilized and stored at -80°C for 4-6 weeks to reduce radioactivity levels. Peptides were reconstituted in 5 µl of 10% (v/v) acetonitrile (ACN) supplememted with 0.1% (v/v) trifluoroacetic acid (TFA) and desalted using ZipTip C18 microcolumns. Peptides were eluted from the ZipTip in 3 µl of 50% (v/v) ACN/10% (v/v) TFA. An aliquot was mixed with an equal volume of α-cyano-hydroxycinnamic acid (10 mg/mL in 50:50 acetonitrile:water supplemented with 0.1% (v/v) TFA), spotted on a gold coated-MALDI target and allowed to dry at room temperature. All spectra were obtained by MALDI MS and MALDI MS/MS using an Ultraflex TOF/TOF II equipped with the control and analysis software Compass v. 1.1 (Bruker Daltonics, Bremen, Germany). The mass spectrometer was operated in the positive ion reflector mode with 150 ns delayed extraction time, the nitrogen laser (337 nm) was set to a repetition rate of 50 Hz and the ion acceleration voltage was 25 kV. Mass measurements were performed automatically through fuzzy logic-based software to accumulate 500-800 single laser shot spectra or

manually to accumulate 2000 single laser shot spectra. All spectra were calibrated externally with the mass signals of the peptide calibrant standard II. Routinely, prior to automate acquisition, two spots were used for signal and parameter optimization. The first monoisotopic signals in the spectra were assigned automatically using the peak detection algorithm SNAP (Bruker Daltonics, Bremen, Germany). The smoothing algorithm of Savitzky-Golay was applied (width 0.2 m/z, cycle number 1). Processed MS and MS/MS spectra were combined through BioTools software (Bruker Daltonics, Bremen, Germany) to search the Uniref100 database (release 6.0), non restricted to the taxonomy, using MASCOT software v. 2.0 (Matrix Science, London, UK). Mass errors of 150 ppm for both, the peptide mass fingerprints and the precursor ions selected for fragmentation were allowed. A maximal tolerance of 0.2 Da was allowed for fragment ions. In addition, the search parameters tolerated oxidation of methionine, carbamidomethylation of cysteine, phosphorylation in threonine and serine as variable modifications were included up to one missed cleavage for trypsin. Probability-based MOWSE above 79 were considered significant.

4.4.7. *In vitro* verification of identified candidate targets using constitutive active AMPK

Incubation of 200 pmol purified glycogen phosphorylase (GP), malate dehydrogenase 2 (MDH), protein disulfide-isomerase A3 (PDI) or glutamate dehydrogenase (GDH) for 3 min at 37°C was performed in the presence or absence of 3.5 pmol AMPK 111TD in kinase buffer containing 200 μM [γ-^{32}P]ATP (specific activity 400 mCi/mmol ATP), 50 μM AMP, 5 mM $MgCl_2$, 1 mM DTT, and 10 mM HEPES (pH 7.4). For negative controls, proteins were incubated without AMPK. Kinase reactions were stopped by addition of SDS-PAGE sample buffer. Proteins were subjected to SDS-PAGE followed by and autoradiography as above or scanning with Typhoon phosphoimager (GE Healthcare).

4.4.8. Assay for association of recombinant AMPK with isolated mitochondria

Enriched liver mitochondria (ca. 5 mg) obtained as described above and resuspended in washing buffer (250 mM sucrose, 10mM HEPES, pH 7.4, 100μM EGTA) were incubated with 0.5 mg purified recombinant AMPK for 30 min at 37°C and washed 1-4 times with washing buffer before subjection to SDS-PAGE and immunoblotting using anti-AMPK antibody (Cell Signaling).

4.5. Supplementary Tables

SUPPL. TABLE 4-1. Proteins identified by MALDI MS/MS mass spectrometry in radiolabeled bands/spots

Swiss Prot ID	*Mass (Da)*	*Score*[a]	*Queries matched*[b]	*Description*
Q6GSZ1	30764	366	13	Voltage-dependent anion channel 3; n=1; Rattus norvegicus
P52873	129608	183	28	Pyruvate carboxylase, mitochondrial precursor; n=1; Rattus norvegicus
P15999	59717	541	25	ATP synthase subunit alpha, mitochondrial precursor; Rattus
Q9DCT2	30189	154	11	NADH dehydrogenase [ubiquinone] Fe-S protein 3; Rattus norvegicus
P11598	56588	150	18	Protein disulfide-isomerase A3 precursor; n=1; Rattus norvegicus|
P08011	17460	102	13	Microsomal glutathione S-transferase 1; n=1; Rattus norvegicus|Rep: Micro
P10860	61377	415	24	Glutamate dehydrogenase 1, mitochondrial precursor; n=1; Rattus norvegicus|Rep: G
P00173	11400	175	5	Cytochrome b5; n=1; Rattus norvegicus|Rep: Cytochrome b5 - Rattus norvegicus [
Q09073	32880	150	9	ADP/ATP translocase 2; n=1; Rattus norvegicus|Rep: ADP/ATP translocase 2 - Rattus
P04905	25897	89	13	Glutathione S-transferase Mu 1 - Rattus norvegicus [Rat]
P10719	56318	124	13	ATP synthase subunit beta, mitochondrial precursor; n=1; Rattus norvegicus|Rep: A
P11884	56488	176	15	Aldehyde dehydrogenase, mitochondrial; Rattus norvegicus
Q68FU3	27670	251	6	Electron transfer flavoprotein subunit beta; n=1; Rattus norvegicus|Rep: Electron
P04636	35574	172	18	Malate dehydrogenase, mitochondrial precursor; n=1; Rattus norvegicus|Rep: Malate
P07756	164476	284	47	Carbamoyl-phosphate synthase [ammonia], mitochondrial precursor; n=1; Ra
P09811	97421	282	24	Glycogen phosphorylase, liver form; n=1; Rattus norvegicus|Rep: Glycogen phosphorylase
P80385	37363	154	14	5'-AMP-activated protein kinase subunit gamma-1; n=1; Rattus norvegicus|Rep: 5'-
P24329	33386	191	10	Thiosulfate sulfurtransferase; n=1; Rattus norvegicus|Rep: Thiosulfate sulfurtrans
P14604	31496	109	8	Enoyl-CoA hydratase, mitochondrial precursor; n=1; Rattus norvegicus|Rep: Enoyl-C

[a] Protein scores above 79 are significant (p<0.05)
[b] Indicates the number of MS/MS spectra that were matched to this protein.

4.6. Supplementary Figures

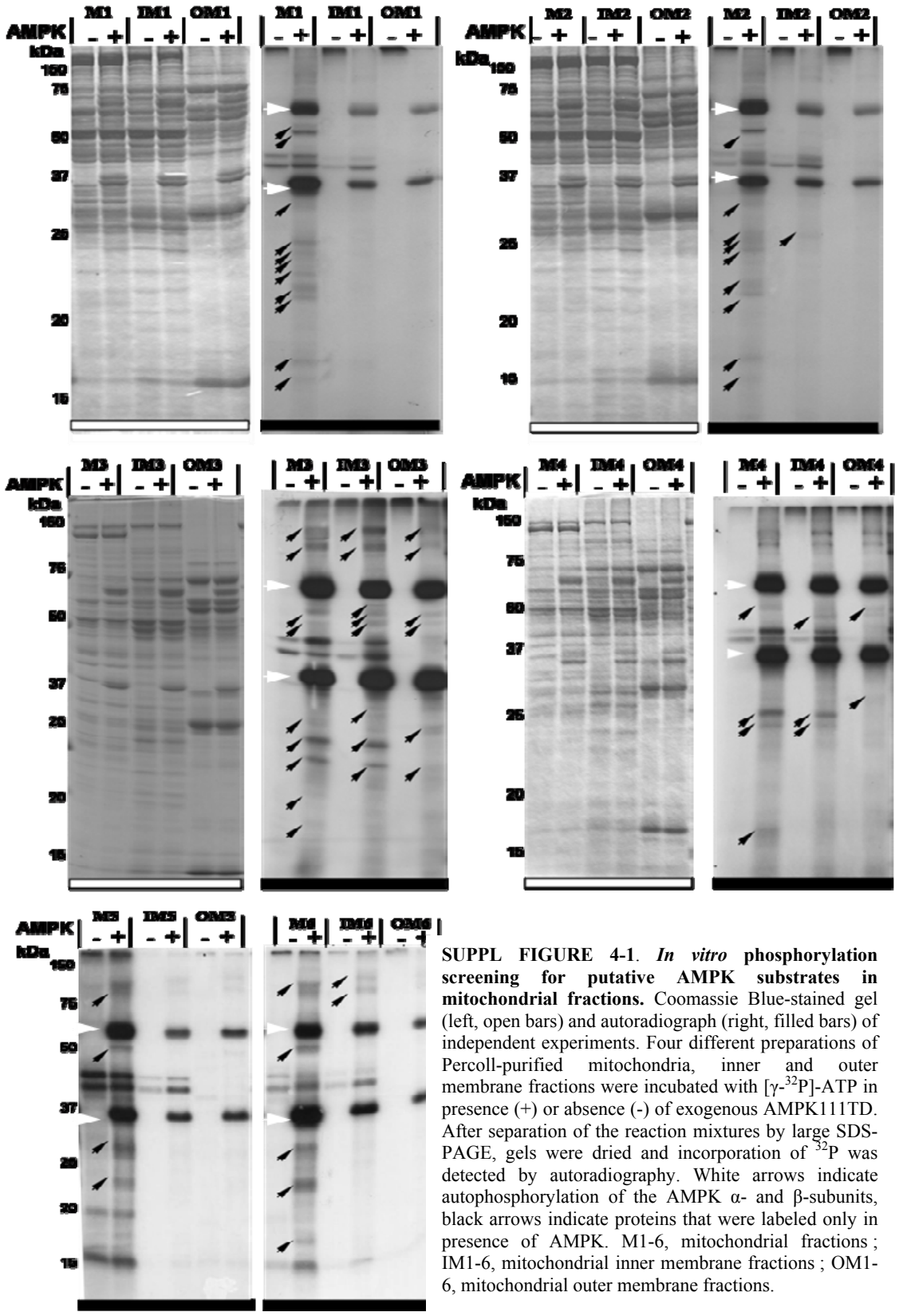

SUPPL FIGURE 4-1. ***In vitro*** **phosphorylation screening for putative AMPK substrates in mitochondrial fractions.** Coomassie Blue-stained gel (left, open bars) and autoradiograph (right, filled bars) of independent experiments. Four different preparations of Percoll-purified mitochondria, inner and outer membrane fractions were incubated with [γ-^{32}P]-ATP in presence (+) or absence (-) of exogenous AMPK111TD. After separation of the reaction mixtures by large SDS-PAGE, gels were dried and incorporation of ^{32}P was detected by autoradiography. White arrows indicate autophosphorylation of the AMPK α- and β-subunits, black arrows indicate proteins that were labeled only in presence of AMPK. M1-6, mitochondrial fractions ; IM1-6, mitochondrial inner membrane fractions ; OM1-6, mitochondrial outer membrane fractions.

4.7. References

Abu-Elheiga, L., W.R. Brinkley, L. Zhong, S.S. Chirala, G. Woldegiorgis, and S.J. Wakil. 2000. The subcellular localization of acetyl-CoA carboxylase 2. *Proc Natl Acad Sci U S A*. 97:1444-9.

Aponte, A.M., D. Phillips, R.K. Hopper, D.T. Johnson, R.A. Harris, K. Blinova, E.S. Boja, S. French, and R.S. Balaban. 2009. Use of (32)P to study dynamics of the mitochondrial phosphoproteome. *J Proteome Res*. 8:2679-95.

Bennett, T.A., B.S. Edwards, L.A. Sklar, and S. Rogelj. 2000. Sulfhydryl regulation of L-selectin shedding: phenylarsine oxide promotes activation-independent L-selectin shedding from leukocytes. *J Immunol*. 164:4120-9.

Bergeron, R., J.M. Ren, K.S. Cadman, I.K. Moore, P. Perret, M. Pypaert, L.H. Young, C.F. Semenkovich, and G.I. Shulman. 2001. Chronic activation of AMP kinase results in NRF-1 activation and mitochondrial biogenesis. *Am J Physiol Endocrinol Metab*. 281:E1340-6.

Carling, D. 2004. The AMP-activated protein kinase cascade--a unifying system for energy control. *Trends Biochem Sci*. 29:18-24.

Chang, T.J., W.P. Chen, C. Yang, P.H. Lu, Y.C. Liang, M.J. Su, S.C. Lee, and L.M. Chuang. 2009. Serine-385 phosphorylation of inwardly rectifying K+ channel subunit (Kir6.2) by AMP-dependent protein kinase plays a key role in rosiglitazone-induced closure of the K(ATP) channel and insulin secretion in rats. *Diabetologia*. 52:1112-21.

Chen, Z.P., K.I. Mitchelhill, B.J. Michell, D. Stapleton, I. Rodriguez-Crespo, L.A. Witters, D.A. Power, P.R. Ortiz de Montellano, and B.E. Kemp. 1999. AMP-activated protein kinase phosphorylation of endothelial NO synthase. *FEBS Lett*. 443:285-9.

Cohen, P., and A. Knebel. 2006. KESTREL: a powerful method for identifying the physiological substrates of protein kinases. *Biochem J*. 393:1-6.

Dasari, V.R., H.K. Anandatheerthavarada, M.A. Robin, E. Boopathi, G. Biswas, J.K. Fang, D.W. Nebert, and N.G. Avadhani. 2006. Role of protein kinase C-mediated protein phosphorylation in mitochondrial translocation of mouse CYP1A1, which contains a non-canonical targeting signal. *J Biol Chem*. 281:30834-47.

de Brito, O.M., and L. Scorrano. 2010. An intimate liaison: spatial organization of the endoplasmic reticulum-mitochondria relationship. *Embo J*. 29:2715-23.

Evans, A.M., D.G. Hardie, C. Peers, C.N. Wyatt, B. Viollet, P. Kumar, M.L. Dallas, F. Ross, N. Ikematsu, H.L. Jordan, B.L. Barr, J.N. Rafferty, and O. Ogunbayo. 2009. Ion channel regulation by AMPK: the route of hypoxia-response coupling in thecarotid body and pulmonary artery. *Ann N Y Acad Sci*. 1177:89-100.

Fraser, S.A., I. Gimenez, N. Cook, I. Jennings, M. Katerelos, F. Katsis, V. Levidiotis, B.E. Kemp, and D.A. Power. 2007. Regulation of the renal-specific Na+-K+-2Cl- co-transporter NKCC2 by AMP-activated protein kinase (AMPK). *Biochem J*. 405:85-93.

Gwinn, D.M., D.B. Shackelford, D.F. Egan, M.M. Mihaylova, A. Mery, D.S. Vasquez, B.E. Turk, and R.J. Shaw. 2008. AMPK phosphorylation of raptor mediates a metabolic checkpoint. *Mol Cell*. 30:214-26.

Ha, J., J.K. Lee, K.S. Kim, L.A. Witters, and K.H. Kim. 1996. Cloning of human acetyl-CoA carboxylase-beta and its unique features. *Proc Natl Acad Sci U S A*. 93:11466-70.

Hardie, D.G. 2007. AMP-activated/SNF1 protein kinases: conserved guardians of cellular energy. *Nat Rev Mol Cell Biol*. 8:774-85.

Hardie, D.G. 2008. AMPK and Raptor: matching cell growth to energy supply. *Mol Cell*. 30:263-5.

Hardie, D.G., S.A. Hawley, and J.W. Scott. 2006. AMP-activated protein kinase--development of the energy sensor concept. *J Physiol*. 574:7-15.

Hatahet, F., and L.W. Ruddock. 2009. Protein disulfide isomerase: a critical evaluation of its function in disulfide bond formation. *Antioxid Redox Signal*. 11:2807-50.

Hawley, S.A., J. Boudeau, J.L. Reid, K.J. Mustard, L. Udd, T.P. Makela, D.R. Alessi, and D.G. Hardie. 2003. Complexes between the LKB1 tumor suppressor, STRAD alpha/beta and MO25 alpha/beta are upstream kinases in the AMP-activated protein kinase cascade. *J Biol*. 2:28.

Hawley, S.A., M. Davison, A. Woods, S.P. Davies, R.K. Beri, D. Carling, and D.G. Hardie. 1996. Characterization of the AMP-activated protein kinase kinase from rat liver and identification of threonine 172 as the major site at which it phosphorylates AMP-activated protein kinase. *J Biol Chem*. 271:27879-87.

Hopkins, T.A., J.R. Dyck, and G.D. Lopaschuk. 2003. AMP-activated protein kinase regulation of fatty acid oxidation in the ischaemic heart. *Biochem Soc Trans*. 31:207-12.

Hovius, R., H. Lambrechts, K. Nicolay, and B. de Kruijff. 1990. Improved methods to isolate and subfractionate rat liver mitochondria. Lipid composition of the inner and outer membrane. *Biochim Biophys Acta*. 1021:217-26.

Hudson, R.C., and R.M. Daniel. 1993. L-glutamate dehydrogenases: distribution, properties and mechanism. *Comp Biochem Physiol B*. 106:767-92.

Jager, S., C. Handschin, J. St-Pierre, and B.M. Spiegelman. 2007. AMP-activated protein kinase (AMPK) action in skeletal muscle via direct phosphorylation of PGC-1alpha. *Proc Natl Acad Sci U S A*. 104:12017-22.

Kahn, B.B., T. Alquier, D. Carling, and D.G. Hardie. 2005. AMP-activated protein kinase: ancient energy gauge provides clues to modern understanding of metabolism. *Cell Metab*. 1:15-25.

King, J.D., Jr., A.C. Fitch, J.K. Lee, J.E. McCane, D.O. Mak, J.K. Foskett, and K.R. Hallows. 2009. AMP-activated protein kinase phosphorylation of the R domain inhibits PKA stimulation of CFTR. *Am J Physiol Cell Physiol*. 297:C94-101.

Kodiha, M., J.G. Rassi, C.M. Brown, and U. Stochaj. 2007. Localization of AMP kinase is regulated by stress, cell density, and signaling through the MEK-->ERK1/2 pathway. *Am J Physiol Cell Physiol*. 293:C1427-36.

Kuramoto, N., M.E. Wilkins, B.P. Fairfax, R. Revilla-Sanchez, M. Terunuma, K. Tamaki, M. Iemata, N. Warren, A. Couve, A. Calver, Z. Horvath, K. Freeman, D. Carling, L. Huang, C. Gonzales, E. Cooper, T.G. Smart, M.N. Pangalos, and S.J. Moss. 2007. Phospho-dependent functional modulation of GABA(B) receptors by the metabolic sensor AMP-dependent protein kinase. *Neuron*. 53:233-47.

Lee, J., R.C. O'Neill, M.W. Park, M. Gravel, and P.E. Braun. 2006. Mitochondrial localization of CNP2 is regulated by phosphorylation of the N-terminal targeting signal by PKC: implications of a mitochondrial function for CNP2 in glial and non-glial cells. *Mol Cell Neurosci*. 31:446-62.

Li, C., A. Allen, J. Kwagh, N.M. Doliba, W. Qin, H. Najafi, H.W. Collins, F.M. Matschinsky, C.A. Stanley, and T.J. Smith. 2006. Green tea polyphenols modulate insulin secretion by inhibiting glutamate dehydrogenase. *J Biol Chem*. 281:10214-21.

Nicolay, K., M. Rojo, T. Wallimann, R. Demel, and R. Hovius. 1990. The role of contact sites between inner and outer mitochondrial membrane in energy transfer. *Biochim Biophys Acta*. 1018:229-33.

Reichert, A.S., and W. Neupert. 2002. Contact sites between the outer and inner membrane of mitochondria-role in protein transport. *Biochim Biophys Acta*. 1592:41-9.

Reinders, J., K. Wagner, R.P. Zahedi, D. Stojanovski, B. Eyrich, M. van der Laan, P. Rehling, A. Sickmann, N. Pfanner, and C. Meisinger. 2007. Profiling phosphoproteins of yeast mitochondria reveals a role of phosphorylation in assembly of the ATP synthase. *Mol Cell Proteomics*. 6:1896-906.

Robin, M.A., H.K. Anandatheerthavarada, G. Biswas, N.B. Sepuri, D.M. Gordon, D. Pain, and N.G. Avadhani. 2002. Bimodal targeting of microsomal CYP2E1 to mitochondria through activation of an N-terminal chimeric signal by cAMP-mediated phosphorylation. *J Biol Chem*. 277:40583-93.

Robin, M.A., S.K. Prabu, H. Raza, H.K. Anandatheerthavarada, and N.G. Avadhani. 2003. Phosphorylation enhances mitochondrial targeting of GSTA4-4 through increased affinity for binding to cytoplasmic Hsp70. *J Biol Chem*. 278:18960-70.

Schagger, H., and G. von Jagow. 1991. Blue native electrophoresis for isolation of membrane protein complexes in enzymatically active form. *Anal Biochem*. 199:223-31.

Schieke, S.M., D. Phillips, J.P. McCoy, Jr., A.M. Aponte, R.F. Shen, R.S. Balaban, and T. Finkel. 2006. The mammalian target of rapamycin (mTOR) pathway regulates mitochondrial oxygen consumption and oxidative capacity. *J Biol Chem*. 281:27643-52.

Scott, J.W., D.G. Norman, S.A. Hawley, L. Kontogiannis, and D.G. Hardie. 2002. Protein kinase substrate recognition studied using the recombinant catalytic domain of AMP-activated protein kinase and a model substrate. *J Mol Biol*. 317:309-23.

Smith, T.J., P.E. Peterson, T. Schmidt, J. Fang, and C.A. Stanley. 2001. Structures of bovine glutamate dehydrogenase complexes elucidate the mechanism of purine regulation. *J Mol Biol*. 307:707-20.

Steinberg, G.R., and B.E. Kemp. 2009. AMPK in Health and Disease. *Physiol Rev*. 89:1025-78.

Suter, M., U. Riek, R. Tuerk, U. Schlattner, T. Wallimann, and D. Neumann. 2006. Dissecting the role of 5'-AMP for allosteric stimulation, activation, and deactivation of AMP-activated protein kinase. *J Biol Chem*. 281:32207-16.

Thali, R.F., R.D. Tuerk, R. Scholz, Y. Yoho-Auchli, R.A. Brunisholz, and D. Neumann. 2010. Novel candidate substrates of AMP-activated protein kinase identified in red blood cell lysates. *Biochem Biophys Res Commun*. 398:296-301.

Tokarska-Schlattner, M., M. Dolder, I. Gerber, O. Speer, T. Wallimann, and U. Schlattner. 2007. Reduced creatine-stimulated respiration in doxorubicin challenged mitochondria: particular sensitivity of the heart. *Biochim Biophys Acta*. 1767:1276-84.

Tuerk, R.D., R.F. Thali, Y. Auchli, H. Rechsteiner, R.A. Brunisholz, U. Schlattner, T. Wallimann, and D. Neumann. 2007. New candidate targets of AMP-activated protein kinase in murine brain revealed by a novel multidimensional substrate-screen for protein kinases. *J Proteome Res*. 6:3266-77.

Turano, C., S. Coppari, F. Altieri, and A. Ferraro. 2002. Proteins of the PDI family: unpredicted non-ER locations and functions. *J Cell Physiol*. 193:154-63.

Winder, W.W., B.F. Holmes, D.S. Rubink, E.B. Jensen, M. Chen, and J.O. Holloszy. 2000. Activation of AMP-activated protein kinase increases mitochondrial enzymes in skeletal muscle. *J Appl Physiol*. 88:2219-26.

Wittig, I., H.P. Braun, and H. Schagger. 2006. Blue native PAGE. *Nat Protoc*. 1:418-28.

Wyatt, C.N., K.J. Mustard, S.A. Pearson, M.L. Dallas, L. Atkinson, P. Kumar, C. Peers, D.G. Hardie, and A.M. Evans. 2007. AMP-activated protein kinase mediates carotid body excitation by hypoxia. *J Biol Chem*. 282:8092-8.

Zhao, X., I.R. Leon, S. Bak, M. Mogensen, K. Wrzesinski, K. Hojlund, and O.N. Jensen. 2010. Phosphoproteome analysis of functional mitochondria isolated from resting human muscle reveals extensive phosphorylation of inner membrane protein complexes and enzymes. *Mol Cell Proteomics*.

- CHAPTER 5 -

Synthetic discussion, conclusions & perspectives

4.8. Synthetic discussion, conclusions & perspectives

The AMPK-activated protein kinase has emerged as a signaling hub in sensing, signaling and regulating energy state at the cellular and whole body level (chapter 1). The work presented in this thesis provides important tools for studying AMPK *in vitro* and extends our knowledge on AMPK signaling for the regulation of cellular energy homeostasis. The developed tools include a novel automized purification protocol for proteins and protein complexes (chapter 2) and protocols to screen for AMPK substrates in the unsoluble cellular fraction containing membranes and others (chapter 4). These advances allowed for the purification of large quantities of recombinant AMPK protein for various studies and provided proof-of principle for unbiased *in vitro* search strategies for AMPK substrates associated with unsoluble cellular structures like mitochondrial membranes. In the following, an AMPK substrate identified in an unbiased *in vitro* screen, the brain-type creatine kinase (chapter 1), has been verified and characterized *in vitro* and *in vivo* (chapter 3). We report for the first time evidence that this key enzyme for energy homeostasis in most non-muscle tissues is regulated by reversible protein phosphorylatiuon at a specific residue via a specific protein kinase, that is AMPK. However, BCK phosphorylation is not affecting CK enzyme activity, as has been suggested by some previous studies that only evidenced phosphorylated BCK species (Chida et al., 1990b; Quest et al., 1990), but affects specifically BCK localized at or localizing to the endoplasmic reticulum. This is also a novel kind of regulatory mechanism for AMPK, which has been known so far only to phosphorylate key enzymes in metabolism or transcription factors to increase or inhibit their enzymatic activity (Carling, 2004; Hardie et al., 2006; McGee and Hargreaves, 2008).

AMPK has been identified as a promising pharmacological target to treat type II diabetes, the metabolic syndrome, and possibly also cancer (Fryer and Carling, 2005; Hardie, 2007; Motoshima et al., 2006; Steinberg and Kemp, 2009), which largely increased interest directed towards AMPK signaling. Different approaches can be applied to screen putative AMPK substrates *in vitro*, including phosphorylation screens (Cohen and Knebel, 2006; Thali et al., 2010; Tuerk et al., 2007) or a scanning peptide library techniques together with bioinformatics tools (Gwinn et al., 2008). The first and most important requirement for *in vitro* phosphorylation assays is the availability of highly pure and enzymatically fully active AMPK isoforms. AMPK purified from tissues like muscle or liver is disadvantagous since only small microgram quantities can be obtained and, in eukaryotic cells, AMPK is expressed as a mixture of different isoforms. A polycistronic bacterial expression system developed in our group (Neumann et al., 2003) allowed obtaining recombinant heterotrimeric and enzymatically active AMPK complex at high yield and containing specific AMPK isoforms or mutants. However, variability within the multi-step purification protocol still limited reproducibility of the procedure and the resulting protein purity. In this thesis work, a thermostated high-end chromatography system (Äkta Explorer) was modified in such a way that an automated 4-dimensional protein purification could be run with interactive remote control (chapter 2). This automated process made it possible to produce in a short time large amounts of highly and freshly isolated AMPK. This is particularly important because AMPK turned out to be a rather unstable protein with a strong tendency to aggregate and

denature *in vitro*. Different AMPKs with defined subunit composition produced by this method presented high specificity activity after full activation via upstream kinases like CaMKKβ. Production and purification of different AMPK isoforms opened the possibility to study isoform-specific functions and to screen for new interaction partners and substrates (Brückner et al., unpublished, and this thesis). The bacterial expression of proteins in sufficient quantity and superior quality has often also been a prerequisite for structural characterization by X-ray crystallography. Our expression and purification protocol is therefore expected to facilitate crystallization of full-length AMPK which will definitely be needed for rational drug design (current collaboration with industry). Recombinant AMPK obtained with our purification method turned out to be a powerful tool for a number of studies related to AMPK structure and function, like a detailed biochemical and biophysical characterization of AMPK (Riek et al., 2008), and already allowed to shed some new light on AMPK signaling (Bhalla et al., 2006; Suter et al., 2006; Xie et al., 2006). Importantly, the automated purification system presented here can be adapted to any protein as e.g. the creatine kinase isoforms used in this thesis.

In vitro phosphorylation screens have been applied so far to cytosolic soluble proteins. Many AMPK substrates may separate in cell fractionation with unsoluble, heavy material, including membranes, cytoskeleton or glycogen bodies. In particular membrane-associated proteins involved in energy transformation and transduction, metabolite and ion transport or signal processing are using-up large amounts of ATP, in particular in the brain. In this thesis, we developed *in vitro* strategies to identify putative AMPK substrates in the unsoluble cellular fraction. These strategies reduce protein complexity in this cellular fraction by two protocols, either by further cellular subfractionation upstream of *in vitro* assays, in particular isolation of mitochondria and mitochondrial inner and outer membranes fractions, or by two-dimensional blue native SDS-PAGE separation of the *in vitro* phosphorylated heavy, unsoluble cellular fraction. Both strategies allowed the identification of several putatively phosphorylated proteins by mass spectrometry. As a proof-of-principle, two of them could be verified by *in vitro* phosphorylation of pure proteins, namely glutamate dehydrogenase and protein disulfide isomerase A3. Further studies are necessary to elucidate whether these are true *in vivo* AMPK targets. This would link AMPK to functions in mitochondria and ER, possibly by controlling the import of the nascent preproteins into these organelles. It is conceivable that such a mechanism also applies to the astonishingly high number mitochondrial proteins identified (but not yet confirmed) and which are located within this organelle. AMPK associated to the mitochondrial surface may play a role in such a type of regulation, since energy state seems to regulate phosphorylation of this AMPK pool (Tokarska-Schlattner, unpublished). The applied screening strategies have to be further optimized for resolving power and enrichment of underrepresented proteins, in particular membrane proteins. Improvements may include a combination of both strategies, membrane subfractionation and blue native 2D-PAGE, improvement of upstream cellular subfractionation e.g. also for the unsoluble heavy cellular fraction, with techniques such as free flow electrophoresis (Islinger et al., 2010; Wildgruber et al., 2008), or also further improvement of protein separation on larger blue native 2D-PAGE. The

presence of membrane proteins in these fractions may be increased by elimination of loosely bound cytosolic proteins or a screening of different neutral detergents for better solubilization.

The main part of this thesis was dedicated to the characterization of a new AMPK target, the brain-type creatine kinase, identified by *in vitro* substrate screening of soluble brain proteins following an earlier published work (Tuerk et al., 2007). AMPK-dependent phosphorylation of BCK occurs in different vertebrate species. We could pinpoint Ser6 as the major site phosphorylated by AMPK by using a panel of methods including mass spectrometry, protein sequencing, site-directed mutagenesis, yeast-two-hybrid analysis, and a generated phosphosite-specific antibody *in vitro* and *in vivo*. In contrast to earlier reports on BCK phosphorylation (Chida et al., 1990a; Chida et al., 1990b; Quest et al., 1990), these data provide first solid evidence for BCK phosphorylation as a regulatory process that is highly specific for a defined protein kinase (AMPK), a specific BCK site (Ser6), and a particular physiological signal (energy stress). Ser6 is localized in the N-terminal domain of the enzyme and is highly conserved in BCKs from different vertebrate species. Only one Ser6 per BCK dimer is exposed at the protein surface due to structural heterogeneity of the two monomers within the BCK dimer (Eder et al., 1999), thus explaining *in vitro* phosphorylation at a 1:1 stoichiometry per BCK dimer that occurs rather rapidly. An important finding supporting BCK phosphorylation by AMPK is the *in vivo* interaction between constitutive active AMPK and BCK wild-type, but not Ser6 phosphomimetic mutant as determined by Y2H analysis. Since interaction is not seen in immunoprecipitation or surface plasmon resonance (not shown), it seems to be of rapid and transient "kiss-and-run" type. In contrast to all earlier studies on BCK phosphorylation (Chida et al., 1990a; Chida et al., 1990b; Quest et al., 1990), we could not confirm strong or even mild inhibition or activation of the BCK enzymatic activity by the Ser6 phosphorylation. However, globally activated AMPK phosphorylated a seemingly minor pool of BCK localized at or localizing to exclusively perinuclear regions identified as ER. This is a first example of an AMPK substrate that is not regulated via its enzymatic activity, but exclusively by its subcellular localization. To confirm that *in vivo* BCK phosphorylation is specific and dependent of AMPK activation, we applied two different pharmacological AMPK activators, AICAR and A-769662, to two cell types, primary astrocytes and fibroblasts, and controlled for specific immunocytochemical staining by either using phosphopeptide-crossabsorption of antibodies or BCK knockout fibroblasts. Further experiments will have to show how Ser6 phosphorylation of BCK promotes its localization to the ER, e.g. by transfecting the phosphosite-mimetic S6D mutant into BCK knockout fibroblats and co-immunoprecipitation of possible protein interaction partners of BCK from ER fractions of astrocytes.

It is well known that specific subcellular localization of cytosolic CK brings the enzyme in close vicinity of ATP-generating (e.g. in glycolysis) or ATP-consuming reactions, like myosin ATPase (Hornemann et al., 2000; Turner et al., 1973) or the sarcomeric/endoplasmic reticulum Ca^{2+} ATPase (SERCA) in muscle (de Groof et al., 2002; Shin et al., 2007). Also BCK is not an exclusively soluble protein as has been shown by many studies. It binds to and activates membrane-associated thrombin receptor PAR-1 (Mahajan et al., 2000) and potassium-chloride-channel KCC2 (Inoue et al., 2004).

BCK also associates transiently with Golgi matrix protein GM130 possibly providing energy for Golgi-fragmentation (Burklen et al., 2007), and with actomyosin in membrane ruffles of astrocytes (Kuiper et al., 2009). However, the mechanisms by which cytosolic CK binds to these specific locations remain largely elusive. Only in case of MCK, the involvement of a specific charge clamp in the interaction of MCK with myomesin and M-protein in the myofibrillar M-band could be shown (Hornemann et al., 2003; Hornemann et al., 2000). Most recently, a putative Ser123 phosphorylation of MCK was found to trigger interaction with the plasma membrane sodium-calcium exchanger (Yang et al., 2010), already suggesting that phosphorylation may be a targeting signal for cytosolic CKs. In case of the phosphorylation-mediated BCK confinement to the ER, this would allow for local ATP delivery at the expense of PCr and could support different ATP-requiring processes. First, local ATP resynthesis could maintain ATP-dependent processes at the ER membrane. These include the SERCA activity which relies on high ATP/ADP ratios and is essential for sequestration of cellular calcium within the ER/SR. It was shown in muscle CK knock-out animals that cytosolic CK is essential for optimal functioning of SERCA during repetitive muscle contraction (de Groof et al., 2002; Steeghs et al., 1997; van Deursen et al., 1993), conditions under which AMPK is activated. Thus, phosphorylation by AMPK could recruit BCK to SERCA sites for fueling of calcium pumps under energy stress. Recent data showed that SERCA activity is altered in AMPK α2-/- endothelial cells and could be restored by transfection of constitutive active AMPK (Dong et al., 2010). Second, local ATP resynthesis could assure ATP supply into the ER lumen, thus supporting different ATP-dependent ER processes like protein synthesis and translocation (Mayinger and Meyer, 1993). This may involve association of phospho-BCK with a putative ER ATP-transporter, which has not yet been identified in mammals, although ATP transport across the ER membranes has been shown (Hirschberg et al., 1998). These different functional advantages of ER-associated phospho-BCK will have to be tested in future experiments. For example, the energy-dependent process of Ca^{2+} removal from the cytosol that is known to be promoted by BCK can be analyzed in AMPK knockout cells. In the absence of AMPK, BCK is no longer phosphorylated which should alter its translocation to and/or function at the ER under condition of energy stress and thus its contribution to Ca^{2+} homeostasis. The Ca^{2+} homeostasis should then be normalized again by transfection with S6D mutant. Finally, MCK phosphorylation by AMPK reported earlier study (Ponticos et al., 1998) should be confirmed, although the reported functional consequences as strong interaction between both proteins and MCK inhibition remain disputed. We suggest that, also in this case, phosphorylation by AMPK could rather induce a specific subcellular localization. Ser6 is conservatively replaced by threonine in MCK and, for example, thr6 is close to the interaction domain that mediates MCK binding to myosine and M-protein in the myofibrillar M-band (Hornemann et al., 2003; Hornemann et al., 2000).

All cellular processes involved in growth and metabolism require high and constant input of energy. Living cells have to maintain a balance between ATP consumption and production to constantly support these processes. AMPK and CK fulfill complementary functions in the complex cellular network that maintains energy homeostasis. While the Cr/PCr system can react very rapidly at

the metabolic level, AMPK is acting via regulation of downstream targets affecting more medium and long term adaptations in the cell. We have here developed different tools and finally, as the main finding of this PhD study, characterized an interplay between both enzymes: AMPK phosphorylates BCK *in vivo* leading to specific localization of phospho-BCK to the endoplasmic reticulum (ER). Thus, AMPK signaling may take advantage of the CK system to assure ATP supply in an ATP-demanding ER microenvironment under energy-compromising conditions. More generally, our data suggest that post-translational modification of cytosolic CKs may be an addressing mechanism for locating the kinase to specific subcellular sites.

4.9. Discution générale, conclusions et perspectives

La protéine kinase activée par l'AMP (AMPK) est une enzyme clée du métabolisme énergétique cellulaire, jouant un rôle central dans la détection, la signalisation et la régulation du statut énergétique. Le travail présenté dans cette thèse fournit des outils importants pour l'étude de l'AMPK *in vitro* et étend nos connaissances sur la participation de l'AMPK dans la régulation de l'homéostasie énergétique cellulaire. Les outils développés comprennent un protocole de purification automatisé pour la purification des protéines et des complexes protéiques (chapitre 2) et des protocoles pour le criblage de cibles de l'AMPK dans la fraction insoluble contenant entre autre des membranes cellulaires (chapitre 4). Ils permettent ainsi la purification de grandes quantités d'AMPK recombinante pour diverses études ainsi qu'une nouvelle méthode applicable pour le criblage *in vitro* des cibles potentielles de l'AMPK associées aux structures cellulaires insolubles comme les membranes mitochondriales. Ainsi, une nouvelle cible de l'AMPK a été identifiée à partir d'un criblage *in vitro*, la créatine kinase de type cerveau (chapitre 1) a été vérifiée et caractérisée *in vitro* et *in vivo* (chapitre 3). Nous rapportons pour la première fois la preuve que cette enzyme clé de l'homéostasie énergétique, présente dans la plupart des tissus non-musculaires, est régulée par une phosphorylation réversible dans un résidu spécifique via une protéine kinase spécifique, l'AMPK. Cependant, la phosphorylation de la BCK n'affecte pas l'activité enzymatique de la kinase comme cela a été suggéré par quelques études antérieures qui montrent uniquement des évidences de la BCK phosphorylée (Chida et al., 1990a; Quest et al., 1990), mais affecte spécifiquement la localisation de l'enzyme dans le réticulum endoplasmique (RE). Cette phosphorylation montre un nouveau type de mécanismes de régulation par l'AMPK, dont on ne connaissait, jusqu'ici, que la capacité de phosphoryler des enzymes clés du métabolisme cellulaire ou des facteurs de transcription afin d'augmenter ou d'inhiber leur activité enzymatique (Carling, 2004; Hardie et al., 2006; McGee and Hargreaves, 2008).

L'AMPK est récemment apparue comme une cible prometteuse pour le traitement pharmacologique du diabète de type II, le syndrome métabolique, et probablement aussi le cancer (Fryer and Carling, 2005; Hardie, 2007; Motoshima et al., 2006; Steinberg and Kemp, 2009), ce qui a largement accru l'intérêt pour la signalisation de l'AMPK. Différentes approches *in vitro* peuvent être appliquées pour le criblage de cibles potentielles de l'AMPK: le criblage par phosphorylation *in vitro* (Cohen and Knebel, 2006; Thali et al., 2010; Tuerk et al., 2007) ou des techniques bioinformatiques pour la recherche de peptides contenant la séquence consensus de l'AMPK (Gwinn et al., 2008). Un haut niveau de pureté et une activité enzymatique élevée des isoformes de l'AMPK sont essentiels pour les essais de phosphorylation *in vitro*. L'AMPK purifiée à partir de tissus comme le muscle ou le foie est désavantageuse puisque seules de petites quantités (quelques microgrammes) peuvent être obtenues. D'autre part, les cellules eucaryotes expriment un mélange de différentes isoformes de l'enzyme. Un système d'expression polycistronique bactérien développé par notre groupe (Neumann et al., 2003) a permis l'obtention de complexes recombinants de l'AMPK hétérotrimérique et d'une activité enzymatique à haut rendement contenant des isoformes de l'AMPK spécifiques ou mutantes. Cependant, les variabilités dans le protocole de purification multi-étapes ont limité la reproductibilité

de la procédure et la pureté des protéines. Dans ce travail de thèse, un système de chromatographie thermostaté haut de gamme (Äkta Explorer) a été modifié de telle manière qu'une purification automatique des protéines en quatre dimensions pourrait être exécutée à distance (chapitre 2). Ce processus automatisé a permis de produire dans un court laps de temps de grandes quantités d'AMPK hautement et fraichement purifiée. Ceci est particulièrement important parce que l'AMPK s'est avérée être une protéine plutôt instable avec une forte tendance à s'agréger et à se dénaturer *in vitro*. Différentes isoformes de l'enzyme produites par cette méthode présentent une grande activité spécifique après activation par des kinases en amont comme CaMKKβ. La production et la purification de différentes isoformes de l'AMPK a ouvert la possibilité d'étudier les fonctions isoforme-spécifiques ainsi que le criblage de nouveaux partenaires d'interactions et de substrats (Brückner et al., non publiées, et cette thèse). L'expression des protéines bactériennes en quantité suffisante et de qualité supérieure a souvent été une condition préalable pour la caractérisation structurelle pour la cristallographie aux rayons X. Notre expression et protocole de purification est donc prévu pour faciliter la cristallisation de l'AMPK hétérotrimérique qui sera certainement nécessaire pour la conception de médicaments (collaboration en cours avec l'industrie). L'AMPK recombinante obtenue avec notre méthode s'est avérée être un outil puissant pour un certain nombre d'études liées à la structure et la fonction de l'AMPK, comme sa caractérisation biochimique et biophysique détaillée (Riek et al., 2008) et a déjà permis de découvrir de nouvelles voies de signalisation de l'AMPK (Bhalla et al., 2006; Suter et al., 2006; Xie et al., 2006). Le système de purification automatisé présenté ici peut être adapté pour la purification de toutes les protéines comme par exemple les isoformes de la créatine kinase utilisées dans cette thèse.

Le criblage de phosphorylation *in vitro* a été principalement appliqué à des protéines cytosoliques solubles. De nombreux substrats de l'AMPK peuvent se séparer par fractionnements cellulaires avec des matériels insolubles, comme les membranes, le cytosquelette ou les corps d'inclusion de glycogène. Certaines protéines, associées aux membranes, sont impliquées dans la transformation et la transduction d'énergie, le transport de métabolites et d'ions ou le traitement du signal en utilisant alors de grandes quantités d'ATP, en particulier dans le cerveau. Dans ce travail de thèse, nous avons développé des stratégies *in vitro* pour identifier des cibles potentielles de l'AMPK dans la fraction insoluble cellulaire. Afin de réduire la complexité des protéines dans cette fraction cellulaire, deux protocoles ont été appliqués : i) un sous-fractionnement cellulaire en amont des essais *in vitro*, comme l'isolement des mitochondries et plus particulièrement les fractions de la membrane internes et externes des mitochondries (ii) des techniques d'électrophorèse telles que l'utilisation de gels natifs en deux dimensions (bleu SDS-PAGE natif) afin de mieux séparer la fraction cellulaire insoluble. Les deux stratégies ont permis l'identification par spectrométrie de masse de plusieurs protéines phosphorylées. Deux d'entre elles ont été confirmée comme cibles de l'AMPK par phosphorylation *in vitro* en utilisant des protéines purifiées, à savoir la glutamate déshydrogénase (GDH) et l'isomérase protéine disulfure A3 (PDI). Des études complémentaires sont nécessaires pour vérifier si ces enzymes sont de vraies cibles de l'AMPK *in vivo*. Cela permettrait de lier l'AMPK à des fonctions des

mitochondries et du RE, probablement en contrôlant l'importation de pré protéines naissantes dans ces organites. Il est concevable qu'un tel mécanisme s'applique également a un nombre étonnamment élevé de protéines mitochondriales identifiées (mais pas encore confirmées) et qui sont situées dans cet organite. L'AMPK associée à la surface mitochondriale peut jouer un rôle dans un tel type de régulation, étant donné que l'état d'énergie semble réguler la phosphorylation de l'AMPK dans ce pool (Tokarska-Schlattner, non publié). Les stratégies de criblage appliquées doivent encore être optimisées pour améliorer l'enrichissement des protéines sous-représentées, particulièrement les protéines membranaires. Les améliorations peuvent comprendre une combinaison des deux stratégies dont le sous-fractionnement des membranes et la séparation par électrophorèse de type blue native PAGE. Des techniques telles que l'électrophorèse libre circulation (Islinger et al., 2010; Wildgruber et al., 2008) peuvent améliorer le sous-fractionnement cellulaire en amont, par exemple pour la fraction insoluble cellulaire. La présence de protéines membranaires dans ces fractions peut être augmentée par l'élimination des protéines cytosoliques faiblement associées ou à une meilleure solubilisation des protéines membranaires en utilisant différents détergents neutres.

La partie principale de cette thèse a été consacrée à la caractérisation d'une nouvelle cible de l'AMPK, la créatine kinase de type cerveau, identifiée par un criblage *in vitro* de protéines solubles du cerveau suite à un travail publié antérieurement (Tuerk et al., 2007). La phosphorylation de la BCK par l'AMPK a été confirmée sur différentes espèces de vertébrés. Nous avons identifié la Ser6 comme le site majeur phosphorylé par l'AMPK en utilisant différentes méthodes, telles que la spectrométrie de masse, le séquençage des protéines, la mutagenèse dirigée, le système de double hybride en levure, et un anticorps généré spécifique de la phospho-Ser6 *in vitro* et *in vivo*. Contrairement aux rapports précédents sur la phosphorylation de la BCK (Chida et al., 1990a; Chida et al., 1990b; Quest et al., 1990), nos données fournissent des preuves solides sur la phosphorylation de la BCK comme un processus de régulation qui est très spécifique d'une protéine kinase définie (AMPK), d'un site particulier de la BCK (Ser6), et d'un signal physiologique caractéristique (stress énergétique). La Ser6 est localisée dans le domaine N-terminal de l'enzyme et est hautement conservée dans la BCK de différentes espèces de vertébrés. Une seule Ser6 par dimère de BCK est exposé à la surface de la protéine en raison de l'hétérogénéité structurelle des deux monomères de BCK (Eder et al., 1999), expliquant ainsi que la phosphorylation *in vitro* a une stœchiométrie 1:1. Une conclusion importante qui soutien la phosphorylation de la BCK par l'AMPK est l'interaction *in vivo* entre l'AMPK constitutivement active et la BCK de type sauvage, mais pas avec la mutante Ser6 tel que déterminée par l'analyse Y2H. Etant donnée que cette interaction n'a pas été confirmé par la résonance plasmonique de surface et l'immunoprécipitation (non représentée), elle semble être rapide et transitoire de type "kiss-and-run". Contrairement à toutes les études antérieures sur la phosphorylation de la BCK (Chida et al., 1990a; Chida et al., 1990b; Quest et al., 1990), nous n'avons pas pu confirmer d'inhibition ou d'activation de l'activité enzymatique de la BCK par la phosphorylation sur la Ser6. Cependant, l'AMPK activée phosphoryle un petit pool de BCK provoquant la localisation ou la rétention de la phospho-BCK dans la région périnucléaire identifiée comme le RE. Il s'agit d'un

premier exemple d'une cible de l'AMPK qui n'est pas régulée via son activité enzymatique, mais exclusivement par sa localisation subcellulaire. Pour confirmer que la phosphorylation *in vivo* de la BCK est spécifique et dépend de l'activation de l'AMPK, nous avons appliqué deux différents activateurs pharmacologiques de l'AMPK, AICAR et A-769662, à deux types de cellules, des astrocytes et des fibroblastes. Par immunocytochimie, nous avons vérifié la spécificité de l'anticorps sur des fibroblastes knockout de la BCK. Des expériences complémentaires devront montrer comment la phosphorylation sur la Ser6 de la BCK favorise sa localisation à RE, par exemple par la transfection de la mutante S6D dans le knock-out BCK des fibroblastes et la co-immunoprécipitation de possibles partenaires d'interaction de la BCK en utilisant des fractions du réticulum endoplasmique d'astrocytes.

Il est bien connu que les CKs cytosoliques sont localisées à proximité des sites de production de l'ATP (par exemple de la glycolyse) ou de réactions de consommation d'ATP, comme la myosine ATPase (Hornemann et al., 2000; Turner et al., 1973) ou du sarcomère/réticulum endoplasmique Ca^{2+} ATPase (SERCA) dans le muscle (de Groof et al., 2002; Shin et al., 2007). Ainsi la BCK n'est pas qu'une protéine exclusivement soluble comme cela a été montré par de nombreuses études. Elle se lie et active le récepteur de la thrombine PAR-1 (Mahajan et al., 2000) et le co-transporteur potassium-chlore neurone spécifique KCC2 (Inoue et al., 2006). La BCK s'associe également de façon transitoire avec la protéine GM130 du Golgi probablement pour fournir de l'énergie pour la fragmentation du Golgi (Burklen et al., 2007), et avec l'actomyosine du lamellipode des astrocytes (Kuiper et al., 2009). Cependant, les mécanismes par lesquels les CKs cytosoliques se lient à ces endroits précis est très incertaine. Dans le cas de la CK du muscle (MCK) la présence d'une serie de quatre lysines dans le N-terminal de l'enzyme permet l'interaction avec la myomesin et la protéine M dans la bande M des myofibrilles a pu être démontrée (Hornemann et al., 2003; Hornemann et al., 2000). Plus récemment, il a été mis en évidence qu'une phosphorylation de la MCK sur la Ser123 permet son interaction avec l'échangeur sodium-calcique de la membrane plasmique (Yang et al., 2010). Ceci suggère que la phosphorylation peut être un signal de ciblage pour les CKs cytosoliques. La présence de la BCK phosphorylée dans le RE peut permettre l'apport local de l'ATP pour supporter différents processus dépendant de l'ATP dans cet organite. Tout d'abord, la resynthèse de l'ATP local pourrait maintenir les processus dépendant de l'ATP à la membrane du RE. Il s'agit notamment de l'activité du SERCA qui repose sur le rapport ATP/ADP et qui est essentiel pour la séquestration du calcium cellulaire dans le RE/SR. Il a été montré que, dans les animaux MCK knock-out, la CK cytosolique est essentielle pour un fonctionnement optimal du SERCA lors de la contraction musculaire répétitive (de Groof et al., 2002; Steeghs et al., 1997; van Deursen et al., 1993), conditions dans lesquelles l'AMPK est active. Ainsi, la phosphorylation par l'AMPK pourrait recruter la BCK au SERCA pour alimenter les pompes à calcium sous stress énergétique. Des données récentes montrent que l'activité du SERCA est altérée dans l'AMPK α2-/- dans les cellules endothéliales (Dong et al., 2010) et pourrait être restaurée par transfection de l'AMPK constitutivement active. Deuxièmement, la resynthèse de l'ATP locale peut être assurée par l'apport de l'ATP dans le lumen du RE, soutenant ainsi les différents processus RE dépendant de l'ATP comme la synthèse des protéines et leur translocation (Mayinger and Meyer,

1993). Il peut s'agir de l'association de la phospho-BCK avec un potentiel transporteur de l'ATP du RE. Cependant même si le transport d'ATP à travers les membranes du RE a été démontré (Hirschberg et al., 1998) ce transporteur n'a pas encore été identifié chez les mammifères. Les différents avantages fonctionnels de la phospho-BCK associée au RE devront être testés dans des expériences futures. Par exemple, le processus dépendant de l'énergie comme la séquestration du Ca^{2+} du cytosol qui est connu pour être promu par la BCK peut être analysé dans les cellules knock out de l'AMPK. En l'absence de l'AMPK, la BCK n'est plus phosphorylée ce qui devrait modifier sa translocation et/ou fonction dans le RE dans des conditions de stress énergétique et donc sa contribution à l'homéostasie du Ca^{2+}. Celle-ci devrait alors être normalisée à nouveau par une transfection avec la forme mutant S6D. Enfin, la phosphorylation de la MCK (Ponticos et al., 1998) devrait être confirmée, bien que les conséquences fonctionnelles comme la forte interaction entre les deux protéines et l'inhibition enzymatique de la MCK restent contestés. Nous suggérons, dans ce cas également, que la phosphorylation de la MCK par l'AMPK pourrait plutôt induire une localisation subcellulaire spécifique. Dans la séquence de la MCK, la Ser6 est remplacé par une thréonine (Thr6), qui est proche du domaine d'interaction intervenant dans la liaison de la MCK à la myosine et à la protéine M dans les bandes myofibrillaires (Hornemann et al., 2003; Hornemann et al., 2000).

Tous les processus cellulaires impliqués dans la croissance et le métabolisme nécessitent un apport élevé et constant en énergie. Les cellules vivantes doivent maintenir un équilibre entre la consommation et la production d'ATP pour supporter ce processus. L'AMPK et la CK remplissent des fonctions complémentaires dans le réseau cellulaire complexe qui maintient l'homéostasie énergétique. Alors que le système Cr/PCr peut réagir très rapidement au niveau métabolique, l'AMPK agit via la régulation des cibles en aval affectant à moyen et long terme des adaptations dans la cellule. Nous avons ici développé différents outils et caractérisé l'interaction entre les deux enzymes: l'AMPK phosphoryle la BCK *in vivo* conduisant à la localisation spécifique de la phospho-BCK vers le réticulum endoplasmique (RE). L'approvisionnement du RE en ATP est nécessaire en cas de stress énergétique et peut alors être assuré par l'utilisation du système CK par la voie de signalisation de l'AMPK. Plus généralement, nos données suggèrent que la modification post-traductionnelle de la CK cytosolique peut être un mécanisme d'adressage de la localisation de la kinase à des sites spécifiques subcellulaires.

4.10. References

Bhalla, V., N.M. Oyster, A.C. Fitch, M.A. Wijngaarden, D. Neumann, U. Schlattner, D. Pearce, and K.R. Hallows. 2006. AMP-activated kinase inhibits the epithelial Na+ channel through functional regulation of the ubiquitin ligase Nedd4-2. *J Biol Chem*. 281:26159-69.

Burklen, T.S., A. Hirschy, and T. Wallimann. 2007. Brain-type creatine kinase BB-CK interacts with the Golgi Matrix Protein GM130 in early prophase. *Mol Cell Biochem*. 297:53-64.

Carling, D. 2004. The AMP-activated protein kinase cascade--a unifying system for energy control. *Trends Biochem Sci*. 29:18-24.

Chida, K., K. Kasahara, M. Tsunenaga, Y. Kohno, S. Yamada, S. Ohmi, and T. Kuroki. 1990a. Purification and identification of creatine phosphokinase B as a substrate of protein kinase C in mouse skin in vivo. *Biochem Biophys Res Commun*. 173:351-7.

Chida, K., M. Tsunenaga, K. Kasahara, Y. Kohno, and T. Kuroki. 1990b. Regulation of creatine phosphokinase B activity by protein kinase C. *Biochem Biophys Res Commun*. 173:346-50.

Cohen, P., and A. Knebel. 2006. KESTREL: a powerful method for identifying the physiological substrates of protein kinases. *Biochem J*. 393:1-6.

de Groof, A.J., J.A. Fransen, R.J. Errington, P.H. Willems, B. Wieringa, and W.J. Koopman. 2002. The creatine kinase system is essential for optimal refill of the sarcoplasmic reticulum Ca2+ store in skeletal muscle. *J Biol Chem*. 277:5275-84.

Dong, Y., M. Zhang, B. Liang, Z. Xie, Z. Zhao, S. Asfa, H.C. Choi, and M.H. Zou. 2010. Reduction of AMP-activated protein kinase alpha2 increases endoplasmic reticulum stress and atherosclerosis in vivo. *Circulation*. 121:792-803.

Eder, M., U. Schlattner, A. Becker, T. Wallimann, W. Kabsch, and K. Fritz-Wolf. 1999. Crystal structure of brain-type creatine kinase at 1.41 A resolution. *Protein Sci*. 8:2258-69.

Fryer, L.G., and D. Carling. 2005. AMP-activated protein kinase and the metabolic syndrome. *Biochem Soc Trans*. 33:362-6.

Gwinn, D.M., D.B. Shackelford, D.F. Egan, M.M. Mihaylova, A. Mery, D.S. Vasquez, B.E. Turk, and R.J. Shaw. 2008. AMPK phosphorylation of raptor mediates a metabolic checkpoint. *Mol Cell*. 30:214-26.

Hardie, D.G. 2007. AMP-activated protein kinase as a drug target. *Annu Rev Pharmacol Toxicol*. 47:185-210.

Hardie, D.G., S.A. Hawley, and J.W. Scott. 2006. AMP-activated protein kinase--development of the energy sensor concept. *J Physiol*. 574:7-15.

Hirschberg, C.B., P.W. Robbins, and C. Abeijon. 1998. Transporters of nucleotide sugars, ATP, and nucleotide sulfate in the endoplasmic reticulum and Golgi apparatus. *Annu Rev Biochem*. 67:49-69.

Hornemann, T., S. Kempa, M. Himmel, K. Hayess, D.O. Furst, and T. Wallimann. 2003. Muscle-type creatine kinase interacts with central domains of the M-band proteins myomesin and M-protein. *J Mol Biol*. 332:877-87.

Hornemann, T., M. Stolz, and T. Wallimann. 2000. Isoenzyme-specific interaction of muscle-type creatine kinase with the sarcomeric M-line is mediated by NH(2)-terminal lysine charge-clamps. *J Cell Biol*. 149:1225-34.

Inoue, K., S. Ueno, and A. Fukuda. 2004. Interaction of neuron-specific K+-Cl- cotransporter, KCC2, with brain-type creatine kinase. *FEBS Lett*. 564:131-5.

Inoue, K., J. Yamada, S. Ueno, and A. Fukuda. 2006. Brain-type creatine kinase activates neuron-specific K+-Cl- co-transporter KCC2. *J Neurochem*. 96:598-608.

Islinger, M., K.W. Li, M. Loos, S. Liebler, S. Angermuller, C. Eckerskorn, G. Weber, A. Abdolzade, and A. Volkl. 2010. Peroxisomes from the heavy mitochondrial fraction: isolation by zonal free flow electrophoresis and quantitative mass spectrometrical characterization. *J Proteome Res*. 9:113-24.

Kuiper, J.W., R. van Horssen, F. Oerlemans, W. Peters, M.M. van Dommelen, M.M. te Lindert, T.L. ten Hagen, E. Janssen, J.A. Fransen, and B. Wieringa. 2009. Local ATP generation by brain-type creatine kinase (CK-B) facilitates cell motility. *PLoS One*. 4:e5030.

Mahajan, V.B., K.S. Pai, A. Lau, and D.D. Cunningham. 2000. Creatine kinase, an ATP-generating enzyme, is required for thrombin receptor signaling to the cytoskeleton. *Proc Natl Acad Sci U S A*. 97:12062-7.

Mayinger, P., and D.I. Meyer. 1993. An ATP transporter is required for protein translocation into the yeast endoplasmic reticulum. *Embo J*. 12:659-66.

McGee, S.L., and M. Hargreaves. 2008. AMPK and transcriptional regulation. *Front Biosci*. 13:3022-33.

Motoshima, H., B.J. Goldstein, M. Igata, and E. Araki. 2006. AMPK and cell proliferation--AMPK as a therapeutic target for atherosclerosis and cancer. *J Physiol*. 574:63-71.

Neumann, D., A. Woods, D. Carling, T. Wallimann, and U. Schlattner. 2003. Mammalian AMP-activated protein kinase: functional, heterotrimeric complexes by co-expression of subunits in Escherichia coli. *Protein Expr Purif*. 30:230-7.

Ponticos, M., Q.L. Lu, J.E. Morgan, D.G. Hardie, T.A. Partridge, and D. Carling. 1998. Dual regulation of the AMP-activated protein kinase provides a novel mechanism for the control of creatine kinase in skeletal muscle. *Embo J*. 17:1688-99.

Quest, A.F., T. Soldati, W. Hemmer, J.C. Perriard, H.M. Eppenberger, and T. Wallimann. 1990. Phosphorylation of chicken brain-type creatine kinase affects a physiologically important kinetic parameter and gives rise to protein microheterogeneity in vivo. *FEBS Lett*. 269:457-64.

Riek, U., R. Scholz, P. Konarev, A. Rufer, M. Suter, A. Nazabal, P. Ringler, M. Chami, S.A. Muller, D. Neumann, M. Forstner, M. Hennig, R. Zenobi, A. Engel, D. Svergun, U. Schlattner, and T. Wallimann. 2008. Structural properties of AMP-activated protein kinase: dimerization, molecular shape, and changes upon ligand binding. *J Biol Chem*. 283:18331-43.

Shin, J.B., F. Streijger, A. Beynon, T. Peters, L. Gadzala, D. McMillen, C. Bystrom, C.E. Van der Zee, T. Wallimann, and P.G. Gillespie. 2007. Hair bundles are specialized for ATP delivery via creatine kinase. *Neuron*. 53:371-86.

Steeghs, K., A. Benders, F. Oerlemans, A. de Haan, A. Heerschap, W. Ruitenbeek, C. Jost, J. van Deursen, B. Perryman, D. Pette, M. Bruckwilder, J. Koudijs, P. Jap, J. Veerkamp, and B. Wieringa. 1997. Altered Ca2+ responses in muscles with combined mitochondrial and cytosolic creatine kinase deficiencies. *Cell*. 89:93-103.

Steinberg, G.R., and B.E. Kemp. 2009. AMPK in Health and Disease. *Physiol Rev*. 89:1025-78.

Suter, M., U. Riek, R. Tuerk, U. Schlattner, T. Wallimann, and D. Neumann. 2006. Dissecting the role of 5'-AMP for allosteric stimulation, activation, and deactivation of AMP-activated protein kinase. *J Biol Chem*. 281:32207-16.

Thali, R.F., R.D. Tuerk, R. Scholz, Y. Yoho-Auchli, R.A. Brunisholz, and D. Neumann. 2010. Novel candidate substrates of AMP-activated protein kinase identified in red blood cell lysates. *Biochem Biophys Res Commun*. 398:296-301.

Tuerk, R.D., R.F. Thali, Y. Auchli, H. Rechsteiner, R.A. Brunisholz, U. Schlattner, T. Wallimann, and D. Neumann. 2007. New candidate targets of AMP-activated protein kinase in murine brain revealed by a novel multidimensional substrate-screen for protein kinases. *J Proteome Res*. 6:3266-77.

Turner, D.C., T. Wallimann, and H.M. Eppenberger. 1973. A protein that binds specifically to the M-line of skeletal muscle is identified as the muscle form of creatine kinase. *Proc Natl Acad Sci U S A*. 70:702-5.

van Deursen, J., A. Heerschap, F. Oerlemans, W. Ruitenbeek, P. Jap, H. ter Laak, and B. Wieringa. 1993. Skeletal muscles of mice deficient in muscle creatine kinase lack burst activity. *Cell*. 74:621-31.

Wildgruber, R., J. Yi, M. Nissum, C. Eckerskorn, and G. Weber. 2008. Free-flow electrophoresis system for plasma proteomic applications. *Methods Mol Biol*. 424:287-300.

Xie, M., D. Zhang, J.R. Dyck, Y. Li, H. Zhang, M. Morishima, D.L. Mann, G.E. Taffet, A. Baldini, D.S. Khoury, and M.D. Schneider. 2006. A pivotal role for endogenous TGF-beta-activated kinase-1 in the LKB1/AMP-activated protein kinase energy-sensor pathway. *Proc Natl Acad Sci U S A*. 103:17378-83.

Yang, Y.C., M.J. Fann, W.H. Chang, L.H. Tai, J.H. Jiang, and L.S. Kao. 2010. Regulation of sodium-calcium exchanger activity by creatine kinase under energy-compromised conditions. *J Biol Chem*. 285:28275-85.

Appendix

5.1. Abbreviations

2-DE	2-Dimensional electrophoresis
A769662	AMPK activator also called Abbott compound
ACC	Acetyl-CoA carboxylase
ADP	Adenosine diphosphate
AGAT	L-arginine:glycine amidinotransferase
AICAR	5-aminoimidazole-4-carboxyamide riboside
AK	Adenylate kinase
AMP	Adenosine monophosphate
AMPK	AMP-activated protein kinase
AMPK111TD	AMPK α1 (T172D) β1γ1
ANT	Adenine nucleotide translocase
AS160	Akt substrate of 160 kDa
ATP	Adenosine triphosphate
BAK (-/-)	Double BCK/AK Knockout
BCK	Cytosolic brain-type creatine kinase
BN-PAGE	Two-dimensional blue native PAGE
CaMKKβ	Ca^{2+}/calmodulin-dependent kinase kinase, especially the β isoform
CFTR	Cystic fibrosis transmembrane conductance regulator $C1^-$ channel
CHAPS	3-[(3-Cholamidopropyl) dimethylammonio]-l-propanesulfonate
CIP	Clean In Place
CK	Creatine kinase
CPT1	Carnitine palmitoyltransferase 1
Cr	Creatine
CREB	cAMP response element-binding protein
CRT	Creatine transporter
CRTC2	CREB regulated transcription coactivator 2
DMEM	Dulbecco's Modified Eagle's Medium
DMSO	Dimethyl sulfoxide
DTT	Dithiothreitol
EDTA	Ethylenediamine tetra-Acetic acid
FA	Fatty acids
FCS	Fetal Calf Serum
GAA	Guanidinoacetate
GAMT	Guanidinoacetate methyltransferase
GFAP	Glial fibrillary acidic protein
GLUT	Glucose transporter
GP	Glycogen Phosphorylase
GS	Glycogen synthase
GTP	Guanosine triphosphate
HDAC	Histone deacetylase
HEPES	4-(2-Hydroxyethyl)piperazine-1-ethanesulfonic acid
HPLC	High Performance Liquid Chromatography
HSL	Hormone-sensitive lipase
IgG	Immunoglobulin G
IRS-1	Insulin receptor substrate 1 (IRS-1)
kDa	Kilo dalton
LKB1	Serine/threonine kinase 11 (STK11)
MALDI	Matrix-assisted laser desorption/ionization
MCK	Cytosolic muscle type creatine kinase
MEF	Mouse Embryonic Fibroblast
MO25	Mouse protein 25

mTOR	Mammalian Target of Rapamycin
Mudseek	Multidimensional substrate-screen for protein kinase
NAD	Nicotinamide adenine dinucleotide
NADH	Reduced nicotinamide adenine dinucleotide
NDPK	Nucleoside diphosphate kinases
OCT1	Organic cation transporter
OxPhos	Oxidative phosphorylation
PAGE	Polyacrylamide gel electrophoresis
PBS	Phosphate buffered saline
PCR	Polymerase chain reaction
PDI	Protein disulfide isomerase
PFK2	6-Phosphofructokinase 2
PGC-1α	Peroxisome proliferator activator receptor gamma coactivator-1alpha
PKA	Protein kinase A
PKC	Protein kinase C
PP2C	Protein phosphatase 2C
SD-AHWL	Supplement deficient medium lacking Ade-His-Trp-Leu
SDS	Sodium dodecyl sulfate
SD-WL	Supplement deficient medium lacking Trp-Leu
sMtCK	Sarcomeric mitochondrial creatine kinase
STRAD	STE 20-related adaptor protein
TAK1	Transforming growth factor-β activated kinase-1
TCA	Tricarboxic acid cycle
TCEP	Tris(2-carboxyethyl)phosphine
TSC2	Tuberous sclerosis complex 2
uMtCK	Ubiquitous mitochondrial creatine kinase
VDAC	Voltage-dependent anion channel
WT	Wild-type
Y2H	Yeast two-hybrid
ZMP	5-aminoimidazole-4-carboxyamide-1-β-D-ribofuranosyl-5’-monophosphate

Acknowledgements

Au terme de ces travaux, mes premières pensées vont à deux personnes, en particulier au Prof. Xavier Leverve à qui je souhaite rendre hommage pour l'ensemble de sa carrière scientifique. Plus personnellement, il m'a accueillie avec gentillesse et m'a permis de réaliser mes études au sein du laboratoire. Je remercie également le Prof. Uwe Schlattner qui a été depuis mon arrivée en France la personne qui m'a encadrée et qui m'a toujours soutenue au niveau scientifique et personnel. Ses remarques scientifiques ainsi que ses idées pour mon projet de thèse ont été très enrichissantes. J'ai sincèrement apprécié de travailler au sein de son groupe.

Je remercie les professeurs Bé Wieringa et Theo Wallimann d'avoir bien voulu être rapporteurs de cette thèse. Je remercie aussi Dr. Marie-Lise Lacombe qui a aimablement accepté d'examiner ce travail.

Un énorme merci aux collègues de l'ETH à Zurich qui ont toujours vivement collaboré avec nous et qui pendant mon séjour chez eux m'ont mis sur la voie de l'AMPK. Encore un grand merci au Prof. Theo Wallimann, pour ses apports lors de ses séjours à Grenoble, sa passion pour nos travaux et ses suggestions ont toujours stimulé ma motivation au profit des recherches sur la CK.

Bien plus que des remerciements, toutes mes amitiés au groupe de LBFA avec qui j'ai eu la chance de travailler et de développer une collaboration fructueuse. Merci pour tout le soutien que j'ai eu depuis mon arrivée au laboratoire. J'ai toujours apprécié l'aide que vous m'avez apportée pour que mon séjour soit à la fois agréable et dynamique.

Un grand merci à mes collègues du groupe 116, Malgorzata, Severine, Laurence, Shuijie, Denis et particulièrement Anna pour les riches moments que nous avons passés ensemble, faits de travail, d'échanges et de beaucoup d'amitié.